Université de Neuchâtel

Cadmium anomalies in Jurassic carbonates (Bajocian, Oxfordian) in western and southern Europe

Mediterranean coast, October 2005

Ph.D thesis presented by

Claire Rambeau

Université de Neuchâtel
Facultés des Sciences - Institut de Géologie

25 January 2006

Thesis Jury:

Prof. Karl B. Föllmi (Neuchâtel)	Director
Prof. T. Adatte (Neuchâtel)	Examinator
Dr. D. Baize (INRA Orléans)	Examinator
Dr. A. Bartolini (Paris VI)	Examinator
Dr. V. Matera (Neuchâtel)	Examinator
Prof. Judith A. McKenzie (Zürich)	Examinator
Prof. E. Verrecchia (Neuchâtel)	Examinator

Key words:

cadmium; carbonates; limestone; oolites; soil;
Jurassic; Bajocian; Oxfordian;
Jura; Burgundy; western Europe; southern Europe;
palaeoenvironment; geochemistry; sedimentology

Abstract

The trace metal cadmium (Cd) is a highly toxic element, with adverse effects both on human health as well as on ecosystem equilibria. Its transfer into the environment occurs by the mediation of natural and anthropogenic processes. Important natural sources comprise volcanic emissions and the biogeochemical weathering of cadmium-enriched rocks, such as phosphorites or organic-rich deposits.

This study considers the Cd concentrations in Jurassic limestone, in particular of Bajocian (Middle Jurassic) and Oxfordian (Late Jurassic) age in western and southern Europe. In the Jura mountains area, carbonate rocks related to these time periods have been shown to contain surprisingly high Cd concentrations, especially since most carbonate rocks are known to be strongly depleted in Cd relative to the average crust. Soils that are developed from bedrocks of these geological ages equally show a strong tendency to be Cd-enriched to anomalously high levels.

One of the specific aims of this study is to trace the geographical and stratigraphical distribution of Cd enrichments in Jurassic carbonates, in western and southern Europe, and consequently to develop a predictive tool to identify the presence of Cd- enriched soils related to Jurassic rock substrata in the investigated areas. A further goal is to reconstruct the sedimentary and environmental conditions that have led to Cd enrichments in Jurassic limestone. Ten sections in carbonate successions of Middle or Late Jurassic age have been analyzed in Switzerland, France, Spain and Italy. Additionally, a specific study aiming at quantifying the relationships between Jurassic limestone and associated soils has been conducted in the Lower Burgundy area (France).

Our results from the analysis of carbonate sections suggest that for both periods cadmium enrichments correspond to a widespread phenomenon in western and southern Europe, unrelated to the specificities of the carbonate facies. Two major features are nevertheless distinguished:

- a general increase in cadmium values is observed in both open-marine and platform settings, and particularly well marked in basin environments; this shift towards more elevated values is interpreted as a witness of general changes in the cadmium cycle at least within the western Tethyan realm, and perhaps on a wider geographical scale;
- shallow-water sections additionally display major enrichments, with cadmium values frequently above 1 µg/g, restricted to narrow stratigraphic intervals. These very high concentrations are attributed to a specific mechanism of enrichment.

Cd enrichments in Jurassic shallow-water calcareous rocks are proposed to be related to (1) the quantity of Cd available in seawater, and (2) important biological activity and organic matter production on the carbonate platform margin. In dynamic sedimentary environments on the carbonate platform, organic matter is trapped by rapid, episodic deposition of sediment bodies. Reducing conditions consequently develop in the uppermost part of deposits, associated with organic matter degradation. In those early diagenetic environments, Cd becomes desorbed and transferred partly into sulphuric phases and partly into surrounding carbonate grains. Calcareous ooids may also be directly enriched in Cd by sequestration of this element within the layers of organic matter associated with the ooid cortex and/or by direct co-precipitation with calcite. Cd enrichments in lagoonal environments are proposed to be related to microbial activity, via micritization and/or by direct bioconcentration in organic layers or carbonate phases.

The general increase of Cd contents in both deep and shallow-water carbonates is tentatively linked to general environment change, and especially to intense volcanic processes, which may have led to an increase in the availability of Cd in the environment. Volcanic processes may explain both the unusual Cd contents of these carbonates as well as the presence of other trace-metals, like Zn Nb, and Zr, in some of the investigated samples. Possible candidates are (1) the important phase of silicic volcanism related to the break-up of Gondwana which has been identified in Patagonia and in Antarctica for the Jurassic period; and (2) the volcanic centre situated in the North Sea which was active during the Jurassic and early Cretaceous.

The results of our investigations with regards to Bajocian and Oxfordian limestone and associated soils in the Lower Burgundy area confirm that a causal link exists between Cd anomalies in soils and high Cd contents in the associated carbonate bedrock. Mean enrichment factors calculated for Cd in the soil relative to the associated carbonate substratum vary from 4.6 to 5.7, those calculated between soil and rock inside restricted geographical areas being around 5.5 - 5.7.
The widespread presence of Cd-enriched carbonates in investigated sections of Middle and Late Jurassic age suggests that these enrichments may occur on a larger geographical scale within western and southern Europe. This would also imply that corresponding soils have the potential to be naturally enriched in Cd, in particular for soils related to the weathering of shallow-water limestone.

Table of contents

IV Geographical and geological settings

V - Anomalous cadmium enrichments in Tethyan Jurassic carbonates : past and present environmental implications

(in prep. for ? Geochimica et Cosmochimica Acta)

VI – Cadmium anomalies in Jurassic limestone as the cause for high cadmium concentrations in associated soils: a case study in Lower Burgundy, France

(in prep. for Environmental Geology)

VII - µ-X-Ray fluorescence determination of cadmium locations and associations with other trace-elements in Jurassic cadmium-enriched limestone - models for the enrichment of cadmium in calcareous rocks

(in prep. for Chemical Geology)

VIII – Cadmium enrichments in Jurassic carbonates : towards the causes and mechanisms – A multivariate statistical analysis approach

IX - Other geochemical investigations

X - Conclusive points and discussion: Towards a model for Cd enrichments in Jurassic carbonates

Annexes

Acknowledgments

First of all, I would like to thank Karl Föllmi for proposing me this subject and therefore allowing me to get involved in a very interesting research topic. Thanks for the discussions, the comments, the interest for my work. Thanks also for having followed my (slow) improvements in English with a lot of encouragements.

I equally acknowledge all the members of my jury, for having accepted to examine my dissertation.

Thanks also to all the other members of the GEA team, Viginie Matera and Tiffany Monnier for the endless ICP-MS analyses, Thierry Adatte, Haydon, Pascal, Raùl, Alexis, Stéphane, for their help in my punctual incursions in the worlds of phosphorus and organic matter measurements, and for field assistance.

A well-deserved thanks goes to Eric Verrecchia, for having introduced me to the wonderful universe of multivariate statistical analyses and helped me for the interpretations.

Thanks also to Christophe Dupraz, who answered my numerous questions about oolitic formation and bacterial activity.

Thanks to André Villard for (sometimes rather complicated) preparation of samples.

Thanks to Annachiara Bartolini, José Sandoval (University of Granada), Markus Geiger (Bremen University) for the samples from Terminilletto, Carcabuey, Casa de Chimeneas and Madagascar, and for having answered all my questions concerning these sections.

I gratefully acknowledge Denis Baize (and all his team) for field assistance, useful comments, and soil analyses.

Thanks to Phillippe Veuve and Wolfgang Hug for giving me access to information and samples, related to the sections they investigated in the Jura Mountains, to Jean-Claude Menot and Jacques Aubry for field assistance, and to Andreas Wetzel for advise.

Thanks also to Andreas Voegelin and Olivier Jacquat (ETH Zurich), as well as to Gerald Falkenberg and Karen Rickers (Hasylab, Hamburg), for analytical assistance and advices during my μXRF measurements.

I furthermore acknowledge financial support from the Swiss National Science Foundation.

A special thanks goes to my three Bachelors students - the "oolite team": Aline Kopf, Patrick Thomet, Robin Dufour, who allowed me to discover the way to supervise a research work. I really appreciate the time we spent together, and I wish you all the best for the years to come!

Thanks to all my friends, especially to the people who encouraged, helped and fed me during these last months. Thanks especially to Anne who helped me go through the last days of writing/correcting/printing.

I owe a lot to my parents, whose confidence never failed. Thanks for everything from my birth to the present day.

And, last but not least, these last months would have been a lot more difficult without François and his love.

I - Introduction
Cadmium enrichments in Jurassic carbonates: aims and problematic

The trace metal cadmium (Cd) is a highly toxic element, which is transferred into the environment by both natural and anthropogenic processes. Cd is extracted from the Earth crust as a by-product from the exploitation and extraction of phosphate, zinc, and lead, and is widely used for a series of industrial applications. Important natural sources are volcanic emissions and the biogeochemical weathering of cadmium-bearing rocks. In the last few decades, much effort has gone into the identification of anthropogenic sources of contamination, whereas natural sources of Cd in the environment have been less intensively considered. Here we suggest that natural sources may be more diverse than previously thought by showing that carbonates – a widespread lithology hitherto thought to be cadmium depleted relative to average terrestrial crust – may be a non-negligible source of cadmium for the environment. In particular, carbonate successions of Bajocian (middle Jurassic) and Oxfordian (upper Jurassic) age tend to present intriguingly high Cd contents. In this manuscript, we will discuss sections of Bajocian and Oxfordian age we have analyzed in western and southern Europe (Switzerland, France, Spain, and Italy), as well as the potential palaeo-environmental conditions/mechanisms that led to the presence of elevated Cd concentrations in Jurassic limestone.

I-1 Origin of the project

Selected soil profiles (e.g., Les Fourgs, Doubs, France; Le Gurnigel near La Vue des Alpes, NE, Switzerland; Dornach, BL, Switzerland; Benitez-Vasquez, 1999; Prudente, 1999; Baize and Sterckeman, 2001; Dubois et al., 2002; Prudente et al., 2002) in the Swiss and French Jura Mountains are characterized by elevated cadmium (Cd) contents (up to 22.3 µg/g; Prudente et al., 2002). These values largely exceed the official Swiss guideline value of 0.8 µg/g, which corresponds to an indicative limit for Cd concentrations in soils (Cd contents above the guideline value indicate that further investigations need to be performed).

J.-P. Dubois and his group (IATE-Pédologie, EPF Lausanne: Benitez-Vasquez, 1999; Prudente, 1999; Dubois et al., 2002; Prudente et al., 2002) as well as Baize and Sterckeman (2001) have demonstrated that this positive anomaly is related to the rock substratum, rather than to anthropogenic pollution, in contrast to earlier suspicions (Atteia et al., 1994, 1995). According to these authors, Cd is included in the carbonate lattice itself, thereby substituting calcium. They also showed that soils in the Jura which include aeolian-derived materials (Havlicek and Gobat, 1996; Havlicek et al., 1998) are less cadmium-enriched, probably because of a dilution effect.

The sedimentary rocks underlying soils concerned by anomalous cadmium contents consist of oolitic, oolitic/bioclastic, oncoidal or micritic limestone of Bajocian and Oxfordian age, and show cadmium enrichments of up to 8.15 µg/g (Benitez-Vasquez, 1999).

These Cd concentrations in Jurassic limestone are surprisingly high, especially since most carbonate rocks are known to be strongly depleted in Cd relative to the average crust and present a mean cadmium concentration around 0.03 - 0.065 µg/g (Kabata-Pendias and Pendias, 1992; Alloway, 1995; Tuchschmid, 1995; Table 1). Generally, sedimentary rocks that are considerably enriched in Cd are phosphorites (up to 1000 µg/g; e.g., Altschuler, 1980; Middleburg and Comans,1991; Jarvis et al., 1994; Nathan et al., 1997) and organic-rich deposits (up to 1500 µg/g; e.g., Heinrichs et al., 1980; Hatch and Leventhal, 1992).

Rock type	Median	Cd (ppb)
Granitic rocks	60	<30-360
Ultrabasic rocks	140	<30-520
Pelitic rocks	210	<30-3700
Sandstones	110	<30-7170
Carbonates	30	<30-2420
Bituminous rocks	450	210-11300

Table 1. Cadmium concentrations in main Swiss rock types (Tuchschmid, 1995)

I-2 Cadmium anomalies in Jurassic limestone: State of the art

In a pilot project conducted by Philippe Veuve (2000) at the University of Neuchâtel, it was shown that the cadmium enrichments in limestone from the Swiss Jura Mountains are contained within specific horizons and that their regional extend is considerable.

This author studied sections of Bajocian and Oxfordian/Kimmeridgian age in Auenstein (AG), Dornach (BL), Le Gurnigel (near La Vue des Alpes, NE), and Pont-de-la-Baleine (Gorges de l'Areuse, NE), and measured Cd values of up to 3.6 µg/g. Veuve (2000) also revealed that the cadmium anomalies mainly concern the cortices of the ooids (2.5 µg/g in a sample from Le Gurnigel), or entire ooids in the case they are micritized (2 µg/g in the same sample from Le Gurnigel; 1.25 µg/g in a sample from Dornach). The nucleus (1.25 µg/g in the same sample from Le Gurnigel) - and to a certain extend the micritic matrix (0.2 µg/g in the same sample from Dornach) - are less Cd-enriched, and the cements - contemporaneous to ooid deposition or related to late veins - show no Cd concentration (0.03 µg/g for both cases in a sample from Le Pont de la Baleine section, which is in contrast to the 0.3 µg/g measured in the cortex and 0.150 µg/g in the nucleus) or a slight enrichment (0.3 µg/g in the same sample from Le Gurnigel).

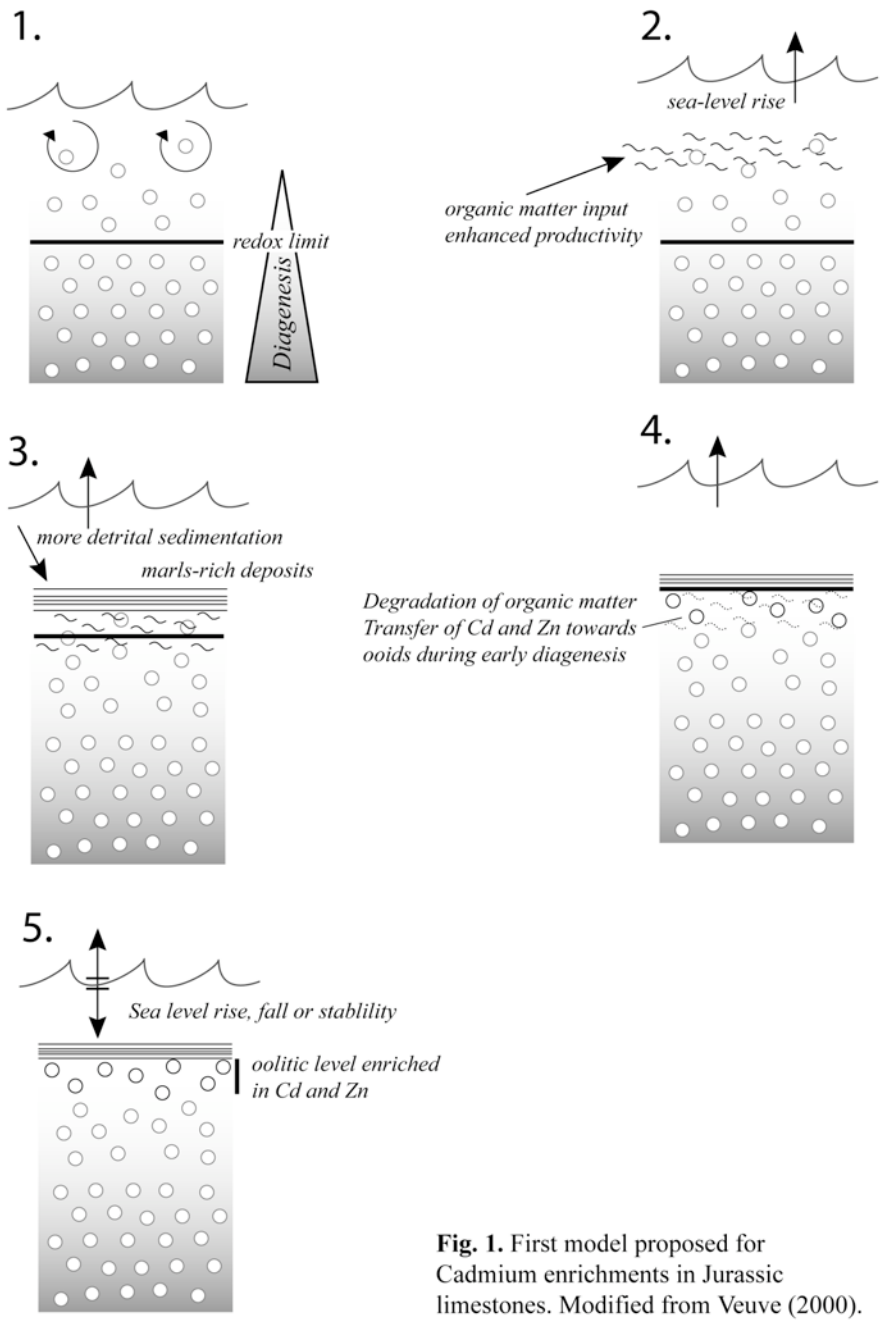

Fig. 1. First model proposed for Cadmium enrichments in Jurassic limestones. Modified from Veuve (2000).

Veuve (2000) also highlighted similar enrichments in zinc (Zn), even if this element seems to behave slightly differently in some cases: in the sample from Dornach mentioned earlier, concentrations of Zn have been shown to be of the same order in the micritized ooids and in the micritic matrix (1.25 µg/g).

In a preliminary model, Veuve (2000) assumed that oolite deposition occurred in a environment rich in organic matter and that Cd (and Zn) was transferred to the ooids upon early diagenetic oxidation of organic matter.
In this model ("secondary way"), the episodic deposition of marls and clays plays an important role in compartmentalizing the vertical distribution of organic matter, which becomes trapped in underlying oolitic levels. After decomposition of the organic matter, the cadmium and zinc became transferred into the cortices of the ooids (Fig. 1).

This model explains part of the anomalic levels that were observed, but does not give satisfactory explanations for enrichments that occur inside thick oolitic beds (e.g., Auenstein; Veuve, 2000) or inside platform barrier to lagoonal deposits (Dornach; Veuve, 2000). Veuve (2000) equally suggested another mode of enrichment, by direct incorporation of Cd and Zn inside the ooid grains during their formation, possibly enhanced by bacterial activity. Cd contents may subsequently be homogenized during micritization, if the ooids are transported and redeposited in quieter environments subjected to intense microbial activity ("primary way").

Questions that arose after this preliminary study are the following:

- what is the exact mechanism responsible for the transfer of cadmium into ooid grains?
- how can we verify the role of organic matter, since very little is preserved in the sediments investigated?
- can this phenomenon be observed on a wider scale, beyond the Jura Mountains?
- is a "secondary way" model a viable alternative to explain the Cd enrichments at Dornach (lagoonal carbonate facies)?
- concerning the "primary way" hypothesis: are bacteria able to sufficiently concentrate Cd and Zn to obtain enrichments similar to those observed? If yes, by which mechanism?
- Can we exclude the participation of micro-organisms in ooid formation? Which physical or chemical mechanism can lead to Cd enrichments in ooids without bacterial activity?
- what are the environmental conditions leading to enhanced cadmium concentrations in the Bajocian and Oxfordian periods?

I-3 Aims of the present study

Keeping these questions in mind, we have articulated this study around the following points:

1 - Carbonates, both modern (e.g., ooids from the Bahamas: 0.016 µg/g; Veuve, 2000) and ancient, are usually highly depleted in cadmium. What are therefore the causes and mechanisms of Cd enrichments in Jurassic oolites?

2 - Are Cd enrichments specifically related to oolites of Bajocian and Oxfordian age, and specifically to the Swiss and French Jura Mountains, or is this a more widespread phenomenon? In summary, what is the distribution of Cd-enriched carbonates in a stratigraphical and regional context?

3 - Are only oolitic facies enriched, or can other types of limestone equally present high Cd concentrations?

4 - Can predictions be made with regard to the eventual presence of cadmium-enriched soils based on a better knowledge of the stratigraphical and regional distribution of carbonate rocks?

Questions 2 and 3 were first investigated, resulting in a better knowledge concerning the geographical and stratigraphical distribution of Cd in western and southern Europe. The results are presented in Chapter V for the main sections investigated, as well as in Chapter IX for additional carbonate successions.

A complementary research on Cd enrichments in Oxfordian limestone from Burgundy and associated soils provided complementary information to point 4 (relationship between Cd-enriched rocks and associated soils). The results are presented in Chapter VI.

Finally, a hypothesis with regards to the causes and mechanisms of Cd enrichments in Jurassic limestone (point 1), is presented and discussed in Chapters VII and VIII.

In parallel, possible links of Cd enrichments with other geochemical tracers were investigated in Chapters V ($\partial^{13}C$), VII / VIII (other chemical elements) and IX (organic matter and total phosphorus contents).

Additional information concerning the general behaviour of Cd in modern and ancient environments, as well as related to the specificities of the Jurassic period, are given in Chapter II and III, respectively. Geographical and geological settings of the investigated sections are presented in Chapter IV.

References

Alloway, B.J., 1995. Cadmium. In: Heavy metals in soils. 2nd edition. Blackie Academic and Professional, 122-147

Altschuler, Z.S., 1980. Geochemistry of trace elements in marine phosphorites. Soc. Econ. Paleontologists Mineralogist Spc. Pub, 29, 19-30

Atteia, O., Dubois, J.P., and Webster, R., 1994. Geostatistical analysis of soil contamination in the Swiss Jura. Environmental Pollution, 86, 315-327.

Atteia, O., Thélin, P., Pfeifer, H.-R., Dubois, J.-P., and Hunziker, J., 1995. A search for the origin of cadmium in the soil of the Swiss Jura. Geoderma, 68, 149-172.

Baize, D., and Sterckeman, T., 2001. Of the necessity of knowledge of the natural pedogeochemical background content in the evaluation of the contamination of soils by trace elements: The Science of the Total Environment, 264, 127-139

Benitez-Vasquez, N., 1999. Cadmium speciation and phyto-availability in soils of the Swiss Jura: hypothesis about its dynamics. Unpublished Ph.D. Thesis, EPF, Lausanne, 132 p.

Dubois, J.P., Benitez, N., Liebig, T., Baudraz, M., and Okopnik, F., 2002. Origine et variabilité spatiale du cadmium dans les sols du Haut Jura suisse. In Baize, D. (ed.), Les éléments traces métalliques dans les sols. Approches fonctionelles et spatiales. INRA Editions, Paris, p. 33-52.

Hatch, J.R., and Leventhal, J.S., 1992. Relationship between inferred redox potential of the depositional environment and geochemistry of the Upper Pennsylvanian Stark Shale Member of the Dennis Limestone, Kansas. Chemical Geology, 99, 65-72.

Havlicek, E., and Gobat, J.-M., 1996. Les apports éoliens dans les sols du Jura. Etat des connaissances et nouvelles données en pâturages boisés. Etude et Gestion des Sols 3, 167-178.

Havlicek, E., Gobat, J.-M., and Gillet, F., 1998. Réflexions sur les relations sol - végétation: trois exemples du Jura sur matériel allochtone. Ecologie 29, 535-546.

Heinrichs, H., Schulz-Dobrich, B., and Wedepohl, K.H., 1980. Terrestrial geochemistry of Cd, Bi, Tl, Pb, Zn and Rb. Geochimica et Cosmochimica Acta, 44, 1519-1533.

Jarvis, I., Burnett, W.C., Nathan, Y., Almbaydin, F., Attia, K.M., Castro, L.N., Flicoteaux, R., Hilmy, M.E., Husain, V., Qutawna, A.A., Serjani, A. and Zanin, Y.N., 1994. Phosphorite geochemistry: state-of-the-art and environmental concerns. In Föllmi, K.B. (ed.), Concepts and controversies in phosphogenesis. Eclogae geologicae Helvetiae, 87: 643-700.

Kabata-Pendias, A. and Pendias, H., 1992. Trace elements in soils and plants. 2nd edition. CRC Press, 365 pp.

Middleburg, J.J. and Comans, R.N.J.J., 1991. Sorption of cadmium on hydroxyapatite, Chemical geology, 90, 45-53

Nathan, Y., Soudry, D., Levy, Y., Shitrit, D., and Dorfman, E., 1997. Geochemistry of cadmium in the Negev phosphorites. Chemical geology, 142, 45-53

Prudente D (1999). Distribution des teneurs naturelles en cadmium dans les sols de la forêt communale des Fourgs (Doubs - France). DES Sciences naturelles de l'environnement. Universités de Genève et de Lausanne. 68 p. + annexes.

Prundente, D., Baize, D., and Dubois, J.P., 2002. Cadmium naturel dans une forêt du Haut-Jura français. In Baize, D. (ed.), Les éléments traces métalliques dans les sols. Approches fonctionelles et spatiales. INRA Editions, Paris, p. 53-70.

Tuchschmid, M., 1995. Quantifizierung und Regionalisierung von Schwermetallen in bodenbildenden Gesteinen der Schweiz. Umwelt-Materialien 32, BUWAL, Berne.

Veuve, P., 2000. Etude géochimique et sédimentaire d'un enrichissement en cadmium observé dans les calcaires oolitiques jurassiques du Jura. Unpublished diploma thesis, Univ. NE, 56 p.

II - “All about” Cadmium - The Cadmium cycle(s)

II-1 Introduction

Cadmium (Cd) is the 48^{e} element of the periodic table and it is classified as a transition metal (e.g., Bentor, 2005). It is also included in the trace elements group III (trace elements whose average concentration in the Earth crust is under 1 µg/g - average concentration for Cd is 0.2 µg/g; Goni and Leleu, 1980; Bourrelier and Berthelin, 1998). The name is derived from the Latin cadmia and the Greek kadmeia (ancient name for calamine, which is a zinc ore-body extracted in the vicinity of the Thebes city, created by Kadmos).

The presence of cadmium and other trace elements in the environment is a function of various inputs from two major categories of sources: natural and anthropogenic sources (e.g., O'Neill, 1993; International Cadmium Association, 2005; Fig. 1; Fig. 2).

The three major compartments of the environment - air, water and soil - are all concerned, with the possibility of considerable Cd transfer between them after initial deposition. Cd amounts released in the atmosphere are considered more mobile than those to water, the less mobile of all being those to soils (International Cadmium Association, 2005).

The natural presence of Cd in the environment is mostly due to gradual phenomena, such as rock weathering or quiescent volcanoes degassing, and more punctual occurrences, such as volcanic eruptions. Cadmium is also transferred to the environment in large amounts by human activity, since its chemical proprieties are of great use for industrial applications ever since its discovery in Germany in 1817 (e.g., International Cadmium Association, 2005). The industrial use of cadmium has resulted in high transfer rates of this element towards all environmental compartments. These emissions reached a peak during the 1960's but have since then been significantly and continuously decreasing (International Cadmium Association, 2005). Anthropogenic emissions of cadmium to the environment arise from either point sources (e.g., large manufacturing or production facilities for emissions related to human activity) or more diffuse sources (e.g., from the use of Cd-bearing products by many consumers over large areas). Total emission rates with regards to Cd have been estimated to approximately 8000 to 10000 ton/year (t/y) compared to 800 to 1000 t/y for natural Cd emissions (Niragu 1980, Niragu 1989, WHO 1992). However, as anthropogenic cadmium emissions have decreased by approximately 90% or more in the past thirty to forty years, they may be nearly equal to natural cadmium emissions today (International Cadmium Association, 2005).

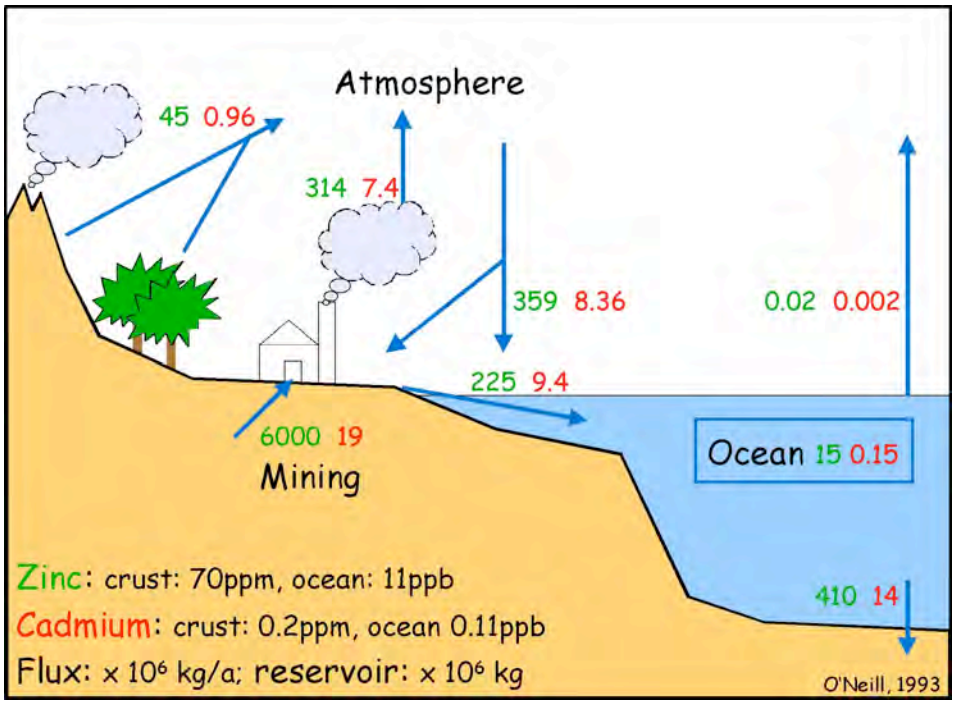

Fig. 1. Global fluxes and reservoirs for the elements Cd and Zn in the present environment. O'Neill, 1993

Cadmium is recognized to have toxic effects on humans, as well as to perturb natural systems, such as soils (e.g., Bourrelier and Berthelin, 1998) or estuaries (e.g., Gonzalez et al., 1999). Long-term exposure can cause health damages to humans, and more specifically to kidneys, lungs and bones (e.g., International Cadmium Association, 2005). The study of its behaviour in the different ecosystems, and of the modalities of its transfer to the various environmental compartments, is therefore important.

II-2 Cadmium, Industry and Environment - Human-related emissions of Cd

Cadmium is a by-product of the non-ferrous metal industry, which has many important industrial applications. Thanks to its unique chemical and physical proprieties - great resistance to corrosion, low melting-point and excellent electrical conduction, excellent resistance of cadmium compounds to chemicals and to high temperatures, production of intense colourings (Cd pigments) in the shades of yellow to red - cadmium is intensively used in special alloys, pigments, coatings stabilisers and, for the greatest part (almost 70% of its use), in rechargeable nickel-cadmium batteries.

Fig. 2. Next page. Global fluxes and reservoirs for Cd in the present environment. Compilation of literature data, modified from Bézier, 2005.

1 Gonzalez et al., 1999
2 Chester, 1990
3 International Cadmium Association, 2005
4 Bourrelier and Berthelin, 1998
5 Cossa and Lassus, 1989
6 Cossa and Lassus, 1989; Miroumana et al., 1989 (Cited by Gonzalez et al., 1999)
7 Nriagu, 1980; Cossa and Lassus, 1989
8 Elbaz-Poulichet, 1988
9 Rubin, 1997

Fig. 2. Cadmium cycle in the present environment

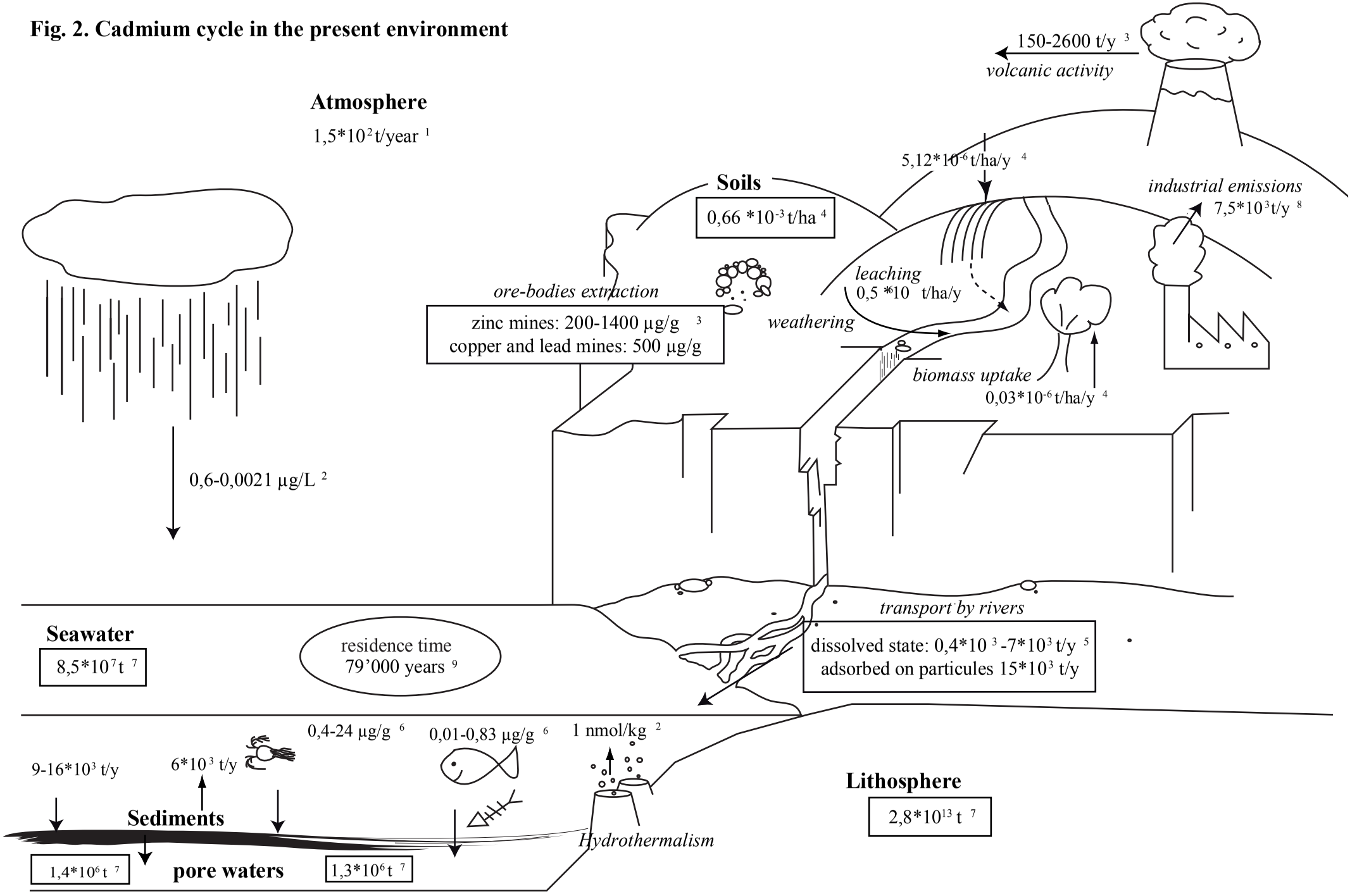

Resulting industrial emissions of cadmium have steadily declined over the past thirty to forty years (e.g., International Cadmium Association, 2005, and references therein). Cd emissions are now tightly controlled as a result of the significant improvement in pollution control technology and to strict regulation and legislation, particularly in the metal industry. Additionally, recycling of Cd-bearing products is in constant improvement, and its transfer towards the environment is therefore supposed to further decrease in the near future.

Cadmium is also present as an impurity in other classes of products: non-ferrous metals (zinc, lead and copper), iron and steel, fossil fuels (coal, oil, gas, peat and wood), cement, and phosphate fertilisers (Cook and Morrow 1995; International Cadmium Association, 2005). Phosphate fertilizers contain from 10 to 200 µg/g Cd (Cook and Morrow 1995).

Cadmium emissions from products in which cadmium is present as an impurity have not been reduced as significantly as those from industral Cd products in the last decades, and remain a source of contamination for which additional reductions might be achieved in the future.

II-3 Natural sources of Cd

Natural levels of cadmium in the environment depend on the specific compartment of consideration. Natural cadmium levels in the environment reach the following values (International Cadmium Association, 2005):

Atmosphere: 0.1 to 5 ng/m³
Earth's crust: 0.1 to 0.5 µg/g
Marine sediment: ~1 µg/g
Sea water: ~0.1 µg/L

Nriagu (1980), as well as Cossa and Lassus (1989) estimate that the Earth crust is the most important reservoir with regards to Cd ($2.8*10^{13}$ t), followed by oceanic waters ($8.5*10^{7}$ t), marine sediments ($1.4*10^{6}$ t) and pore waters ($1.3*10^{6}$ t), which represent the other main geochemical reservoirs of Cd (Fig. 2). The atmosphere is not considered to be of quantitative importance.

Natural cadmium emissions to the environment are mostly dependent of the weathering of Cd-bearing rocks and volcanic activity. An additional source to atmosphere by forest fires has also been reported (1 to 70 t/y; Nriagu, 1980).

II-3-1 Cd contents in various types of rocks

The mean concentration of cadmium in the Earth's crust is between 0.1 and 0.5 µg/g. Igneous and metamorphic rocks are generally displaying lower concentrations, from 0.02 to 0.2 µg/g (International Cadmium Association, 2005). Higher Cd levels have been measured in specific types of sedimentary rocks.

Phosphorites

Cd contents as high as 500 µg/g have been reported for marine phosphates and phosphorites (WHO 1992; Cook and Morrow, 1995). Phosphorites constitute therefore excellent traps for Cd.

Altschuler (1980), and Middleburg and Comans (1991) have postulated that Cd enrichments in phosphorites are the result of the substitution between Cd^{2+} and Ca^{2+}, which have very similar ionic radii (0.94 Å and 0.99 Å, respectively).
Nevertheless, Nathan et al. (1997) have demonstrated that no direct correlation exists between Cd and phosphate concentrations in the Negev phosphorites (Israel) and that increased Cd concentrations in these deposits are more likely related to high organic matter contents.

Organic-rich deposits

Generally, organic-rich deposits exhibit high cadmium concentrations. Heinrichs et al. (1980) clearly demonstrated the relationship between Cd and organic matter in sediments. A positive correlation has been also established by Nathan et al. (1997) between Cd and organic matter contents in the Negev phosphorites, with Cd concentrations up to more than 100 µg/g for the samples showing the highest organic matter contents - up to 15% - and 0 to 50 µg/g for the less enriched samples with regards to organic matter.
Additionally, Cd contents in fossil fuels are reported to be between 0.5 to 1.5 µg/g (Cook and Morrow, 1995) or 0.4 and 3.3 µg/g (BUWAL, 1997).

Ore-bodies

Zinc, lead and copper ores - mainly composed of sulfides and oxides - contain generally high Cd levels (200 to 1400 µg/g for zinc ores and around 500 µg/g for typical lead and copper ores; International Cadmium Association, 2005; Fig. 2).

Carbonates

Cd may be incorporated in the calcareous shells of marine organisms and therefore be included in carbonate rocks. However, Cd levels in the shells of calcareous foraminifers do not surpass 0.01 µg/g (Boyle, 1988; Rickaby and Elderfield, 1999; Lynch-Stieglitz and Fairbanks, 1994). The mean values given for the different types of carbonates rocks usually vary between 0.030 and 0.065 µg/g (Kabata-Pendias and Pendias, 1992; Alloway, 1995, Tuchschmid, 1995).
Some recent studies (Benitez-Vasquez, 1999; Veuve, 2000; Baize and Sterckeman, 2001; Dubois et al., 2002; Prudente et al., 2002) have shown that limestone of Bajocian and Oxfordian age, in particular in the Jura Mountains (France/Switzerland) are generally characterized by high cadmium contents (frequently above 1µg/g). Exactly these calcareous rocks are the subject of the present work.

II-3-2 Rock weathering and subsequent Cd transfer to the environment

Weathering of Cd-bearing parent rocks results in the transport of large quantities of cadmium to the world's oceans by rivers. This total amount has been recently estimated at 15,000 t/y (WHO, 1992; OECD, 1994).

Additionally, recent studies conducted in the French and Swiss Jura area (e.g, Benitez-Vasquez, 1999; Prudente, 1999; Baize and Sterckeman, 2001; Dubois et al., 2002; Prudente et al., 2002) have pointed out a relationship between anomalously high cadmium contents in soils and the weathering of associated bedrocks, which consist of the limestone of Oxfordian and Bajocian age mentioned above, which present unexpectedly high cadmium concentrations.

II-3-3 Volcanic emissions and hydrothermalism

Volcanic activity is considered to be a major natural source of cadmium release to the atmosphere. Estimations of yearly inputs are generally placed between 150 and 2600 t/y; a value of 820 t/y has been estimated by several authors (Nriagu, 1980; Nriagu, 1989; WHO, 1992; OECD, 1994).

Volcanic aerian systems

Cd has been demonstrated to be highly enriched in vapours emitted by various kind of aerian volcanoes, as well as in deposits related to their eruptions. Vapor associated with intermediate-to-silicic aerian systems has been shown to contain high contents of elements like As, Sb, Hg, Bi, Cd, Cu, In, Ag, Au, Re, Mo, Sn, W, and Pb (Stimac et al., 1996, and references therein). The high temperature fumaroles of the andesitic-dacitic Augustine volcano (Alaska) are enriched in B, K, Na, Fe, As, Pb, Sb, Cd, Mn, Li, and Ni (Symonds et al., 1992). Elements measured in the emissions from different volcanoes worldwide and in those registered in ice strata almost always include Cd, along with Pb, Cu and Zn; the more occasional presence of As, Sb, in, Bi, Ag, Tl, Se, Sn, and Te is equally reported (Hinkley et al., 1999). Measurements of basalt degassing of Stromboli volcano (Allard et al., 2000) have shown high enrichment factors concerning Cd (by a factor of 10^2), as well as Bi, Au, Pb, an Zn. Gases from Merapi volcano (andesitic stratovolcano, Indonesia; Symonds et al., 1987) are strongly enriched in Cd (by a factor $>10^5$) relative to magma. Fluxes of Cd strongly varies from one volcano to another: 180 g/d for the Merapi fumaroles, $2.8*10^4$ g/d for the Mt Etna (Italy; Buat-Menard and Arnold, 1978), 5'000 g/d for Mt St Helens (USA; Phelan et al., 1982), and about $1.5*10^4$ g/d for the Stromboli (Italy; Allard et al., 2000), and even from one eruption to another.

However, it must be noted that some elements have been shown to preferentially concentrate in deposits immediately surrounding the volcanic vents (Symonds et al., 1987). These elements comprise Bi, Cd, Pb, W, Mo, Zn, Cu, K, Na, V, Fe and Mn.

Degassing from submarine oceanic plateaus

Volcanic eruptions related to oceanic plateaus may be sufficiently large to reach enough heat and energy and thereby influence surface circulation. Trace metals are in this case provided by gas-rich magmatic fluids, abundant in volatile elements, and fractionate and precipitate out depending on their residence time in seawater (Fig. 3). Pb, Cu and Zn are considered as "near-field" elements, as they precipitate out close to the source (Snow et al., 2005). "Far-field" elements comprise Au, Bi and Cd. These metals may additionally enter into various chemical cycles, mainly bio-mediated, before they are removed from the surface and incorporated in the sediment.

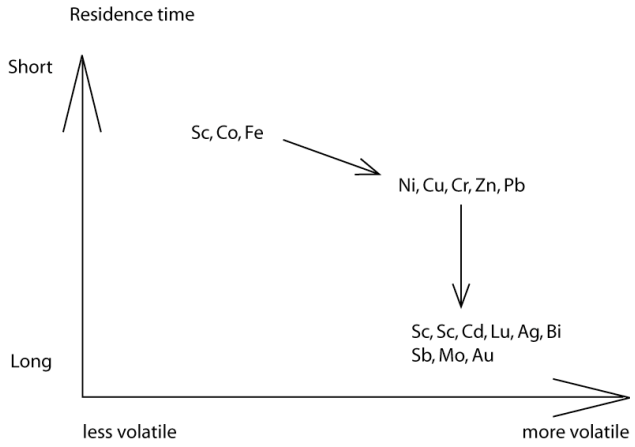

Fig. 3. Distribution of various elements in deposits related to oceanic plateau eruption, related to their reactivity in sea-water (residence time). Modified from Snow et al., 2005.

Hydrothermal activity

Hydrothermal activity may also represent a source of Cd for both continental and oceanic realms, through the circulation of hydrothermal fluids along major faults (e.g., mineralizations of sedimentary rocks in contact with ancient crystalline massifs: Morvan, France; Caillère et al., 1968) or direct input into oceanic waters by the hydrothermal release of Cd along oceanic ridges. However, oceanic hydrothermal activity is generally not considered to be a major source of Cd for oceanic waters, as this element is not particularly enriched in hydrothermal effluents, in comparison with volcanic submarine degassing ("event plumes"; Rubin, 1997; Snow et al., 2005). Hydrothermal effluents are particularly enriched in Al, Zn, Fe, Mn, Au and Ir, relative to Mo, W, Re, Hg, Bi, Se, Cd and As, which are present in greater concentrations in volcanic submarine effluents.

II-4 Cadmium partitioning in the environment:

II-4-1 Cadmium in soils

Cadmium in soils is both of natural and anthropogenic origin. Natural sources comprise underlying bedrock, as well as transported parent material such as alluvium or glacial till. Anthropogenic sources include aerial deposition, sewage sludge application, and the use of fertilizers (in particular for agricultural soils; Jensen and Bro-Rasmussen, 1992, Van Assche and Ciarletta, 1992). The vast majority of cadmium emissions of anthropogenic origin (80 to 90%) pass initially to the soil environment (International Cadmium Association, 2005, and references therein).

The net flux into the soil is regarded as positive since the transfer of Cd occurs both from the atmosphere and water into this compartment, and since this transfer is not counterbalanced by equal outputs, which usually arise from soil leaching and biomass uptake. These output fluxes are generally low, except for those linked to erosion, which contributes to the contamination of rivers and coastal areas. Soils are therefore considered as a sink for cadmium. An example is given here for Swiss soils in 1990 (data from BUWAL, 1997; Fig. 4), for which global inputs of Cd largely exceeded the outputs.

Cd speciation, adsorption, and distribution in soils are mainly governed by pH, soluble organic matter content, hydrous metal oxide content, clay content and type, presence of organic and inorganic binders, and competition from other metal ions (OEDC, 1994). In soils, cadmium is supposed to be largely bound to the non-exchangeable fraction, e.g., on clays, manganese, and iron oxides, and its mobility and subsequent transfer into the chain food may be considered as limited (International Cadmium Association, 2005). However, approximately 2000 t of Cd has been estimated to be stored in the upper soil layers in Switzerland, and part of this considerable stock is subjected to rapid mobilization if the pH drops (BUWAL, 1997).

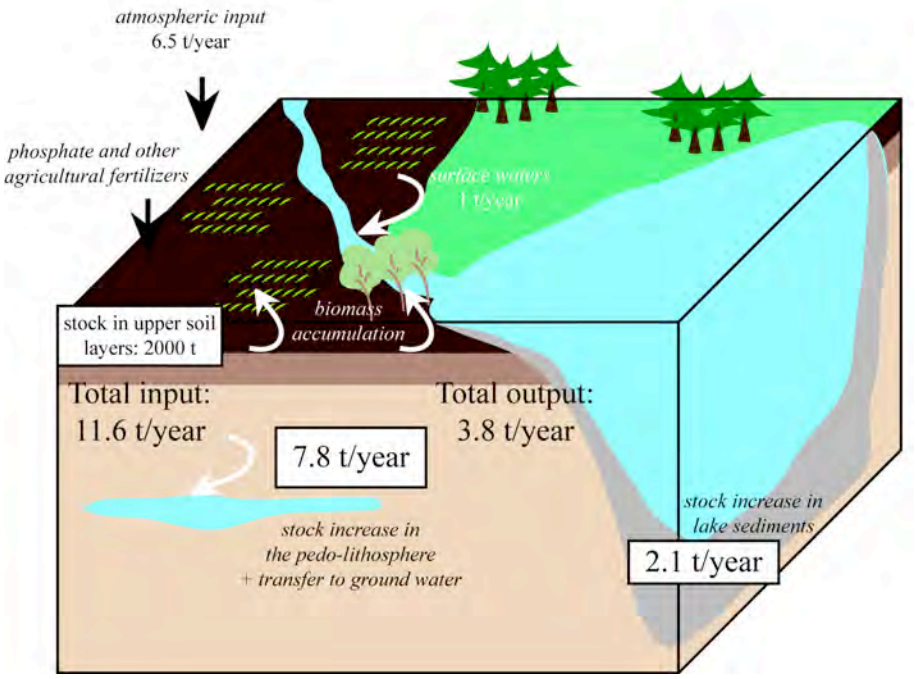

Fig. 4. Global Cd fluxes and reservoirs estimated for the Swiss "environmental partial system" in 1997. Inputs are represented by black arrows, whereas outputs are symbolized by white arrows. Data from BUWAL, 1997.

II-4-2 Cadmium in oceanic waters

Cadmium behaviour in ocean waters is of particular interest for this study since the here considered Jurassic carbonate rocks that presently outcrops in larger areas in Europe were deposited in the former Tethyan ocean realm, in shallow-water to basin environments.

In actual environments, Cd is transferred into rivers and costal areas through the weathering of soils and rocks, atmospheric deposition, leakage from landfills and contaminated sites, and the use of sludge and fertilizers in agriculture. Rivers have been shown to transport Cd for considerable distances from the source (up to 50 km; WHO, 1992). The residence time of Cd in oceanic waters has been estimated as 79’000 years (Rubin, 1997).

Cd concentrations in ocean waters have variously been reported to correspond to approximately 0.11 ng/L (O'Neill, 1993), <5 ng/L (WHO, 1992), 5-20 ng/L (OECD, 1994; Jensen and Bro-Rasmussen, 1992), 110 ng/L (CRC, 1996), 100 ng/L (Cook and Morrow, 1995), and 10 to 100 ng/L (Elinder, 1985). Cd concentrations, particularly in surface waters, of the different oceans vary as a function of different factors including anthropogenic inputs and primary biological production.

Higher levels have been observed in certain coastal areas (Elinder, 1985). In deeper waters cadmium concentrations may considerably increase, mainly because of the decomposition of organic matter (e.g., Boyle, 1988; WHO, 1992; OECD, 1994).

In natural waters, Cd is found in different physical forms, i.e., in the form of a dissolved phase, in colloids, or adsorbed onto particles.

Most of the cadmium entering the water systems is rapidly adsorbed by particulate matter, and consequently trapped in the sediment (WHO, 1992). Cd partitioning between the adsorbed and dissolved states is therefore an important factor controlling the bioavailability of Cd (Gonzalez et al., 1999; International Cadmium Association, 2005).

Dominant forms of Cd, and Cd associations, in oceanic waters and sediments

The different physical and chemical parameters (pH, salinity, redox potential, nature and abundance of particles, presence of chemical binders - e.g., OH^-, HCO_3^-, Cl^-, SO_4^{2-} in oxic environments, HS^-, polysulfides in anoxic environments, humic substances, organic compounds or metabolites…) of the environment control the dominant forms of Cd (e.g., Ramamoorthy and Kushner, 1975; Stevenson, 1976; Fisher and Fabris, 1982; Gonzalez et al., 1999). In ocean waters, Cd appears mainly in dissolved form, associated with chlorides in very stable complexes (Gonzales et al., 1999). As a consequence, the levels of dissolved Cd vary as a function of salinity. $CdCl_2$ is the major form of chloro-complexes in marine waters, whereas $CdCl^+$ dominates for lower salinities (Long and Angino, 1977).

Gobeil et al. (1987) have postulated that solid particles represent the vector that delivers Cd to the sediment-water interface. In the oxic zone, processes of adsorption - desorption mostly control the repartition between dissolved Cd and Cd associated to particles (Gonzalez et al., 1999). Association with particulate matter includes:

- an integration in the crystalline lattice of different detrital minerals
- a link with organic fractions (carbonates, remains of organisms, fecal pellets)
- a precipitation or co-precipitation with various mineral fractions (carbonates, phosphates, iron or manganese oxides and hydroxides, sulfides)
- an adsoption onto different phases (clay minerals, organic matter, iron or manganese oxides and hydroxides…)

In zones depleted in oxygen (e.g., in muddy deposits associated to estuaries, or inside the sediment column), reactions of dissolution - precipitation, linked with local redox conditions, become predominant, and the presence of dissolved sulfides lead to the precipitation of sulfide minerals, with which a significant part of Cd is purported to co-precipitate (e.g., in FeS_2; Gonzales et al., 1999).

Processes related to life are also of great importance: Cd is bio-concentrated by phytoplanctonic species; reactions of oxidation-reduction that predominate in suboxic environments are often controlled by biological processes; and degradation of organic matter by bacterial activity leads to the solubilization of the Cd associated to organic matter (Gonzales et al., 1999).

In the sediment pore water of coastal areas, dissolved Cd concentrations are highly variable. For example, in the St-Laurent, concentrations range from 582 ng/L in well-oxygenized levels, to lower than 5.6 ng/L in reduced horizons (Gobeil et al., 1987).

The principal forms of Cd in marine waters are compiled in Fig. 5.

Relationship with phosphorus and "nutrient-like" elements

Bio-limiting trace-elements include Fe, Ni, Co, Zn, Cu, V and Mo (Gonzales et al., 1999; Algeo, 2004; Böning et al., 2004 and references therein). Cd, and, to a lesser extend, As, are equally considered to follow a "nutrient-like" behaviour in seawater (e.g., Boyle et al., 1976; Böning et al., 2004). Indeed, in oceanic surface waters, the distributions of Cd and phosphorus – one of the bio-limiting nutrients - are closely related. As a consequence, Cd contents in the shells of calcareous foraminifers have been used to quantify the nutrient levels in the parent waters (Boyle et al., 1976; Bruland et al., 1978; Boyle, 1988; Elderfield and Rickaby, 2000), rather than phosphorus concentrations, which have been shown to be less conservative in the sediment.

Relationship with increasing organic matter contents and suboxic conditions

Previous studies highlighted a positive correlation between Cd and organic matter contents and/or reducing conditions in sedimentary rocks (e.g., Heinrichs et al., 1980; Rosenthal et al., 1995; van Geen et al., 1995; Il'in and Kiperman, 2001).

In oxygen-depleted environments, Cd precipitates in the form of a sulfide phase (CdS).

In highly anoxic zones (restricted basins, pore waters), Cd concentrations have been measured that surpass those corresponding to the solubility product of Cd with sulfides (Boulègue, 1977; Boulègue et al., 1979; Kremling, 1983; Gaillard et al., 1986). This may be explained by the formation of stable complexes with organic compounds or with different species of sulfides (polysulfides, thiosulfates, sulfites, colloidal sulphur).

Van Geen et al. (1995) confirmed that Cd accumulation is favoured by an oxygen deficit in freshly deposed sediments. These authors observed a anti-correlation between cadmium contents and oxygenation levels inside the sediment, and postulated that Cd was derived from the degradation of organic matter under suboxic conditions.

Fig. 5. Next page. Principal Cd forms and associations in coastal seawater. Compilation of literature data, principally from Gonzalez et al., 1999.

Fig. 5. Principal chemical forms of cadmium in sea water

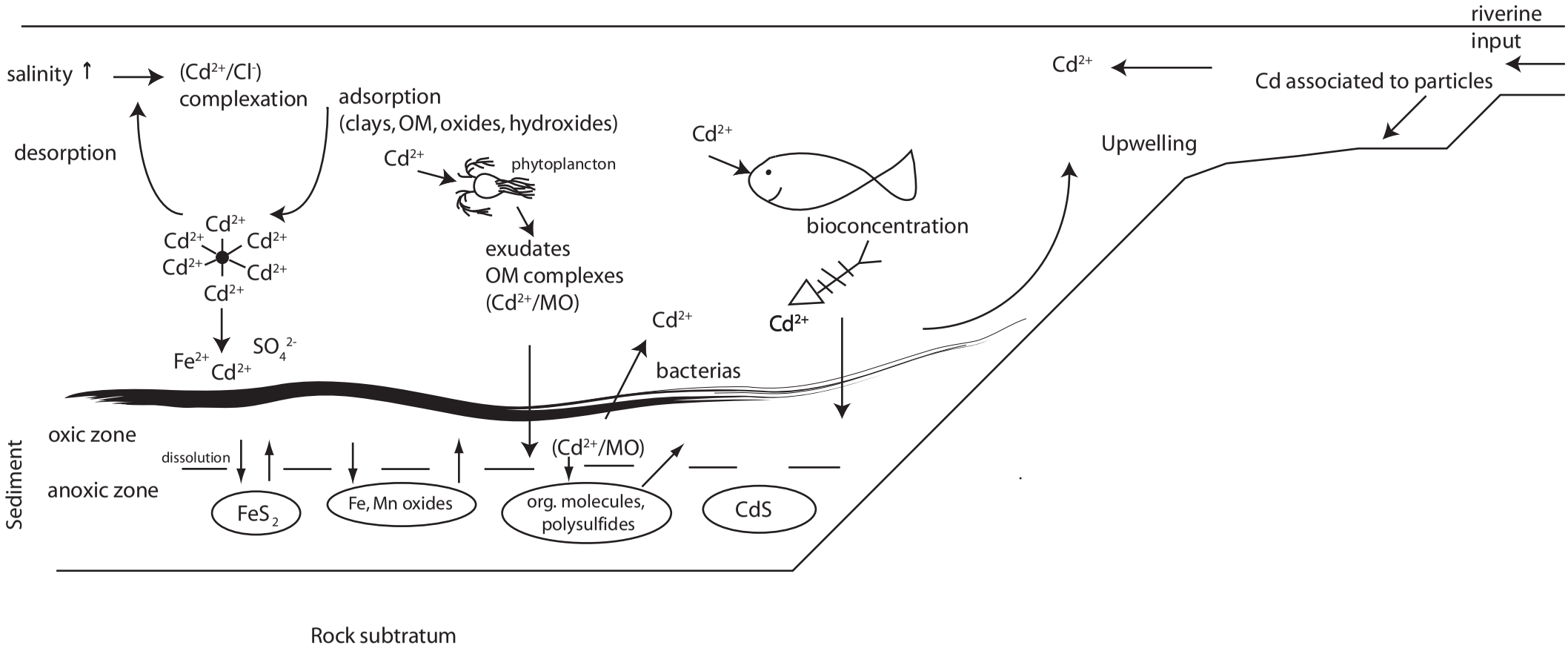

Other elements that may be influenced by suboxic or anoxic conditions are Mo, Pb, U, V, Zn (via uptake by organic matter or authigenic minerals; Algeo, 2004 and references therein), Cr, Ni, Cu (which, along with V and Zn seem to covariate with organic carbon contents; Algeo, 2004), Re (which requires suboxic conditions for its removal from solutions, whereas Mo is accumulating under anoxic (sulfidic) conditions; Böning et al., 2004 and references therein), and Bi (which has been shown to concentrate in correlation with increasing total sulphur contents, rather than with organic matter contents, in black shale also containing high Cd and Tl levels; Heinrichs et al., 1980).

Relationship with microbial activity

Bacterial activity is known to play a major role in the degradation of organic matter and the subsequent release of the Cd initially adsorbed onto organic matter particles (Gonzales et al., 1999). In areas subjected to intense micritization (e.g., lagoonal environments), microbial activity may have a preponderant influence on Cd distribution, as some bacteria have been shown to concentrate several trace elements, including Cd, with great efficiency (e.g., Loaëc et al., 1997; Boyanov et al., 2003 and references therein; Kemner et al., 2005 and references therein).

II-5 Cadmium and human health

Virtually all chemicals are dangerous for human life at sufficiently high concentrations. Certain elements are essential to human life - like copper and zinc, and a deficiency as well as an excess in these elements can lead to adverse health effects. Cd is not considered as necessary for human life.

Since the 1950's, the consciousness of the scientific community with regards to the toxicity of cadmium, and to the consequences of its accumulation in mankind, has grown, and the potential risks related to human exposure have been extensively studied.

As tobacco leaves naturally accumulate high levels of Cd, smoking of tobacco is an important source of exposure for smokers (estimated to 50% of the total uptake; Van Assche, 1998). For non-smokers, Cd is principally taken in by ingestion (about 95%; Van Assche, 1998), due to the presence of trace levels of cadmium in food. This Cd is of natural origin or is related to the use of phosphate fertilisers and sludge on agricultural soils. Phosphate fertilizers have been shown to be the most important Cd source to human exposure (41.3%; Van Assche, 1998).

Cd contents vary widely in the different types of food, depending on the levels of Cd available in the environment, as well as on specific uptakes and accumulations. Lettuce, spinach, potatoes and grain foods contain rather high Cd concentrations, from 30 to 150 ng/g. Peanuts, soybeans and sunflower seeds equally show high natural Cd contents. Meat and fish generally exhibit lower Cd values, from 5 to 40 ng/g. Animal kidneys and livers can present important Cd levels, up to 1000 ng/g, as Cd is principally concentrated in these organs (International Cadmium Association, 2005).

For the general population, the current daily Cd intake remains very low, at the lower end of the total range of 10-25 µg/day. The tolerable daily cadmium intake has been established for adult women and men, at 60 and 70 µg, respectively (WHO, 1992).

Cd principally accumulates in the kidneys, for a relatively long residence time – from 20 to 30 years. At high exposures, Cd levels can reach a critical threshold and can lead to serious kidney failure, as well as to adverse heath effects on the respiratory system and bone disease. An example is given by rice crops in Japan in the 1950's and 1960's, where concentrations from 200 to 2000 ng/g where measured (Elinder, 1985). These high Cd concentrations, along with nutritional deficiencies for iron, zinc and other minerals led to both renal impairment and bone disease (Itaï Itaï disease). However, these levels of Cd contamination remain exceptional, and recent studies by Roels et al. (1997) have shown that, at least at low exposures, these effects are reversible, once the exposure to cadmium has been reduced.

A carcinogenic risk of Cd by inhalation has been equally suspected, but is increasingly contested by newer studies (Sorahan et al., 1995; Sorahan and Lancashire, 1997).

II-6 Conclusive points and discussion: The cadmium cycle(s) and anomalous cadmium contents in Jurassic rocks

As Cd is an element that may endanger life, its concentration in the environment needs to be closely monitored. Direct emissions of Cd to the atmosphere due to anthropogenic activities are in a steady decrease since the 1960's, and are now strictly controlled. Natural inputs of Cd, by the way of weathering of Cd-bearing parent rocks remain a source of increasing Cd values in soils, along with sewage sludge application, and the use of phosphate fertilizers. In this optic, the identification and geographical delimitation of soil areas contaminated with regards to Cd contents, and associated with the weathering of limestone that contain anomalously high Cd levels, is of considerable environmental importance.

Concerning the processes of Cd concentration in carbonate sediments related to past marine environments, they are likely linked to one or a combination of the following sources or mechanisms:

- increasing organic matter contents in the environment, as Cd is known both to follow a "nutrient-like" behaviour in oceanic waters and to accumulate in sediments in positive correlation with organic matter
- preferential concentration under specific chemical conditions inside the sediment, including oxygen depletion and sulfide precipitation
- preferential uptake and concentration via bacterial activity
- increasing inputs of Cd into the environment, by the way of increasing continental weathering, or provided by volcanic inputs, from either aerial systems or submarine volcanoes.

Enhanced hydrothermal activity is not supposed to be of major importance relative to Cd concentrations in ocean waters, as hydrothermal fluids are not particularly Cd-enriched (Rubin, 1997; Snow et al., 2005).

With regards to continental volcanic systems, Cd is known to mostly precipitate close to the volcanic vents. In the case of aerian Cd inputs, we therefore admit that this element has only a chance to be transferred into remote areas, if one or more of the following conditions is fulfilled:

1. strong and violent explosive events leading to the transfer of Cd by volcanic exhalations into the stratosphere and their subsequent redistribution worldwide.
2. volcanic deposits in nearby seawater and concomitant changes in the transport phase (e.g., emission of Cd as an elemental gas, with subsequent chemical associations in seawater under the form of chloro-complexes, which may lead to a final deposition in remote areas). This is valid for elements that have a residence time in the ocean that is superior to the mixing time of ocean waters (actually >1500 years).
   This condition is fulfilled for Cd – with an actual ocean residence time of about 79000 years, and for several elements including Na, Mg, K, Sr, B, Li, Mo, As, V, Cs, Sb, Se, W, Bi, Tl, Au, Re, Ag, Hg and Ir, but not for elements such as Zn, Cu, Pb and Sn (Rubin, 1997). Ni and Cr have residence times close to the mixing time of ocean waters.

In a further hypothesis, volcanic activity is foreseen in areas nearby the regions which are marked by enrichments in various trace-elements, and the transfer of these elements into those regions may occur directly by ash deposits, and/or by continental weathering of volcanic deposits and subsequent transport of Cd into the depositional environment by rivers.

References

Algeo, T.J., 2004. Can marine anoxic events draw down the trace element inventory of seawater? Geology, 32 (12), 1057-1060

Allard, P., Aiuppa, A., Loyer, H., Carrot, F., Gaudry, A., Pinte, G., Michel, A. and Dongarrà, G., 2000. Acid gas and metal emission rates during long-lived basalt degassing at Stromboli volcano. Geophysical Research Letters, 27, 1207-1210

Alloway, B.J., 1995. Cadmium. In: Heavy metals in soils. 2nd edition. Blackie Academic and Professional, 122-147

Altschuler, Z.S., 1980. Geochemistry of trace elements in marine phosphorites. Soc. Econ. Paleontologists Mineralogist Spc. Pub, 29, 19-30

Baize, D., and Sterckeman, T., 2001. Of the necessity of knowledge of the natural pedo-geochemical background content in the evaluation of the contamination of soils by trace elements. The Science of the Total Environment, 264, 127-139

Benitez-Vasquez, N., 1999. Cadmium speciation and phyto-availability in soils of the swiss Jura : hypothesis about its dynamic. Ecole Polytechnique Fédérale de Lausanne. 132 pp.

Bentor, Y., 2005. Chemical Element.com - Cadmium. Available on http://www.chemicalelements.com/elements/cd.html

Bézier, P., 2005. Le cycle du Cadmium. Unpublished report, University of Neuchâtel. 21 pp. Available on request, claire.rambeau@unine.ch

Böning, P., Brumsack, H.-J., Böttcher M.E., Schnetger, B., Kriete, C., Kallmeyer, J. and Borchers, S.L., 2004. Geochemistry of Peruvian near-surface sediments. Geochimica et Cosmochimica Acta, 68 (21), 4429-4451

Boulègue, J., 1977. Equilibria in a sulfide rich water from Enghien-les-Bains, France. Geochimica et Cosmochimica Acta, 41 (12), 1751-1758

Boulègue, J., Ciabrini, J.-P., Fouillac, C., Michard, G. and Ouzounian, G. 1979. Field titrations of dissolved sulfur species in anoxic environments — Geochemistry of Puzzichello waters (Corsica, France). Chemical Geology, 25 (1-2), 19-29

Bourrelier, P.-H and Berthelin, J., 1998. Contamination des sols par les éléments en traces: les risques et leur gestion. Rapport de l'Académie des Sciences, 42, Technique et Documentation, Paris, 440 pp.

Boyanov, M.I., Kelly, S.D., Kemner, K.M., Bunker, B.A., Fein, J.B. and Fowle, D.A., 2003. Adsorption of cadmium to Bacillus subtilis bacterial cell walls: A pH-dependent X-ray absortion fine structure spectrometry study. Geochimica et Cosmochimica Acta, 67 (18), 3299-3311

Boyle, E.A., Sclater, F.R. and Edmond, J.M., 1976. On the marine geochemistry of cadmium. Nature, 263, 42-44

Boyle, E.A., 1988. Cadmium: chemical tracer of deepwater paleoceanography. Paleoceanography, 3, 471-489

Buat-Ménard, P. and Arnold, M., 1978. The Heavy metal chemistry of atmospheric particulate matter emitted by mount Etna volcano. Geophysical Research Letters, 5 (4), 245-248

Bruland, K.W., Knauer, G.A. and Martin, J.H, 1978. Cadmium in northeast Pacific waters: Limnology and Oceanography, 23, 618-625

BUWAL, 1997. Stoffflussanalyse Cadmium. Umweltgefährdende Stoffe. Schriftenreihe Umwelt 295. Herausgegeben vom Bundesamt für Umwelt, Wald und Landschaft. Bern, 74 pp.

Caillère S., Kraut F., Horon O., Lefavrais-Raymond A., and Rouire J. (1968) - Carte géologique France (1/50 000), feuille Quarré-les-Tombes (467), et notice explicative, 8 p. - Orléans: Bureau de recherches géologiques et minières.

Chester, R., 1990. Marine Geochemistry. Unwin Hyman: London, 698 pp.

Cook, M.E. and Morrow, H., 1995. Anthropogenic Sources of Cadmium in Canada. National Workshop on Cadmium Transport Into Plants, Canadian Network of Toxicology Centres, Ottawa, Ontario, Canada, June 20-21

Cossa, D. and Lassus, P., 1989. Le cadmium en milieu marin. Biogéochimie et écotoxicologie. Rapports scientifiques et techniques de l'IFREMER, 16, 111 pp.

CRC Handbook of Chemistry and Physics, 77th Edition, 1996. Lide, D.R. and Frederikse, H. P. R. (Eds.). CRC Press, Inc., Boca Raton, Florida. 2608 pp.

Dubois, J.P., Benitez, N., Liebig, T., Baudraz, M. and Okopnik, F., 2002. Le cadmium dans les sols du haut Jura suisse, in Les éléments traces métalliques dans les sols. Approches fonctionnelles et spatiales, D.Baize, M.Tercé, editors, INRA Editions, Paris, 33-52

Elbaz-Poulichet, F., 1988. Apports fluviatiles et estuariens de plomb, cadmium et cuivre aux océans; comparaison avec l'apport atmosphérique. Unpublished PhD thesis. Univ. Pierre et Marie Curie, Paris. 288 pp.

Elderfield, H., and Rickaby, R.E.M., 2000. Oceanic Cd/P ratio and nutrient utilization in the glacial Southern Ocean. Nature, 405, 305-310.

Elinder, C.-G., 1985. Cadmium: Uses, Occurrence, and Intake, Cadmium and Health: A Toxicological and Epidemiological Appraisal, CRC Press, Inc., Boca Raton, Florida, 23-63

Fisher, N.S. and Fabris, J.G., 1982. Complexation of Cu, Zn and Cd by Metabolites Excreted from Marine Diatoms. Marine Chemistry, 11(3), 245-255

Gaillard, J.F., Jeandel, C., Michard, G., Nicolas, E. and Renard, D., 1986. Interstitial Water Chemistry of Villefranche Bay Sediments: Trace Metals Diagenesis. Marine Chemistry, 18, 233-247

Gobeil C., Silverberg, N., Sundby, B. and Cossa, D., 1987. Cadmium diagenesis in Laurentian Trough sediments. Geochim. Cosmochim. Acta, 51, 589-596

Goni, J., and Leleu, M. 1980. Traces (Eléments en). Encyclopedia Universalis, 224-226

Gonzalez, J.-L., Chiffoleau, J.-F., Miramand, P., Thouvenin, B. and Guyot, T., 1999. Le cadmium : comportement d'un contaminant métallique en estuaire. IFREMER publications, Programme scientifique Seine-Aval, 10, J.-L. Gonzalez (coord.), Plouzané, France, 31 pp.

Heinrichs H.B., Schulz-Dobrick B., Wedepohl K.H., 1980. Terrestrial geochemistry of Cd, Bi, Tl, Pb, Zn and Rb. Geochim. Cosmochim. Acta, 44, 1519-1533

Hinkley, T.K., Lamothe, P.J., Wilson, S.A., Finnegan, D.L. and Gerlach, T.M., 1999. Metal emissions from Kilauea, and a suggested revision of the estimated worldwide metal output by quiescent degassing of volcanoes. Earth and Planetary Science Letters, 170, 315-325

Il'in A.V. and Kiperman Y.A., 2001. Geochemistry of Cadmium in Mesozoic Phosphorites of the East European Platform. Lithology and Mineral Resources, 36 (6), 576-581

International Cadmium Association, 2005. Available on http://www.cadmium.org/

Kabata-Pendias, A. and Pendias, H., 1992. Trace elements in soils and plants. 2nd edition. CRC Press, 365 pp.

Kemner, K.M., O'Loughlin, E.J., Kelly, S.D. and Boyanov, M.I., 2005. Synchrotron X-ray Investigations of Mineral-Microbe-Metal Interactions. Elements, 1 (4), 217-221

Kremling, K., 1983. Trace metal fronts in European shelf waters. Nature, 303, 225-227

Loaëc, M., Olier, R. and Guezennec, J., 1997. Uptake of lead, cadmium and zinc by a novel bacterial exopolysaccharide. Water Research, 31 (5), 1171-1179

Long, D.T. and Angino, E.E., 1977. Chemical speciation of Cd, Cu, Pb and Zn in mixed freshwater, seawater and brine solutions. Geochimica et Cosmochimica Acta, 41 (9), 1183-1191

Lynch-Stieglitz, J. and Fairbanks, R.G., 1994. A conservative tracer for glacial ocean circulation from carbon isotope and palaeo-nutrient measurements in benthic foraminifera. Nature, 369, 308-310

Middleburg, J.J. and Comans, R.N.J.J., 1991. Sorption of cadmium on hydroxyapatite, Chemical geology, 90, 45-53

Nathan, Y., Soudry, D., Levy, Y., Shitrit, D. and Dorfman, E., 1997. Geochemistry of cadmium in the Negev phosphorites. Chemical Geology, 142, 45-53

Nriagu, J. 0., 1980. Cadmium in the Atmosphere and in Precipitation, Cadmium in the Environment, Part 1, Ecological Cycling, JohnWiley & Sons, 71-114

Nriagu, J. 0., 1989. A Global Assessment of Natural Sources of Atmospheric Trace Metals, Nature, 338, 47-49

Jensen,A. and Bro-Rasmussen,F., 1992. Environmental Contamination in Europe, Reviews of Environmental Contamination and Toxicology, 125, 101-181

O'Neill, P. 1993. Environmental chemistry (2nd edition). Chapman and Hall, London, 230 pp.

Organisation for Economic Co-operation and Development (OECD), 1994. Risk Reduction Monograph No. 5: Cadmium OECD Environment Directorate, Paris, France.

Phelan, J. M., Finnegan, D. L., Ballantine, D. S., Zoller, W. H., Hart, M. A. and Moyers, J. L., 1982. Airborne aerosol measurements in the quiescent plume of Mount Saint Helens September, 1980. Geophysical Research Letters, 9, 1093-1096

Prudente D (1999). Distribution des teneurs naturelles en cadmium dans les sols de la forêt communale des Fourgs (Doubs - France). DES Sciences naturelles de l'environnement. Universités de Genève et de Lausanne. 68 p. + annexes.

Prudente, D., Baize, D., Dubois, J.P., 2002. Le cadmium naturel dans une forêt du haut Jura français, in Les éléments traces métalliques dans les sols. Approches fonctionnelles et spatiales, D. Baize, M. Tercé, editors, INRA Editions, Paris, 53-70

Ramamoorthy, S. and Kushner, D.J., 1975. Heavy metal binding sites in river water. Nature, 256, 399-401

Rickaby, R.E.M., and Elderfield, H., 1999. Planktonic foraminiferal Cd/Ca: Paleonutrients or paleotemperature. Paleoceanography, 14, 293-303

Roels, H. A., Van Assche, F. J., Oversteyns, M., De Groof, M., Lauwerys, R. R. and Lison, D., 1997. Reversibility of microproteinuira in cadmium workers with incipient tubular dysfunction after reduction of exposure. Amer. J lnd. Med., 31, 645-652

Rosenthal, Y., Lam, P., Boyle, E.A. and Thomson, J., 1995. Authigenic cadmium enrichments in suboxic sediments: precipitation and postdepositional mobility. Earth and Planetary Science Letters, 132, 99-111

Rubin, K., 1997. Degassing of metals and metalloids from erupting seamount and mid-ocean ridge volcanoes: observations and predictions. Geochimica et Cosmochimica Acta, 61, 3525-3542.

Sorahan, T., Lister, M., Gilthorpe, S. and Harrington, J. M., 1995. Mortality of copper cadmium alloy workers with special reference to lung cancer and non-malignant diseases of the respiratory system, 1946-92, Occupational and Environmental Medicine, 52 (12), 804-812.

Sorahan, T. and Lancashire, R. J., 1997. Lung cancer mortality in a cohort of workers employed at a cadmium recovery plant in the United States: an analysis with detailed job histories, Occupational and Environmental Medicine, 54 (3), 194-201

Snow, L. J.,. Duncan, R. A, and Bralower, T. J., 2005. Trace element abundances in the Rock Canyon Anticline, Pueblo, Colorado, marine sedimentary section and their relationship to Caribbean plateau construction and oxygen anoxic event 2, Paleoceanography, 20, 1029-1093

Stevenson, F. J., 1976. Stability constants of Cu^{2+}, Pb^{2+} and Cd^{2+} complexes with humic acids. Soil Sci. Soc. Am. J., 40, 665-672

Stimac, J., Hickmott, J., Abell, R., Larocque, A.C.L., Broxton, D.E., Gardner, J., Chipera, S., Wolff, J. and Gaueke, E., 1996. Redistribution of Pb and Other Volatile Trace Metals During Eruption, Devitrification, and Vapor-Phase Crystallization of the Bandelier Tuff, New Mexico. Journal of Volcanology and Geothermal Research, 73, 245-266

Symonds, R. B., Rose, W. I., Reed, M. H., Lichte, F. E., and Finnegan, D. L.1987. Volatilization, transport and sublimation of metallic and non-metallic elements in high temperature gases at Merapi Volcano, Indonesia. Geochim. Cosmochim. Acta, 51, 2083-2101

Symonds, R. B., Reed, M. H. and Rose, W. I., 1992. Origin, speciation, and fluxes of trace-element gases at Augustine volcano, Alaska: Insights into magma degassing and fumarolic processes: Geochimica et Cosmochimica Acta, 56, 633–657

Tuchschmid, M., 1995. Quantifizierung und Regionalisierung von Schwermetallen und Fluorgehalten bodenbildender Gesteine der Schweiz. Umwelt-Materialien, 32 (BUWAL, Berne).

Van Assche, F. J. and Ciarletta, P., 1993. Environmental exposure to cadmium in Belgium: Decreasing trends during the 1980s. Heavy Metals in the Environment, 1, 34-37

Van Assche, F. J., 1998. A Stepwise Model to Quantify the Relative Contribution of Different Environmental Sources to Human Cadmium Exposure, Paper to be presented at NiCad '98, Prague, Czech Republic, September 21-22.

van Geen A., McCorkle, D.C. and Klinkhammer, G.P., 1995. Sensitivity of the phosphate-cadmium-carbon isotope relation in the ocean to cadmium removal by suboxic sediments, Paleo Currents, 10, 159-169

Veuve, P., 2000. Etude géochimique et sédimentaire d'un enrichissement en cadmium observé dans les calcaires oolitiques jurassiques du Jura. Unpublished diploma thesis, Univ. NE, 56 pp.

World Health Organisation (WHO), 1992. Environmental Health Criteria 134 - Cadmium International Programme on Chemical Safety (IPCS) Monograph.

III - The Jurassic system

Here we present the main climatic and geochemical conditions which are related to the Jurassic period, as well as major tectonic and volcanic events which occurred during the same period. A special emphasis is placed on the Bajocian and Oxfordian.

III-1 Jurassic Climate

The Mesozoic climate has been described by several authors as warm and "equable" (e.g., Frakes, 1979; Hallam, 1985). Particularly, the Mesozoic is usually considered as free of major polar ice caps (Price, 1999, and references therein; Fig. 1)

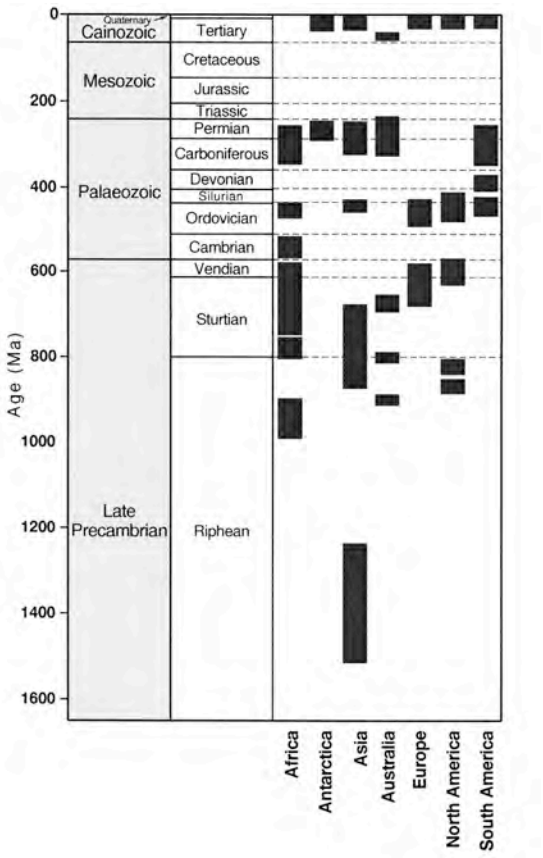

Fig. 1. The Earth's glacial record from the late Precambrian to Cainozoic.
Price (1999).

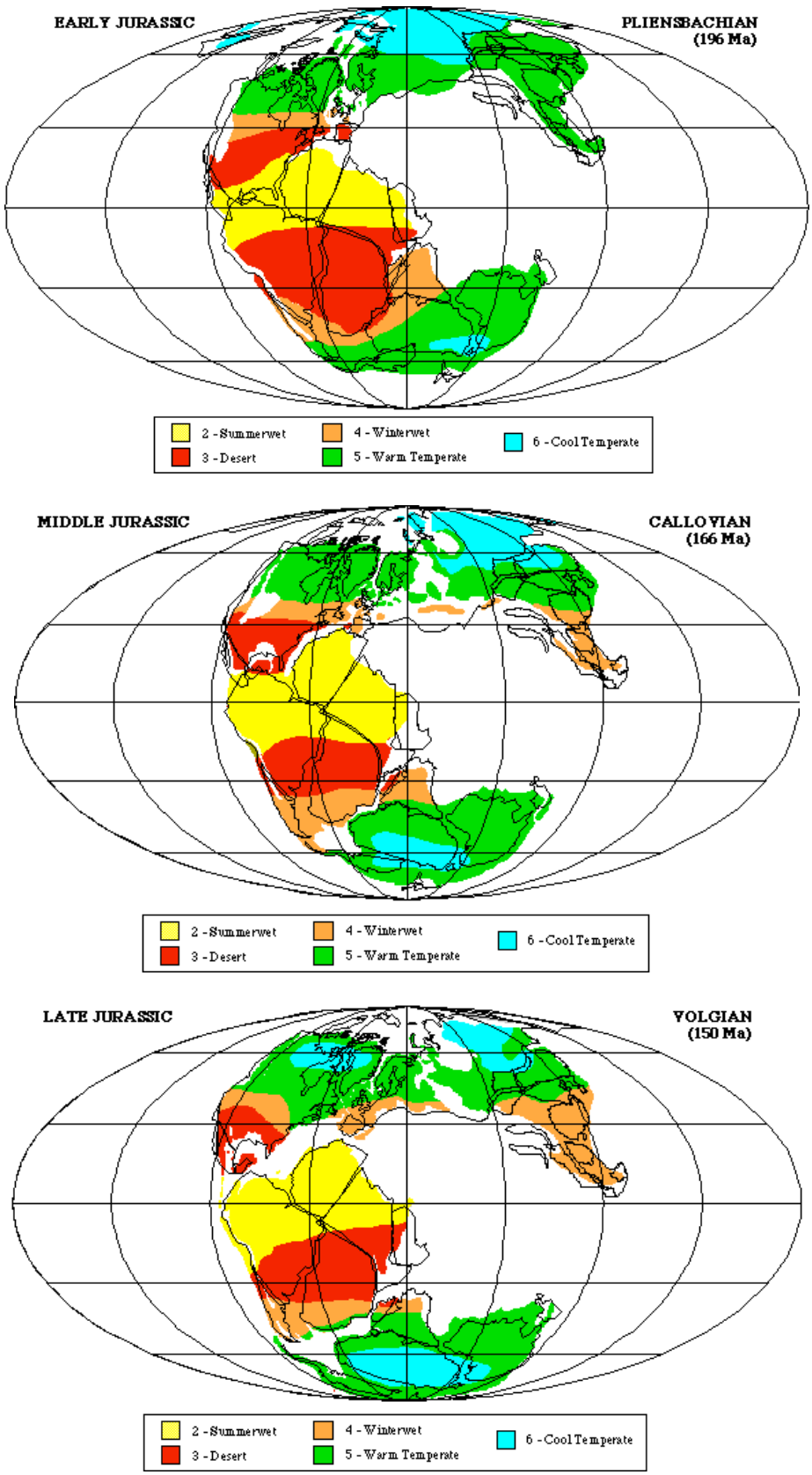

Fig. 2. Jurassic evolution of continents and climate: combination of lithological and paleobotanical indicators, treated by multivariate statistical analysis. Rees et al (2000).

Global climate zones for the Jurassic have been deduced from both lithological indicators, such as the presence of evaporites and coals, and changes in plant foliar morphologies (Rees et al., 2000; Fig. 2). In this context, terrestrial areas corresponding to western and southern Europe were likely part of a rather warm, seasonally dry (winterwet) climate zone.

However, this vision of an ever-warm climate during Jurassic times has been contested by several authors. Price (1999) established a record of possible indicators of polar ice during the Mesozoic (including faunal and floral evidences, abraded rock surfaces, dropstones, tillites, glendonites, which are carbonate nodules composed of ikaite - a calcium carbonate polymorph that crystallise at temperatures around 0ºC, clay-mineral distribution and changes in global sea level, and concluded that several periods during the Mesozoic may have been characterized by cooler events. This concerns, in particular, the time interval ranging from the Late Aalenian to the Oxfordian, which is marked by a global increase in glendonite occurrences in higher latitudes (Fig. 3). However, it should be noted here that the witnesses of colder events used in this study are dispersed and frequently controversially debated.

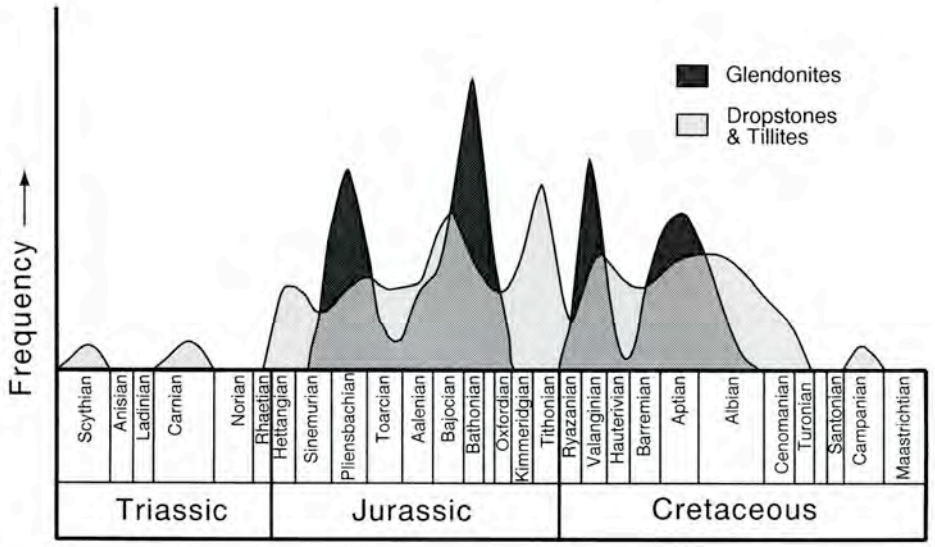

Fig. 3. Distribution of possible glacially derived sediments and glendonites through the Mesozoic. A semi-quantitative measure of the extend of the Earth surface affected is indicated by the heights of the peaks. Price (1999).

The variations of the global $\partial^{18}O$ curve, calculated for the Cambrian to recent times from measurements realized on brachiopods and belemnites, as well as on mollusc shells consisting of preserved aragonite, equally suggest the development of a cold period (seawater enrichment in ^{18}O) during Middle and Late Jurassic times (Veizer et al., 1999: Fig. 4). Additionally, $\partial^{18}O$ measurements realized on Jurassic brachiopods from the high latitude archipelago of Svalbard (Ditchfield, 1997) indicate a marked drop of temperature between the Aalenian - Bajocian and Bathonian - Kimmeridgian times (mean calculated temperatures of 14.8 - 11.4 ºC and 7.6ºC, respectively), with the settling of a colder period that continue during the Tithonian to Valanginian time period (mean calculated temperatures of 7.7 to 8.4ºC).

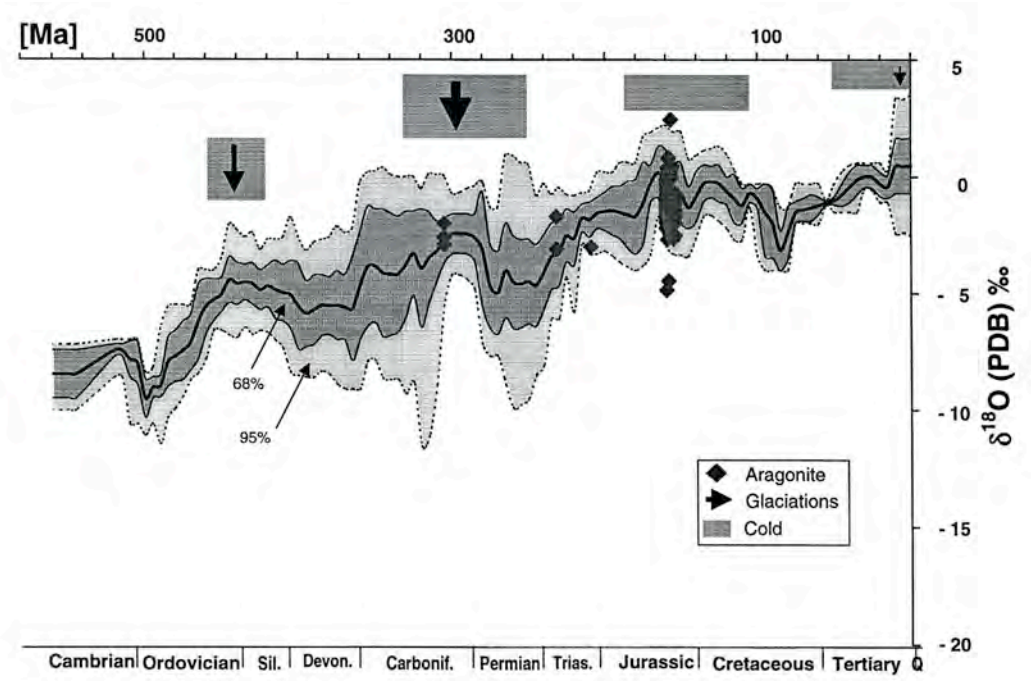

Fig. 4. ∂^{18}O variations from Cambrian to recent times. Veizer et al. (1999).

III-2 Middle to Late Jurassic geodynamic evolution

During Middle Jurassic times, the Neotethys extended towards the northwest, which resulted in a connexion with the Central Atlantic, which was itself in an advanced drift stage (Ford and Golonka, 2003). The Gulf of Mexico and Central America were put in connection with southern Europe through the opening of a major Jurassic seaway (Ricou, 1996). Meanwhile, rifting in the North Sea and in the northern proto-Atlantic was still active (Ziegler, 1989; Doré, 1991). Fast spreading is also recorded for the Pacific, along with associated increased volcanism in circum-Pacific subduction zones (Larson and Sager, 1992). Opening of the Liguro-Piemontese oceanic basin, with rearrangement of the prevailing oceanic current patterns began during the early Middle Jurassic (Favre and Stampfli, 1992; Bill et al., 2001). During the late Jurassic, the Atlantic began to extend towards the area between Iberia and Canada (Ziegler, 1988; Sinclair et al., 1993) whereas reduced, transcontinental sea channels developed across Europe and the North Atlantic (Ford and Golonka, 2003).

III-3 Active volcanic centres

A large aerial volcanism event is recorded in Antarctica and Patagonia during Jurassic times (Pankurst et al., 2000). This important episode of silicic volcanism related to the break-up of Gondwana contain two major events, which have been dated at 172-162 Ma and 157-153 Ma (Pankhurst et al., 2000), which correspond to the latest Aalenian to Callovian and Late Oxfordian to Kimmeridgian, respectively (Gradstein et al., 2004). This volcanism seems to have been particularly active during the Late Aalenian-Early Bajocian (Courtillot, 1995; Dromart et al., 1996).

Additionally, Jurassic and Lower Cretaceous volcanogenic sediments have been reported from the northern North Sea area (Hansen and Lindgreen, 1989; Lindgreen, 1989; Jeans et al., 2000). This volcanic event was invoked to explain Fe enrichments and specific host phases in Lower Jurassic to Lower Cretaceous ironstones, as these deposits have few chances to have been derived from deeply weathered lateritic soils, which have not been observed in sediments of the same age in adjacent areas (Jeans et al., 2000).

III-4 Geochemical and sedimentological features during the Bajocian and Oxfordian time periods

The Bajocian and Oxfordian are stages that are characterized, in present-day central Europe, by the widespread deposition of iron- and chert-rich sediments and by the abundance of condensed horizons and omissions surfaces (e.g., Burkhalter, 1995, 1996, Bartolini et al., 1996). Both are periods of major sea-level rise (e.g., Price, 1999; Fig. 1). The Bajocian and Oxfordian are also related to a "calcite-sea" state of ocean chemistry, which signifies that precipitation of the majority of non-skeletal carbonates is in calcitic mineralogy, rather than in aragonite (e.g., Philip, 2003, and references therein).

With regards to shallow-water carbonate deposition, carbonates are partly deposited as heterozoan or foramol-type carbonates, indicative of higher nutrient levels and eventually colder waters (Lees and Buller, 1972; Föllmi et al., 1994; Gonzales and Wetzel, 1996). For the Oxfordian, higher nutrient supplies are also indicated by the phosphorus-accumulation curve compiled for the last 160 my, which gives a relative maximum for this time period (Föllmi, 1995). Phosphorite deposits - i.e. rocks containing more than 18% P_2O_5 - are known from both the Bajocian and the Oxfordian, and the Middle and Upper Jurassic periods are represented by two distinct maxima in the estimated abundance of economic phosphate deposits (Cook and McElhinny, 1979).

A majority of the carbonate platforms in the western Tethys experienced low growth rates during the period between the Late Bajocian and the Oxfordian, wich lead to the hypothesis of unfavourable conditions with regards to carbonate productivity (e.g., Bartolini et al., 1996; Weissert and Mohr, 1996; Cobianchi and Picotti, 2001 and references therein).
This crisis in carbonate production has been linked to a gradual increase in trophic resources (e.g., Bartolini et al., 1996; Cobianchi and Picotti, 2001), which is concomitant with a sea-surface temperature drop (Veizer et al., 1999; Cobianchi and Picotti, 2001). This increase in nutrient levels has been related to an increase in continental weathering and run-off, which may have been triggered by an increase in atmospheric pCO_2 due to endogenic degassing during sea-floor spreading (Bartolini et al., 1996; Cobianchi and Picotti, 2001). A pronounced negative excursion in the $^{87}Sr/^{86}Sr$ curve is indeed recorded for Middle to Late Jurassic times, and may be interpreted in terms of increased hydrothermal activity (Jones and Jenkyns, 2001).

In parallel, coeval changes in seawater chemistry such as high concentrations of dissolved carbon dioxide may have led to unfavourable conditions for carbonate-producing organisms (Bartolini and Cecca, 1999). A change towards more humid conditions (increase in continental precipitation), which is postulated for the Early to Late Jurassic time period (Gibbs et al., 1999), was also proposed as a driving factor for increasing trophic levels in the western Tethys (Cobianchi and Picotti, 2001). All these environmental changes are expressed by perturbations in the carbon and silica cycles (Bartolini et al., 1996; Bartolini and Cecca, 1999; Cobianchi and Picotti, 2001). Radiolarian-derived deposits replaced the platform-derived carbonates in the Umbria-Marche basins, whereas a large hiatus developed in the adjacent platforms (Early Bajocian to late early Kimmeridgian; Bartolini and Cecca, 1999). Additionally, two positive excursions in stable carbon isotopes are observed for the Bajocian and Oxfordian times (Bartolini et al., 1996; Weissert and Mohr, 1996), which may reflect both an increase of organic carbon burial and/or a reduction in the global production of carbonates.

III-5 Conclusion

The Bajocian to Oxfordian period is characterized by major changes in nutrient levels and coeval changes in sedimentation patterns, and in particular platform carbonate accumulation and crises therein in the western Tethys. Possible climate changes include a shift toward cooler or more humid conditions. Enhanced hydrothermal activity, which may be in relation with continental break-up and increasing spreading rates at middle oceanic ridges, as well as intense volcanic activity, both in the Patagonia/Antartica area and in the northern North Sea area, are recorded. During the Jurassic, volcanic events as well as hydrothermal activity may have acted as principal elements of perturbation in the carbonate system, by triggering CO_2 inputs in the atmosphere and leading to changes in seawater composition.

References

Bartolini, A., Baumgartner, P.O., and Hunziker, J., 1996. Middle and late Jurassic carbon stable-isotope stratigraphy and radiolarite sedimentation of the Umbira-Marche basin (central Italy). Eclogae geologicae Helvetiae, 89, 811-844

Bartolini, A. and Cecca, F., 1999. 20 My hiatus in the Jurassic of Umbria-Marche Apennines (Italy): carbonate crisis due to eutrophication. Comptes Rendus de l'Académie des Sciences de Paris, Earth and Planetary Sciences, 329, 587-595

Bill, M., O'Dogherty, L., Guex, J., Baumgartner, P.O. and Masson, H., 2001. Radiolarite ages in Alpine-Mediterranean ophiolites: Constraints on the oceanic spreading and the Tethys-Atlantic connection. GSA Bulletin, 113 (1), 129-143

Burkhalter, R.M., 1995. Ooidal ironstones and ferruginous microbialites: origin and relation to sequence stratigraphy. Sedimentology, 42, 57-74

Cobianchi, M. and Picotti, V., 2001. Sedimentary and biological response to sea-level and palaeoceanographic changes of a Lower-Middle Jurassic Tethyan platform margin (Southern Alps, Italy). Paleogeography, Paleoclimatology, Paleoecology, 169, 219-244

Cook, P.J. and McElhinny, M.W., 1979. A re-evaluation of the spatial and temporal distribution of sedimentary phosphate deposits in the light of plate tectonics: Economic Geology, 74, 315-330

Courtillot, V., 1995. La vie en catastrophes. Fayard, Paris, 278 pp.

Ditchfield, P.W., 1997. High northern paleolatitude Jurassic-Cretaceous paleotemperature variation: new data from Kong Karls Land, Svalbard. Paleogeography, Paleoclimatology, Paleoecology, 130, 163-175

Doré, A.G., 1991. The structural foundation and evolution of Mesozoic seways between Europe and the Arctic. Paleogeography, Paleoclimatology, Paleoecology, 97, 441-492

Dromart, G., Allemand, P., Garcia, J.P. and Robin, C., 1996. Variation cyclique de la production carbonatée au Jurassique le long d'un transect Bourgogne-Ardèche, Est-France, Bulletin de la Société géologique de France, 167 (3), 423-433.

Favre, P. and Stampfli, G.M., 1992. From rifting to passive margin : the example of the Red Sea, Central Atlantic and Alpine Tethys. Tectonophysics, 215, 69-97

Föllmi, K.B., Weissert, H., Bisping, M. and Funk, H., 1994. Phosphogenesis, carbon-isotope stratigraphy, and carbonate-platform evolution along the Lower Cretaceous northern Tethyan margin. GSA Bulletin, 106 (6), 729-746

Föllmi, K.B., 1995. 160 m.y. record of marine sedimentary phosphorus burial: coupling of climate and continental weathering under greenhouse and icehouse conditions. Geology, 23, 859-862

Ford, D. and Golonka, J., 2003. Phanerozoic paleogeography, paleoenvironment and lithofacies maps of the circum-Atlantic margins. Marine and Petroleum Geology, 20 (3), 249-285

Frakes, L.A., 1979. Climates throughout Geologic Time. Elsevier, Amsterdam, 310 pp.

Gibbs, M.T., Bluth, G.J.S., Fawcett, P.J. and Kump L.R., 1999. Global chemical erosion over the last 250 My: variations due to changes in paleogeography, paleoclimate, and paleogeology. American Journal of Science, 299, 611–651

Gradstein, F.M., Ogg, J.G., Smith, A.G. et al., 2004. A Geologic Time Scale 2004. Cambridge University Press, ~ 500 pp.

Gonzales, R., and Wetzel, A., 1996. Stratigraphy and paleogeography of the Hauptrogenstein and Klingnau Formation (middle Bajocian to late Bathonian), northern Switzerland. Eclogae geologicae Helvetiae, 89, 695-720

Hallam, A., 1985. A review of Mesozoic climates. J. Geol. Soc. London, 142: 433-445.

Hansen P.L. and Lindgreen H. 1989.Mixed-layer illite-smectite diagenesis in Upper Jurassic claystones from the North Sea and onshore Denmark. Clay Minerals 24, 197-213

James, N.P., 1997. The cool-water carbonate deposition realm. Cool-water carbonates, James, N.P., Clarke, J.A.D (Eds.), SEPM, Society for Sedimentary geology, Special Publication 56, 1-20.

Jeans, C.V., Wray, D.S., Merriman, R.J. and Fisher, M.J., 2000. Volcanogenic clays in Jurassic and Cretaceous strata of England and the North Sea Basin. Clay Minerals 35, 25-55

Jones, C.E. and Jenkyns, H.C., 2001. Seawater strontium isotopes, oceanic anoxic events, and seafloor hydrothermal activity in the Jurassic and Cretaceous. American Journal of Science, vol. 301, 112-149

Larson, R.L., and Sager, W.W., 1992. Skewness of magnetic Anomalies M0 to M29 in the northwestern Pacific. In Larson, R.L., Lancelot, Y., et al., Proc. ODP, Sci. Results, 129: College Station, TX (Ocean Drilling Program), 471–481

Lees, A. and Buller, A.T., 1972. Modern temperate-water and warm-water shelf carbonate sediments contrasted. Marine Geology, 13, (5), M67-M73

Lindgreen H. 1989. Elemental and structural changes in illite/smectite mixed-layer minerals during diagenesis in Kimmeridgian-Volgian (-Ryazanian) clays in the Central Trough, North Sea and the Norwegian-Danish Basin. Bull. Geol. Soc. Denmark, 39, 1-82

Morettini, E., Santantonio, M., Bartolini, A., Cecca, F., Baumgartner, P.O., and Hunziker, J.C., 2002. Carbon isotope stratigraphy and carbonate production during the Early-Middle Jurassic: examples from the Umbria-Marche-Sabina Apennines (central Italy). Paleogeography, Paleoclimatology, Paleoecology, 184, 251-273

Pankhurst, R. J., Riley, T. R., Fanning, C. M. and Kelley, S. P., 2000. Episodic Silicic Volcanism in Patagonia and the Antarctic Peninsula: Chronology of Magmatism Associated with the Break-up of Gondwana. Journal of Petrology, 41, 605-625.

Philip, J., 2003. Peri-Tethyan neritic carbonate areas: distribution through time and driving factors. Paleogeography, Paleoclimatology, Paleoecology, 196, 19-37

Price, G.D., 1999. The evidence and implications of polar ice during the Mesozoic. Earth-Sci. Rev. 48, 183-210

Rees, P.M., Ziegler, A.M. and Valdes, P.J. 2000. Jurassic phytogeography and climates: new data and model comparisons. In: Huber et al. (Eds), Warm climates in Earth History: 297-318. Also available on http://pgap.uchicago.edu/Jurassic.html.

Ricou, L.E., 1996. The Plate tectonic History of the Past Tethys Ocean. In A.E.M. Nain, L.E. Ricou, B. Vrielynck and J. dercourt (Eds.), The Ocean Basins and Margin 8, The Tethys Ocean, Plenum Press, New York, 3-70

Sinclair, I.K., Shannon, P.M., Williams, B.P.J., Harkers, S.D. and Moore, J.G., 1994. Tectonic control on sedimentary evolution of the three North Atlantic borderland Mesozoic basins. Basin Research, 6, 193-217

Veizer, J., Ala, D., Azmy, K., Bruckschen, P., Buhl, D., Bruhn, F., Carden, G.A.F., Diener, A., Ebneth, S., Godderis, Y., Jasper, T., Korte, C., Pawellek, F., Podlaha, O.G., and Strauss, H., 1999. $^{87}Sr/^{86}Sr$, d ^{13}C and d ^{18}O evolution of Phanerozoic seawater. Chemical Geology, 161, 59-88

Weissert, H. and Mohr, H.,1996. Late Jurassic climate and its impact on carbon cycling. Paleogeography, Paleoclimatology, Paleoecology, 122, 27-43

Ziegler, P. A., 1988. Evolution of the Arctic-North Atlantic and the Western Tethys. American Association of Petroleum Geologists, Memoir 43, 198 pp.

Ziegler, P. A., 1989. Evolution of Laurussia. Kluwer Academic Publishers, Dordrecht, 102 pp.

IV - Geographical and geological settings

Here a description is given of the sections from western and southern Europe which - in the framework of this study - were sampled and analyzed for their Cd contents. Firstly, I present the geographical and palaeogeographical context and in the following, I provide information on their specific ages and finally, I describe each of the sections in further detail.

IV-1 Geographical and palaeogeographical settings

Seven geographical areas have been investigated. Six of them are located in southern or western Europe (Fig. 1) and related to the former western Tethyan realm (Fig. 2):

- *Swiss Jura Mountains*
  sections of Lausen-Schleifenberg, Gorges du Pichoux
- *Burgundy, France*
  sections of Vergisson-Davayé, Lucy-le-Bois, Rochers du Saussois, Roche aux Poulets
  outcrops of the Frétoy forest, Clamecy, Blacy, Précy-le-Sec
- *Normandy, France*
  section of Sainte Honorine des Pertes
- *Southeastern France (Digne area)*
  section of Chaudon-Norante
- *Southern Spain*
  sections of Carcabuey, Casa de Chimeneas
- *Central Italy*
  section of Terminilletto

The geographical location of the European sections is shown in Fig 1, and the corresponding geographical coordinates are presented in Table 2. The geographical and palaeo-geographical locations of the sections previously described and studied by Veuve (2000) in the Swiss Jura Mountains are also provided here: Pont de la Baleine, Vue-des-Alpes, Gurnigel, Dornach, Auenstein (Fig. 1; Table 2).

Fig. 1. Next page. Geographical and palaeogeographical location of sections from western and southern Europe.

Geographical location of the studied sections

1000 km

Jura Mountains
- Lausen-Schleifenberg
- Gorges du Pichoux
- La Vue-des-Alpes / Le Gurnigel / Pont-de-la-Baleine
- Auenstein
- Dornach

Burgundy
- Le Saussois/Frétoy forest/Clamecy/Blacy
- Vergisson-Davayé

Normandy
- Sainte-Honorine des Pertes

Southeastern France
- Chaudon-Norante

South Spain
- Carcabuey
- Casa de Chimeneas

Central Italy
- Terminilletto

Palaeogeographical location of the studied sections

1000 km

Middle Jurassic (Bajocian-Bathonian)

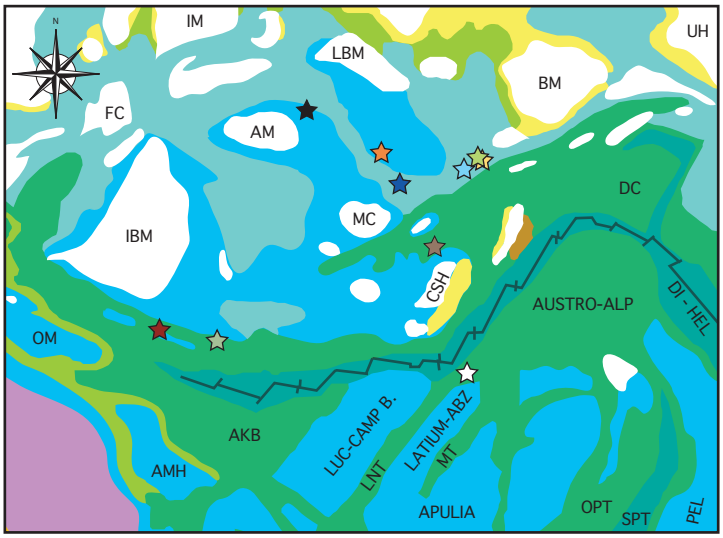

- Carcabuey
- Casa de Chimeneas
- Lucy le Bois / Blacy
- Vergisson-Davayé
- Sainte-Honorine des Pertes
- La Vue-des-Alpes / Le Gurnigel / Pont-de-la-Baleine
- Lausen-Schleifenberg
- Auenstein
- Chaudon-Norante
- Terminilletto

Late Jurassic (Oxfordian-Tithonian)

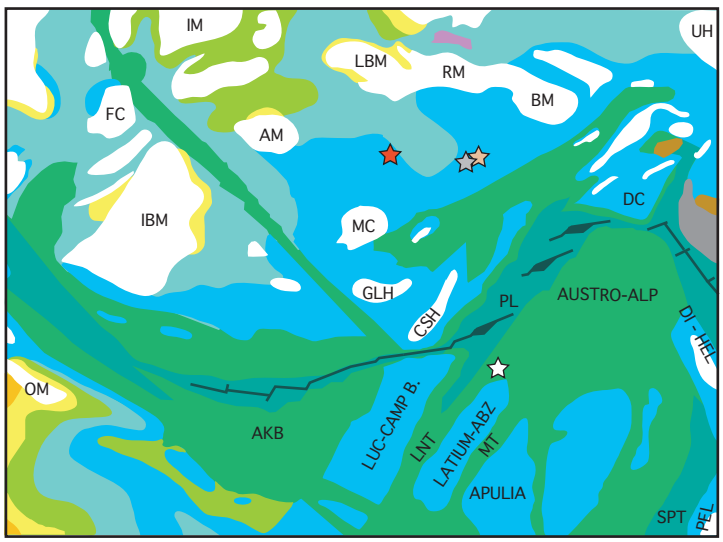

- Le Saussois/Frétoy forest/Clamecy
- Gorges du Pichoux
- Dornach
- Terminilletto

Legend

- emerged areas
- deltaic-shallow marine, mainly sands
- shallow marine, carbonates and clastics
- shallow marine, mainly carbonates
- deeper marine mainly sands (flysch)
- mainly evaporites
- mainly continental clastics
- shallow marine, mainly shales
- deeper marine, clastics and/or carbonates
- basins floored by oceanic crust

AKB	ALBORAN-KABYLIAN BLOCK
AM	ARMORICAN MASSIF
AMH	AIN M`LILA HIGH
AUSTRO-ALP	AUSTRO ALPINE BLOCK
BM	BOHEMIA MASSIF
CSH	CORSICA-SARDINA HIGH
DC	DACIDES BLOCK
DIN. HELL	DINARIC-HELLENIC BASIN
FC	FLEMISH CAP
GLH	GOLFE DU LION HIGH
IBM	IBERIA MESETA
IM	IRISH MASSIF
LATIUM-ABZ	LATIUM-ABRUZZI BLOCK
LBM	LONDON-BRABANT MASSIF
LNT	LAGONEGRO TROUGH
LUC-CAMP B.	LUCANIA-CAMPANIA BLOCK
MC	MASSIF CENTRAL
MT	MOLISE TROUGH
OM	ORAN MESETA
OPT	OLENOS-PINDOS TROUGH
PEL	PELAGONIA
PL	SOUTH PENINIC-PIEDMONT-LIGURIAN BASIN
RM	RHENISH MASSIF
SPT	SUB-PELAGONIAN TROUGH
UH	UKRAINIAN HIGH

The seventh geographical area is represented by Madagascar.
Samples from sections in Anjeba, Dangovato, Analamanga, Atainakanga, Tongobory, Ankazomiheva, and Amparambato have been analyzed to obtain information on Cd contents in Jurassic carbonates outside the Tethyan realm. These sections have previously been described by Markus Geiger (Bremen university, Germany; Geiger et al., 2004), and samples studied here have been provided by this author. The paleogeographical location of sections from Madagascar is presented on Fig 2.; their geographical coordinates and detailed description are given in Geiger et al., (2004).

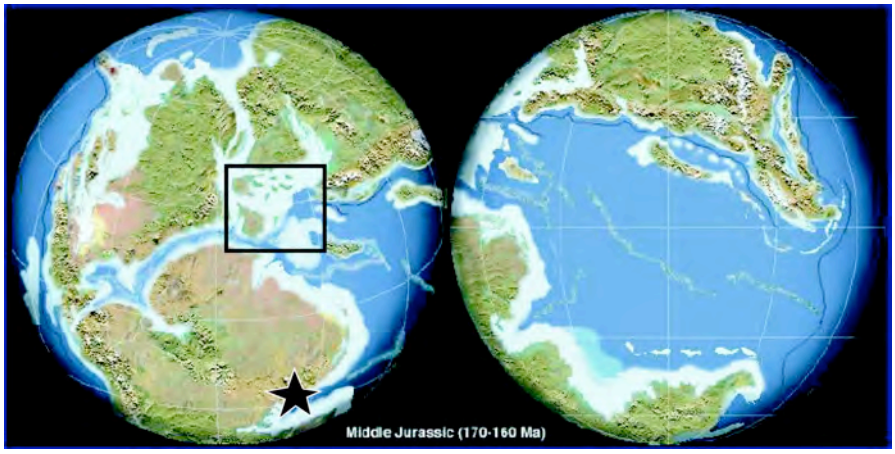

Fig. 2. Palaeogeographic map of the middle Jurassic time period and studied areas. The western Tethyan realm is located inside the black-framed box. The star marks the location of Madagascar sections. Palaeogeographic map modified from Blakey, 2005.

IV-2 Geological time-scale and biostratigraphy

Chonostratigraphical units (Gradstein et al., 2004), for the geological period ranging from the Aalenian to the Kimmeridgian, as well as biostratigraphical intervals (ammonite Zones and Subzones; Hardenbol et al., 1998) for both the Bajocian and the Oxfordian, are presented in Table 1.

IV-3 Description of the different sections investigated

IV-3-1 Bajocian sections

IV-3-1-1 Lausen-Schleifenberg section; Swiss Jura mountains

The Lausen-Schleifenberg section is located in the Jura Mountains (BL, Switzerland). The upper 95 metres of this composite section is exposed near Liestal on the slope of the Schleifenberg hill (Gonzales, 1993; Table 2). We also explored a nearby section, which crops out in a quarry nearby the Lausen rail-station (Table 2), and extends stratigraphically further downwards, and which permitted us to obtain a composite section of 100.06 metres thickness, ranging from the late early Bajocian (*humphriesianum* Zone) to the late Bajocian (*parkinsoni* Zone).

CHRONO-STRATIGRAPHY AGES	BIOSTRATIGRAPHY AMMONITE ZONES		AMMONITE SUBZONES		
Tithonian					
150.8 +/- 4.0					
Kimmeridgian					
155.7 +/- 4.0					
Oxfordian	PLANULA		GALAR / GRANDIPLEX		
			PLANULA		
	BIMAMMATUM		HAUFFIANUM		
			BIMAMMATUM		
			BERRENSE		
			SEMIMAMMATUM		
	BIFURCATUS		GROSSOUVREI		
			STENOCYCLOIDES		
	TRANSVERSARIUM		ROTOIDES		
			SCHILLI		
			LUCIAEFORMIS / WARTAE		
			PARANDIERI		
	PLICATILIS	PATURAT-TENSIS	ANTECEDENS		
			VERTEBRALE		
	CORDATUM	CLAROMO-TANUS	CORDATUM		
			COSTICARDIA		
			BUKOWSKII		
	MARIAE		PRAECORDATUM		
			SCARBURGENSE		
161.2 +/- 4.0					
Callovian					
167.7 +/- 3.5					
Bathonian					
167.7 +/- 3.5					
Bajocian	PARKINSONI		BOMFORDI	BOMFORDI	DIMOR ass.
			DENSICOSTATA		DAUB / ACRIS ass.
			ACRIS	PARKINSONI	
	GARANTIANA	ANNU-LATUM	TETRAGONA		
			SUBGARANTI / TRAUTHI		
			DICHOTOMA		
	NIORTENSE / SUBFURCATUM	LEPTO-SPHINCTITES	SAUZEANUM	BACU-LATA	"SCHROEDERI"
					BACULATA
			PHAULUS		POLYGIRALIS
			?	APLOUS / BANKSI	
	HUMPHRIESIANUM		?	BLAGDENI	
			HUMPHRIESIANUM		
			ROMANI / CYCLOIDES		
	SAUZEI / PROPINQUANS		"HEBRIDICA" / PINGUIS		
			SAUZEI / PATELLA		
	SOWERBYI	LAEVIUSCULA	LAEVIUSCULA		
			OVALIS		
		DISCITES	DISCITES	"EUHOPLOCERAS'	
			WALKERI	ASPERA/MUNDUM "TOXOLIOCERAS"	
171.6 +/- 3.0					
Aalenian					

Table 1. Chronostratigraphy and biostratigraphy of the Middle to Late Jurassic

This carbonate succession belongs to the Hauptrogenstein Formation, which was deposited in a shallow-marine environment in the southeastern part of the Burgundy platform. This carbonate platform became installed along the central European portion of the northern Tethyan margin during the Middle Jurassic, and is characterized by the development of a broad oolitic belt in the central and eastern areas (Gonzales, 1993; Gonzales and Wetzel, 1996).
The lithology of the Lausen-Schleifenberg composite section is predominantly composed of oolitic carbonates, i.e., oolitic and locally bioclastic grainstone and packstone (*sensu* Dunham, 1962). Two major marly intervals are present in the lower part of the section (blue marls intercalated with oolitic packstones) and around 80 m, at the limit between the Early and Late Bajocian. The second detrital episode began with the settling of a ferruginous hardground, followed by the deposit of red, yellow and grey marls intercalated with oolitic packstone. Packstone samples corresponding to the lower part of the section display blue cores contrasting with yellow-orange borders, which hints at the former presence of reducing conditions inside the sediment.
Sedimentary structures include cross-stratifications inside thick oolitic grainstone beds, and erosional surfaces and channel infills, separating thin layers of packstone. Depositional depths are interpreted as varying from shoreface to upper offshore environments.

IV-3-1-2 Vergisson-Davayé section; Burgundy, France

The Vergisson-Davayé section is located near Mâcon, Burgundy. The lower part of this composite section crops out on the Vergisson cliff, whereas the upper part is visible in a former quarry near the Davayé village (Thiry-Bastien, 2002; Table 2). The total section is of about nearby 38 metres thickness, and is dated as latest Aalenian to earliest Late Bajocian (niortense Zone).
These carbonate successions are related to the southwestern part of the Burgundy platform, which - during the Bajocian - was dominated by bioclastic limestone, mainly composed of echinoderms, molluscs and brachiopods (Gonzales and Wetzel, 1996).
The lower part of the section is composed of reddish, crinoid-rich grainstone, and dated as late Aalenian. The sedimentary succession subsequently comprises nodular packstone rich in crinoid and bioclasts, intercalated by thin, red marly levels, and characterized by the presence of numerous perforated surfaces. This succession corresponds to the *discites* and *propinquans* Zones of the Early Bajocian. During the *humphriesianum* Zone, crinoid-rich grainstone was deposited in a succession of wave dunes marked by cross-stratifications, followed by grainstone rich in layers of crinoids and coral clasts. The *blagdeni* Subzone is characterized by the deposition of packstone rich in crinoids and dissolved coral clasts, followed by the deposits of a marly level and by the installation of a small coral bioherm, which is located at the top of the Vergisson section. The Davayé section displays a succession of reddish crinoidal grainstone to packstone arranged in wave dunes and topped by a perforated surface. These carbonates correspond in age to the end of the *humphriesianum* Zone and are laterally equivalent to the top of the Vergisson section. They are followed by siliciclastic grey packstone, rich in crinoids, characterized by channels and erosional surfaces, and dated as Late Bajocian.

These sediments were deposited on a carbonate platfom margin, in shoreface to upper offshore environments. The small bioherm corresponds to a reef barrier environment.

IV-3-1-3 Lucy le Bois section and Blacy area; Lower Burgundy, France

This section is 8.5 metres thick and crops out in a former quarry near the Lucy-le-Bois village (close to Avallon, Burgundy; Table 2).
These carbonate successions were deposited in the western part of the Burgundy platform (Gonzales and Wetzel, 1996). Calcareous deposits are highly condensed and the whole section is dated as uppermost Toarcian to Late Bajocian/Bathonian (Mégnien et al., 1971). Deposits of Aalenian and perhaps earliest Bajocian age are missing.
The lower part of the section is characterized by reddish, crinoid-rich packstone to grainstone levels of early Bajocian age, which are locally rich in bioclasts (bivalves, gastropods), and separated by erosional surfaces and channels. The presence of several marly levels is also noted. These deposits are followed by crinoidal grainstone beds, which are characterized by the presence of cross-stratifications. This succession ends up with an erosional surface, overlapped by marly deposits and siliceous grey packstone, which correspond in age to the Late Bajocian to Bathonian.
Depositional depths are similar to those observed for the Davayé section.

Carbonate rocks laterally correlated to this section have been sampled in soils in the Blacy area (Table 2). They display reddish, crinoid-rich packstone facies.

IV-3-1-4 Sainte Honorine des Pertes; Normandy, France

The carbonate succession which crops out at Sainte Honorine des Pertes - on the Normandy coast near Bayeux (Table 2) corresponds to the historical Bajocian stratotype (d'Orbigny, 1849-1852; Rioult, 1964; Rioult et al., 1991; Préat et al., 2000) and belongs to the Anglo-Paris basin (Rioult et al., 1991).
The section measures about 15.5 metres. Its basis is composed of micritic limestone and ribbon chert and dated as Early Bajocian (*laeviuscula* Zone). The top of this stratigraphic level is phosphatized. Sediments equivalent to the uppermost part of the Early Bajocian and early part of the Late Bajocian are very condensed and reduced to a few decimetres. An erosional surface precedes the deposit of a bioclastic and phosphatized conglomerate, corresponding to the *sauzei* Zone. Deposits associated to the *humphriesianum*, *niortense*, *garantiana* Zones, and *parkinsoni* Zone pro part, are composed both of phosphatized stromatolites, as well as ferruginous oolites and oncolites, which include bioclastic levels. The sediments corresponding to the remainder of the *parkinsoni* Zone are characterized by well-developed sponge-rich limestone beds. The basis of this succession is equally enriched in ferruginous ooids. These beds are overlapped by an alternation of marl and limestone, dated as Bathonian.
Depositional environments for the Bajocian are interpreted as upper offshore conditions, situated on a carbonate platform slope.

IV-3-1-5 Chaudon-Norante; Vocontian basin, southeast France

The Chaudon-Norante section is located near Digne (Table 2) and belongs to the Vocontian Basin of southeastern France, which developed as a consequence of east-west rifting of the west European margin of the Tethys ocean during the Triassic (Corbin et al., 2000 and references therein). The section sampled in the framework of this study consists of the lower part of a thick hemipelagic succession, for which a detailed ammonite biostratigraphic zonation has been realized by Didier Bert (University of Burgundy, Dijon, France). The measured section corresponds in age to the interval around the limit between the Early and Late Bajocian, i.e., to the uppermost part of the *propinquans* Zone and to the *garantiana* Zone pro parte, and is approximately 80 metres thick.
The lithology corresponds to a rather monotonous hemipelagic succession of marl, marly limestone and limestone (mudstone, *sensu* Dunham, 1962). Faunal assemblages comprise ammonites, bivalve fragments, calcified radiolarians and foraminifera. Trace-fossils such as *Zoophicos* and *Chondrites* are frequent.
Deposits are related to a lower offshore environment. All rocks are dark-coloured and rich in pyrite nodules, which is consistent with an oxygen-depleted environment.

IV-3-1-6 Carcabuey and Casa de Chimeneas sections; southern Spain

These two sections are located in the provinces of Córdoba (Andalusia, southern Spain) and Murcia (southeastern Spain), respectively (Table 2). They correspond to the external zones of the Betic Cordillera, which is a 600 km long by 200 km wide, WSW-ENE trending belt extending from the Cádiz to the Valencia provinces, which incorporates the western extreme of the European Alpine mountain belt. More precisely, the sections belong to the Subbetic Domain (Sandoval, 1983), an area remote from the continent in which pelagic facies were deposited from the beginning of the main intracontinental phase of rifting onwards (190 My ago; García-Hernández et al., 1989). The Sierra de Gaena (central sector of the External Subbetic) and Sierra Ricote (eastern sector of the Median Subbetic) are the Subbetic areas in which the Early/Late Bajocian transition is best documented with abundant, representative and relatively well-preserved ammonites, which allow a detailed biostratigraphical analysis (Sandoval, 1983). Samples corresponding to these two sections were obtained from Dr. Annachiara Bartolini (University ParisVI) and Prof. José Sandoval (University of Granada).

The Carcabuey section (Sierra de Gaena) is 36 metres thick and crops out along the Puerto Escaño path, 1200 m W of the village of Carcabuey, province of Córdoba (Table 2).
The section has previously been studied by Delgado et al. (1980), who analyzed the "ammonitico rosso" facies. Sandoval (1983, 1986, 1990, 1998) carried out biostratigraphic and paleontologic analyses. In this section, the Bajocian/lower Bathonian interval is relatively well represented. Ammonite assemblages permit to recognize the *discites*, *laeviuscula*?, *propinquans*, *humphriesianum*, *niortense*, *annulatum* and *parkinsoni* ammonite Zones within the Bajocian (Sandoval, 1983, 1986, 1990).
The studied part of this section spans the time interval from the early Bajocian (*discites* Zone) to the Bathonian.

Lower Bajocian beds (*discites*, *laeviuscula*?, and *propinquans* pro parte Zones) consists of 15 m of light-grey micritic limestone (mudstone and wackestone with radiolarians and crinoids). Chert nodules are abundant in this interval. The *propinquans* (pro parte) to *niortense* Zones (9.2 m thickness) are composed of grey to reddish nodular limestone (wackestone to packstone, containing echinoderms fragments, radiolarians, and benthic foraminifera in particular). Small sedimentary hiatuses have been identified (Delgado et al., 1980; Sandoval, 1983). The *annulatum* and *parkinsoni* Zones are represented by 7.5 m of yellowish to red marl, nodular marly limestone and red nodular limestone (wackestone to packstone). Some episodes of turbiditic deposits are recorded. The uppermost part of the section corresponds to the Early to Middle Bathonian and consists of 4.3 m of alternating reddish nodular limestone and marl with microfacies similar to those of the underlying beds.
General depositional conditions correspond to a lower offshore environment with possible incursions into the upper offshore.

The Casa de Chimeneas section (Sierra Ricote) is approximately 102 metres thick and crops out along a local road, nearly 1800 m south of the Cabezo Inés and 1500 m NW of the Cerro Mahoma, Mula, province of Murcia (Table 2). An abundant and diversified ammonite fauna allowed for a detailed biostratigraphic analysis. No biostratigraphic gaps were detected in this stratigraphical interval. Within the *humphriesianum* Zone the *romani*, *humphriesianum* and *blagdeni* Subzones have been recognized, and within the *niortense* Zone the of *banksi*, *polygyralis* and *baculata* Subzones, although some of the subzonal ammonite index species were scarcer or even absent.
The lower part of the section (belonging to the Early Bajocian *humphriesianum* Zone, pro parte) is made out of approximately 56 m of grey-whitish marls and marly limestone (mudstone and wackestone, *sensu* Dunham, 1962). At the base of the section (*romani* Subzone), marl predominates over marly-limestone; in the middle part (*humphriesianum* Subzone), calcareous beds become thicker and chert - in the form of nodules and thin intercalations - is relatively common. In the upper part of the *humphriesianum* Zone (*blagdeni* Subzone), two small slump levels occur; cherty concretions and chert intercalations disappear, and bioturbation, especially *Zoophycos*, is very common. The lower part of the Late Bajocian, belonging to the *niortense/leptosphinctes* Zone, is approximately 46 m thick. Lithology and microfacies are similar to those of the sediments of the underlying *humphriesianum* Zone but marly intercalations clearly dominate with regards to marly-limestone beds. The bivalve *Bositra* is very abundant throughout the section. Some belemnoids and gastropods are also presents in sediments of the Late Bajocian.
The here analyzed deposits are characteristic of a lower offshore environment.

IV-3-2 Oxfordian sections

IV-3-2-1 Gorges du Pichoux section; Swiss Jura mountains

The Gorges du Pichoux section crops out in the Jura Mountains (JU, Switzerland). The profile is located between Sornetan and Undervelier in the southern part of the Gorges du Pichoux (Table 2).

This succession is part of a wide-scale carbonate platform which extended from the Aquitaine toward the Bohemian area during the Oxfordian.

This platform was located on the northern margin of the Ligurian Tethys, which was subjected to an extensional phase (Ziegler, 1988).
This section was first decribed by Hug (2003) and the samples analyzed in the framework of this study have been provided by this author.

The here considered calcareous succession is 80 metres thick and spans the time interval from the Late Oxfordian (*bimammatum* Zone pro part) to the lower part of the Early Kimmeridgian.
The profile starts with lagoonal sediments with oncoids, followed by beds richer in ooids and quartz (6 -12.4 m). All these limestone beds present fluctuating evaporitic contents. From 6.8 to 9.9 metres the banks are strongly dolomitized, and show the presence of peloids and high amounts of organic matter. A level rich in gastropods can be observed between 12 and 12.4 m. Beginning at 12.4 m, a pronounced change in carbonate facies is determined. Black-coloured ooids are abundant in a level of a few centimetres thickness. Above this level, the sediments become marlier, perhaps recording the presence of a maximum flooding zone. After 18.2 m the bioturbation intensity and marl ratio decrease. In this part of the section, sediments comprise thin stratigraphic layers of limestone rich in oncoids, gastropods and coral fragments. From approximately 18.2 to 19.7m, beds are affected by dolomitization and include pseudomorphoses after gypsum and anhydrite. The overlying peloidal mudstone facies shows an increase in the quartz content. Sedimentation then comprises elevated contents of quartz and organic material, gypsum- and anhydrite-pseudomorphoses, as well as reddish oncoids, and records an emersion episode occurring at 23 m. The overlying banks are thicker and vary between peloidal micritic facies to oolitic bars. They correspond to a semi-restricted lagoonal system with middle to high energy. From 31 to 50 m, thick oolitic sandbars characterize sedimentation patterns. The last centimetres are increasingly affected by evaporation, which may indicate an emersion under sabkha-like conditions. After 50 m the number of peloids increase, as well as the ooid and oncoid contents. A highly bioturbated bank of 34 cm thickness is visible at 51 m. Subsequent sediment layers are first characterized by a high amount of peloids, and show in the following a strongly oolitic facies. Starting at 60 m the layering is disturbed by tectonic fracturation and minor faults; consequently, errors of several cm thickness in the measuring are possible. Finally, at 74.4 m, a distinctive facies change occurs. The high-energy, intertidal and oolitic bar depositional system is replaced by a low-energy, subtidal depositional system characterized by increasing peloidal production.

The fauna is mainly represented by echinoids (mostly observable in the lower and uppermost parts), and for the lower part brachiopods, gastropods and bivalves. At the basis of this succession, coral fragments are found, which were likely derived from the destruction of a nearby reef. Depositional conditions range from restricted to semi-restricted lagoonal environments to more open-marine settings related to the oolitic barrier (subtidal to supratidal bathymetry).

IV-3-2-2 Rochers du Saussois, Roche aux Poulets, and outcrops of the Frétoy forest, Précy-le-Sec, Clamecy; Lower Burgundy, France

The carbonate succession which crops out in the Lower Burgundy area belongs to the same palaeogeographical realm as that of the Pichoux section (Fig. 1). They particularly correspond to the Late Oxfordian Mailly-le-Château reef complex (Ménot, 1991).

Le Saussois section has been studied at the Le Saussois cliff, which outcrops 5500 m southwest of the village of Mailly-la-Ville, in the vicinity of the Merry-sur-Yonne village (Table 2). The upper 25 m of this outcrop have been studied; they correspond in age to the Late Oxfordian *bimammatum* Zone (Ménot, 1991).
This section is composed of a rather homogeneous alternation of thick, weathering-resistant layers, rich in coral (*Madreporas*) build-ups, and more micritic (wackestone to packstone) beds, locally rich in coral clasts, which are more deeply eroded. Depositional conditions are characteristic of shallow-water, lagoonal environments, ranging from the reef barrier to the more restrictive lagoonal micritic facies.

The base of the Roche aux Poulets section is stratigraphically equivalent to the upper part of the Le Saussois section (Menot, 1991; Chevalier et al., 2001) and displays similar carbonate facies. The uppermost part of this section is characterized by the development of a beach facies (bioclastic grainstone with *fenestrae*, graded bedding, and slightly oblique stratifications).

Six small sections, related to the upper part of the Late Oxfordian Mailly-le-Château reef complex (Mégnien et al., 1970; Mégnien et al., 1971, 1972), have been investigated along a NW-SE transect inside the Frétoy Forest. This transect is situated between the villages of Courson-les-Carrières (north) and Coulanges-sur-Yonne (south), between the junction point of the road D.130 and the Grange Cathelin Line and the junction point of the road D.39 and the Lac Marry Line (Table 2). Each section is a few metres thick. Most of the carbonate successions display a rather homogeneous facies corresponding to very white, almost pure lagoonal micrite lacking sedimentary structures, containing sparse clasts of corals or bivalves. In contrast, the section situated at the southeastern extremity of the transect is composed of thin limestone beds rich in bioclasts.

Laterally equivalent carbonate rocks have equally been sampled in soils corresponding to the Précy-le-Sec and Clamecy area (Table 2). They present carbonate facies similar to those of the Frétoy forest section (white lagoonal micrite).

IV-3-3 Aalenian to Kimmeridgian/Tithonian section

Terminilletto section; central Italy

This carbonate succession crops out in central Italy, along the E-SE side of Monte Terminilletto (Table 2). It belongs to the Umbria-Marche Basin, which, during Jurassic times, was part of the southern continental margin of the western Tethys.

The Terminilletto section was previously studied by Bartolini et al. (1996), and samples analyzed in the framework of this study were obtained from Dr. Annachiara Bartolini (University ParisVI).
The Terminilletto section is dated as early Aalenian to early Tithonian in age and is 235 metres thick. Carbonate rocks present in this section were deposited along a N-S fault separating the Umbria-Marche Basin from the Lazio-Abruzzi carbonate platform (Bartolini et al., 1996 and references therein). The sediment succession is therefore composed of both cherty pelagic limestone, as well as platform-derived carbonates in the form of gravity-flow deposits and exported peri-platform ooze.
The interval corresponding to the Early to Middle Aalenian (0 - 40 m) is composed of micritic limestone (mudstone to wackestone), with intercalations of platform resediments of 20-30 cm thickness (oolitic grainstone) to 40-90 cm thickness (pebbly mudstone). Chert nodules are episodically present. The interval ranging from the Middle Aalenian to Early Bajocian (40 - 110 m) comprises mudstone as well as resedimented beds, which decrease upward in abundance. Chert occurrences in the form of nodules and ribbons become frequent, and display reddish colours beginning at 45 m. Resedimented beds composed of oolitic grainstone are frequent in the last part of this interval, as well as during the Early Bajocian to Middle Bathonian (110 - 160 m). The lithology of this latter interval is dominated by bioclastic packstone to grainstone, and mainly composed of echinoderm fragments, alternating with mudstone to packstone. Chert is only sporadically present, and disappears totally between 130 and 160 m. The sediments corresponding to Middle Bathonian - Late Oxfordian (160 - 196 m) are constituted of radiolarian mudstone with abundant red or green chert, with intercalations of resedimented beds comprising ooids, crinoids and bioclasts. The Late Oxfordian to Kimmeridgian/Tithonian deposits (196 - 256 m) display alternating beds of radiolarian-rich mudstone, cherty limestone (more abundant up to 236 m), and resedimented beds (mainly oolitic up to 220 m, and principally bioclastic afterward).
This carbonate succession is characteristic of a depositional environment located in the lower offshore.

Table. 2. Next page. Approximated geographical coordinates of the sections (western and southern Europe) related to this study, as well as of the sections previously described and studied by Veuve (2000) in the Swiss Jura Mountains.

Table 2. International coordinates of studied sections (1/3)

Lausen/Schleifenberg

Lower part
Lat:
47:28:07N (47.4687)
Lon:
7:46:04E (7.7678)

Upper part
Lat:
47:29:31N (47.4919)
Lon:
7:44:29E (7.7415)

Vergisson/Davayé

Lower part
Lat:
46:18:42N (46.3116)
Lon:
4:43:20E (4.7222)

Upper part
Lat:
46:18:08N (46.3023)
Lon:
4:44:30E (4.7417)

Lucy-le-Bois

Lat:
47:33:30N (47.5584)
Lon:
3:53:37E (3.8937)

Blacy-fields

Lat:
47:34:02N (47.5673)
Lon:
4:02:30E (4.0417)

Blacy-forest

Lat:
47:34:00N (47.5666)
Lon:
4:02:29E (4.0413)

Sainte-Honorine des Pertes

Lower part
Lat:
49:21:12N (49.3533)
Lon:
0:47:18W (-0.7883)

Upper part
Lat:
49:21:17N (49.3548)
Lon:
0:47:57W (-0.7992)

Chaudon-Norante

Lat:
43:59:33N (43.9924)
Lon:
6:19:17E (6.3214)

Carcabuey

Lat:
37:26:38N (37.4439)
Lon:
4:17:06W (-4.2851)

Local equivalent coordinates
UTM UG855447, Scheet 989, Lucena (South Spain)

Casa de Chimeneas

Lat:
38:07:33N (38.1257)
Lon:
1:30:52W (-1.5157)

Local equivalent coordinates
UTM XH316209, Scheet 912, Mula (South Spain)

Table 2. International coordinates of studied sections (2/3)

Pichoux		
	Lat:	47:17:10N (47.2862)
	Lon:	7:13:39E (7.2275)
Le Saussois		
	Lat:	47:33:58N (47.5662)
	Lon:	3:38:42E (3.6449)
Roche aux Poulets		
ME	Lat:	47:33:53N (47.5648)
	Lon:	3:37:52E (3.6312)
FE	Lat:	47:33:55N (47.5658)
	Lon:	3:37:51E (3.6309)
Frétoy Forest		
Transect	Lat:	47:35:11N (47.5863)
	Lon:	3:33:52E (3.5644)
	Lat:	47:33:20N (47.5555)
	Lon:	3:35:40E (3.5945)
Detailed		
FM	Lat:	47:33:56N (47.5656)
	Lon:	3:35:12E (3.5866)
FR	Lat:	47:34:41N (47.5779)
	Lon:	3:34:14E (3.5706)
RA	Lat:	47:35:05N (47.5846)
	Lon:	3:33:59E (3.5663)
CH	Lat:	47:33:20N (47.5555)
	Lon:	3:35:40E (3.5945)

Frétoy Forest (continued)		
AN	Lat:	47:35:11N (47.5863)
	Lon:	3:33:52E (3.5644)
FF	Lat:	47:33:43N (47.562)
	Lon:	3:34:57E (3.5825)
Fret 1/2	Lat:	47:34:09N (47.569)
	Lon:	3:35:04E (3.5844)
Précy le Sec		
	Lat:	47:36:40N (47.6112)
	Lon:	3:50:41E (3.8447)
Clamecy		
	Lat:	47:27:19N (47.4554)
	Lon:	3:29:42E (3.4951)
Terminilletto		
	Lat:	42:27:05N (42.4515)
	Lon:	12:58:50E (12.9807)

Table 2. International coordinates of studied sections (3/3)
Sections studied by Philippe Veuve

Pont-de-la-Baleine

Lat:
46:57:13N (46.9536)
Lon:
6:44:21E (6.7391)

La Vue-des-Alpes

Lat:
47:04:31N (47.0752)
Lon:
6:52:31E (6.8752)

Le Gurnigel

Lat:
47:05:10N (47.0861)
Lon:
6:54:09E (6.9025)

Auenstein

Lat:
47:25:30N (47.4251)
Lon:
8:08:53E (8.148)

Dornach

Lat:
47:28:16N (47.4712)
Lon:
7:36:39E (7.6107)

References

Bartolini, A., Baumgartner, P.O., and Hunziker, J., 1996. Middle and late Jurassic carbon stable-isotope stratigraphy and radiolarite sedimentation of the Umbira-Marche basin (central Italy). Eclogae geologicae Helvetiae, 89, 811-844

Blakey, R., 2005. Paleogeography Through Geologic Time. Available at http://jan.ucc.nau.edu/~rcb7/global_history.html.

Chevalier F., Garcia JP, Quesne D., Guiraud M. and Menot JC (2001). Corrélations et interprétations génétiques dans les formations récifales oxfordiennes de la haute vallée de l'Yonne (sud-est du bassin de Paris, France). Bull. Soc. géol. France, 172 (1), 69-84

Corbin, J.C., Person, A., Iatzoura, A., Ferré, B., Renard, M., 2000, Manganese in pelagic carbonates: indication of major tectonic events during the geodynamic evolution of a passive continental margin (the Jurassic Europeann margin of the Tethys-Ligurian Sea). Palaeogeography, Palaeoclimatology, Palaeoecology, 156, 123-138

Delgado, F., Linares, A. Sandoval, J. and Vera, J.A., 1980. Contribution à l'étude de l'Ammonico Rosso du Dogger dans la Zone Subbétique. In: Rosso Ammonitico Symp. Proc., Farinacci, A., Ed., Tecnosscienza, Roma, 181-197

Dunham, R. J., 1962. Classification of carbonate rocks according to depositional texture. American Association of Petroleum Geologists Memoir 1, 108-121

García-Hernández, M., López-Garrido, A.C., Martín-Algarra, A., Molina, J.M., Ruiz-Ortiz, P.A and Vera, J.A., 1989. Las discontinuidades mayors del Jurásico de las Zonas Externas de las Cordilleras Béticas: análisis e interpretacíon de ciclos sedimentarios. Cuadernos de Geología Ibérica, 13, 35-52

Geiger M., Clark, D.N. and Mette W., 2004. Reappraisal of the timing of the breakup of Gondwana based on sedimentological and seismic evidence from the Morondava Basin, Madagascar. Journal of African Earth Sciences, 38, 363-381

Gonzales, R., 1993. Die Hauptrogenstein-Formation der Nordwestschweiz (mittleres Bajocien bis unteres Bathonien). Unpublished Ph.D. thesis, University of Basel, 191p.

Gonzales, R., and Wetzel, A., 1996. Stratigraphy and paleogeography of the Hauptrogenstein and Klingnau Formation (middle Bajocian to late Bathonian), northern Switzerland. Eclogae geologicae Helvetiae, 89, 695-720

Gradstein, F.M., Ogg, J.G., Smith, A.G. et al., 2004. A Geologic Time Scale 2004. Cambridge University Press, ~ 500 pp.

Hug, W.A., 2003. Sequenzielle Faziesentwicklung der karbonatplattform des Schweizer Jura im Späten Oxford und frühensten Kimmeridge. Geofocus, 7, 156 pp.

Mégnien, C., Mégnien, F. and Turland, M., 1970. Le récif oxfordien de l'Yonne et son emplacement sur la feuille Vermenton (1/50 000). Bull. BRGM (deuxième série), I(3), 83-115

Mégnien, C., Mégnien, F., Turland, M. and Villalard, P., 1971. Carte géologique de la France au 1/50 000, feuille Vermenton. Bull. BRGM, XXVII (21)

Mégnien, C., Mégnien, F., Turland, M. and Villalard, P., 1972. Carte géologique de la France au 1/50 000, feuille Courson-les-Carrières. Bull. BRGM, XXVII(21)

Ménot, J.C., 1991. Formations d'âge Oxfordien dans la vallée de l'Yonne. In: Sédimentation, diagenèse et séquences de dépôt dans les séries carbonatées de plate-forme d'âge bathonien à oxfordien en Bourgogne. In: Floquet M., Javaux C., Menot JC and Purser BH. Livret-Guide A.S.F., 27-29 June 1991, 125-174

d'Orbigny, A., 1849-1852. Cours élémentaire de Paléoécologie et de Géologie Stratigraphique. Masson, vol. 2, 846 pp.

Préat, A., Mamet, B., De Ridder, C., Boulvain, F. and Gillan, D., 2000. Iron bacterial and fungal mats, Bajocian stratotype (Mid-Jurassic, northern Normandy, France). Sedimentary Geology, 137, 107-126

Rioult, M., 1964. Le stratotype du Bajocien. Coll Jurassique, Luxembourg 1962. Publ. Inst.Grand Ducal Luxembourg. Sci. Nat. Phys. Math., 239-258

Rioult, M., Dugué, O., Jan du Chêne, R., Ponsot, C., Fily, G., Moron, J.M. and Vail, P.R., 1991. Outrop sequence stratigraphy of the Anglo-Paris Basin, Middle to Upper Jurassic (Normandy, Maine, Dorset). Bull. centres Rech. Explor.-Prod. Elf Aquitaine, 15 (1), 101-194

Sandoval, J., 1983. Bioestratigraphía y Paleontología (Stephanocerataceae y Perisphinctaceae) del Bajocense y Bathonense de las Cordilleras Béticas. PhD Thesis, Servicio de Publicaciones, University of Granada, 613 pp.

Sandoval, J., 1986. Middle Jurassic Haploceratidae (Ammonitina) from the Subbetic Zone (South Spain). Geobios, 19, 435-463

Sandoval, J., 1990. A revision of the Bajocian divisions in the Subbetic Domain (Southern Spain). In: Cresta, S. and Pavia, G., Eds, Proceeding Meeting on Bajocian Stratigraphy, Memorie descrittive della Carta geologica d'Italia, 40, 237-255

Sandoval, J., 1998. The Bajocian/Bathonian boundary in the Subbetic domain, Betic Cordillera (southern Spain): a typical Mediterranean domain. In: 5th International Symposium on the Jurassic System: Abstract and Program. International Union of Geological Sciences, p. 80

Thiry-Bastien, P., 2002. Stratigraphie séquentielle des calcaires bajociens de l'Est de la France (Jura - Bassin de Paris). PhD Thesis, Université Claude Bernard - Lyon 1, Lyon, France, 410 pp.

Veuve, P., 2000. Etude géochimique et sédimentaire d'un enrichissement en cadmium observé dans les calcaires oolitiques jurassiques du Jura. Unpublished diploma thesis, Univ. NE, 56 pp.

Ziegler, PA, 1988. Evolution of the Arctic-North Atlantic and Western Tethys. AAPG Memoir 43, 198 pp.

V - Anomalous cadmium enrichments in Tethyan Jurassic carbonates: past and present environmental implications

(in prep. for ? Geochimica et Cosmochimica Acta)

Claire Rambeau[1*], Karl B. Föllmi[1], Thierry Adatte[1] , Denis Baize[2], Annachiara Bartolini[3], Wolfgang A. Hug[4], Virginie Matera[1], José Sandoval[5], Philipp Steinmann[1], Philippe Veuve[1]

[1]*Institut de Géologie, Université de Neuchâtel, rue Emile-Argand 11, CH-2007 Neuchâtel, Switzerland*
[2] *Unité de Science du Sol, Institut National de la Recherche Agronomique, Av. de la Pomme de Pin, Ardon, F-45166 Olivet Cedex, France*
[3] *Laboratoire de Micropaléontologie, Université Pierre et Marie Curie, 4 Place Jussieu, F-75252 Paris 05, France*
[4]*Section d'archéologie et de paléontologie, Office de la Culture, République et Canton du Jura, Hôtel des Halles,CP 64, CH-2900 Porrentruy 2, Switzerland*
[5]*Departamento de Estratigrafía y Paleontología, Universidad de Granada, Campus Fuentenueva, E-18002 Granada, Spain*

[*]To whom correspondence should be addressed.
Telephone number: ++41 32 718 25 96. Fax number: ++41 32 718 26 01.
E-mail: claire.rambeau@unine.ch

Abstract

Cadmium is a highly toxic element which is transferred into the environment by natural and anthropogenic processes. Important natural sources are volcanic emissions and the biogeochemical weathering of cadmium-bearing rocks. Carbonate rocks are generally depleted in cadmium relative to average continental crust and are not considered to be a major source of cadmium to the environment. Here we describe the occurrence of Middle and Upper Jurassic carbonates of Tethyan origin in western and southern Europe, which are considerably enriched in cadmium, independent of their particular facies. These carbonates constitute area sources for soils, which have a strong tendency to be naturally contaminated in cadmium. Furthermore, the periods of preferential cadmium enrichment appear to be contemporaneous with positive anomalies in the $\delta^{13}C$ and the phosphorus burial records. This may point to a relationship between changes in the carbon cycle, intensity in weathering and volcanism, and cadmium release and accumulation during the Jurassic.

Keywords: cadmium, carbonates, Jurassic, Tethys, Europe, contaminated soils

V-1 Introduction

Cadmium (Cd) is extracted from the Earth's crust as a by-product from the exploitation of phosphate and non-ferrous metal deposits such as zinc, lead and copper. Approximately 20,000 metric tonnes are extracted each year by man (19,700 metric tonnes in 2000; COWI A/S, 2003), a quantity that is comparable to the amount of Cd released by natural processes involving the weathering and erosion of Cd-bearing parent rocks (estimated to be 15,000 metric tonnes per year; Dobson, 1992). Cd-bearing parent rocks such as ore bodies, phosphorites, and organic-rich sediments are generally limited in their lateral extension and act as point or line sources rather than an area source, which restricts the transfer of Cd into the soil to small and rather well-defined areas. Here, we describe a newly identified Cd-bearing parent rock, Tethyan carbonate rocks of Middle and Upper Jurassic age, which are unusually rich in Cd and which may act as an area source for the transfer of natural Cd to associated soils and vegetation.

V-2 Cadmium in Jurassic carbonates and their associated soils

Carbonates and carbonate rocks are generally strongly depleted in Cd (0.03-0.035 mg/g on average; Gong et al., 1977; Tuchschmid, 1995) in comparison to average continental crust (0.1 mg/g; Wedepohl, 1995). In the Swiss and French Jura Mountains, however, soil scientists have established that soils with anomalously high Cd concentrations are consistently associated with carbonate rocks that are exceptionally rich in Cd (Baize and Sterckeman, 2001; Dubois et al., 2002; Prudente et al., 2002). These rocks have been assigned to the Bajocian and Oxfordian-Kimmeridgian (approximately 172-168 and 161-151 Ma; Gradstein et al., 2004) stages of the Jurassic period, and have been shown to contain Cd concentrations of up to 8.15 µg/g (Baize and Sterckeman, 2001; Dubois et al., 2002). Soils associated with these carbonate rocks contain up to 22.3 µg/g Cd (Prudente et al., 2002); a value that exceeds by one order of magnitude the Swiss and French official tolerance guideline values of 0.8 µg/g (Osol, 1986, 1998) and 2 µg/g (AFNOR, 1996), respectively.

The purpose of this contribution is to show the importance of these Cd enrichments on a stratigraphic and regional scale. We examined a series of representative carbonate successions of Middle and Upper Jurassic age in different regions of Switzerland, France, Spain (all belonging to the former NW Tethyan margin - Fig.1) and Italy (belonging to the SW Tethyan margin - Fig.1), with different marine sedimentary origins (near-shore to open-marine settings) (Fig. 2; Table 1). One of the studied sections, the deeper-water section at Terminilletto, central Italy (Bartolini et al., 1996), is of particular interest, since it covers carbonate sediments from the Aalenian (lowest Middle Jurassic) to the Tithonian (uppermost Jurassic), thereby providing information on the general evolution of Cd contents for this interval. The set of samples analyzed was the same as that used previously to generate a detailed whole-rock stable carbon ($\delta^{13}C$) isotope record for the succession (Bartolini et al., 1996; Fig. 2).

V-2-1 Measurement of cadmium contents

Inductively Coupled Plasma-Mass Spectrometry (ICP-MS) analyses were performed on bulk rock samples. Powders were obtained using a mechanic agate crusher. A portion of approximately 250 mg was transferred into a PTFE digestion vessel and 10 ml of concentrated nitric acid (65 %, suprapur, Merck) were added. The sample was digested in a microwave oven (MSL-Ethos plus, Milestone) using the heating program recommended by the EPA 3051 procedure. After cooling, the resulting solution was filtered (0.45 μm) and diluted to 100 ml with ultrapure water. A second dilution (1/20) was then performed prior to analysis. Rhodium was used as the internal standard, in order to correct for matrix-induced ion signal variations and instrumental drift. The element concentrations of the acid digests were determined by ICP-MS (ELAN 6100, Perkin Elmer) using full mass-spectra scans (panoramic method). Certified reference materials (CRMs) for trace metals in natural water (NIST 1640) and lake sediments (LKSD-1) were used to estimate the accuracy of the method. The mean recovery rates for cadmium in these CRMs were 99% and 101.1%, respectively.

Figure 1. Next Page. Palaeogeographic maps of western and southern Europe for the Middle and Late Jurassic (modified from Ziegler, 1988) showing the original location of the studied sections.

Figure 2. Page 55. Cd contents in mg/g for a selection of sections of Middle and Upper Jurassic age (Lausen-Schleifenberg, NW Switzerland: lower part 47:28:07N - 7:46:04E, upper part 47:29:31N - 7:44:29E, shallow-water oolitic facies; Vergisson-Davayé, eastern France: lower part 46:18:42N - 4:43:20E, upper part 46:18:08N - 4:44:30E, shallow-water crinoidal facies; Ste-Honorine-des-Pertes, NW France: lower part 49:21:12N - 0:47:18W, upper part 49:21:17N - 0:47:57W, ferruginous oolitic and spongy micritic facies; Carcabuey, southern Spain: 37:26:38N - 4:17:06W, open-marine micritic facies; Gorges du Pichoux, NW Switzerland: 47:17:10N - 7:13:39E, oolitic, oncolitic and lagoonal micritic facies; Terminilletto, central Italy: 42:27:05N - 12:58:50E, open-marine micritic carbonates), and d13C values (relative to V-PDB; from Bartolini et al., 1996) measured on the same set of whole-rock samples for the Terminilletto section. Note the different scale for Cd concentrations at the Terminilletto section. Aal. = Aalenian; Baj. = Bajocian; Bat. = Bathonian; Cal. = Callovian; Oxford. = Oxfordian; Ear = Early; Mid. = Middle; Z. = Zone(s); d. = *discites*; l. = *laeviuscula*; pr./p. = *propinquans*; humphr./h. = *humphriesianum*; n. = *niortense*; g. = *garantiana*; pa. = *parkinsoni*. The Cd and d13C measurements are represented by black dots. The grey curves correspond to a five-point moving average.

Fig. 1

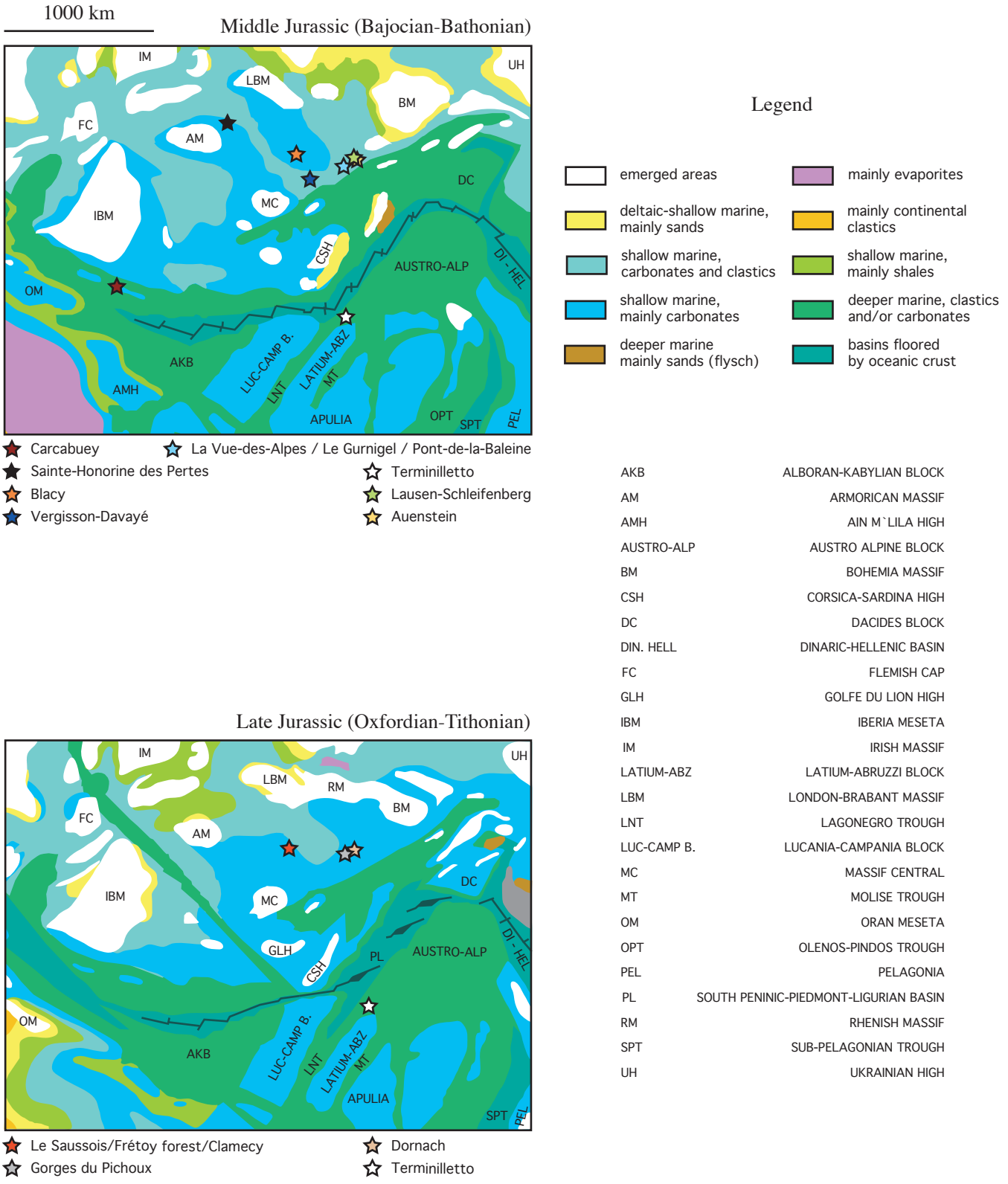

AKB	ALBORAN-KABYLIAN BLOCK
AM	ARMORICAN MASSIF
AMH	AIN M`LILA HIGH
AUSTRO-ALP	AUSTRO ALPINE BLOCK
BM	BOHEMIA MASSIF
CSH	CORSICA-SARDINA HIGH
DC	DACIDES BLOCK
DIN. HELL	DINARIC-HELLENIC BASIN
FC	FLEMISH CAP
GLH	GOLFE DU LION HIGH
IBM	IBERIA MESETA
IM	IRISH MASSIF
LATIUM-ABZ	LATIUM-ABRUZZI BLOCK
LBM	LONDON-BRABANT MASSIF
LNT	LAGONEGRO TROUGH
LUC-CAMP B.	LUCANIA-CAMPANIA BLOCK
MC	MASSIF CENTRAL
MT	MOLISE TROUGH
OM	ORAN MESETA
OPT	OLENOS-PINDOS TROUGH
PEL	PELAGONIA
PL	SOUTH PENINIC-PIEDMONT-LIGURIAN BASIN
RM	RHENISH MASSIF
SPT	SUB-PELAGONIAN TROUGH
UH	UKRAINIAN HIGH

Fig. 2

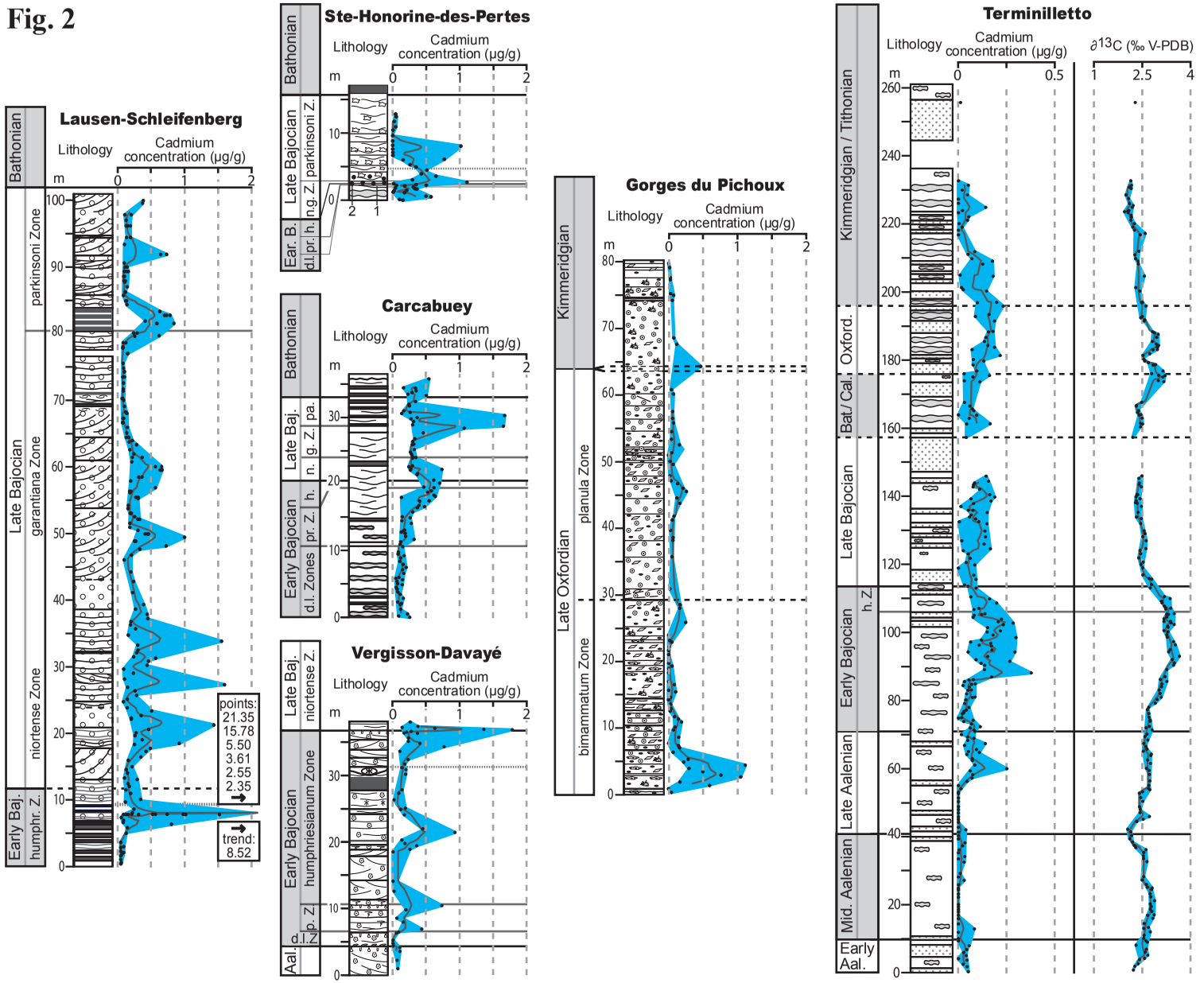
Lausen-Schleifenberg
Lithology
Cadmium concentration (µg/g)
Bathonian
Late Bajocian
parkinsoni Zone
garantiana Zone
niortense Zone
Early Baj.
humphr. Z.
points:
21.35
15.78
5.50
3.61
2.55
2.35
trend:
8.52
Ste-Honorine-des-Pertes
Bathonian
Late Bajocian
parkinsoni Z.
n.g. Z.
Ear. B.
d.l.
pr.
h.
Carcabuey
Bathonian
Late Baj.
pa.
n. g. Z.
h.
Early Bajocian
pr. Z.
d.l. Zones
Vergisson-Davayé
Late Baj.
niortense Z.
Early Bajocian
humphriesianum Zone
p. Z.
d.l.Z
Aal.
Gorges du Pichoux
Kimmeridgian
Late Oxfordian
planula Zone
bimammatum Zone
Terminilletto
Kimmeridgian / Tithonian
Oxford.
Bat./ Cal.
Late Bajocian
h. Z.
Early Bajocian
Late Aalenian
Mid. Aalenian
Early Aal.
∂13C (‰ V-PDB)
Lithology
limestone
cherty limestone
nodular limestone
marly limestone
calcareous conglomerate
marl
resedimented limestone
Non-skeletal grains
oolites
pebbles
ferruginous oolites
oncoids
ferruginous oncolites
peloids
chert nodules
dolomite
Fauna
coral reef
sponges
coral clasts
bivalve clasts
crinoids
echinids
Sedimentary structures
erosional surfaces
channels
cross stratification
Biological structures
bioturbation
stromatolites
Surfaces
bored surface
hardground
Composite sections
correlation surface between two neighbouring sections
Tectonics
minor faults/fracturation

V-2-2 Cadmium contents of Middle and Upper Jurassic carbonates

The carbonate rocks analyzed show a general increase in Cd concentrations for samples which are associated with the Bajocian stage (*propinquans* to *parkinsoni* Zones; Fig. 2). In the sections from the NW Tethyan margin (Fig. 1), Bajocian carbonate rocks attributed both to shallow-water settings (oolitic and bioclastic carbonate rocks; Fig. 2, Table 1) and to open-marine settings (micritic carbonate rocks, Fig. 2) exhibit background values of 0.2-0.4 µg/g Cd. Furthermore, these successions contain intervals in the high Lower and Upper Bajocian (*humphriesianum* Zone to *parkinsoni* Zone: Fig. 2), which are consistently enriched in Cd, with maximum values of 1-2 µg/g Cd. An exceptionally enriched sample in the Lausen-Schleifenberg section contained up to 21.4 µg/g Cd (Fig. 2). Carbonate rocks of the Terminilletto section, which are attributed to an open-marine setting (micritic carbonate rocks) along the SW Tethyan margin (Fig. 1), show an interval of increased Cd contents (values of 0.1-0.3 µg/g Cd), in the uppermost Aalenian - Bajocian (Fig. 2). Oxfordian near-shore carbonate deposits (oolitic, oncolitic, and lagoonal micritic carbonates) from Switzerland and France (Fig. 1, Table 1) also show background concentrations varying from <0.04 µg/g (detection limit) to 0.2-0.4 µg/g Cd, and include enriched levels with a maximum value of 1.34 µg/g Cd (Fig. 2). Intervals with the highest Cd contents occur in the Upper Oxfordian (*bimammatum* Zone). The Terminilletto section also shows a general increase in Cd contents, with values up to almost 0.25 µg/g Cd, in the Oxfordian - Lower Kimmeridgian (Fig. 2). In general, the sections show enrichments in Cd contents for intervals which are dated as Late Aalenian - Bajocian, and Oxfordian – Early Kimmeridgian in carbonate rocks of shallow-water to open-marine facies, with the NW Tethyan successions being consistently more enriched in Cd than the SW Tethyan succession at Terminilletto, both with regards to the background values and to the maximum values.

V-2-3 Cadmium contents in soils developed from cadmium-enriched Jurassic carbonates

In soils associated with Cd-enriched carbonate rocks, Cd has been suggested to concentrate by progressive carbonate dissolution and in-situ adsorption on clay minerals and iron oxyhydroxides (Prudente et al., 2002). At the Frétoy forest, a site near Avallon (Burgundy, France), an enrichment factor of 5.7 is observed in soils associated with an Upper Oxfordian carbonate reef complex. At Blacy, a site also near Avallon, an enrichment factor of 5.5 is estimated for soils developed from Bajocian crinoidal limestones (Table 1). These enrichment factors are comparable to those derived from literature data (Baize and Sterckeman, 2001; Dubois et al., 2002) for the Swiss sites at Le Gurnigel and Dornach (Table 1). This demonstrates that soils developed from Cd-enriched carbonates have considerable potential to be naturally contaminated with Cd, if the Swiss (0.8 µg/g) or French (2 µg/g) tolerance guideline values are applied. This is all the more important since the Cd-enriched carbonates may reach stratigraphic thicknesses of several 10's of meters, which renders them diffuse area sources of Cd to the environment.

Table 1. Cd concentration in Middle and Upper Jurassic carbonates and their associated soils in Switzerland and France

Sample location	Stratigraphy	Carbonate facies	Cd concentration (µg/g) in carbonate rocks			Cd concentration (µg/g) in soils			Enrichment factor
			N	Mean value (SD)	Range	N	Mean value (SD)	range	
Pont-de-la-Baleine Jura, Switz.	Upper Bajocian	oolitic limestone; marly limestone	23	**0.43** (0.90)	0.01 - 3.42	-	-	-	-
La Vue-des-Alpes Jura, Switz	Bajocian	micritic, oolitic, bioclastic limestone	52	**0.21** (0.17)	0.02 - 0.79	-	-	-	-
Le Gurnigel Jura, Switz.	Upper Bajocian	oolitic limestone; bioclastic limestone	12 (1)	**0.84** (0.57)	0.14 - 1.62 (1)	9 (1)	**6.11** (2.93)	2.21 - 10.30 (1)	**7.3**
Auenstein Jura, Switz.	Bajocian	oolitic limestone	20	**0.14** (0.24)	0.04 - 1.11	-	-	-	-
Blacy (fields/forest) Burg., France	Bajocian	crinoïdal limestone	7(**)	**0.27** (0.20)	0.04 - 0.63	9	**1.47** (0.45)	-	**5.5**
Dornach Jura, Switz.	Upper Oxfordian	oolitic, bioclastic, micritic limestone	7	**0.65** (0.35)	0.33 - 1.34	15 (2)	**4.12** (3.80)	0.87 - 11.04 (2)	**6.3**
Frétoy forest Burg., France	Upper Oxfordian	reef barrier lagoonal micrite	21(*)	**0.28** (0.99)	0.12 - 0.55	4	**1.58** (0.67)	1.20 - 2.59	**5.7**
Le Saussois Burg., France	Upper Oxfordian (*bimammatum* Zone)	reef barrier lagoonal micrite	10	**0.20** (0.21)	0 - 0.66	-	-	-	-

N = number of samples; SD = standard deviation; Switz. = Switzerland; Burg. = Burgundy; (*) samples of the rock substratum; (**) samples of rock fragments within the soil; (1) data from Dubois et al. (2002); (2) data from Baize and Sterckeman (2001).
Enrichment factors calculated between the mean cadmium concentrations in carbonates and in associated soils.

V-3 A link between Jurassic cadmium enrichments and global environmental change?

V-3-1 Stable carbon isotope record

A comparison of the Cd record for the Terminiletto section with the previously established $\delta^{13}C$ record (Bartolini et al., 1996), demonstrates a good correspondence between the high Lower Bajocian interval of maximum Cd values and a positive excursion in $\delta^{13}C$ values (Fig. 2). For the Oxfordian/Lower Kimmeridgian interval of high Cd values, the maxima in Cd contents and $\delta^{13}C$ values show a stratigraphic offset, with Cd enrichment occuring above the $\delta^{13}C$ maximum. The $\delta^{13}C$ record determined at Terminilletto for the Bajocian has been reproduced from other sections in Europe (Bartolini and Cecca, 1999; Jenkyns et al., 2002), whereas the evolution for the Oxfordian part is less well constrained. In fact, published $\delta^{13}C$ records of the Oxfordian show consistently high values (up to approximately 5‰; Jenkyns et al., 2002) for the entire Oxfordian or a maximum for the higher Oxfordian (Wierzbowski, 2004). The positive excursions in the $\delta^{13}C$ record of the Bajocian and Oxfordian stages have been associated with periods of carbonate production crisis, nutrient mobilisation, increased productivity and organic C burial (Bartolini et al., 1996).

V-3-2 Phosphorus record

A close correlation between Cd and phosphorus (P) contents in marine waters is known on a global scale, and Cd contents in sediments have been employed as an approximation of nutrient availability at the time of their formation (Boyle et al., 1976, 1988) in spite of a certain sensitivity of Cd to the redox state in sediments (Rosenthal et al., 1995). In a compilation of averaged P burial rates in marine sediments that extends back to 160 Ma (base Callovian), the Oxfordian is characterized by a maximum in P accumulation (Föllmi, 1995).

Phosphorite deposits - i.e. rocks containing more than 18% P_2O_5 - are known from both the Bajocian and the Oxfordian, and the Middle and Upper Jurassic periods are represented by two distinct maxima in the estimated abundance of economic phosphate deposits (Cook and McElhinny, 1979).

V-4 Discussion and conclusions

1 We suggest a possible link between the positive Cd anomalies measured in carbonates of the Late Aalenian to Late Bajocian and the Oxfordian to Early Kimmeridgian, and associated changes in the C and P cycles as expressed in the $\delta^{13}C$ record, in the estimated abundance of economic phosphate deposits and, for the Oxfordian, in the marine P burial record. These changes are probably related to changes in the intensity of hydrothermal and volcanic processes (Bartolini et al., 1996), which may have led to an increase in the availability of Cd to the environment, and an increase in continental biochemical weathering rates (Föllmi, 1995), eustatic sea-level rise (Hallam, 2001), and higher biological productivity rates (Bartolini et al., 1996; Bartolini and Cecca, 1999).

An important phase of silicic volcanism related to the break-up of Gondwana has been identified both in Patagonia and in Antartica for the Jurassic time, with two major events occurring at 172-162 Ma and 157-153 Ma (Pankhurst et al., 2000), which correspond to latest Aalenian to Callovian and Late Oxfordian to Kimmeridgian times, respectively (Gradstein et al., 2004).

2 At the present day, Cd is preferentially concentrated in organic-rich sediments with reducing conditions near the sediment-water interface (Rosenthal et al., 1995), and in such environments, the release and precipitation of Cd occur during the early diagenetic oxidation of organic matter. Higher productivity rates and the increased transfer of organic matter into the sedimentary reservoir may have been instrumental in the increased transfer and precipitation of Cd during the Middle and Upper Jurassic.

3 The presence of Cd-enriched carbonates of Middle and Late Jurassic age in all investigated sections suggests that this enrichment may occur on a wider scale within western and southern Europe. This would also imply that soils associated with these sedimentary rocks have the potential to be naturally enriched in Cd to levels considerably higher than recommended tolerance guideline levels.

Acknowledgments

We would like to thank Jean-Pascal Dubois, Jean-Michel Gobat, Andreas Wetzel and Ian Jarvis for advice, and Alexis Godet, Stéphane Bodin and Pascal Linder for field assistance. We acknowledge financial support from the Swiss National Science Foundation (projects no. 21-65183.01, 200020-101718/1), from the National Centre of Competence in Research ("Plant Survival") and the Ministerio de Ciencia y Tecnología, Spain (project BTE 2001-3020).

References

AFNOR, NF U44-041, 1996. In: *Qualité des sols. Recueil de normes françaises*. 3e édition, Paris-La Défense, 534 p.

Baize, D., and Sterckeman, T., 2001. Of the necessity of knowledge of the natural pedo-geochemical background content in the evaluation of the contamination of soils by trace elements. *The Science of the Total Environment*, **264**, 127-139.

Bartolini, A., Baumgartner, P. and Hunziker, J., 1996. Middle and late Jurassic carbon stable-isotope stratigraphy and radiolarite sedimentation of the Umbria-Marche basin (central Italy). *Eclogae geologicae Helvetiae*, **89**, 811-844.

Bartolini, A. and Cecca, F., 1999. 20 My hiatus in the Jurassic of Umbria-Marche Apennines (Italy): carbonate crisis due to eutrophication. *Comptes Rendus de l'Académie des Sciences de Paris, Earth and Planetary Sciences*, **329**, 587-595.

Boyle, E.A., Sclater, F.R. and Edmond, J.M., 1976. On the marine geochemistry of cadmium. *Nature*, **263**, 42-44.

Boyle, E.A., 1988. Cadmium: chemical tracer of deepwater paleoceanography. *Paleoceanography*, **3**, 471-489.

Cook, P.J. and McElhinny, M.W., 1979. A re-evaluation of the spatial and temporal distribution of sedimentary phosphate deposits in the light of plate tectonics. *Economic Geology*, **74**, 315-330.

COWI A/S, 2003. *Cadmium review: Report to the Nordic Council of Ministers*. Available at www.norden.org/miljoe/sk/kemirapp_cadmium.asp?lang=6.

Dobson, S., 1992. *Cadmium: environmental aspects*. Environmental Health Criteria 135, World Health Organization, Geneva. Available at www.inchem.org/documents/ehc/ehc/ehc135.htm

Dubois, J.P., Benitez, N., Liebig, T., Baudraz, M. and Okopnik, F., 2002. Le cadmium dans les sols du haut Jura suisse. In: *Les éléments traces métalliques dans les sols. Approches fonctionnelles et spatiales* (D.Baize and M.Tercé, eds) INRA Editions, Paris, 33-52.

Föllmi, K.B, 1995. 160 m.y. record of marine sedimentary phosphorus burial: coupling of climate and continental weathering under greenhouse and icehouse conditions. *Geology*, **23**, 859-862.

Gong, H., Rose, A.W. and Suhr, N.H, 1977. The geochemistry of cadmium in some sedimentary rocks. *Geochimica et Cosmochimica Acta*, **41**, 1687-1692.

Gradstein, F.M., Ogg, J.G., Smith, A.G. et al., 2004. *A Geologic Time Scale 2004*. Cambridge University Press, ~ 500 pp.

Hallam, A., 2001. A review of the broad pattern of Jurassic sea-level changes and their possible causes in the light of current knowledge. *Palaeogeography, Palaeoclimatology, Palaeoecology*, **167,** 23-37.

Jenkyns, H.C., Jones, C.E., Gröcke, D.R. et al., 2002. Chemostratigraphy of the Jurassic system: applications, limitations and implications for palaeoceanography. *Journal of the Geological Society, London*, **159**, 351-378.

OSol: *Ordonnance sur les polluants du sol de 9 juin 1986, and Ordonnance sur les atteintes portées au sol du 1er juillet 1998.* SR 814.12. Conseil Fédéral, Berne.

Pankhurst, R. J., Riley, T. R., Fanning, C. M. and Kelley, S. P., 2000. Episodic Silicic Volcanism in Patagonia and the Antarctic Peninsula: Chronology of Magmatism Associated with the Break-up of Gondwana. *Journal of Petrology*, **41**, 605-625.

Prudente, D., Baize, D. and Dubois, J.P., 2002. Le cadmium naturel dans une forêt du haut Jura français. In: *Les éléments traces métalliques dans les sols. Approches fonctionnelles et spatiales* (D.Baize and M.Tercé, eds) INRA Editions, Paris, 53-70.

Rosenthal, Y., Lam, P., Boyle, E.A. and Thomson, J., 1995. Authigenic cadmium enrichments in suboxic sediments: precipitation and postdepositional mobility. *Earth and Planetary Science Letters*, **132**, 99-111.

Tuchschmid, M., 1995. Quantifizierung und Regionalisierung von Schwermetallen und Fluorgehalten bodenbildender Gesteine der Schweiz. Schriftenreihe Umwelt-Materialien 32, Bundesamt für Umwelt, Wald und Landschaft (Hrsg.), Bern, 130 pp.

Wedepohl, K. H., 1995. The composition of the continental crust. *Geochimica et Cosmochimica Acta*, **59**, 1217-1232.

Wierzbowski, H., 2004. Carbon and oxygen isotope composition of Oxfordian–Early Kimmeridgian belemnite rostra: palaeoenvironmental implications for Late Jurassic seas. P*alaeogeography, Palaeoclimatology, Palaeoecology*, **203**, 153-168.

Ziegler, PA, 1988. *Evolution of the Arctic-North Atlantic and Western Tethys*. AAPG Memoir 43, 198 pp.

VI - Cadmium anomalies in Jurassic limestone as the cause for high cadmium concentrations in associated soils: a case study in Lower Burgundy, France

(in prep. for Environmental Geology)

Claire Rambeau[1*], Denis Baize[2], Nicolas Saby[2], Karl B. Föllmi[1], Virginie Matera[1], Thierry Adatte[1]

[1]*Institut de Géologie, Université de Neuchâtel, rue Emile-Argand 11, CH-2007 Neuchâtel, Switzerland*
[2]*Unité de Science du Sol, Institut National de la Recherche Agronomique, Av. de la Pomme de Pin, Ardon, F-45166 Olivet Cedex, France*

[*]To whom correspondence should be addressed.
Telephone number: ++41 32 718 25 96. Fax number: ++41 32 718 26 01.
E-mail: claire.rambeau@unine.ch

Abstract

Cadmium is a highly toxic element and its presence in the environment needs to be closely monitored. Recent systematic surveys with regards to cadmium concentrations in French soils have revealed the existence of areas in eastern and central France, which systematically show high concentrations for this element. It has been suggested that these anomalous values are of natural origin, independent of human pollution. For the Lower Burgundy area in particular, a direct heritage from the bedrock, which consists of Jurassic limestone, is highly suspected. We have studied this potential relationship in several localities around Avallon and report new evidence for a direct link between anomalous cadmium contents of Middle (Bajocian) and Upper (Oxfordian) Jurassic carbonates and high cadmium concentrations in associated soils. Soils in this area are anomalously rich in cadmium also from a statistical point of view, their cadmium contents being frequently higher than the "upper whisker" value (0.8 µg/g, calculated at a national scale). In parallel, the carbonates studied in the same area have been shown to contain cadmium concentrations frequently exceeding the mean value of 0.030 - 0.065 µg/g given for this kind of rocks by one order of magnitude, with a maximum of 2.6 µg/g. Mean enrichment factors between these calcareous rocks and associated soils have been calculated for the different localities studied here, which range from 4.6 to 5.7. Calculations based on analyses of soils from a restricted area and fragments of bedrock sampled in the immediate vicinity of soil enrichments are around 5.5 - 5.7.

VI-1 Introduction

Trace element contents in soils are a subject of increasing concern for the environment since the last few decades. Our consciousness with regards to possible health problems linked with high metal or, more generally, trace element concentrations in soils has grown. As a consequence, systematic studies have been performed across France on trace-element concentrations in soils, focusing especially on those that have a noxious effect on human health (mercury, lead, cadmium, arsenic; ASPITET program - Baize, 1997, 2000; and ADEME program - Baize et al., in press), and guideline values have been introduced which serve as a reference in the monitoring of soil quality (e.g., Décret N° 97.1133 du 8 Décembre 1997 and Arrêté du 8 janvier 1998 for France; OSol, 1998 for Switzerland). On the other hand, soil scientists and geochemists have introduced and used the notion of "pedo-geochemical context" (e.g., Baize, 1997; Baize and Sterckeman, 2001; Palumbo et al., 2000; Colinet et al., 2004), which permit to define specific areas of similar "background" chemical concentrations, independent of anthropogenic pollutions. Pedo-geochemical backgrounds directly depend of natural local conditions, including soil types and particular parent materials.

In spite of its rather low flux rates and concentrations in the soil environmental compartment, cadmium is on top of the list of potentially toxic metals and therefore in need to be closely monitored. With regards to this element, several areas in central and eastern France show anomalously high Cd concentrations in soils that seem independent of human activity (e.g., the Burgundy and Jura regions; Baize and Chrétien, 1994; Baize, 1997; Baize et al., 1997, 1999; Prudente, 1999; Prudente et al., 2002). These high concentrations continue in the adjacent Swiss Jura area (Atteia et al., 1994, 1995; Okopnik, 1997; Benitez-Vasquez, 1999; Baize and Sterckeman, 2001; Dubois et al., 2002). Recent studies conducted in the French and Swiss Jura area (e.g, Benitez-Vasquez, 1999; Prudente, 1999; Baize and Sterckeman, 2001; Dubois et al., 2002; Prudente et al., 2002) have pointed out a relationship between anomalously high cadmium contents in soils and the weathering of associated bedrocks, which consist of limestone of specific Jurassic ages and show unexpectedly high cadmium concentrations. This apparent relation is all the more surprising since, following previous surveys of cadmium concentrations in major rock types, limestone is supposed to be depleted in cadmium relative to average continental crust, with a mean cadmium concentration of around 0.030 - 0.065 µg/g (Kabata-Pendias and Pendias, 1992; Alloway, 1995; Tuchschmid, 1995). However, investigations concerning cadmium contents in Jurassic limestone in western and southern Europe (Rambeau et al., in prep.) have highlighted a general increase of cadmium contents in calcareous rocks for both the Bajocian and Oxfordian periods, that renders these rocks possible sources for cadmium enrichments in the associated soils.

This study provides complementary information about a causal link between cadmium anomalies in Jurassic limestone and in associated soils in the Lower Burgundy area, which has been already proposed by several authors (Baize et al., 1999; Baize and Roddier, 2002). Limestone sampling has been carried out in selected localities of established cadmium anomalies in soils. Special attention has been paid to two sites:

(1) the Frétoy forest and adjacent fields, where all analyzed soils, which developed from a reef complex of Late Oxfordian age, have shown outlying cadmium contents; and (2) the Blacy area, where the soils containing high cadmium concentrations appear to be related to the weathering of crinoidal limestone of Bajocian age. In addition to the sampling and analyses of carbonate rocks in the immediate vicinity of the soils anomalously rich in cadmium (rock fragments inside the soil and/or underlying bedrock), a more detailed stratigraphic section outcropping a few kilometers from the investigated localities has been studied in both cases, in order to establish the general evolution of cadmium contents, during the Late Oxfordian for the Le Saussois section, and during the Bajocian for the Lucy-le-Bois section, respectively.

VI-2 Material and methods

VI-2-1 Soil samples

We have used the results of two national surveys about trace element contents in French soils:
- "Collecte nationale ADEME / INRA" (Baize et al., in press; see also Baize et al., 1999), concerning ploughed topsoils of agricultural lands selected to be spread with urban sewage sludge
- “ASPITET” program (Baize, 1997, 1999) - Lower Burgundy part, concerning surface and deep horizons of both agricultural and forest soils.

With regards to general statements about cadmium anomalies in French soils and their possible relationships with limestone weathering (Fig. 1, Table 1), only data from the ADEME / INRA program have been used (which corresponds to 10 634 samples, geographically well-distributed within the French territory).

For the part focused on the Lower Burgundy, soil analyses related to this area have been considered from both the ADEME / INRA and the “ASPITET” programs, (total of 262 samples; Fig. 2). Samples related to geographical zones, which have been studied for Cd contents in the corresponding bedrock, have been listed in Table 2. Associated sample localities have been plotted in Fig 2: Frétoy forest, point 1; Coulanges zone, point 2; Clamecy fields, point 3; Précy-le-Sec zone, point 4; Blacy area and laterally equivalent soils, points 7, 9 and 12; Pousseau, point 11).

VI-2-2 Rock samples

All sample localities have been reported in Fig. 2. N corresponds to the number of samples related to each locality.

Oxfordian limestone

Samples of the carbonate bedrock (Oxfordian Mailly-le-Château reef complex; N=21) have been taken for analysis along a NW-SE transect inside the Frétoy Forest, situated between the villages of Courson-les-Carrières (north) and Coulanges-sur-Yonne (south), between the junction point of the road D.130 and the Grange Cathelin Line and the junction point of the road D.39 and the Lac Marry Line (Fig. 2, point 1).

Six small sections, each a few meters thick, have been investigated. In each section carbonates just underneath the soils have been sampled, and wherever possible additional samples have been taken at 20 to 40 cm intervals down section.

Rock fragments have also been sampled in the Clamecy fields (N=4; Fig. 2, point 3) and in the Précy-le-Sec zone (Cravant limestone; N=3; Fig. 2, point 4), which both represent areas concerned by high Cd contents in the corresponding soils.

A more detailed stratigraphic section corresponding to the Oxfordian Mailly-le-Château reef complex has been studied at the Le Saussois cliff, which outcrops 5500 m southwest of the village of Mailly-la-Ville, in the vicinity of the Merry-sur-Yonne village (Fig. 2, point 5). 25m of the upper part of the section have been sampled (N=10). This section has been completed by a sampling at the Roche aux Poulets outcrop, situated a little further to the northern side of Merry-sur-Yonne (Fig. 2, point 6; N=5).

Bajocian limestone

Large fragments of rocks (N=7) have been sampled from shallow soils in the Blacy area (Fig. 2, point 7). Additionally, the Lucy-le-Bois section, which outcrops in a former quarry (Fig. 2, point 8), has been studied to analyse the stratigraphic distribution of cadmium concentrations during the Bajocian (N=19) in detail.

VI-2-3 Measurement of cadmium contents

Two methods have been used for the determination of cadmium concentrations in soils:

- cadmium measurements by Inductively Coupled Plasma-Mass Spectrometry (ICP-MS) after dissolution by HF + $HClO_4$ = "total" concentrations (following the French standard NF X 31-147 – AFNOR, 1999)
- cadmium measurements by ICP-MS after dissolution by *aqua regia* = "pseudo-total" concentrations (according to the international standard ISO 11466 - AFNOR, 1999).

Cadmium concentrations obtained by both methods are of the same order of magnitude, and no distinctions have been established between the two populations.

Concerning rock samples, ICP-MS analyses (ELAN 6100, Perkin Elmer) were performed on bulk rock samples, after microwave-assisted (MSL-Ethos plus, Milestone; EPA 3051 procedure) nitric-acid digestion (250 mg of powered sample + 10 ml of concentrated nitric acid -65 %, suprapur, Merck). The element concentrations of the acid digests were determined using full mass-spectra scans (panoramic method). Certified reference materials (CRMs) for trace metals in natural water (NIST 1640) and lake sediments (LKSD-1) were used to estimate the accuracy of the method. The mean recovery rates for cadmium in these CRMs were 99% and 101.1%, respectively.

VI-2-4 Statistical analysis (soil samples)

The research and definition of anomalous contents ("outlier" values) for cadmium concentrations in soils was carried on using the *Exploratory Data Analysis* method (Tukey, 1977; McGrath and Loveland, 1992):

- on an sample population, an "interquartile distance" (ID) is arithmetically defined, spreading between the 1st and 3rd quartiles.
- by adding 1.5 times the ID to the 3rd quartile, we define the "upper whisker".
- all values higher than the upper whisker are considered as "upper outliers" (referred in the text as "outliers"), i.e. anomalous values for the particular population under consideration.

VI-3 General statement about cadmium anomalies in French soils, and possible relationships with limestone outcrops

Data obtained from the national survey ADEME / INRA have permitted to establish different maps showing the cadmium distribution in France (based on number of "outliers", or mean values; Baize et al., 1999). We have chosen to present here a new map based on the ratio number of "outliers"/total number of values available per Agricultural Areas (AAs), which permit to highlight the zones showing anomalous cadmium contents (Fig.1.A) and compare them with the outcropping of Mesozoic calcareous rocks (Fig.1.B).

VI-3-1 Comparison between occurrences of cadmium anomalies in soils and outcrops of Mesozoic limestone

17 AAs in France present a ratio NO/NS higher than 15%. At least 8 of them: Plateaux Moyens du Jura, Bourgogne nivernaise, Plateaux Supérieurs du Jura, Plateaux de Bourgogne, Saintonge viticole, Vignoble du Barrois, Saintonge agricole, Aunis, correspond to zones where Jurassic calcareous rocks represent the dominant or (almost) exclusive lithology (for the "Saintonge agricole" and "Aunis" AAs, Cretaceous limestone also form part of the bedrock).

Fig. 1. A. Next page. Ratio Number of Outliers (NO)/total Number of Samples (NS) for cadmium concentrations, in percents, per Agricultural Area (AA).
Definition of AAs: the subdivision of the French territory into Small Agricultural Areas (SAAs) results from an intra-departmental cutting carried out by geographers. The SAAs, constituted of groupings of communes, are supposed to constitute homogeneous zones considering as well soil and climate conditions as the dominant vocation of farms. This zoning was carried out at the request of authorities in the fifties to be used as a territorial framework for the production of many agricultural statistics. The adjacent SAAs of close characteristics were gathered in the same Agricultural Area (AA) at a national level. Only the Agricultural Areas (AAs) for which more than 21 analyses were available have been taken into account. 1 - Plateaux Moyens du Jura; 2 - Bourgogne nivernaise; 3 - Plateaux Supérieurs du Jura; 4 - Plateaux de Bourgogne; 5 - Saintonge viticole; 6 - Vignoble du Barrois; 7 - Saintonge agricole; 8 - Aunis; 9 - Autunois-Auxois; 10 - Pevèle; 11 - Haut Limousin.

Fig. 1. B. Next page. Simplified map of dominant outcropping lithologies and major orogenic complexes in France and its immediate vicinity.

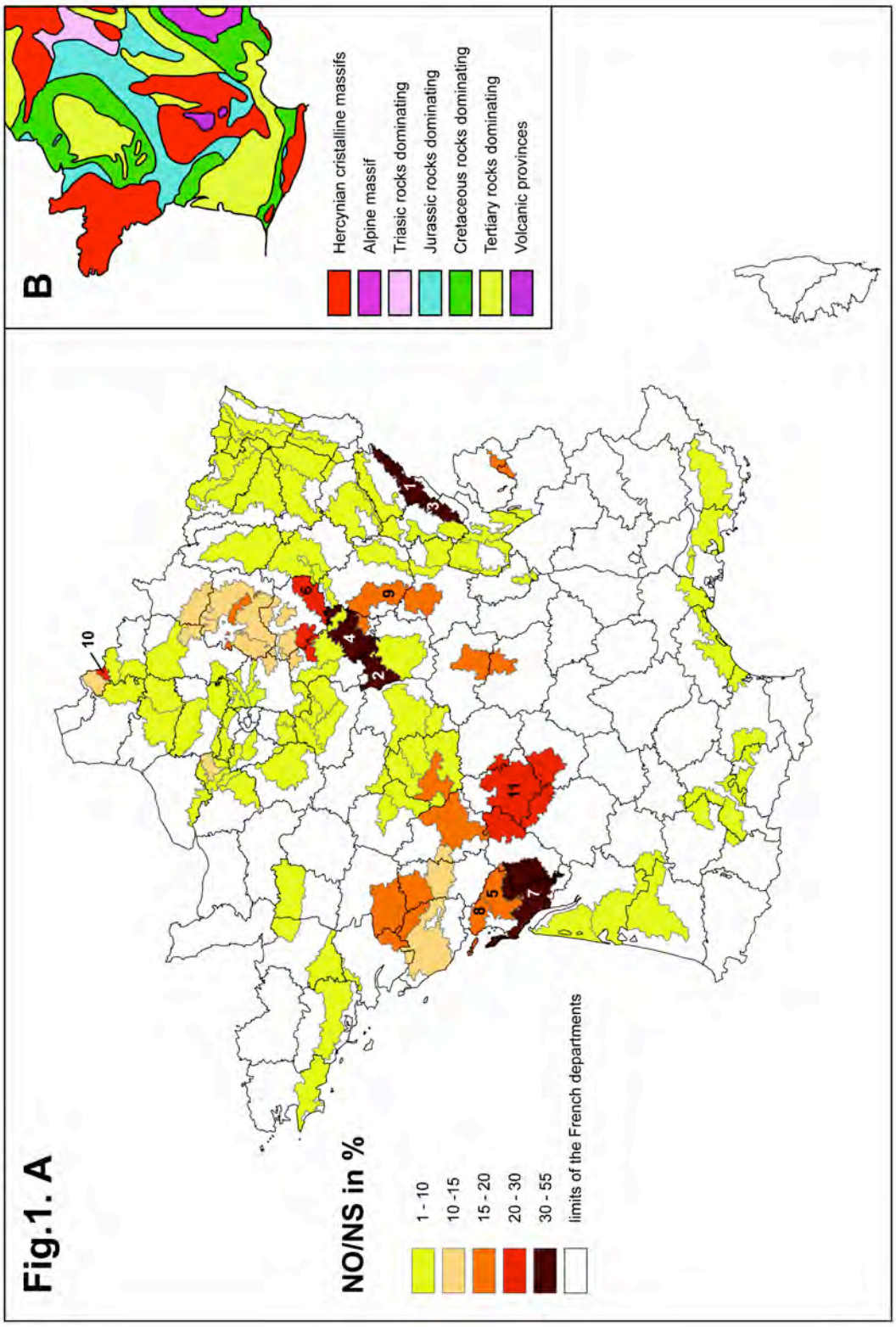
B
Hercynian cristalline massifs
Alpine massif
Triasic rocks dominating
Jurassic rocks dominating
Cretaceous rocks dominating
Tertiary rocks dominating
Volcanic provinces
Fig.1. A
NO/NS in %
1 - 10
10 -15
15 - 20
20 - 30
30 - 55
limits of the French departments
1
2
3
4
5
6
7
8
9
10
11

VI-3-2 Possible relationships between cadmium enrichments in soils and weathering of Jurassic limestone

The Jura Mountains comprise two most anomalous AAs (1 - 3, Table 1, Fig.1) with regards to cadmium; this area has been the frame of specific studies (Dubois et al., 2002; Prudente, 1999; Prudente et al., 2002) in which a geogenic origin for most of the cadmium discovered in soils - both in forest and agricultural contexts -was concluded on.

In Burgundy, which also holds an important anomalous zone distributed over two AAs (2 - 4, Table 1, Fig.1), a link between cadmium anomalies in Jurassic limestone and related anomalies in soils is also highly suspected (Baize, 1999, 2002). The results of specific investigations concerning cadmium contents in Jurassic limestone in selected localities of Lower Burgundy, which are concerned by cadmium anomalies in soils, are presented in this paper. The goal of this study is an investigation of the role of limestone weathering on the general cadmium enrichment of soils related to this geographical zone.

Table 1 Cadmium NO/NS ratios of 8 anomalous Agricultural Areas (France) and relationships with cadmium anomalies in the Jurassic calcareous bedrock

AA name	NO/NS ratio	Relationship	
		argued	suspected
Plateaux Moyens du Jura - *Jura Medium Plateaus* (1)	55%	X (a)	
Bourgogne nivernaise - *Burgundy in the vicinity of Nevers* (2)	54%	X (b)	
Plateaux Supérieurs du Jura - *Jura Higher Plateaus* (3)	44%	X (a)	
Plateaux de Bourgogne - *Burgundy Plateaus* (4)	32%	X (b)	
Saintonge viticole - *Vineyard of Saintonge* (5)	31%		X
Vignoble du Barrois - *Barrois Vineyard* (6)	23%		X
Saintonge agricole - *Agricultural Saintonge* (7)	15%		X
Aunis (8)	15%		X

AA: Agricultural Area. The numbers following AAs names are reported to corresponding locations on Fig. 1. NO/NS: number of outliers/total number of samples. Data from the ADEME/INRA program, Baize et al., in press. (a) Prudente et al., 2002; (b) this study

VI-4 Cadmium anomalies in soils in relation with anomalous concentrations in Jurassic limestone: the case of the Burgundy Plateaus

VI-4-1 Cadmium contents in soils

The region of the Burgundy Plateaus is one of the most anomalous areas in France with regards to cadmium concentrations; when considering data from the ADEME / INRA program, 32% of the cadmium concentrations measured in soil samples are "upper outliers" at the national scale (Table 1), which comes to 48 % when compiling data from both ADEME / INRA and ASPITET surveys.

The cadmium anomalies in this region are related to several specific pedo-geological contexts and the cadmium enrichments may therefore be related to different processes. The whole region can be divided into seven categories of pedo-geological units (Fig. 2):

- the major alluvial valleys
- the Morvan uplifted block, consisting of crystalline and metamorphic rocks, sporadically overlain by silicified and mineralized sedimentary rocks of early Jurassic age (Caillère et al., 1968)
- The “Terre Plaine”, which is a large depression due to the occurrence of easily weatherable sedimentary rocks of early Jurassic age (mainly micaceous clays and marls)
- the “Non-Calcareous Residual Cover”, which consists of residual soils sometimes reaching more than one metre thickness. This category comprises: (1) the “Terres d’Aubues”: reddish iron-rich soils developed in residual clays resulting from the total dissolution of various types of limestone; (2) the “argiles à chailles” ("clay with cherts"): thick formations containing large amounts of siliceous cobbles, and resulting from the weathering of Callovian cherty limestone by total calcite removal; and (3) ancient (Mio-Pliocene) alluvial sediments

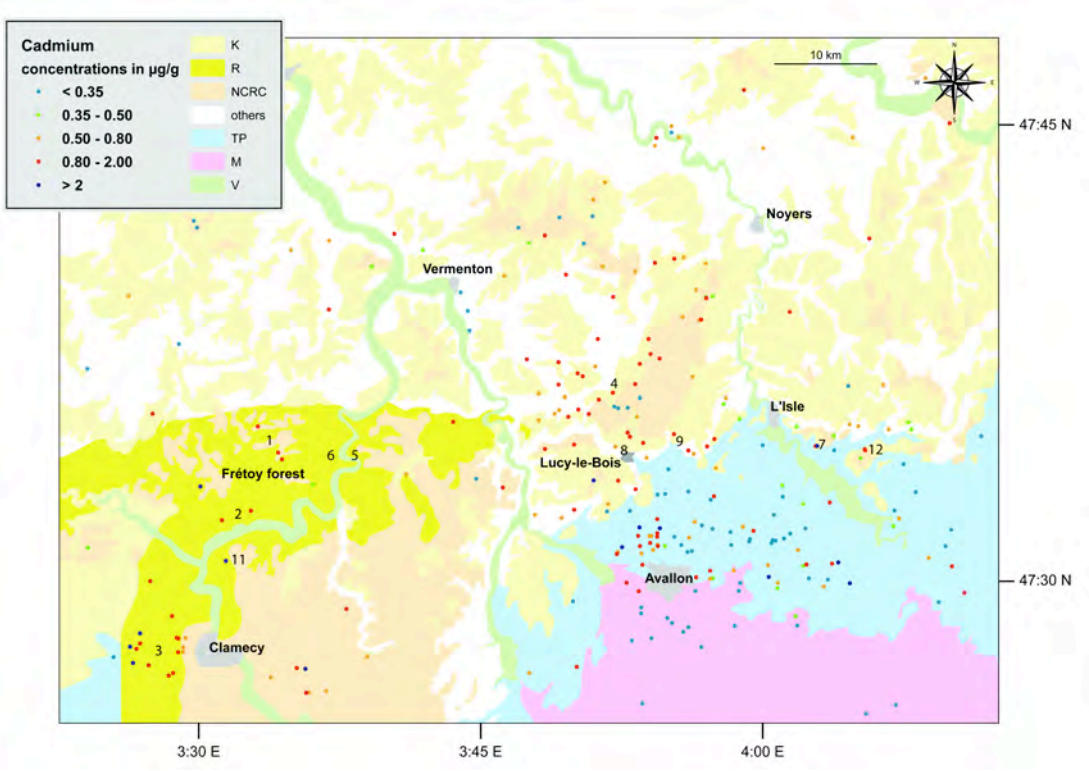

Fig. 2. Map of cadmium concentrations in soils from Lower Burgundy

Cadmium analyses in soils from ADEME / INRA and ASPITET programs. Cartographic data from Baize, 1993 and Baize, 1996. Pedo-geological categories: K: Jurassic “hard” limestones; R: Oxfordian reef complex of Mailly-le-Château; NCRC: Non-Calcareous Residual Cover; TP: Terre Plaine; M: Morvan; V: major alluvial valleys. The numbers refer to places cited in the text and in Table 2, which have been the locality of detailed studies concerning cadmium concentrations in soils and/or rocks.

- shallow soils overlying Jurassic "hard" (i.e., well-resistant to weathering) limestone (Bajocian, Bathonian, Callovian, Oxfordian, Lower Kimmeridgian, Portlandian)
- soils associated with limestone of the large Oxfordian reef complex of Mailly-le-Château
- others: areas not classified in previous categories, including zones where the pedo-geological context is less well constrained, areas with very pronounced slopes, small valleys with temporary streams, etc.

In the framework of this study, we have focused on cadmium anomalies related to soils developed from the Oxfordian reef complex of Mailly-le-Château, as well as from Bajocian limestone. This choice has been deduced from preliminary studies (e.g., Benitez-Vasquez, 1999; Dubois et al., 2002; Prudente, 2002; Rambeau et al., in prep.), which concluded on generally high cadmium contents for European calcareous rocks of this age. Moreover, it is highly suspected that part of the cadmium enrichments in Lower Burgundy (areas in contact with the Morvan ancient crystalline massif: Morvan, Terre Plaine) are not related to Jurassic bedrock weathering but to hydrothermal mineralizations due to fluids migrations along major faults (Caillère et al., 1968). These specific zones have therefore not been considered for this study.

Cadmium concentrations in selected soils related to the here considered specific bedrocks are presented in Table 2, for soils derived from the weathering of Oxfordian rocks, and Table 3, for those corresponding to Bajocian limestone. For both categories, cadmium contents are generally high, and frequently surpass the 0.8 µg/g whisker value. However, concentrations are highly variable, even within the same sampling area (e.g., Clamecy measurements - “Cla”, Table 2). This may be related either to specific pedogenic processes or to differences in original cadmium concentrations of the parent rock (Rambeau et al., in prep.).

VI-4-2 Cadmium contents in parent rocks

Oxfordian limestones

Analyses of rocks in the immediate vicinity of cadmium-enriched soils

The Frétoy forest (Fig. 2, point 1) is characterized by generally high cadmium contents in soils (Table 2). There, carbonate rocks have been sampled along a transect and analyzed for their cadmium contents. These carbonate rocks correspond to the upper part of a fossil reef complex dated as Late Oxfordian (Mégnien et al., 1970; Mégnien et al., 1971, 1972). The facies is relatively homogeneous along the transect and corresponds to very white, almost pure lagoonal micrite with no sedimentary structures, containing sometimes clasts of corals or bivalves, with the exception of the section situated at the southeastern extremity of the transect, which is composed of thin limestone beds rich in bioclasts.

Table 2 - Cadmium concentrations in soils and carbonate rocks Burgundy, Mailly-le-Château Oxfordian reef and lateral equivalents

Soils					Carbonate rocks		
Samples	Sampling depth in cm from the surface	forest	fields	Cd concentrations in µg/g	Samples	Sampling depth in cm from the section top	Cd concentrations in µg/g
Frétoy Forest (top of Mailly-le-Château reef)							
Frét1 (1)	0-15	X		1.29	**Frétoy Forest (top of Mailly-le-Château reef)**		
Mais (1)	10-20	X		1.2	FM 1 (1)	5	0.19
Rabo (1)	20-35	X		1.24	FM 2 (1)	5	0.20
Frét2 (1)	45-75	X		2.59	FM 3 (1)	35	0.20
Soils associated to other outcrops of the Mailly-le-Château reef					FM 4 (1)	35	0.21
					FM 5 (1)	65	0.12
Coul (2)	0-5	X		2.14	FM 6 (1)	80	0.15
Cimt (2)	0-10			1.26	FR 1 (1)	5	0.20
Crai (2)	0-15			1.13	FR 2 (1)	30	0.23
Cla1 (3)	0		X	1.56	RA 1 (1)	5	0.27
Cla2 (3)	0		X	1.56	RA 2 (1)	35	0.29
Cla3 (3)	0		X	0.94	RA 3 (1)	75	0.34
Cla4 (3)	0		X	2.78	CH 1 (1)	5	0.37
Cla5 (3)	0		X	2.86	CH 2 (1)	35	0.55
Cla6 (3)	0		X	1.42	CH 3 (1)	65	0.29
Cla7 (3)	0		X	2.3	AN 1 (1)	30	0.34
Cla8 (3)	0		X	1.25	AN 2 (1)	60	0.31
Cla9 (3)	0		X	0.99	AN 3 (1)	90	0.36
Cla10 (3)	0		X	1.26	FF 1 (1)	5	0.39
Cla11 (3)	0		X	0.6	FF 2 (1)	35	0.28
Cla12 (3)	0		X	0.79	FF 3 (1)	65	0.36
Cla13 (3)	0		X	0.76	FF 4 (1)	105	0.22
Cla14 (3)	0		X	1.02			
Cla15 (3)	0		X	0.48			
Cla16 (3)	0		X	0.99			
Cla18 (3)	0		X	0.78			
Cla19 (3)	0		X	0.52	**Other outcrops of the top of Mailly-le-Château reef**		
Cla20 (3)	0		X	1.07	CL5-1 (3)	-	0.25
Cla21 (3)	0		X	1.15	CL5-2 (3)	-	0.52
Cla22 (3)	0		X	0.28	CL5-3 (3)	-	0.20
Cla23 (3)	0		X	1.26	CL5-4 (3)	-	0.44
Oisy (3)	0-5			1.16			
Varv (3)	0-20			1.27			
Pous (11)	0-15		X	2.66			
Soils associated to lateral equivalents of the Mailly-le-Château reef					**Lateral equivalents of the Mailly-le-Château reef**		
Précy (4)	0-20			1.7	CRA 1 (4)	-	0.34
Suchy (4)	0-20			1.57	CRA 2 (4)	-	0.22
Rompi (4)	0-15			1.14	CRA 3 (4)	-	0.23
Frétoy Forest (Mailly-le-Château reef)				Soils			Rocks
Average cadmium concentration				1.58	Average cadmium concentration		0.28
Median cadmium concentration				1.27	Median cadmium concentration		0.29
Mean enrichment factor EF: 5.7							
All outcrops of the Mailly-le-Château reef				Soils			Rocks
Average cadmium concentration				1.33	Average cadmium concentration		0.29
Median cadmium concentration				1.22	Median cadmium concentration		0.28
Mean enrichment factor EF: 4.6							
Total				Soils			Rocks
Average cadmium concentration				1.34	Average cadmium concentration		0.29
Median cadmium concentration				1.24	Median cadmium concentration		0.28
Mean enrichment factor EF: 4.7							

Cadmium concentrations determined in these carbonate samples vary from 0.12 to 0.55 µg/g with a mean value and a median value at 0.28 µg/g (Table 2). The four samples of corresponding soils taken in this area display cadmium contents of 1.20 to 2.59 µg/g; values that correspond well to other analyses of soil samples which developed from the upper part of the reef complex of Mailly-le-Château or its lateral equivalents (Table 2).

Samples of bedrock fragments associated with the soils of the Clamecy fields characterized by positive outliers in cadmium contents, display comparable cadmium concentrations (Fig. 2, point 3; Table 2). Identical results have been obtained on fragments of the Cravant limestone – a micritic, sublithographic limestone that represents the lateral equivalent of the beach facies directly overlapping the uppermost part of the Mailly-le-Château reef complex - inside the cadmium-rich soils of the Précy-le-Sec zone (Fig. 2, point 4; Table 2).

Additional rock samples: Le Saussois section and lateral equivalents

The reef complex outcropping at Le Saussois is composed of reef build ups which alternate with lagoonal micrites rich in coral bioclasts (Fig. 3). Considering the cadmium contents in carbonates from this section, the lower part of the cadmium curve is considered as displaying "background" cadmium values for carbonate rocks (Fig. 3). In contrast, a distinct shift towards more elevated concentrations is observed in the upper part of the curve (probably corresponding to the Late Oxfordian, *bimammatum* Zone, *hypselum* Subzone; Menot, 1991; Fig. 3). Samples showing this positive excursion represent the lateral equivalent of the calcareous bedrock that outcrops in the Frétoy forest and display similar cadmium contents (Table 3). This increase in cadmium concentrations in the upper part of the reef complex of Mailly-le-Château is also confirmed by the analyses of several samples from the outcrop of the Roche aux Poulets (Fig. 2, point 6; Fig. 3). The base of the Roche aux Poulets section is stratigraphically equivalent to the upper part of the Le Saussois section (Menot, 1991; Chevalier et al., 2001). In addition, analyses from the top of the Roche aux Poulets section show that high cadmium contents also concern the beach facies overlapping the uppermost part of the reef complex.

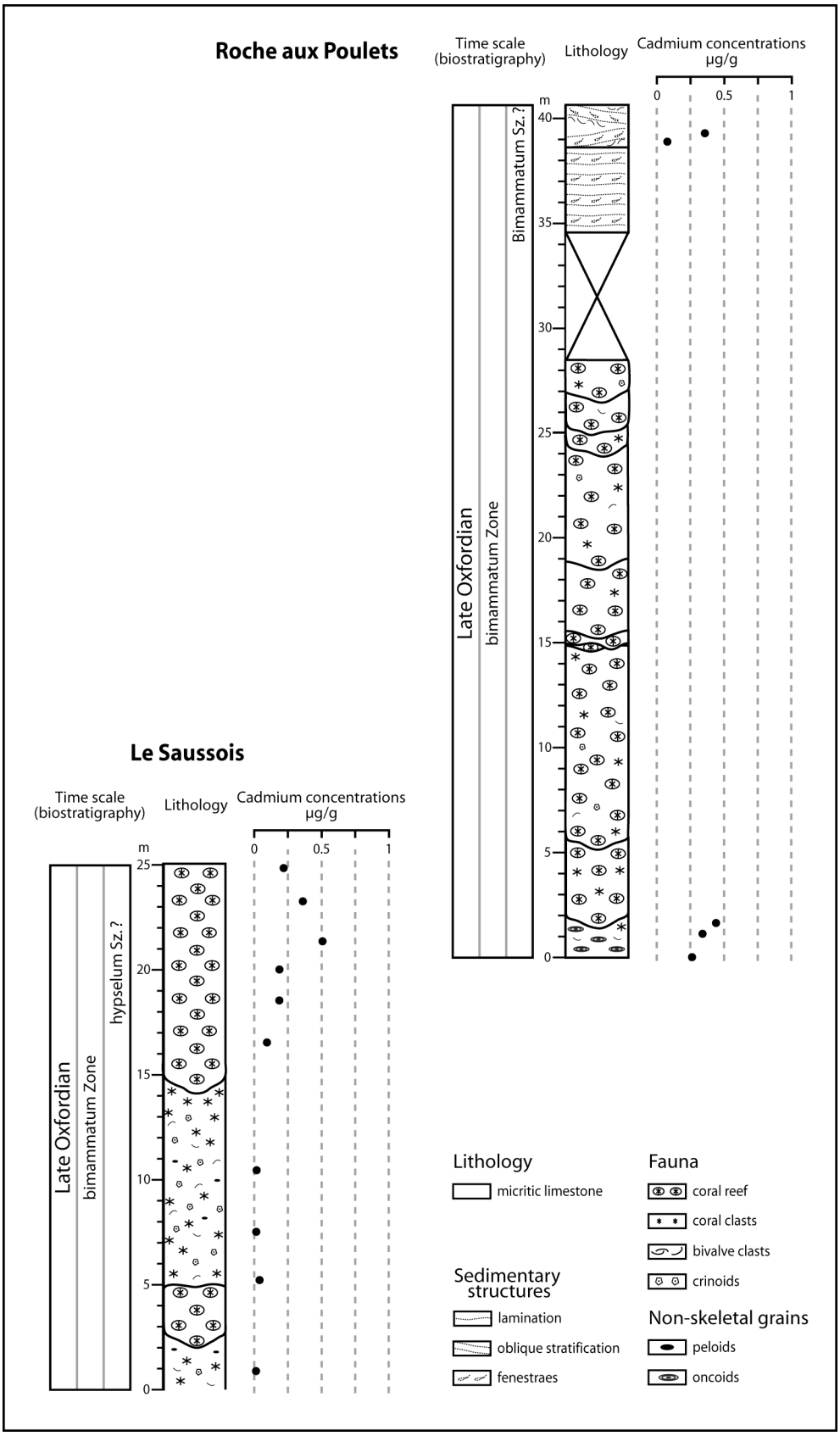

Fig. 3. Biostratigraphy, lithology and cadmium concentrations in Upper Oxfordian carbonates at Le Saussois and Roche aux Poulets sections. Biostratigraphy from Menot, 1991.

Bajocian limestone

In Lower Burgundy, soils associated with bedrock composed of Bajocian crinoidal limestone are generally characterized by elevated cadmium contents. Soils of the Blacy area (Fig. 2, point 7) are representative for soils developed from Bajocian crinoidal facies in this area with regards to the cadmium contents, which very often exceed the 0.8 µg/g whisker value (Table 3 – Fig. 2 points 7, 9, 12).

The majority of the bedrock fragments sampled in the Blacy zone displays cadmium values similar to those in the Oxfordian limestone from the Frétoy forest or other investigated sites in the Lower Burgundy area, with a mean cadmium concentration of 0.27 µg/g (Table 3). Cadmium measurements performed on the carbonate successions of the Lucy-le-Bois section (Fig. 4) show that the lower part of the section is characterized by great heterogeneity in cadmium contents, with one value reaching 2.6 µg/g, in contrast to the upper part of the section which displays lower and more homogeneous values.

Table 3 - Cadmium concentrations in Burgundian Bajocian crinoidal limestones and associated soils

Soils					Carbonate rocks		
Samples	Sampling depth in cm from the surface	forest	fields	Cd concentrations in µg/g	Samples	Sampling depth in cm from the section top	Cd concentrations in µg/g
PAJ 1(9)	0-15			1.37			
PAJ 2 (9)	0-15			0.68	BL 1 (7)	-	0.23
PAJ 3 (9)	0-15			0.97	BL 2 (7)	-	0.04
PA1F1 (7)	0-4	X		1.8	BL 3 (7)	-	0.05
PA1F2 (7)	10-20	X		2.07	BLC 1 (7)	-	0.63
PA1C (7)	0-20		X	1.72	BLC 2 (7)	-	0.32
PA2F1 (12)	0-4	X		1.56	BLC 3 (7)	-	0.34
PA2F2 (12)	10-20	X		1.81	BLF-S (7)	-	0.26
PA2C (12)	0-20		X	1.25			
Total				Soils			Rocks
Average cadmium concentration				1.47	Average cadmium concentration		0.27
Median cadmium concentration				1.56	Median cadmium concentration		0.26
Mean enrichment factor EF: 5.5							

VI-4-3 Enrichment factors between rocks and soils

With the assumption of a direct chemical heritage from the bedrock for soils in the investigated areas, enrichments factors (EFs) between rocks and soils were calculated (Table 2 and 3). To consider both statistical accuracy (numerous values give better evaluation) and pedo-geochemical homogeneity (a reduced area gives more precise results), we calculated mean EFs for different geographical contexts (Table 2). In each case, mean values were calculated for soils and rocks, respectively, and the mean EFs are obtained by dividing the first value by the second one. Cadmium concentrations measured in the sections of Le Saussois, Roche aux Poulets and Lucy-le-Bois have not been taken into account, considering the large stratigraphical scale represented and the associated large variations in cadmium contents.
Values obtained vary from 4.6 to 5.7 (Table 2 and 3) in function of the different sets of samples taken into account.

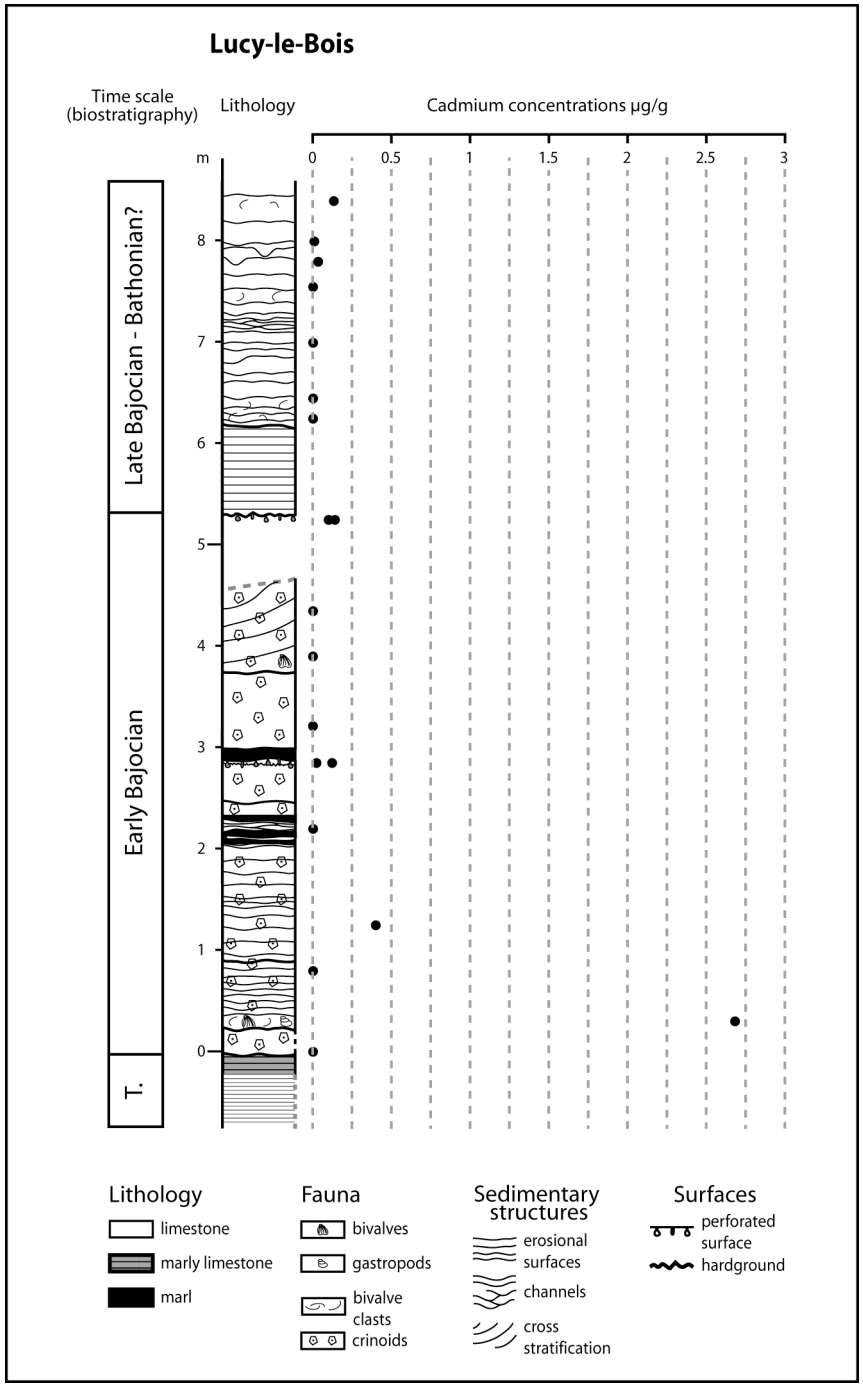

Fig. 4. Biostratigraphy, lithology and cadmium concentrations of the Bajocian Lucy-le-Bois section, Burgundy, France. T. = Toarcian. Biostratigraphy in comparison with other Bajocian formations from Burgundy (Thiry-Bastien, 2002).

VI-5 Discussion

VI-5-1 Cadmium contents of Jurassic limestone in the Lower Burgundy area

Jurassic bedrock, both of Oxfordian and Bajocian age, has been shown to present rather high cadmium contents (average concentrations of 0.29 and 0.27 µg/g, respectively) in the Lower Burgundy area. This values are quite elevated if compared to the mean cadmium concentration given for carbonate rocks in the literature (0.030 - 0.065 µg/g; Tuchschmid, 1995; Kabata-Pendias and Pendias, 1992; Alloway, 1995). Moreover, the cadmium curve corresponding to the carbonate successions of Le Saussois/Merry sur Yonne (Oxfordian) present a positive shift in the uppermost part of the reef complex (Le Saussois), which represent the lateral equivalent of carbonates oucropping in the Frétoy forest, as well as in the overlying beach facies (Merry-sur-Yonne). Cadmium concentrations obtained for the Lucy-le-Bois stratigraphic section show that carbonates of early Bajocian age in the Lower Burgundy area may present rather high cadmium concentrations (up to 2.6 µg/g), and that the vertical distribution of cadmium concentrations strongly varies on the scale of a few tens of centimetres. These results are in complete accordance with those obtained by recent studies on cadmium contents of Bajocian and Oxfordian carbonates in western and southern Europe in general (Rambeau et al., in prep.). This last study has permitted to establish that for one or both periods, cadmium contents are highly variable, with very high concentrations often limited to layers of a few centimetres thickness.

Carbonates rocks in Lower Burgundy represent, therefore, good candidates as a source for cadmium anomalies in associated soils; however, the great variability of cadmium contents in limestone must be of some repercussion to the cadmium concentrations displayed in soils which derives from these rocks.

VI-5-2 Processus involved in cadmium anomalies in the Lower Burgundy area

Two major phenomena may be involved in the development of soil cadmium anomalies in this region:

- for areas directly in contact with the Morvan ancient crystalline massif, enrichments may be due to mineralizations of sedimentary rocks by the way of hydrothermal fluids following major faults (Morvan, Terre Plaine; Caillère et al., 1968)
- for the zones that are not concerned by major faulting and hydrothermal mineralization (“Non-Calcareous Residual Cover”, Jurassic “hard” limestone, Oxfordian reef complex of Mailly-le-Château), anomalous cadmium values are proposed to be inherited from the bedrock composition (Baize et al., 1999; Baize and Roddier, 2002; this study).

VI-5-3 Role of specific carbonate facies

The conclusion of previous studies is that in Burgundy, biogenic limestone (reef or bioclastic carbonates) are often anomalous with regards to cadmium concentrations (Baize, 1997; Baize et al., 1999); these authors also concluded that,

however, not all bedrocks consisting of biogenic carbonates are associated with soils rich in cadmium (Baize et al., 1999). To this comes that in the Jura area, most of the calcareous rocks showing unexpectedly high cadmium concentrations present an oolitic/oncoidal facies, whereas bioclastic rocks are generally less rich in cadmium (Benitez-Vasquez, 1999; Dubois et al., 2002). In this study we show that cadmium concentrations are quite independent of the specific rock facies, as similar kinds of limestone may present very different cadmium concentrations (e.g., at Le Saussois section, Fig. 3). Cadmium anomalies in limestone from Lower Burgundy seem to be especially related to stratigraphic levels, which influence the cadmium concentrations of related soils along distances of several tens of km.

VI-5-4 Enrichment factors between rocks and soils

The wide range of concentrations obtained for both the Jurassic limestone and the associated soils renders the calculation of enrichment factors less accurate. Considering that cadmium concentrations sometimes varies by a factor of ten in a few decimetres (e.g., Lucy le Bois section, Fig. 4), and that the layers from which soils have developed are no longer present, it is quite difficult to calculate a realistic enrichment factor by measuring cadmium contents in the soil and in the directly underlying rock. One possibility is to take into account all values corresponding to a defined area, for both soils and rocks. Another problem immediately arises, with the frequent differences in the locations of rocks and soils sampling. The difficulty is thus to balance between statistical accuracy and pedo-geochemical homogeneity, and this is well expressed by the various mean enrichment factors obtained for different geographical settings (from 4.6 to 5.7; Table 2 and 3).

Data sets for the Oxfordian from the Frétoy forest and for the Bajocian from the Blacy area allow for realistic calculations: they both contain soils from a restricted area and fragments of bedrock sampled in the immediate vicinity of soil enrichments. The very good accordance between the two mean EFs obtained (5.7, Table 2, and 5.5, Table 3, respectively) plays in favour of realistic values despite the rather low number of samples available. It also may indicate that mechanisms of enrichments do not varies as a function of specific rock age or facies.

Although the EFs calculated for soils developed from Oxfordian limestone are based on more measurements, they are skewed by heterogeneities in the location of rocks and soils samplings and/or in soil types. Inclusion of soils developed from non-anomalous rocks and/or of "normal" carbonate bedrocks in the calculations may explain the slightly lower values obtained for the mean EFs corresponding to larger areas in Lower Burgundy (“all outcrops of the Mailly-le-Château reef”: 4.6 and “total”: 4.7; Table 2).

VI-5-5 Mechanism of soil enrichment

In soils associated with carbonate rocks presenting high cadmium concentrations, cadmium has been suggested to concentrate by progressive carbonate dissolution and in-situ adsorption on clay minerals and iron and manganese oxi-hydroxides (Baize et al., 1999; Benitez-Vasquez, 1999; Prudente et al., 2002). Other processes should, however, be taken into account to explain the actual cadmium distribution in soils

(Baize et al., 1999). In the case of Lower Burgundy, these processes include in particular vertical transfer by lixiviation and biogeochemical recycling. Lateral transfer is not considered as having a major influence on the evolution of cadmium concentrations in these soils, which are in majority related to areas of very slight slopes. The summary of chemical heritage from the geological background, itself subjected to high fluctuations related to the extreme variability of the rock chemistry, and subsequent soil evolution, therefore produce a large range of cadmium concentrations in soils.

VI-6 Conclusions

The cadmium analyses performed on Oxfordian and Bajocian carbonate rocks and associated soils in Lower Burgundy have permitted to highlight the following points:

- Bajocian and Oxfordian carbonates in Lower Burgundy display a wide range of cadmium concentrations, which is in accordance with the spatial variability of cadmium contents observed in the corresponding soils.
- Limestone fragments sampled within cadmium-rich soils present cadmium concentrations higher than those commonly found in calcareous rocks.
- The analysed carbonate sections show stratigraphic intervals in which cadmium contents are unusually high for limestone in general but similar to those discovered in carbonate rocks of the same age in western and southern Europe (Rambeau et al., in prep.). These layers stratigraphically correspond to the parent rocks of soils presenting anomalously high cadmium contents.
- Cadmium contents in these carbonates are highly independant of their specific facies and rocks of comparable facies may show highly different cadmium concentrations (e.g., at Le Saussois section).
- Mean enrichment factors calculated range from 4.6 to 5.7, the most realistic values being around 5.5 - 5.7. However, the calculation of enrichment factors is delicate, considering the wide variability of rock chemistry with regards to cadmium, and the possibilities of remobilization and transfer of this element inside soil horizons after bedrock dissolution.

The geochemical investigations conducted on Jurassic rocks in Lower Burgundy therefore confirm that for a large part of the soils present in this area which are anomalously rich in cadmium, a chemical heritage from the weathering of the associated bedrock is the most likely source of cadmium. These observations are in complete agreement with previous results obtained with the studies on Bajocian and Oxfordian carbonates and associated soils in the Jura area (Genolet and Dubois, 1996; Liebig, 1996; Baize and De Pury, 1997; Okopnik, 1997; Benitez-Vasquez, 1999; Prudente, 1999; Baize and Sterckeman, 2001; Dubois et al., 2002; Prudente et al., 2002), and on cadmium contents of Bajocian and Oxfordian calcareous rocks in western and southern Europe (Rambeau et al., in prep.). High variability in cadmium contents for limestone of Bajocian and Oxfordian age in Lower Burgundy may explain the wide range of cadmium concentrations, and their spatial variability, obtained for the corresponding soils, and renders enrichment factor between soils and rocks difficult to calculate.

Acknowledgments

We would like to thank Jean-Claude Menot for field assistance and advice, as well as the ADEME / INRA and the "ASPITET" programs for data provision. We acknowledge financial support from the Swiss National Science Foundation (projects no. 21-65183.01, 200020-101718/1) and from the National Centre of Competence in Research ("Plant Survival").

References

AFNOR (1999). *Qualité des sols. Recueil de normes françaises. 2 volumes* (4e édition), Paris-La Défense

Alloway BJ (1995). Cadmium. In: Heavy metals in soils. 2nd edition. Blackie Academic and Professional. pp 122-147

Arrêté du 8 janvier 1998 fixant les prescriptions techniques applicables aux épandages de boues sur les sols agricoles en application du décret N° 97.1133 du 8 Décembre 1997. Journal Officiel du 31 Janvier 1998

Atteia O, Dubois JP, Webster R (1994). Geostatistical analysis of soil contamination in the swiss Jura. Environmental pollution 86:315-327

Atteia O, Thélin Ph, Pleifer HR, Dubois J P, Hunziker JC (1995). A search for the origin of cadmium in the soil of the Swiss Jura. Geoderma 68:149-172

Baize D, Deslais W, Saby N (In press). Teneurs en huit éléments en traces (Cd, Cr, Cu, Hg, Ni, Pb, Se, Zn) dans les sols agricoles en France. Résultats d'une collecte de données à l'échelon national. ADEME

Baize D (1993). Petites régions naturelles et paysages pédologiques du département de l'Yonne. Carte à 1/200.000

Baize D, Chrétien, J (1994). Les couvertures pédologiques de la plate-forme sinémurienne en Bourgogne. Particularités morphologiques et pédogéochimiques. Etude et Gestion des Sols, 1(2):7-27

Baize D (1996). Carte des sols de l'Yonne. Feuille Vermenton. Notice et carte à 1/50.000. 116 p. Conseil Général de l'Yonne et INRA Orléans

Baize D (1997). Teneurs totales en éléments traces métalliques dans les sols (France). Références et stratégies d'interprétation. INRA Editions, Paris, 410 p.

Baize D, De Pury P (1997). Etude de quelques fosses pédologiques sur la commune de Boncourt (Jura). Ecole Polytechnique Fédérale de Lausanne. Rapport interne. Unpublished

Baize D, Deslais W, Gaiffe M (1999). Anomalies naturelles en cadmium dans les sols de France. Etude et Gestion des Sols, 2:85-104

Baize D (2000). Teneurs totales en « métaux lourds » dans les sols français. Résultats généraux du programme ASPITET. Le Courrier de l'Environnement de l'INRA 39:39-54

Baize D, Sterckeman T (2001). Of the necessity of knowledge of the natural pedogeochemical background content in the evaluation of the contamination of soils by trace elements: The Science of the Total Environment 264:127-139

Baize D, Roddier S (2002). Approche typologique d'une cartographie pédogéochimique. Exemple de l'Avallonnais. in: Les éléments traces métalliques dans les sols. Approches fonctionnelles et spatiales, D.Baize, M.Tercé, Eds. (INRA Editions, Paris), pp. 123-134

Benitez-Vasquez N (1999). Cadmium speciation and phyto-availability in soils of the swiss Jura : hypothesis about its dynamic. Ecole Polytechnique Fédérale de Lausanne. 132 p.

Caillère S., Kraut F., Horon O., Lefavrais-Raymond A., and Rouire J. (1968) - Carte géologique France (1/50 000), feuille Quarré-les-Tombes (467), et notice explicative, 8 p. - Orléans: Bureau de recherches géologiques et minières.

Chevalier F., Garcia JP, Quesne D., Guiraud M. and Menot JC (2001). Corrélations et interprétations génétiques dans les formations récifales oxfordiennes de la haute vallée de l'Yonne (sud-est du bassin de Paris, France). Bull. Soc. géol. France 172(1): 69-84

Colinet G, Laroche J, Etienne M, Lacroix D, Bock L (2004). Intérêt d'une stratification pédologique pour la constitution de référentiels régionaux sur les teneurs en éléments traces métalliques dans les sols de Wallonie. Biotechnol. Agron. Soc. Environ. 8(2):83–94

Décret N° 97.1133 du 8 Décembre 1997 relatif à l'épandage des boues issues du traitement des eaux usées. Journal Officiel de 10 Décembre 1997.

Dubois JP, Benitez N, Liebig T, Baudraz M, Okopnik F (2002). Le cadmium dans les sols du haut Jura suisse, in Les éléments traces métalliques dans les sols. Approches fonctionnelles et spatiales, D.Baize, M.Tercé, editors, INRA Editions, Paris, pp 33-52

Genolet F, Dubois JP (1996). Etude de la teneur en cadmium dans les sols de la région de Blauen-Nenzlingen (canton de Basel-Campagne). Lausanne: EPF, 1996:27

Kabata-Pendias A, Pendias H (1992). Trace elements in soils and plants. 2nd edition. CRC Press, 365 p.

Liebig T (1996). Untersuchungen zu den Bindungsformen und der Bioverfügbarkeit von Cadmium in den Böden des Schweizer Jura. Diplomarbeit. Berlin: Universität Berlin, 1996:69

McGrath SP, Loveland PJ (1992). The Soil Geochemical Atlas of England and Wales. Blackie Academic and Professional. Glasgow. 101 p.

Mégnien C, Mégnien F, Turland M (1970). Le récif oxfordien de l'Yonne et son emplacement sur la feuille Vermenton (1/50 000). Bull. BRGM (deuxième série), I(3):83-115

Mégnien C, Mégnien F, Turland M, Villalard P (1971). Carte géologique de la France au 1/50 000, feuille Vermenton. Bull. BRGM, XXVII(21)

Mégnien C, Mégnien F, Turland M, Villalard P (1972). Carte géologique de la France au 1/50 000, feuille Courson-les-Carrières. Bull. BRGM, XXVII(21)

Menot JC (1991). Formations d'âge Oxfordien dans la vallée de l'Yonne. In: Sédimentation, diagenèse et séquences de dépôt dans les séries carbonatées de plate-forme d'âge bathonien à oxfordien en Bourgogne. In: Floquet M., Javaux C., Menot JC and Purser BH. Livret-Guide A.S.F., 27-29 June 1991, pp 125-174

Okopnik F (1997). Relation entre la variabilité spatiale du cadmium et la couverture pédologique de la région du Mont d'Amin. Travail de fin de 3e cycle. EPFL Lausanne. 45 p.

OSol. (1998). Ordonnance du 1er juillet 1998 sur les atteintes portées aux sols. Swiss Federal Council, RS 814.12, Bern. 4 pp.

Palumbo B, Angelone M, Bellanca A, Dazzi C, Hauser S, Neri R, Wilson J (2000) Influence of inheritance and pedogenesis on heavy metal distribution in soils of Sicily, Italy. Geoderma 95:247–266

Prudente D (1999). Distribution des teneurs naturelles en cadmium dans les sols de la forêt communale des Fourgs (Doubs - France). DES Sciences naturelles de l'environnement. Universités de Genève et de Lausanne. 68 p. + annexes.

Prudente D, Baize D, Dubois JP (2002). Le cadmium naturel dans une forêt du haut Jura français, in Les éléments traces métalliques dans les sols. Approches fonctionnelles et spatiales, D. Baize, M. Tercé, editors, INRA Editions, Paris, pp 53-70

Rambeau C, Adatte T, Baize D, Bartolini A, Hug WA, Matera V, Sandoval J, Steinmann Ph, Veuve Ph, Föllmi KB (submitted). Anomalous cadmium enrichments in Tethyan Jurassic carbonates: past and present environmental implications.

Thiry-Bastien (2002). Stratigraphie séquentielle des calcaires bajociens de l'Est de la France (Jura - Bassin de Paris). PhD Thesis, Université Claude Bernard - Lyon 1, Lyon, France, 410 p.

Tuchschmid M (1995). Quantifizierung und Regionalisierung von Schwermetallen und Fluorgehalten bodenbildender Gesteine der Schweiz: Umwelt-Materialien 32 (BUWAL, Berne).

Tukey JW (1977). Exploratory data analysis. Addison Wesley, Reading, Massachusetts.

VII - µ-X-Ray fluorescence determination of cadmium locations and associations with other trace-elements in Jurassic cadmium-enriched limestone - models for the enrichment of cadmium in calcareous rocks

(in prep. for Chemical Geology)

Claire Rambeau*, Karl B. Föllmi, Virginie Matera, Thierry Adatte

Institut de Géologie, Université de Neuchâtel, rue Emile-Argand 11, CH-2007 Neuchâtel, Switzerland

*To whom correspondence should be addressed.
Telephone number: ++41 32 718 25 96. Fax number: ++41 32 718 26 01.
E-mail: claire.rambeau@unine.ch

Abstract

Carbonate rocks of Jurassic (Bajocian and Oxfordian) age in western and southern Europe (in particular Switzerland, France, and Italy) have been shown to present anomalously high cadmium (Cd) contents (Rambeau et al., in prep (a)). The range of cadmium concentrations obtained by bulk-rock ICP-MS analyses in such carbonates is wide, sometimes varying from a few hundreds of ng/g to as high as 21.35 µg/g in samples less than 10 cm apart. We have used a Synchrotron µ-XRF (beamline L, Hasylab, Hamburg, Germany) and an Eagle X-ray microfluorescence spectrometer (Institute of Terrestrial Ecology, ETH Zürich, Switzerland), to investigate the microscale distribution of cadmium, as well as its association with other chemical elements, in samples which are highly enriched in Cd. The results obtained (1) confirm the heterogeneous character of Cd distribution in the selected carbonate samples also on a micrometer-scale; and (2) provide information about other chemical elements and their degree of association with cadmium: Surprisingly, only a few elements (Zn, Fe, S) appear associated with Cd, and this not always in a consistent way. Based on these data and the observations by Veuve (2000) we propose a model for cadmium enrichment in the investigated samples, which takes into account our observations on the sedimentological and (micro-)facies context of the samples and sections and our interpretation of the specific depositional environments. We propose that (1) direct incorporation of cadmium into carbonate phases occurred during carbonate precipitation, which was probably assisted by microbial activity; and (2) cadmium enrichment took place via organic matter, which first adsorbed Cd and then was buried inside sediments, particularly in the form of pellets. The subsequent establishment of reducing conditions in the early diagenetic environment allowed for the transfer of Cd into carbonate phases and partly also into sulphidic phases.

The source of cadmium remains uncertain, but external inputs, triggered by volcanic events or enhanced continental weathering, are highly suspected.

VII-1 Introduction

A small selection of sediments and sedimentary rocks include Cd in quantities which are anomalously high, relative to the average crust (0.1-0.2 μg/g, Wedepohl, 1995). This is particularly the case for black-shale deposits (Heinrichs et al., 1980) and phosphorites (Altschuler, 1980; Middleburg and Comans,1991; Nathan et al., 1997). According to several authors, the high concentrations in sedimentary deposits is related to the presence of organic matter (Heinrichs et al., 1980; Nathan et al., 1997; van Geen et al., 1995; Il'in and Kiperman, 2001).

Calcareous rocks show an average Cd concentration of approximately 0.030 - 0.065 μg/g (Kabata-Pendias and Pendias, 1992; Alloway, 1995; Tuchschmid, 1995;) and are generally considered to be depleted in cadmium in comparison to the average crust. However, in recent studies, carbonate rocks of Jurassic age have been identified which contain unexpectedly high Cd contents, and which are held responsible for high Cd contents in associated soils (Benitez-Vasquez, 1999; Baize and Sterckeman, 2001; Dubois et al., 2002; Prudente et al., 2002). More specifically, cadmium anomalies have been discovered in a wide range of Bajocian and Oxfordian carbonate sections located in western and southern Europe (Switzerland, France, Spain, Italy; Veuve, 2000; Rambeau et al., in prep (a)). Quadrupole ICP-MS analyses on bulk-rock samples from these carbonate successions indicate an increase in "background" cadmium contents from <0.04 – 0.10 μg/g to 0.20 - 0.40 μg/g for the entire Bajocian period and during the Oxfordian (Rambeau et al., in prep (a)). Moreover, in the investigated shallow-water carbonate sections of Ste Honorine des Pertes (Bajocian, Normandy, France), Davayé and Lucy-le-Bois (Bajocian, Burgundy, France), Merry sur Yonne (Oxfordian, Burgundy, France), Lausen, Schleifenberg, Auenstein, Gurnigel, and Pont-de-la-Baleine (Bajocian, Swiss Jura), and Gorges du Pichoux and Dornach (Oxfordian, Swiss Jura), discrete, cm-thin stratigraphic levels are characterized by very high (>1 μg/g) cadmium contents (Veuve, 2000; Rambeau et al., in prep (a)). A further distinctive feature of these carbonate successions is the highly inhomogeneous distribution in Cd concentrations obtained on whole-rock samples, which may vary between a few hundreds ng/g to as high as 21.35 μg/g in less than ten cm vertical distance (e.g. Lausen section, Switzerland; Rambeau et al., in prep (a); this study).

In the aforementioned carbonates, the specific location of Cd inside carbonate phases has already been suggested by Benitez-Vasquez (1999). This is compatible with the postulation of Altschuler (1980) and Middleburg and Comans (1991), who linked Cd enrichments in phosphorites with a substitution between Cd^{2+} and Ca^{2+} in the apatite lattice. Indeed, Cd^{2+} and Ca^{2+} have a very similar ionic radius (0.99 Å and 0.94 Å, respectively) and substitution of Cd in carbonates is feasible.

The specific mechanisms leading to exceptional Cd enrichments in calcareous rocks, however, remain poorly known. In the Swiss Jura region, Veuve (2000) has identified both well-preserved ooid grains with Cd-enriched cortices, as well as micritized ooids, which are entirely Cd-enriched. He has also highlighted a preferential association between Cd and Zn enrichments. According to Veuve (2000), cadmium enrichments in these carbonates are related to the enhanced presence of organic matter during early diagenesis. In this model, the episodic deposition of marls was important in compartmentalizing the vertical distribution of organic matter, and trapping and concentrating it in porous oolitic layers just underneath the more impermeable marly layers. In these discrete organic matter-enriched layers, suboxic conditions were created. Once the organic matter underwent decomposition, Cd and Zn contained within the organic matter became transferred into the rims of the ooids (see also Additional material - Annex 1).

This model is in accordance with previous studies in which a positive correlation between Cd and organic matter contents and/or reducing conditions in sedimentary rocks was highlighted (e.g., Heinrichs et al., 1980; Rosenthal et al., 1995; van Geen et al., 1995; Il'in and Kiperman, 2001). The presence of pyrite in these oolitic carbonates is a further indication pointing to the early diagenetic presence of organic matter. However, the Cd-enriched carbonates are not in every case associated with a marly interval and may occur in the middle of thick and homogeneous oolitic carbonate beds (Rambeau et al., in prep (a)). We therefore propose a follow-up model, which is more detailed and complementary to the one proposed by Veuve (2000), and which take a suite of geochemical and sedimentological observations into account. In this model, we include new data for the location of cadmium on a micrometer scale and its chemical associations for a selection of Jurassic calcareous samples.

VII-2 Material and methods

VII-2-1 Samples

We have used a selection of samples which are highly enriched in Cd and listed in the following both for Synchrotron μ-XRF investigations at beamline L, Hasylab, Hamburg (Germany) as well as for μ-XRF mapping using an Eagle X-ray microfluorescence Spectrometer of the Institute of Terrestrial Ecology, ETH Zürich (Switzerland). The μ-XRF analyses were performed on 100 μm thin sections of the cadmium-enriched samples. These thin sections were both produced from bulk rock slices, as well as from specific components (oncoids), which were manually separated from the original rock, concentrated and cemented in an inert resin.

The samples used are the following:

- **S 156, Schleifenberg section**
  BL, Swiss Jura. International coordinates: 47:29:31N - 7:44:29E
  Early Bajocian, oolitic limestone
  Cadmium contents of 3.46 - 4.91 μg/g (2 replicates)
  Synchrotron μXRF measurements

- **LA 24 – LA 24epm1 – LA 24epm2, Lausen section**
  BL, Swiss Jura. International coordinates: 47:28:07N - 7:46:04E
  Early Bajocian, oolitic limestone
  Cadmium contents of 2.55 (La24) and 21.35 (LA 24epm1 – LA 24epm2) μg/g
  Synchrotron μXRF measurements (LA 24 – LA 24epm1 – LA 24epm2) and μ-Eagle XRF measurements (LA 24epm1)

- **OOF2**, **Ste Honorine des Pertes section**
  Normandy, France. International coordinates: 49:21:12N - 0:47:18W
  Early Bajocian, spongy, micritic limestone with ferruginous ooids
  Cadmium contents of 1.09 μg/g
  μ-Eagle XRF measurements

- **Lu2, Lucy-le-Bois section**
  Burgundy, France. International coordinates: 47:33:30N - 3:53:37E
  Early Bajocian, crinoidal/micritic limestone
  Cadmium contents of 2.68 μg/g
  μ-Eagle XRF measurements

- **DA 4b, Davayé section**
  Burgundy, France. International coordinates: 46:18:08N - 4:44:30E
  Early Bajocian, crinoidal limestone
  Cadmium contents of 1.76 μg/g
  Synchrotron μXRF measurements

Samples used for comparison:

- **ME 2, Merry-sur Yonne section**
  Burgundy, France. International coordinates: 47:33:53N - 3:37:52E
  Isolated and hand-picked grains: oncoids, cemented within resin
  Late Oxfordian, oncoidal micritic limestone
  Cadmium contents of 0.32 μg/g
  μ-Eagle XRF measurements

- **a recent lacustrian oncoid**
  Marin, Lake of Neuchâtel, Switzerland
  μ-Eagle XRF measurements

- **Bahamian recent ooids**
  Bay Cah, Bahamas, USA.
  Isolated and hand-picked grains: oncoids, cemented within resin
  μ-Eagle XRF measurements

Sedimentological context (marine samples)

The facies and microfacies associated with the sections of Schleifenberg, Lausen, Ste Honorine des Pertes, Lucy-le-Bois, and Davayé are characteristic of carbonate deposition on the margin of a carbonate platform. Samples belonging to these sections are composed of a mix of remobilized elements (ooids, crinoids) that formed higher on the margin and on top of the platform, in-situ precipitation (micritic matrix) as well

as, for the most agitated environments, sparitic matrix (e.g., cross-bedded oolitic beds of the Lausen-Schleifenberg section; not considered in this study).

In contrast, the Merry-sur Yonne section corresponds to the internal platform characterized by lagoonal environments. The recent ooids of the Bahamas were deposited in well-agitated shallow-water environments.

VII-2-2 Synchrotron μ-XRF analyses

We have used the setup at beamline L of the Synchrotron-X-Ray Fluorescence Microprobe at Hasylab (Hamburg, Germany), which allows for simultaneous multi-element analysis. This technology uses the highly brilliant synchrotron source, with its white and linearly polarized radiation, for fluorescence excitation. Detection of any element with atomic numbers (Z) between 20 and 92 is possible, using the K lines as analytical signal. Detection limits vary from 0.1 to 1 μg/g (Z = 20 to 50) to 1 to 10 μg/g (Z > 50). We have used an ML monochromator and a single-bounce capillary (Falkenberg et al., 2001, 2003) at an incident energy of 30 KeV, and a dwell time varying from 10 to 60s. The spatial resolution (beam diameteter) reaches 15-20 μm in diameter; however, the footprint is enlarged in the horizontal direction because of the 45 degree geometry of the beam-sample-detector. For several measurements (general mappings concerning larger areas of the samples) we moved out the capillary and used a large beam, collimated by slits. The presence of "hot spots" (small areas showing very high concentrations) of several elements have induced analytical problems, by saturation of the detector. After the first tries, a 90 μm thick Al absorber have been intercalated between the beam and the sample (see also specificities of measurements in the figure captions). We have operated on thin sections of 100 μm thickness, without glass support.

VII-2-3 Eagle X-ray microfluorescence spectrometer analyses

Preparatory scans for the above-described Synchrotron μ-XRF analyses at Hasylab, and supplementary investigations have been realized using a Eagle X-ray microfluorescence spectrometer at the Institute of Terrestrial Ecology (ETH Zürich, Switzerland). Beam resolution is approximately 40 μm and detection limits of a few μg/g. This technique allowed for the detection of Cd-enriched zones. Furthermore, it provided information on elements with atomic numbers below 20 (e.g., S), and permitted to obtain concentration maps and associated elemental spectra. We have used an incident energy of 40 KeV - 400-700 μA, with an amplificator time of 17 μs and a dwell time varying between 200 and 600 ms. Measurements were realized both on thin sections of 100 μm thickness, without glass support, and on uncovered glass-supported thin sections of 30 μm thickness.

VII-3 Results

VII-3-1 General chemical associations in investigated samples

Preliminary scans using the Eagle X-ray microfluorescence spectrometer and μ-XRF maps and associated spectra using the Synchrotron have permitted to establish the general chemical associations in the investigated samples (see also additional material, Annex 2: charts of observed chemical associations).

μ-Eagle XRF measurements show the omnipresence of Ca, except for areas rich in Si. Si enrichments occur most frequently in association with enrichments in Al, K, Mg, and Na, which are sometimes complemented by Fe, Mn, Ti, Ba, or occur in independent spots. Ti is preferentially associated with Ba, either within the spots of Si enrichments or outside.

Enrichments in S are systematically observed, but their amounts vary from one sample to another. La24epm1, OOF2, Lu2 frequently include S-enriched zones; in these samples the S spots are usually associated with Zn and/or Fe. S tends also to be associated with Ca (+/- Fe, Cd). In contrast, in sample ME2 S is present as a minor component exhibiting a rather homogeneous distribution, and is mostly associated with Ca and P. In μ-Eagle XRF measurements, the observed preferential "association" between Mo and S must be taken with caution, as it is certainly due to signal interference between both elements, leading to a "contaminated" signal (XRF peaks overlapping may occur if high concentrations of one of these two elements are detected).

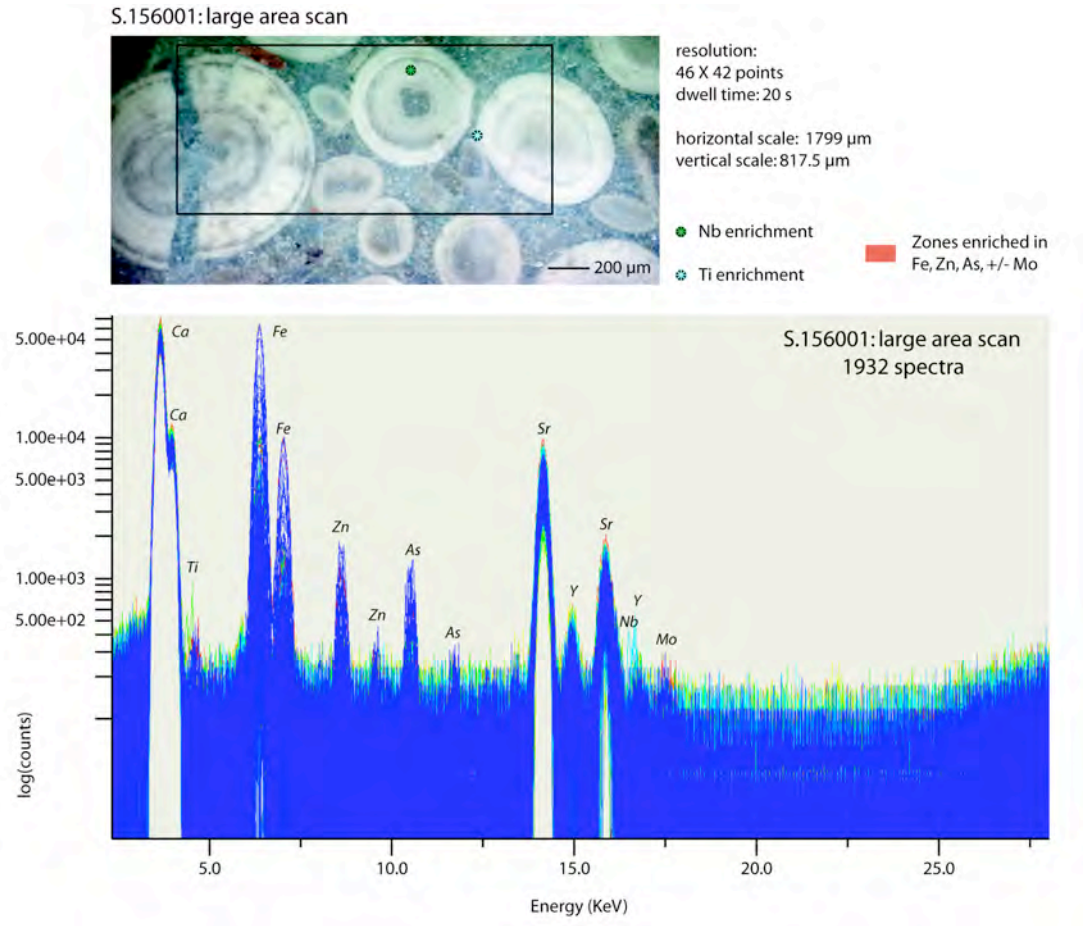

Fig. 1. Image, distribution of specific chemical elements and sum of all spectra measured for a selected area of sample S 156.

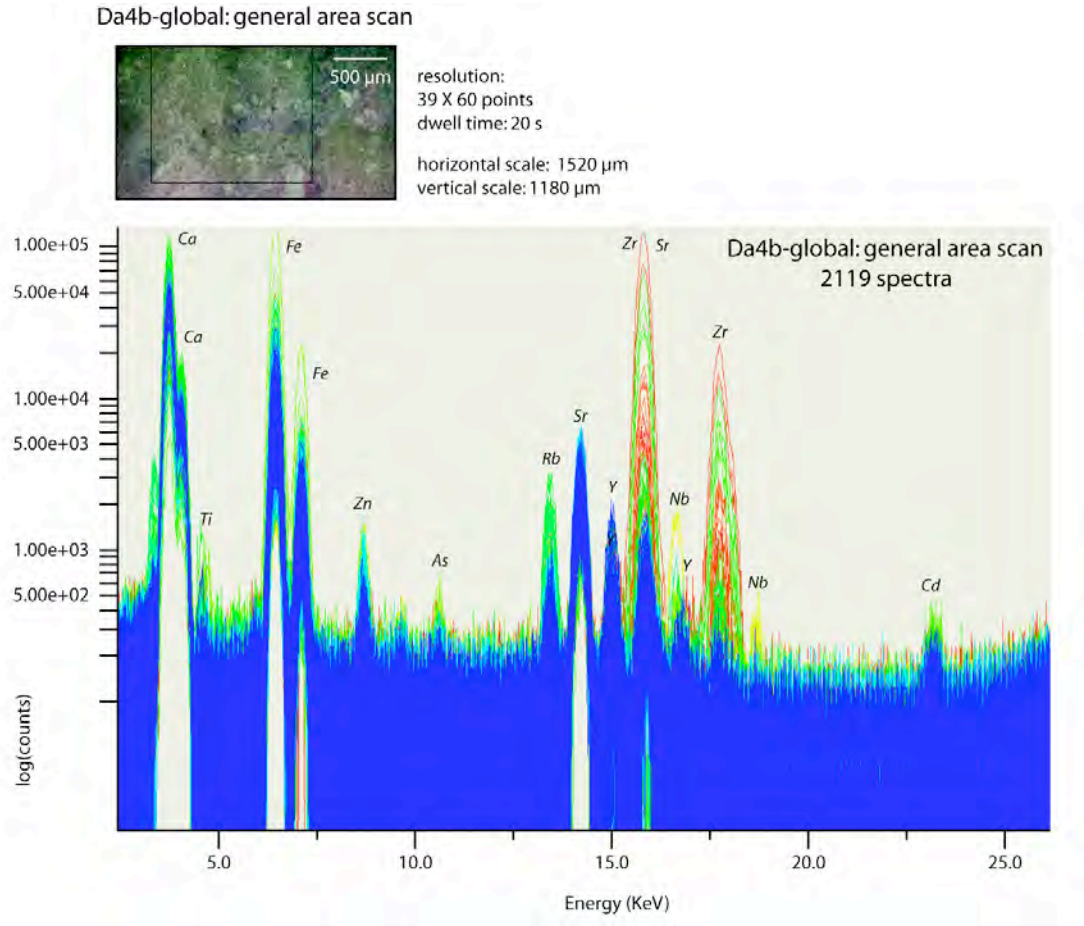

Fig. 2. Image and sum of all spectra measured for a selected area of sample Da4b.

Zn and Fe are equally two frequent components in the here analyzed carbonate rocks, which appear in some cases associated. Cd occurs in individual spots in most of the mapped areas (see also the specific paragraph on Cd location).

Chemical concentration maps and associated spectra obtained on the samples by Synchrotron µXRF display usual element associations comprising Ca, Fe, and Sr, which are often accompanied by Y, Zn, As +/- Mo (e.g., S 156 - Fig. 1). This association is in some cases complemented by Cd (Da4b - Fig 2; La24epm2 - Fig. 3) as well as elements like Ti (as already observed within the µ-Eagle XRF measurements), Zr, Nb, Pb, and Rb (S 156: Fig. 1; Da4b: Fig 2; La24epm2: Fig. 3; La24: Fig 4). These latter elements are sometimes in association or present unrelated concentration patterns (e.g., S 156: Fig. 1; La24: Fig 4). A preferential association is also observed between Fe and Mo (S 156, La24).

VII-3-2 The distribution of cadmium and its specific associations

Specific and well-defined Cd "hot spots" have been observed by both µ-XRF techniques, even if an important part of the realized maps - and in particularly the most precise ones by Synchrotron measurements, did not show the presence of Cd to measurable levels.

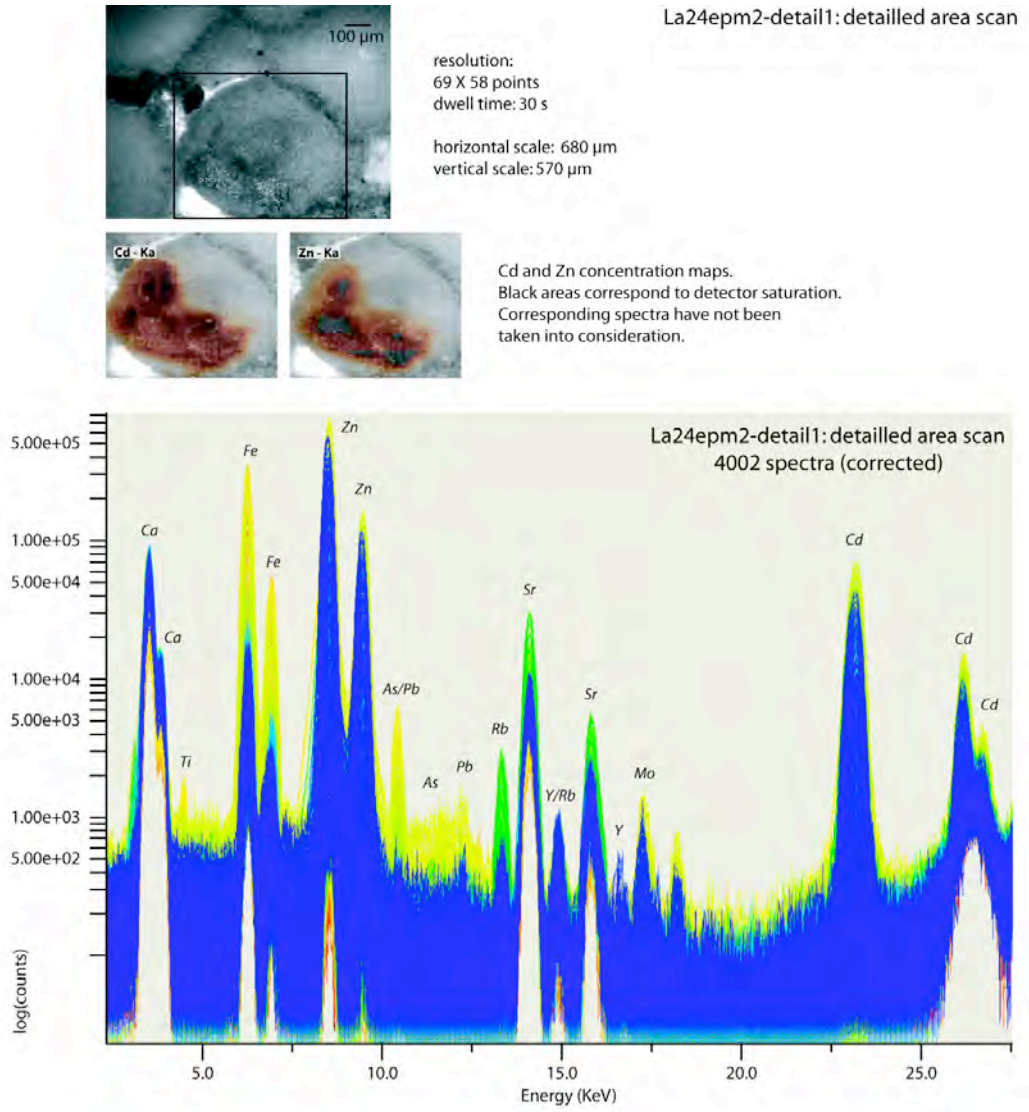

Fig. 3. Image, elemental distribution maps regarding Cd and Zn, and sum of all spectra measured for a selected area of sample La24epm2.

As was already suggested by the results from ICP-MS analyses, the spatial distribution of Cd is highly heterogeneous, and quantities may range from below detection limits to very enriched levels along a few micrometers distance (Synchrotron measurements; La24epm1: Fig. 5A). The same observation was made for the spatial distribution of Zn, which was associated with Cd in several cases (only observed by Synchrotron μ-XRF measurements; La24epm2: Fig. 3; La24epm1: Fig. 5A and B). Hot spots showing high concentrations of these two elements are sometimes - but not systematically – accompanied by enrichments in Mo (La24epm1 - Fig. 5A).

However, Cd enrichments appear in most cases not associated to any of the other measured elements with the possible exception of Ca (μ-Eagle XRF measurements: La24epm1, OOF2, Lu2). In one case a clear association of Cd enrichments with high contents of Fe and S is observed (ME2: Fig. 6).

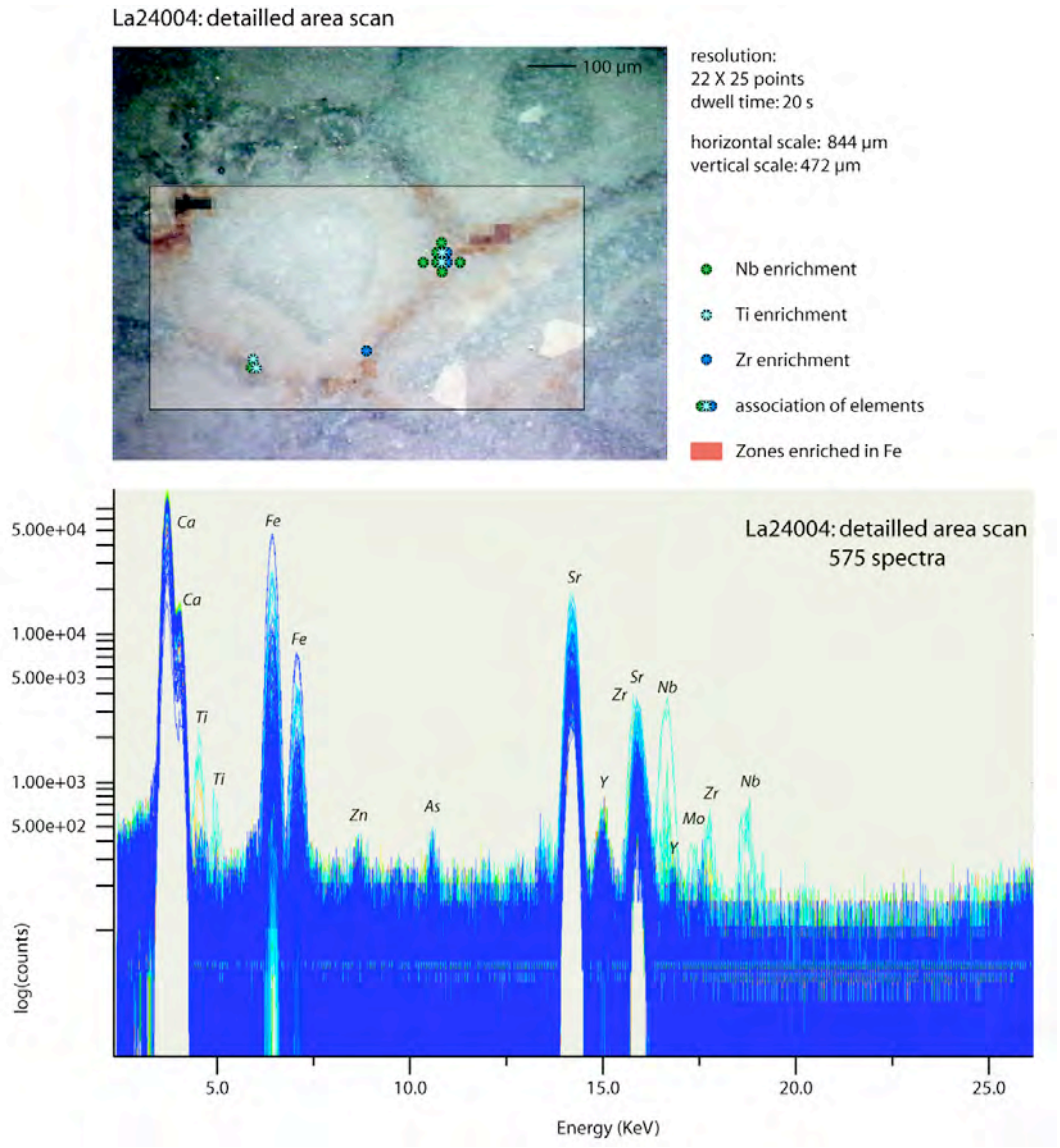

Fig. 4. Image, distribution of specific chemical elements and sum of all spectra measured for a selected area of sample La24.

A Cd enrichment was observed around a S- and Fe-enriched spot, which itself was not Cd-enriched (La24epm1: Fig. 7).

In most investigated samples, high concentrations of Cd are spatially limited to 100-200 μm spots, which occur both in the micritic matrix (OOF 2, Lu2, La24epm1: Figs. 5B and 7), as well as within ooids (La24epm2: Fig. 3; La24epm1: Figs. 5B and 7). In the latter case, Cd enrichment is sometimes observed to be only limited to a discrete zone within the ooid cortex, and is usually but not systematically associated with Zn (e.g., La24epm1: Fig. 7; La24epm2: Fig. 3; La24epm1: Fig. 5B), and to a lesser extend with Mo (La24epm1: Fig. 5B). It should be noted here that Cd enrichments occupy larger areas within the ooid cortices than other elemental hot spots (La24epm2: Fig. 3; La24epm1: Fig. 5B). Elemental spectra obtained from the Cd hot spots show a systematic association of Cd with Ca, even if the relative amount of Ca diminishes in most Cd- and Zn-enriched zones (La24epm2: Fig. 3).

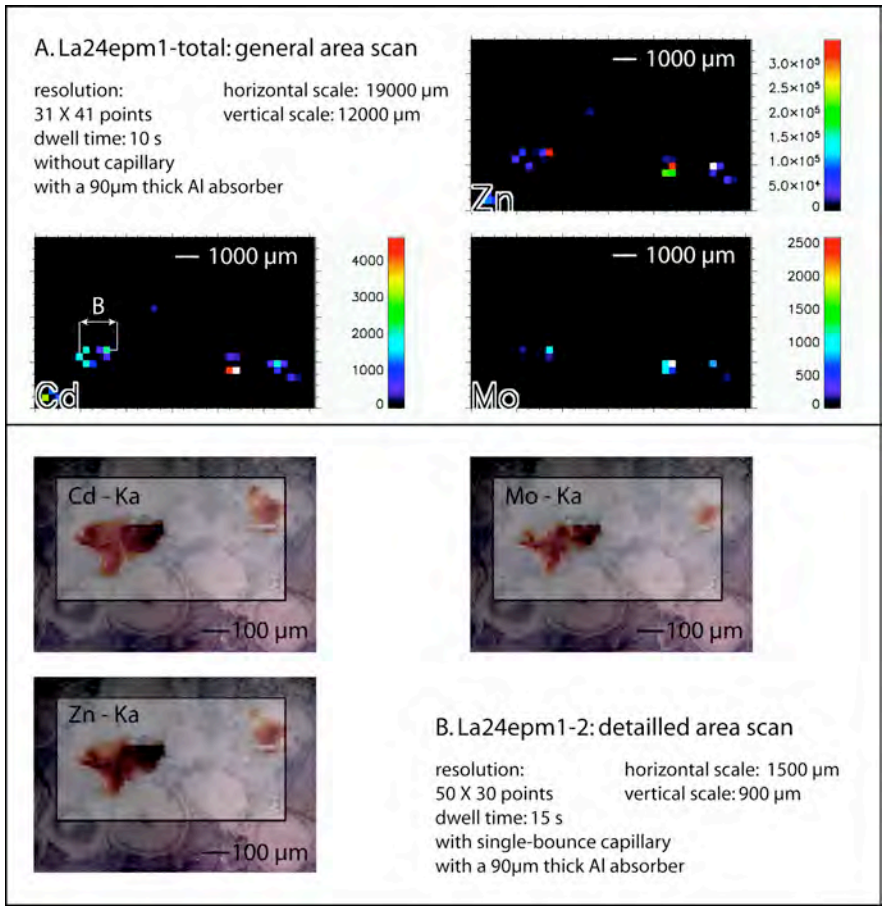

Fig. 5A. Large-scale Cd, Zn and Mo distribution in thin section La24epm1. Relative intensities of elements are given in counts per line. **Fig. 5B.** Image and superimposed elemental distribution maps of Cd, Zn and Mo for a selected area of sample La24epm1, corresponding to one of the enriched zones observed in Fig. 5A.

In addition, smaller amounts of Cd may also be incorporated into the outer rings of oncoids (ME2: Fig 6, recent lake oncoid). In this sample Cd is associated with Ca, P, K, Cl, and S in various amounts. Cd has not been observed in recent Bahamian ooids.

VII-3-3 Zn distribution

We did not observe a coincidence in the locations of Cd and Zn in the µ-Eagle XRF measurements. In most samples, Zn appears to be located either in association with S (Me2: Fig. 6), Fe (Lu2, ME2), or in spots independent from other elemental enrichments (La24epm1, OOF 2). In most cases, the outer rings of ooids or oncoids are not enriched in Zn to a measurable level (Bahamian ooids, recent lake oncoid).

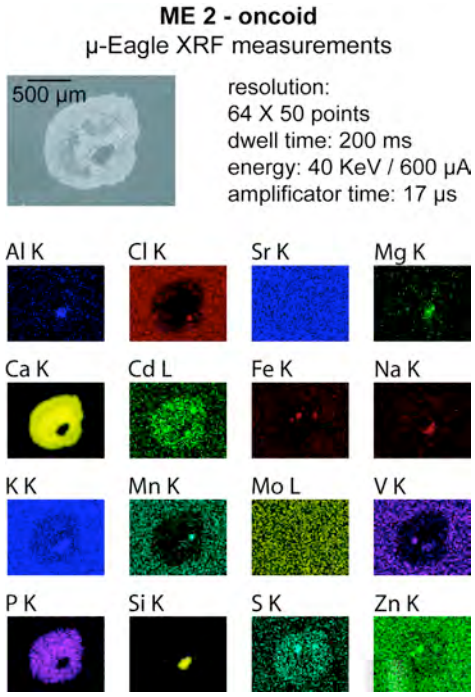

Fig. 6. Image and elemental distribution maps of Al, Cl, Sr, Mg, Ca, Cd, Fe, Na, K, Mn, Mo, V, P, Si, S, and Zn for a selected oncoid from sample ME2. N.B. For some elements (e.g., Sr, K, Mo...) concentrations are not sufficient, which results in an similar, patchy color for both the calcitic grain and the background.

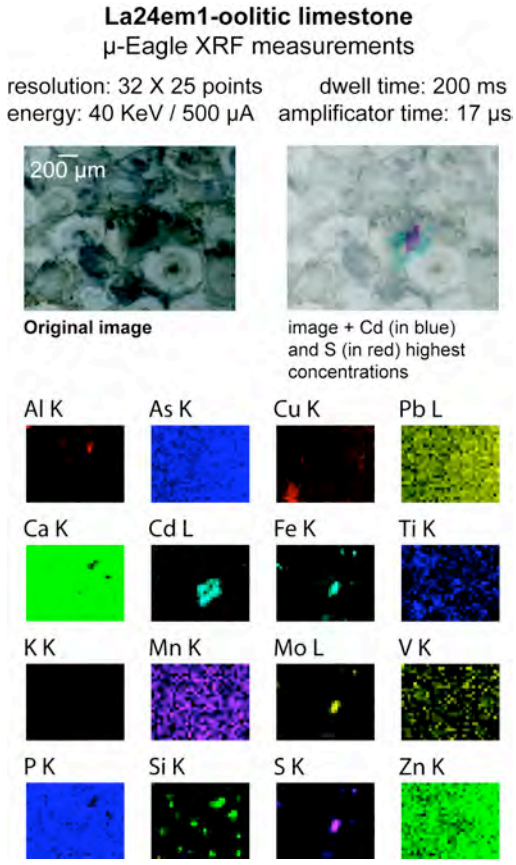

Fig. 7. Image and superimposed Cd concentration map, and elemental distribution maps of Al, As, Cu, Pb, Ca, Cd, Fe, Ti, K, Mn, Mo, V, P, Si, S, and Zn for a selected area of sample La24epm1. N.B. Same remark than for Fig. 6.

In contrast to Cd, most of the maps realized by Synchrotron technics show high concentrations of Zn, which were preferentially located inside the micritic matrix and principally associated with Fe, As +/- Mo (S 156: Fig.1). As already mentioned in the previous paragraph, a positive correlation was observed between Cd and Zn in some of the Synchrotron maps; in these cases, Zn enrichments occur both in the micritic matrix as well as in the surrounding ooid grains (La24epm1: Fig. 5), and there sometimes in discrete zones within the ooid cortices (La24epm2: Fig. 3). In most thin sections (such as La24s), numerous Zn spots were observed, which are not associated with Cd enrichments.

VII-4 Interpretation and discussion

VII-4-1 General chemical associations and environmental conditions

All analyzed Cd-enriched rock samples (S156, La24s, Da4b, OOF2, Lu2) are for a large part composed of calcitic grains (bioclasts, lithoclasts, ooids) and include a micritic matrix in the form of calcite. Detrital components are invariably present in subordinate amounts and are marked by various elemental associations, depending on their mineralogy. Detrital grains also serve as a nucleus for oncoid precipitation (Me2, recent lacustrian oncoid). Usual compositions of detrital grains include Si +/- Al, and K, and in minor amounts Ti, Fe, Mg, and Na. Si individual spots my be either related to purely siliceous detrital phases or to authigenic Si precipitation.

Observed spots of enriched S concentrations in the thin sections of samples La24epm1, OOF2, Lu2 are located in the micritic matrix, and correspond probably to sulphide grains. The presence of numerous S-enriched grains in these sections hint at the importance of pyrite, which is interpreted as a witness of reducing conditions during early diagenesis (Raiswell and Berner, 1986; Raiswell et al., 1988). Less important S contents in sample Me2, associated with Ca/P enrichment, may be related to direct incorporation during the cortex formation.

VII-4-2 Relationship between Cd and Zn

We do not observe a systematic coincidence in the locations of Cd and Zn in the analyzed samples; however, some of the Cd enrichments equally present high Zn contents (La24epm2: Fig. 3; La24epm1: Fig. 5B). We therefore postulate a rather different chemical behavior during diagenesis for Zn in comparison to Cd. This includes a preferential location of Zn inside sulphide lattices (under reducing conditions) and the existence of additional Zn host phases, such as a carbonate phase, and an iron oxy-hydroxide mineral in the case the sedimentary rock underwent oxydation through rock exposure. In both cases, Zn shows a rather strong association with Fe. ICP-MS measurements as well as multivariate statistical analyses reveal that concentrations of these two elements are generally positively correlated, at least for samples from the Lausen-Schleifenberg section (Rambeau et al., in prep (b)). These elements may therefore have a similar source, as well as partially similar concentration mechanisms.

VII-4-3 Other trace-element occurrences

In several of the investigated thin sections (S 156: Fig. 1; Da4b: Fig 2; La24epm2: Fig. 3; La24: Fig 4), the presence of Ti, Zr, Nb, Pb, and/or Rb have been observed. Possible host phases for these elements may be partly carbonate grains, partly clay or authigenic precipitates. An example is given by Nb enrichments, which occur both inside the ooid cortex (S 156: Fig. 1), as well as in the matrix bounding the carbonate grains (La24: Fig. 4). The specific distribution and concentration mechanisms of these elements will not be discussed here. However, their rather widespread presence in the investigated sections let us speculate about their origin. These elements are mostly present in high concentrations in the Earth crust; they may be transferred into the carbonate systems either through the mediation of detrital phases (which may be the case at least for Ti; Jimenez-Espinoza et al., 1997), or by aerial volcanic inputs. Pb is indeed an element frequently associated with volcanic emissions (e.g., Hinkley et al., 1999) and is, like Cd and Zn, and to a lesser extend, Rb, highly enriched in volcanic gases by comparison with lava extrusions (e.g., Symond et al., 1987; Allard et al., 2000). Pb, Zr and Nb has been found in high concentratins in the volcanic assemblage of Bandelier Tuff, New Mexico (1.61-1.22 My; Stimac et al., 1996) an some Jurassic smectite-rich bentonites have been shown to be enriched in Zn, Zr, and Nb (Jeans et al., 2000).

VII-4-4 Cd location and concentration mechanism: towards a model of cadmium enrichment in carbonate rocks

In the here investigated samples related to the platform margin, Cd concentrations have been shown to not only occur in specific grains like ooids but also in small spots both in a micritic matrix, or within part of ooids cortices. These enrichments are either independent of the concentrations of other elements (La24epm1: Fig. 7) or related to Zn +/- Mo enrichments (La24epm2: Fig. 3 and La24epm1: Fig. 5B). Furthermore, Cd spots have been observed to envelop S- and Fe-enriched spots which themselves are not enriched in Cd (La24epm1: Fig. 7). Oncoids (lagoonal environments) have been shown to contain moderate but rather homogeneous Cd concentrations. These new observations are in some contrast to previous results where a preferential concentration of Cd inside the entire cortices of ooids, and entire ooids in the case the grain is micritized, was reported (oolitic barrier and lagoonal environments; Veuve. 2000). The here proposed model permits to reconcile all observations of Cd enrichments in calcareous rocks.

In Fig. 8, we trace the processes leading to Cd enrichment on an oolite-dominated carbonate platform along a transect from the internal platform realm to the margin. Ooid grains form in shallow-water environments and are exported towards more open-marine settings by wave currents, where they are mixed with authochtonous sediment such as micrite and clay, as well as towards inner shelf environments, where they underwent intensive micritization.

All investigated sections related to oolitic and oncoidal sedimentation (Lausen-Schleifenberg, Pont-de-la-Baleine, Dornach, Auenstein, Merry-sur-Yonne, Gorges du Pichoux; Veuve, 2000; Rambeau et al., in prep (a); this study) have been placed in this model with regards to their respective depositional environments.

For comparison, the sections related to other types of calcareous accumulations have also been placed on this transect (Davayé and Lucy-le-Bois sections: mostly crinoidal deposits; Ste Honorine des Pertes section: ferruginous ooids and spongy micrite).

Cd enrichment - case 1: platform margins

Enhanced primary productivity rates are responsible for an enhanced flux of organic matter exported towards the sediments. This may include primary organic matter and organic-rich pellets. Cd is supposed to concentrate by adsorption onto particles of organic matter (Gonzalez et al., 1999), or more generally onto solid particles, which represent the vector that delivers Cd to the sediment-water interface (Gobeil et al., 1987).

Organic-rich agglomerates and pellets reaching the sea bottom become incorporated into the oolitic sedimentary waves and dunes, especially since their (re-) deposition is a rapid process. Within the sediments, the organic particles are decomposed by bacterial respiration, thereby creating local reducing conditions (as is suggested by high levels of S in the investigated samples) and imposing a redox boundary, which is probably located near the surface of the freshly deposed sediment.

The early diagenetic environment may be characterized by complex redox gradients and associated pH variations, which may lead to the formation of sulphide phases within and near the organic pellets, as well as to the desorption and transfer of the Cd adsorbed onto the organic matter into different mineral phases, such as sulphide minerals and carbonates. A partial association of Cd with sulphide minerals is suggested by the association of Cd with Zn and Mo (La24epm1: Fig. 5B) in spots located in the micritic matrix. Cd - and eventually other elements like Zn - may also be transferred to surrounding carbonate grains, where it becomes incorporated by a process of probably pH-induced carbonate dissolution and reprecipitation allowing for the replacement of Ca ions in carbonates phases by Cd (La24epm1: Figs. 5B and 7). A carbonate hosting phase is indeed suggested by the systematic association of Cd with Ca in the Cd enriched zones. Furthermore, it appears that relative to Zn and Mo, Cd enrichments extend slightly deeper into carbonate grains (La24epm2: Fig. 3, and La24epm1: Fig. 5B). This may indicate that Cd is a preferred substituting element of Ca, due to specific chemical affinities between these two elements - which have very comparable ionic radii (0.94 Å for Cd versus 0.99 Å for Ca), in comparison to Zn and Mo (ionic radii of 0.74 Å and 0.59 Å, respectively) - as was already pointed out by Altschuler (1980) and Middleburg and Comans (1991) in the case of Cd substitution with Ca in phosphorite.

The sediments that are enriched in cadmium in this manner, may become remobilized again and single cadmium-enriched grains may become mixed with non-enriched oolites in new deposits. This mechanism may be responsible for the presence of isolated Cd-enriched ooids in association with non-enriched micritic grains and ooids (La24epm2: Fig 3).

Fig. 8. Next page. Model of Cd enrichment along an oolite-dominated carbonate platform transect from the slope to the internal platform realm.

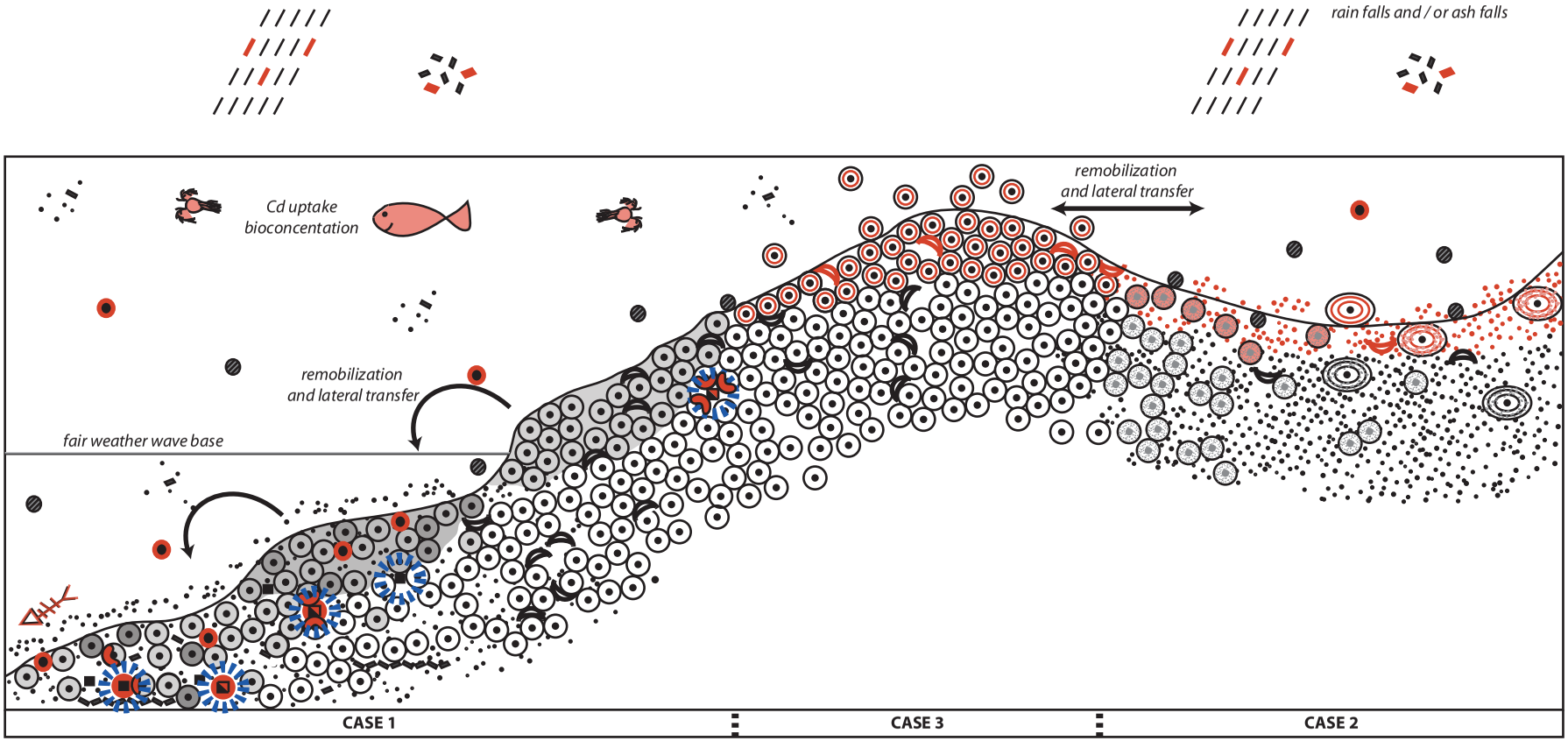

Schleifenberg (lower part)
Lausen
by analogy (different kind of deposits):
Lucy-le-bois
Davayé
Ste-Honorine-des-Pertes

Pont-de-la-Baleine
Auenstein
Schleifenberg (upper part)

Gurnigel *Dornarch*
Vue-des-Alpes

Le Saussois / **Merry-sur-Yonne**
Gorges du Pichoux

LEGEND

Pelagic organisms

Sedimentary grains / minerals

- *ooid*
- *oncoid*
- *bioclast*
- *clay particle*
- *micrite*
- *organic mater particle (e. g. pellet)*
- *sulphide grain (FeS_2, ZnS_2)*

Processes

- *early degradation of organic mattter*
- *micritization*
- *local transition between oxygenized and reduced conditions*
- *remobilization*
- *high Cd contents*
- *moderate to high Cd contents*

The case 1 scenario is related to the platform margin and implies an intervention by organic matter, principally in the form of pellets - which is more likely than finely dispersed organic matter in the dynamic sedimentary environment - and sulphide grain formation. A rather similar model has been proposed by Rosenthal et al. (1995), who assumed an immobilization of Cd in sulphidic sediments in the form of CdS. However, recent observations on actual sedimentation processes in the Laurentian Trough, Gulf of St. Lawrence, tend to negate the importance of such a mechanism (Sundby et al., 2003). These authors show that authigenic Cd accumultion is insensitive to sulphide abundance.

We postulate here that Cd is precipitated in carbonate grains surrounding the organic-matter from which it was desorbed, rather than in in a sulphidic phase (even if part of disponible Cd may enter this phase). It is evident that such a mechanism is unlikely to occur in sediments dominated by detrital components, like in the Gulf of St. Lawrence (Sundby et al., 2003). It becomes, however, far more probable in carbonate platform environments, where calcareous deposits may react strongly to local diminutions of pH, by dissolution and quasi-immediate reprecipitation due to a buffering effect. In this case, elements present in pore fluids (e.g., Cd) are likely to enter the new-formed carbonate phases.

Cd enrichments - case 2: lagoonal environments

Cd is also incorporated in moderate and rather homogeneous amounts in the outer rims of the here analyzed oncoid grains (ME2) - in association with Ca, P, K, Cl, and S in various proportions.

We postulate, therefore, that in lagoonal environments, Cd becomes incorporated into carbonate grains and especially into oncoids, via co-precipitation with calcium carbonate phases, favored by the comparable chemical affinities of Cd and Ca (Altschuler, 1980; Middleburg and Comans, 1991; see also Thakur et al., 2005), and probably aided by bacterial activity during the intensive post-depositional processes of micrititisation that operate in this kind of environments, and/or by direct microbial bioconcentration, eventually within or near organic-rich biofilms that are present in the oncoids.

Many investigations have been made concerning the sorption rate of dissolved metals, including Cd, with calcite, and the results hint invariably at a rapid initial removal of metals from the solution, which - in the case of Cd -, is in the form of surface precipitation of (Cd, Ca)CO_3 solid solutions (Prieto et al., 2003), followed by much slower uptake (e.g., Prieto et al., 2003 and references therein). However, in case of precipitation of successive carbonate layers, the process may have been repeated for each outer ring with renewed efficiency.

In addition, bacterial cells are known to adsorb different types of trace elements such as Cd and U with great efficiency (Boyanov et al., 2003 and references therein; Kemner et al., 2005 and references therein). A similar mechanism of enrichment may have played a major role in trace-metal distributions in carbonate systems which are dominated by microbial activity.

Cd enrichments - case 3: platform barrier

Certain types of ooid grains related to platform barrier environments (packed ooid grains cemented by sparite) show a preferential enrichment of Cd in the entire outer cortex layers (Veuve, 2000). This enrichment is proposed to occur directly during ooid cortex formation, by incorporation of the Cd disponible in the environment at the time of precipitation. This assessment is corroborated by the fact that the nuclei of the ooid grains studied by Veuve (2000) equally show an enrichment in Cd relative to the sparitic matrix, but not as high as the outer cortex. The observation of homogeneously distributed Cd values within micritized ooids (Veuve, 2000) is equally in accordance with the hypothesis of a direct enrichment during ooid precipitation.

This type of enrichments during ooid formation may be related to the particular structure of ooids, which may include – similar to oncoids - layers rich in organic matter in alternance with carbonate layers (Folk and Lynch, 2001). If the organic matter incorporated during ooid development was enriched in Cd, this may result in high levels of Cd in the whole ooid cortex. However, high concentrations of Cd were in this case directly dependent on the availability of Cd in the parent waters, since recent Bahamian ooids do not show Cd enrichments (0.016 μg/g: ICP-MS measurement - Veuve, 2000; Cd not detected during μ-XRF analyses - this study).

These processes of cadmium incorporation and enrichment seem to directly depend on the specific environmental conditions during the deposition of sediments and on the quantity of Cd available in seawater at the time of ooid and oncoid formation. This latter point is underlined by the fact that most oolitic carbonate rocks, and calcareous rocks in general, are not Cd-enriched to measurable levels, even in the carbonate sections which have shown the presence of highly enriched levels in cadmium (Rambeau et al., in prep (a)). We therefore propose that occasional events of preferential cadmium input occurred during the Jurassic, especially during the Bajocian and Oxfordian periods, each event being of a short duration. Volcanic events may be responsible for episodic inputs of Cd in these sedimentary systems, and for the presence of other trace-elements like Nb, Zr, and Pb in the investigated samples. However, input by enhanced continental weathering cannot be excluded either, even if this hypothesis seems less probable, due to the very punctual occurrence of Cd enrichments in Jurassic carbonate.

VII-5 Conclusions

Cd in calcareous rocks of the Jurassic period has been shown to concentrate in shallow-water environments depending on (1) biological activity and (2) amounts of Cd available in seawater. This is in accordance with previous studies in which a positive correlation between Cd and organic matter and/or suboxic conditions was established (e.g., Heinrichs et al., 1980; Rosenthal et al., 1995; Van Geen et al., 1995; Il'in and Kiperman, 2001). A model, subdivided into three specific cases, has been established for the preferential enrichment of Cd in platform settings. The case one is in association with:

- enhanced bioproductivity and related organic matter production, and subsequent enhanced input of organic matter inside sediments, particularly in the form of pellets
- high sedimentation rates on the platform slope,
- the establishment of reducing conditions in the uppermost part of deposits associated with organic matter degradation
- and subsequent Cd transfer, for a minor part into sulphidic phases, and for a major part into surrounding carbonate grains.

This case takes into account our observations of Cd enrichments occurring both in the matrix, where they sometimes occur in the immediate vicinity of S-enriched grains, as well as in discrete zones within the ooid cortices. It also give an explanation for the highly heterogeneous contents of cadmium present in the investigated samples.

Cd enrichments in lagoonal environments are proposed to be related to microbial activity, via micritization and/or by direct bioconcentration in carbonate phases (case 2). Calcareous ooids may also be directly enriched in Cd by sequestration of this element within the layers of organic matter these grains may comprise (case 3).

This model permits to reconcile new observations realized at micrometre scale by μ-XRF measurements on limestone related to platform margin environments (this study) with previous observations mostly obtained on limestone from barrier or inner-shelf environments (Veuve et al., 2000). Our results equally highlight the probable external origin for Cd in these environments. One possible source of Cd, and perhaps of other trace-elements present in the investigated samples, is by aerial volcanism; another possibility, although less probable due to the short duration of cadmium enrichment events, is represented by enhanced continental weathering.

Acknowledgments

We would like to thank Gerald Falkenberg, Karen Rickers, Andreas Voegelin and Olivier Jacquat for analytical assistance and advise. We also acknowledge financial support from the Swiss National Science Foundation (projects no. 21-65183.01, 200020-101718/1).

Additional material

Additional material

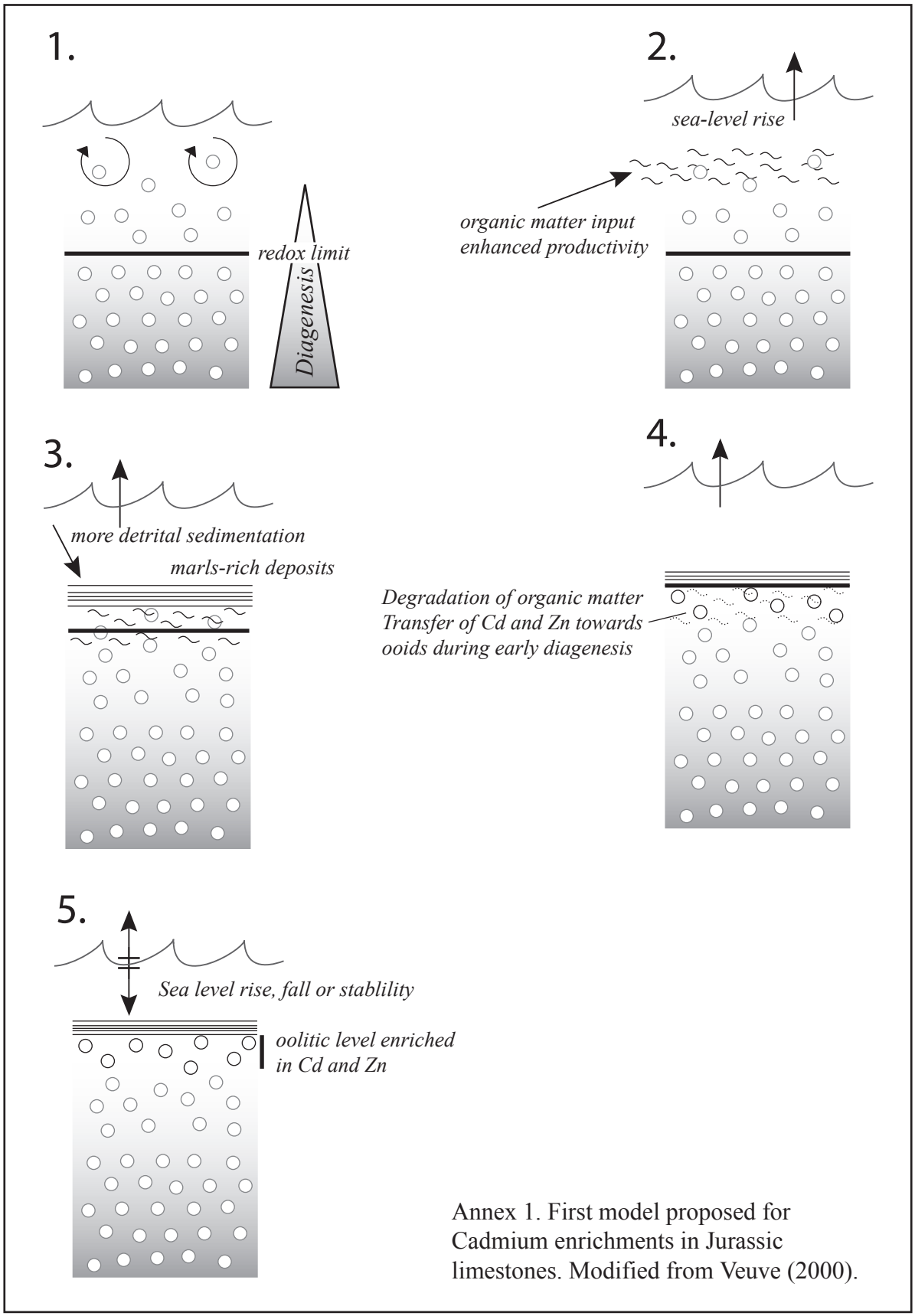

Annex 1. First model proposed for Cadmium enrichments in Jurassic limestones. Modified from Veuve (2000).

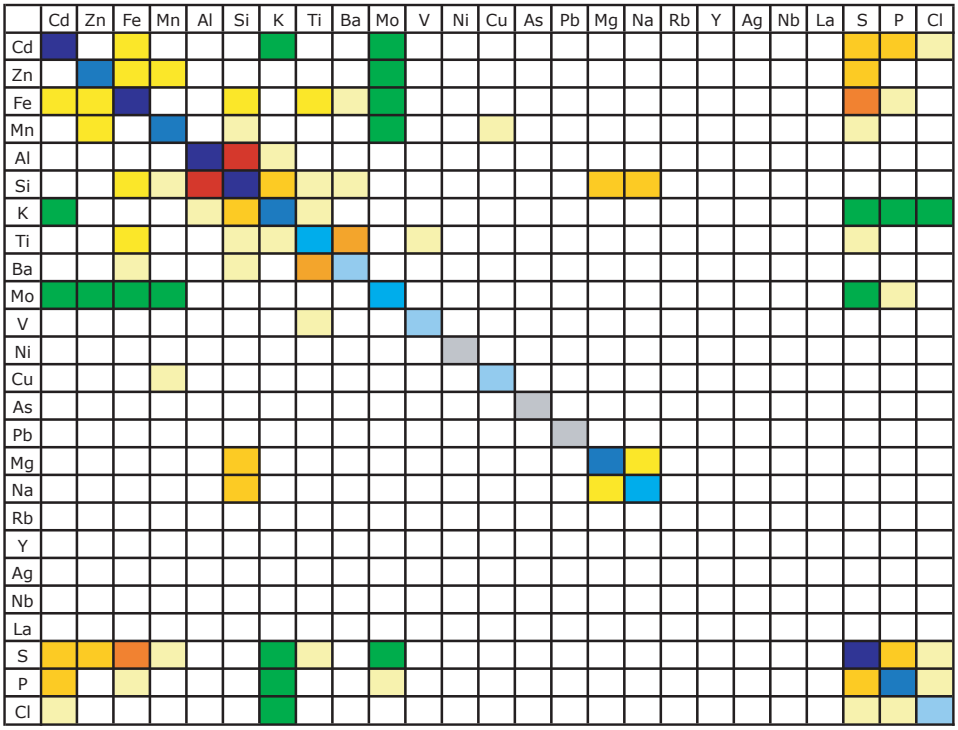

Table 1
apparent chemical associations observed after µ-Eagle XRF concentration maps

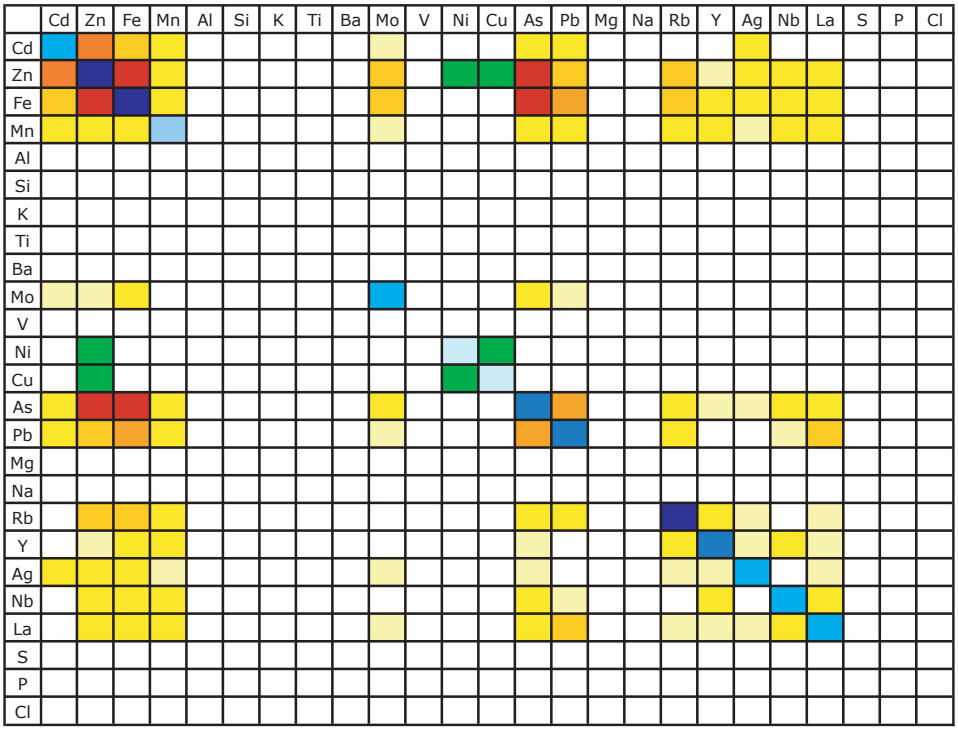

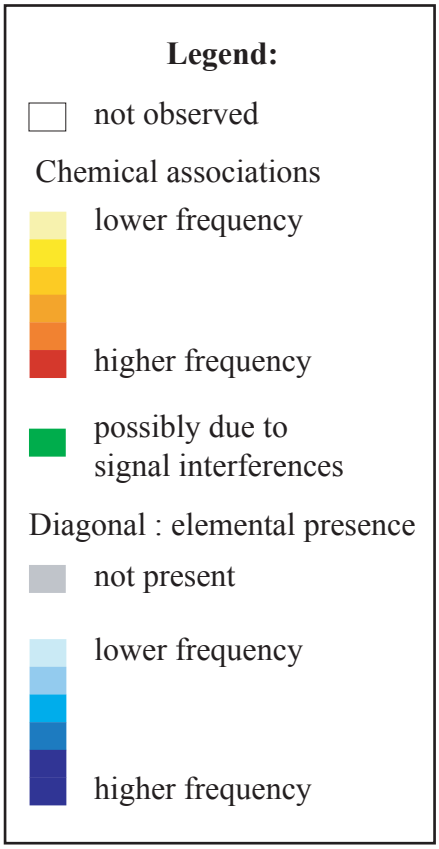

Table 2
apparent chemical associations observed after Synchrotron µXRF concentration maps

Annex 2. Charts of observed chemical associations (non quantitative).
Table 1: observed chemical associations by µEagle microfluorescence elemental maps
Table 2: observed chemical associations by Synchrotron µXRF elemental maps
Ca and Sr have not been taken into account in the compilation of the elemental associations.
This is related to the omnipresence of Ca, and, to a lesser extend, Sr, in these samples, which renders any determination of specific associations with this element uncertain. In these table, possible interferences beween chemical elements, leading to a "contaminated" signal (high concentrations of some elements lead to an enlargment of the associated XRF peaks, and may induce a artificial detection of elements which peaks are located in the immediate vicinity) have been highlighted in green. These interferences are dependant of the specific elemental lines used for elemental detection, which varies for several element between µ-Eagle XRF and Synchrotron µ-XRF measurements.
The diagonal line is used for an appreciation of the relative presence of the elements of interest (gray to dark blue colors).
Specific associations are plotted in yellow to red colors following the number of observations.

References

Allard, P., Aiuppa, A., Loyer, H., Carrot, F., Gaudry, A., Pinte, G., Michel, A. and Dongarrà, G., 2000. Acid gas and metal emission rates during long-lived basalt degassing at Stromboli volcano. Geophysical Research Letters, 27, 1207-1210

Alloway, B.J., 1995. Cadmium. In: Heavy metals in soils. 2nd edition. Blackie Academic and Professional, 122-147

Altschuler, Z.S., 1980. Geochemistry of trace elements in marine phosphorites. Soc. Econ. Paleontologists Mineralogist Spc. Pub, 29, 19-30

Baize, D., and Sterckeman, T., 2001. Of the necessity of knowledge of the natural pedogeochemical background content in the evaluation of the contamination of soils by trace elements: The Science of the Total Environment, 264, 127-139

Benitez-Vasquez, N., 1999. Cadmium speciation and phyto-availability in soils of the swiss Jura : hypothesis about its dynamic. Ecole Polytechnique Fédérale de Lausanne. 132 pp.

Boyanov, M.I., Kelly, S.D., Kemner, K.M., Bunker, B.A., Fein, J.B. and Fowle, D.A., 2003. Adsorption of cadmium to Bacillus subtilis bacterial cell walls: A pH-dependent X-ray absortion fine structure spectrometry study. Geochim Cosmochim Acta, 67 (18), 3299-3311

Dubois, J.P., Benitez, N., Liebig, T., Baudraz, M. and Okopnik, F., 2002. Le cadmium dans les sols du haut Jura suisse, in Les éléments traces métalliques dans les sols. Approches fonctionnelles et spatiales, D.Baize, M.Tercé, editors, INRA Editions, Paris, 33-52

Falkenberg, G., Clauss, O., and Tschentscher, Th., 2001. X-ray Optics for the Microfocus Beamline L. Hasylab Annual Report, available on http://www-hasylab.desy.de/science/annual_reports/2001_report/index.html

Falkenberg, G., Rickers, K., Bilderback, D.H. and Huang, R., 2003. A Single-bounce Capillary for Focusing of Hard X-rays. Hasylab Annual Report, available on http://www-hasylab.desy.de/science/annual_reports/2003_report/index.html

Folk, R.L. and Lynch, F.L., 2001, Organic matter, putative nannobacteria and the formation of ooids and hardgrounds. Sedimentology, 48, 215-229

Gobeil C., Silverberg, N., Sundby, B. and Cossa, D., 1987. Cadmium diagenesis in Laurentian Trough sediments. Geochim. Cosmochim. Acta, 51, 589-596

Gonzalez, J.-L., Chiffoleau, J.-F., Miramand, P., Thouvenin, B. and Guyot, T., 1999. Le cadmium : comportement d'un contaminant métallique en estuaire. IFREMER publications, Programme scientifique Seine-Aval, 10, J.-L. Gonzalez (coord.), Plouzané, France, 31 pp.

Heinrichs H.B., Schulz-Dobrick B., Wedepohl K.H., 1980. Terrestrial geochemistry of Cd, Bi, Tl, Pb, Zn and Rb. Geochim. Cosmochim. Acta, 44, 1519-1533

Hinkley, T.K., Lamothe, P.J., Wilson, S.A., Finnegan, D.L. and Gerlach, T.M., 1999. Metal emissions from Kilauea, and a suggested revision of the estimated worldwide metal output by quiescent degassing of volcanoes. Earth and Planetary Science Letters, 170, 315-325

Il'in, A.V. and Kiperman, Y.A., 2001. Geochemistry of Cadmium in Mesozoic Phosphorites of the East European Platform. Lithology and Mineral Resources, 36 (6), 576-581

Jeans, C.V., Wray, D.S., Merriman, R.J. and Fisher, M.J., 2000. Volcanogenic clays in Jurassic and Cretaceous strata of England and the North Sea Basin. Clay Minerals 35, 25-55

Jiménez-Espinoza, R., al., Jiménez-Millán, J. and Nieto, L., 1997. Factors controlling the genesis of Fe-Mn crusts in stratigraphic breaks of the eastern Betic Cordillera (SE Spain) deduced from numerical analysis of geological data. Sedimentary Geology, 114, 97-107

Kabata-Pendias, A. and Pendias, H., 1992. Trace elements in soils and plants. 2nd edition. CRC Press, 365 pp.

Kemner, K.M., O'Loughlin, E.J., Kelly, S.D. and Boyanov, M.I., 2005. Synchrotron X-ray Investigations of Mineral-Microbe-Metal Interactions. Elements, 1 (4), 217-221

Middleburg, J.J. and Comans, R.N.J.J., 1991. Sorption of cadmium on hydroxyapatite, Chemical geology, 90, 45-53

Nathan, Y., Soudry, D., Levy, Y., Shitrit, D., and Dorfman, E., 1997. Geochemistry of cadmium in the Negev phosphorites. Chemical geology, 142, 45-53

Prieto, M., Cubillas, P, and Fernández-Gonzales A., 2003. Uptake of dissolved Cd by biogenic and abiogenic aragonite: a comparison with sorption onto calcite. Geochim Cosmochim Acta, 67 (20), 3859-3869

Prudente, D., Baize, D., Dubois, J.P., 2002. Le cadmium naturel dans une forêt du haut Jura français, in Les éléments traces métalliques dans les sols. Approches fonctionnelles et spatiales, D. Baize, M. Tercé, editors, INRA Editions, Paris, 53-70

Raiswell, R. and Berner, R.A., 1986. Pyrite and organic matter in Phanerozoic normal marine shales. Geochim Cosmochim Acta, 50, 1967-1976

Raiswell, R., Buckley, F., Berner, R.A. and Anderson, T.F., 1988. Degree of pyritization of iron as a paleoenvironmental indicator of bottom water oxygenation. Jrnl Sed Petrology, 58, 812-819

Rambeau, C., Föllmi, K.B., Adatte, T., Baize, D., Bartolini, A., Hug, W.A., Matera, V., Sandoval, J., Steinmann, P., and Veuve, P., in prep (a). Anomalous cadmium enrichments in Tethyan Jurassic carbonates: past and present environmental implications. In prep (a).

Rambeau C., Föllmi, K.B., Adatte, T., Bartolini, A., Hug, W.A., Matera, V., Verrecchia, E., in prep (b). Cadmium enrichments in Jurassic carbonates: towards the causes and mechanisms. In prep (b).

Rosenthal, Y., Lam, P., Boyle, E.A., and Thomson, J., 1995. Authigenic cadmium enrichments in suboxic sediments: precipitation and postdepositional mobility. Earth and Planetary Science Letters, 132, 99-111

Stimac, J., Hickmott, J., Abell, R., Larocque, A.C.L., Broxton, D.E., Gardner, J., Chipera, S., Wolff, J. and Gaueke, E., 1996. Redistribution of Pb and Other Volatile Trace Metals During Eruption, Devitrification, and Vapor-Phase Crystallization of the Bandelier Tuff, New Mexico. Journal of Volcanology and Geothermal Research, 73, 245-266

Sundby, B., Martinez, P. and Gobeil, C., 2003. Comparative geochemistry of cadmium, rhenium, uranium, and molybdenium in continental margin sediments. Geochim. Cosmochim. Acta, 68 (11), 2485-2493

Symonds, R. B., Rose, W. I., Reed, M. H., Lichte, F. E., and Finnegan, D. L.1987. Volatilization, transport and sublimation of metallic and non-metallic elements in high temperature gases at Merapi Volcano, Indonesia. Geochim. Cosmochim. Acta, 51, 2083-2101

Thakur, S.K., Tomar, N.K. and Pandeya S.B. In Press, Corrected Proof. Influence of phosphate on cadmium sorption by calcium carbonate. Geoderma

Tuchschmid, M., 1995. Quantifizierung und Regionalisierung von Schwermetallen und Fluorgehalten bodenbildender Gesteine der Schweiz: Umwelt-Materialien 32 (BUWAL, Berne)

van Geen A., McCorkle, D.C. and Klinkhammer, G.P., 1995. Sensitivity of the phosphate-cadmium-carbon isotope relation in the ocean to cadmium removal by suboxic sediments, Paleo Currents, 10, 159-169

Veuve, P., 2000. Etude géochimique et sédimentaire d'un enrichissement en cadmium observé dans les calcaires oolitiques jurassiques du Jura. Unpublished diploma thesis, Univ. NE, 56 pp.

Wedepohl, K.H., 1995. The composition of the continental crust. Geochimica et Cosmochimica Acta, 59 (7), 1217-1232

VIII - Cadmium enrichments in Jurassic carbonates: towards the causes and mechanisms
A multivariate statistical analysis approach

VIII-1 Introduction

Cadmium (Cd) anomalies have recently been discovered in Bajocian and Oxfordian carbonate rocks in western and southern Europe (Rambeau et al., in prep.a). These anomalies appear to be correlatable in time, although two main features may be distinguished: a general increase in cadmium "background" values (i.e., increase in mean concentrations as well as in the lowest concentrations for both periods) is recorded on both open-marine and platform settings; in this latter environment, major enrichments ("Cd peaks") are also observed, with cadmium values frequently above 1 μg/g. These values largely surpass the mean value for Cd in carbonates of around 0.030 - 0.065 μg/g (Kabata-Pendias and Pendias, 1992; Alloway, 1995; Tuchschmid, 1995). High cadmium concentrations in shallow-water environments have been related to (1) biological activity and (2) amounts of Cd available in seawater (Rambeau et al., in prep.b), and has been related to preferential concentration processes. The general increase in cadmium values during the Late Aalenian to Late Bajocian and the Oxfordian to Early Kimmeridgian has been suggested to be linked with environmental change in general, such as changes in the intensity of hydrothermal and volcanic processes, eustatic sea-level rise, increase in continental biochemical weathering rates, and higher biological productivity rates (Rambeau et al., in prep.a).

Cadmium anomalies in Jurassic times are indeed synchronous with times of decreased growth rates for many carbonate platforms of the western Tethys (Late Bajocian to Oxfordian; e.g., Charrière, 1992; Bartolini et al., 1996; Weissert and Mohr, 1996; Cobianchi and Picotti, 2001, Morettini et al., 2002), which suggests a time of environmental stress leading to unfavourable conditions for carbonate productivity. This stress may be related to increasing trophic resources in the western Tethys (e.g., Bartolini et al., 1996; Cobianchi and Picotti, 2001, Morettini et al., 2002), induced by increased continental weathering and runoff (e.g., Cobianchi and Picotti, 2001), that in turn may be triggered by changes in the intensity of global weathering accompanying the break-up of Pangea (Zempolich, 1993; Gibbs et al., 1999) and/or elevated atmospheric CO_2 related to endogenic degassing during increased sea-floor spreading (Bartolini et al., 1996, Bartolini and Larson, 2001). The latest early Bajocian to Oxfordian are also characterized by a long-term drop in the $^{87}Sr/^{86}Sr$ curve (Jones and Jenkyns, 2001), which may be interpreted in terms of increasing hydrothermal activity, and which is concomitant with both a carbonate crisis in the Umbria-Marche Basin (central Italy; e.g., Bartolini et al., 1996; Morettini et al., 2002) and enhanced extensional rates in the Pacific ocean as well as

palaeogeographic rearrangements in the Alpine Tethys (e.g., new ridge formation, new basins and changes in oceanic currents; Morettini et al., 2002 and references therein). These events may be responsible of the increasing availability of cadmium in the environment, by the way of increased continental weathering or by direct input via enhanced hydrothermalism, as well as by preferential concentration in sediments due to biological uptake. Another possible source of Cd is the transfer of this element in the atmosphere, and subsequently to the marine system through rainfall, by aerian volcanic eruptions (Rambeau et al., in prep.b), as this element is often present in high concentrations in volcanoes vapours (e.g., Symond et al., 1987; Stimac et al., 1996; Allard et al., 2000).

Here we provide an analysis of the different potential cadmium sources and mechanisms leading to cadmium enrichment using our current sedimentological and geochemical knowledge of cadmium occurrences in Jurassic carbonates, as well as multivariate statistical analyses applied on three carbonate sections: Terminilletto, open-marine environment, Aalenian to Kimmeridgian, central Italy (Bartolini et al., 1996; ref Rambeau et al., in prep.a); Lausen-Schleifenberg, oolitic platform barrier and margin, Bajocian, Swiss Jura (Gonzales, 1994; Rambeau et al., in prep.a); and Gorges du Pichoux, lagoonal environment, Late Oxfordian, Swiss Jura (Hug, 2003; Rambeau et al., in prep.a).

VIII-2 Geological settings

VIII-2-1 Terminilletto section

This section crops out in the Umbria-Marche Basin, central Italy, along the E-SE side of Monte Terminilletto (Bartolini et al., 1996). In terms of palaeogeography, during Jurassic times, the section was located along a N-S fault separating the Umbria-Marche Basin from the Lazio-Abruzzi carbonate platform (Bartoloni et al., 1996 and references therein). The sediment succession includes, therefore, abundant layers of carbonate resediments (mainly oolitic grainstone, pebbly mudstone, crinoidal packstone-grainstone), derived from the nearby platform, which are intercalated with autochtonous wackestones and mudstones. Chert occurrences in the form of nodules and ribbons are frequent and increase in abundance between 40 to 110 m and 160 to 236 m (Bartolini et al., 1996; Fig. 1).

VIII-2-2 Lausen-Schleifenberg section

The Lausen-Schleifenberg section is located in the Jura Mountains (BL, Switzerland). The lower part of this composite section crops out in a quarry nearby the Lausen rail-station, whereas the upper part is located a few kilometers farther to the northwest, near Liestal, on the slope of the Schleifenberg hill (Gonzales, 1994). This section is mostly composed of oolitic and locally of bioclastic packstone to grainstone (Fig. 1), which are interrupted by marly deposits, with the major detrital episodes being located in the lower part of the section (blue marls intercalated with oolitic packstones) and around 80 m (red, yellow and grey marls separated from the underlying oolitic grainstone by a ferruginous hardground and intercalated with oolitic packstone).

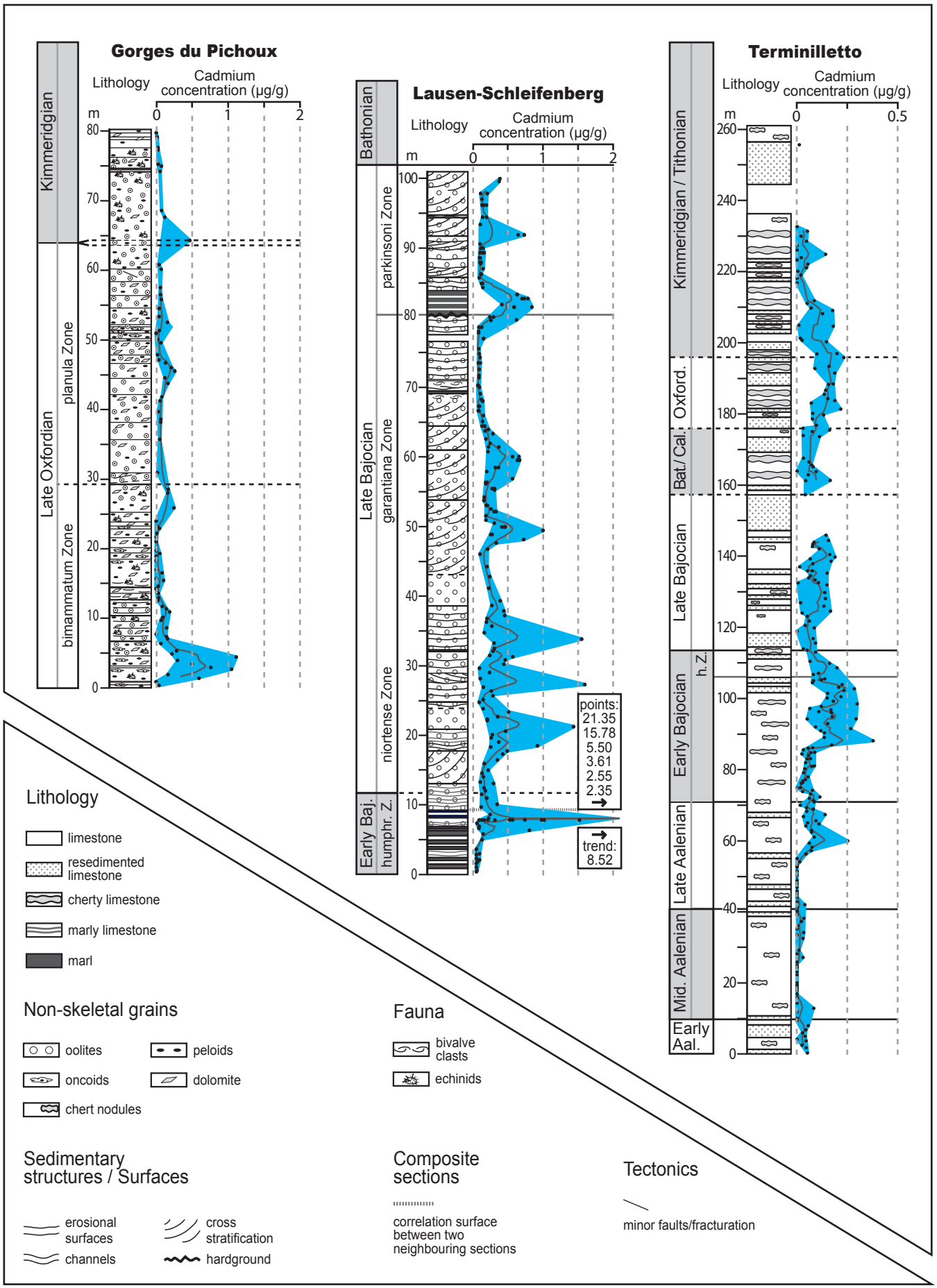

Fig. 1. Carbonate successions and cadmium concentrations of the Gorges du Pichoux, Lausen-Schleifenberg and Terminilletto sections. Note the different scale for Cd concentrations at the Terminilletto section. Aal. = Aalenian; Baj. = Bajocian; Bat. = Bathonian; Cal. = Callovian; Oxford. = Oxfordian; Mid. = Middle; Z. = Zone; humphr./h. = humphriesianum. The Cd measurements are represented by black dots. The grey curves correspond to a five-point moving average.

VIII-2-3 Gorges du Pichoux section

The Gorges du Pichoux section crops out in the Jura Mountains (JU, Switzerland) a few kilometres south from Undervelier (Hug, 2003).This section is composed of lagoonal micrites (Fig. 1) rich in oncoids (lower part), ooids (abundance increasing upwards), peloids in various abundance throughout the section, dolomite (present in the whole section but decreasing in the uppermost part) and evaporites. The fauna is mainly represented by echinoids (mostly observable in the lower and uppermost parts), and for the lower part brachiopods, gastropods, bivalves, and corals (Hug, 2003).

VIII-3 Methods

VIII-3-1 Determination of elemental contents

Multi-element analyses were performed on bulk rock samples using Inductively Coupled Plasma-Mass Spectrometry (ICP-MS). Powders were obtained using a mechanic agate crusher. A portion of approximately 250 mg was transferred into a PTFE digestion vessel and 10 ml of concentrated nitric acid (65 %, suprapur, Merck) were added. The sample was digested in a microwave oven (MSL-Ethos plus, Milestone) using the heating program recommended by the EPA 3051 procedure. After cooling, the resulting solution was filtered (0.45 µm) and diluted to 100 ml with ultrapure water. A second dilution (1/20) was then performed prior to analysis. Rhodium was used as the internal standard, in order to correct for matrix-induced ion signal variations and instrumental drift. The element concentrations of the acid digests were determined by ICP-MS (ELAN 6100, Perkin Elmer) using full mass-spectra scans (panoramic method).

VIII-3-2 Statistical analyses

The main goal of the multivariate statistical analyses used here is to transform our complex, multivariate chemical systems in new systems, for which the maximum of variance is held by a few number of axes. They permit to gain information on the degree of correlation between the different chemical elements and to distinguish the chemical poles (i.e, associations of elements), which govern the global geochemical variability of the here considered carbonate successions.
The data obtained by ICP-MS measurements were transformed in standardized values, in order to allow for direct comparison of variables of very different orders of magnitude (e.g., concentrations between <0.04 and 21.4 µg/g for Cd, and varying from 730 to 46900 µg/g for Mg) and subjected to multivariate statistical analyses, using the MATLAB program (e.g., Reyment and Savazzi, 1999). The whole chemical system for each of the three sections was first considered, with statistical treatments that include the production of correlation matrices, which give information about the degree of correlations between the measured variables (i.e., the chemical components). Principal Component Analyses (PCAs) led both to the construction of new matrices (PC) providing new coordinates of each object in the PCA multi-dimensional system, as well as of matrices showing the relationships between variables and PCA axes (referred to in the text as rPC matrices).

Associated correlation circles show the relationships between variables and selected PCA axes in 2D diagrams. Correlation circles can be considered as "lecture keys" for associated diagrams showing the distribution of each object in the PCA system.

Global chemical systems were characterized by using as many samples as possible (see specificities for each section in the paragraphs below) and all available chemical variables at disposal, excepting:

- elements which were suspected of analytical problems (e.g., B, Na, Bi),
- wich display general concentrations above detection limits (about 0.04 µg/g; e.g., Ag),
- which were not systematically measured in all samples (e.g., Fe for the Lausen-Schleifenberg section; Fe, As, W, Zn for the Gorges du Pichoux carbonate successions)

After the first characterizations by PCA (realized on the Terminilletto section), the number of rare-earth elements has been reduced to those holding a maximum of information relative to the total variance (i.e., La, Th, Y, Sc).

Multivariate analyses were then applied using selected variables (chemical "sub-systems") in order to reduce the complexity of the entire dataset and as such facilitate interpretations. Variables of these sub-systems have been chosen according to the two following indications:

- results from preliminary global analyses (chemical elements that were associated to the construction of first PCA axes
- preferential choice of elements which are generally associated in oceanic waters and sediments due to similar sources (external inputs: weathering, volcanism) or behaviour (nutrient-like elements, elements related to preferential accumulation/preservation in the sediment).

Chemical elements that generally follow a "nutrient-like" behaviour in oceanic water are Fe, Ni, Co, Zn, Cu, V. Mo, Cd, As, Cr (e.g., Boyle et al., 1976; Gonzalez et al., 1999; Algeo, 2004, and references therein; Böning et al., 2004, and references therein; Snow et al., 2005, and references therein).

Elements that have been related to preferential accumulation/preservation in the sediment under dysoxic conditions comprises Mo, Pb, U, V, Zn, Ni, Cu, Cr, As (e.g., Morford and Emerson, 1999; Algeo, 2004, and references therein; Böning et al., 2004, and references therein).

Chemical elements, which are highly enriched in the continental crust (e.g., Taylor and McLennan, 1985), which not participate to the nutrient cycles, and which not show preferential concentrations in sediments have been here associated to external inputs. This chemical association comprises Ga, Rb, Cs, Th, +/- Li, Al, Ba, Sr, and La. All these elements are likely to be related to continental weathering, and may be transferred to the oceanic realm through riverine transport or atmospheric inputs (eolian particles). However, a volcanic (e.g., OIB type) origin for these elements can not be excluded (Halliday et al., 1995; Niu and O'Hara, 2003).

Finally, two sub-systems were defined for each section: an “external inputs” sub-system and a “nutrients-preservation” one. In the case that information was not clearly displayed on the “nutrient-preservation” sub-system, an additional, “nutrients” sub-system was considered, which only comprises elements that follow a "nutrient-like" behaviour in oceanic waters. These sub-systems underwent slight modifications between the three sections of consideration, in relation with the different variables that dominate the general variability of each geochemical system and the number of variables available for each section.

Terminilletto section

Data available:
PCA have been conducted using 183 samples, and 29, 12, 10 and 10 chemical elements for the global system, and the “external inputs”, “nutrients-preservation” and “nutrients” sub-systems, respectively.

Chosen chemical elements
global system:
Li; Be; Mg; Al; Ti; V; Cr; Mn; Fe; Co; Ni; Cu; Zn; Ga; As; Rb; Sr; Zr; Mo; Cd; Cs; Ba; W; Pb; U; La; Th; Y; Sc
“external inputs”:
Li; Mg; Al; Zn; Ga; Rb; Sr; Zr; Cd; Cs; Ba; Th
“nutrients-preservation”:
Cr; Fe; Co; Cu; Zn; As; Mo; Cd; Pb; U
“nutrients”:
V; Cr; Fe; Co; Ni; Cu; Zn; As; Mo; Cd;

Diagrams colour codes
Data have been encoded in three categories following the Cd contents of each object: the first category (referred as “normal” in the text) comprises the samples with Cd contents below 0.065 µg/g (maximum mean value given for carbonates in the literature; Kabata-Pendias and Pendias, 1992; Alloway, 1995; Tuchschmid, 1995). Two others categories have been arbitrarily defined as a function of increasing Cd contents: an “intermediate” category that include samples with Cd concentrations between 0.065 µg/g and 0.100 µg/g, and a category comprising maximum Cd concentrations for this section (i.e., > 0.100 µg/g; “Cd-enriched” samples).

Lausen-Schleifenberg

Data available
PCA have been realized using 79 samples, and 23, 9 and 8 variables for the global system, and the “external inputs” and “nutrients-preservation” sub-systems, respectively.

Chosen chemical elements:

global system

Mg; V; Cr; Mn; Co; Ni; Cu; Zn; Ga; As; Rb; Sr; Zr; Mo; Cd; Cs; Ba; La; Th; Y; Sc; Pb; U

"external inputs"

Zn; Ga; Rb; Sr; Zr; Cd; Cs; La; Th

"nutrients-preservation"

V; Co; Zn; As; Mo; Cd; Pb; U

Diagrams colour codes

Different colours have been attributed to the sample plots in relation to increasing Cd contents. Separations have been made at 0.065 µg/g (considered as the maximum limit for "normal" Cd concentrations), 100 µg/g and 300 µg/g. Samples whose Cd concentrations are above 300 µg/g may be considered as anomalous with regards to this element, since they show Cd contents four orders of magnitude above the 0.030 µg/g mean Cd concentration given for carbonate rocks by several authors (e.g., Tuchschmid, 1995). On some diagrams this latter limit has been moved upwards to 0.800 µg/g (refer to corresponding text for further explanation). Samples between 0.065 and 0.300 / 0.800 µg/g Cd have been referred in the text as "intermediate" samples.

Gorges du Pichoux

Data available:

PCA have been realized using 80 samples, and 25, 11, 7 and 5 variables for the global system, and the "external inputs", "nutrients-preservation" and "nutrients" sub-systems, respectively.

Chosen chemical elements:

global system

Li; Mg; Al; Sc; Ti; V; Cr; Mn; Fe; Co; Ni; Cu; Zn; Ga; As; Rb; Sr; Y; Zr; Mo; Cd; Cs; Ba; La; W; Pb; Th; U

"external inputs"

Li; Al; Ga; Rb; Y; Zr; Cs; Ba; La; Th; Cd

"nutrients-preservation"

V; Co; Cu; Mo; Cd; Pb; U

"nutrients"

V; Co; Cu; Mo; Cd

A comparative global system has been established with fewer samples (49) and 28 variables for considering the specific role of Zn, As and W, which has not been measured in all cases.

Diagrams colour codes

They are similar to those used for the Lausen-Schleifenberg section, with the upper limit put at 0.300 µg/g.

VIII-4 Results and interpretation of the multivariate statistical analyses

VIII-4-1 Terminilletto section

VIII-4-1-1 Terminilletto global system: results

With regards to Cd, the correlation matrix indicates an independent behaviour of this element relative to other variables, with the exception of Zn, with which Cd forms a partial association (Fig. 2a). The only strong associations observable in this matrix concern the Li, Al, Ga, Rb, and to a lesser extend, Cs, Ba and Th positive correlation, and the positive correlation between Y and La.

The results of the PCA reflects the complexity of the Terminilletto system: the first PCA axis only holds 31.60% of the total variance, and 9 axes are necessary to surpass the 75% of variance explained.
The rPC matrix (Fig. 2b) indicates that the first PCA axis is principally constructed following the variations of Li, Al, Ga, Rb, Cs, Ba and Th. Other elements are also associated to the first axis but to a lesser extend (Fe, Co, As, Sr, Zr, La, Y). Cd is strongly anti-correlated to the second axis, principally in association with Zn and to a lesser extend with V, Cu and Pb, whereas Mg is positively correlated to the same axis.

The two first principal components were plotted against each other on a diagram and the associated correlation circle was drawn (PCA axes one and two; 42.17% of the total variance) (Fig. 3b). An examination of the thus obtained correlation circle (Fig. 3b) suggests the presence of three major chemical poles. The first one comprises Li, Al, Rb, Ga, Th, Ba, Cs, and - to a lesser extend, Fe, Co, As, Zr and Y. These elements are strongly associated with the first axis (especially those near the circle periphery) and almost independent of the second axis. A second pole is constituted by Cd and Zn, which represent elements mostly associated with the second axis, and Pb, La, Cu (+/- V), for which the influence of the second axis becomes even more important. A third pole corresponds to Mg and Sr, which are related to both the first and second axes. Less information is given for Mn (which plots in the vicinity of the first pole but far away from the circle periphery), Sc (which plots near the second pole), and U, Mo, Cr, Be, W, Ni, Ti.

Considering the data plotted on the two first components diagram (Fig. 3a), objects are distributed in a fan between these three poles. The point cluster of “normal” samples (i.e., with Cd concentrations <0.065 µg/g) shows a trend towards elongation into two directions, the principal of them pointing towards the first pole (Li, Al...), the second one directed towards the third pole (Mg and Sr). Nevertheless, a minority of these samples is pulled to the second pole (Cd and Zn). "Intermediate" and Cd-enriched samples are principally distributed between minor to increasing influences of the first and second poles; some members of the intermediate group show also a slight influence of the third pole, which tends to disappear for the samples most enriched in Cd.

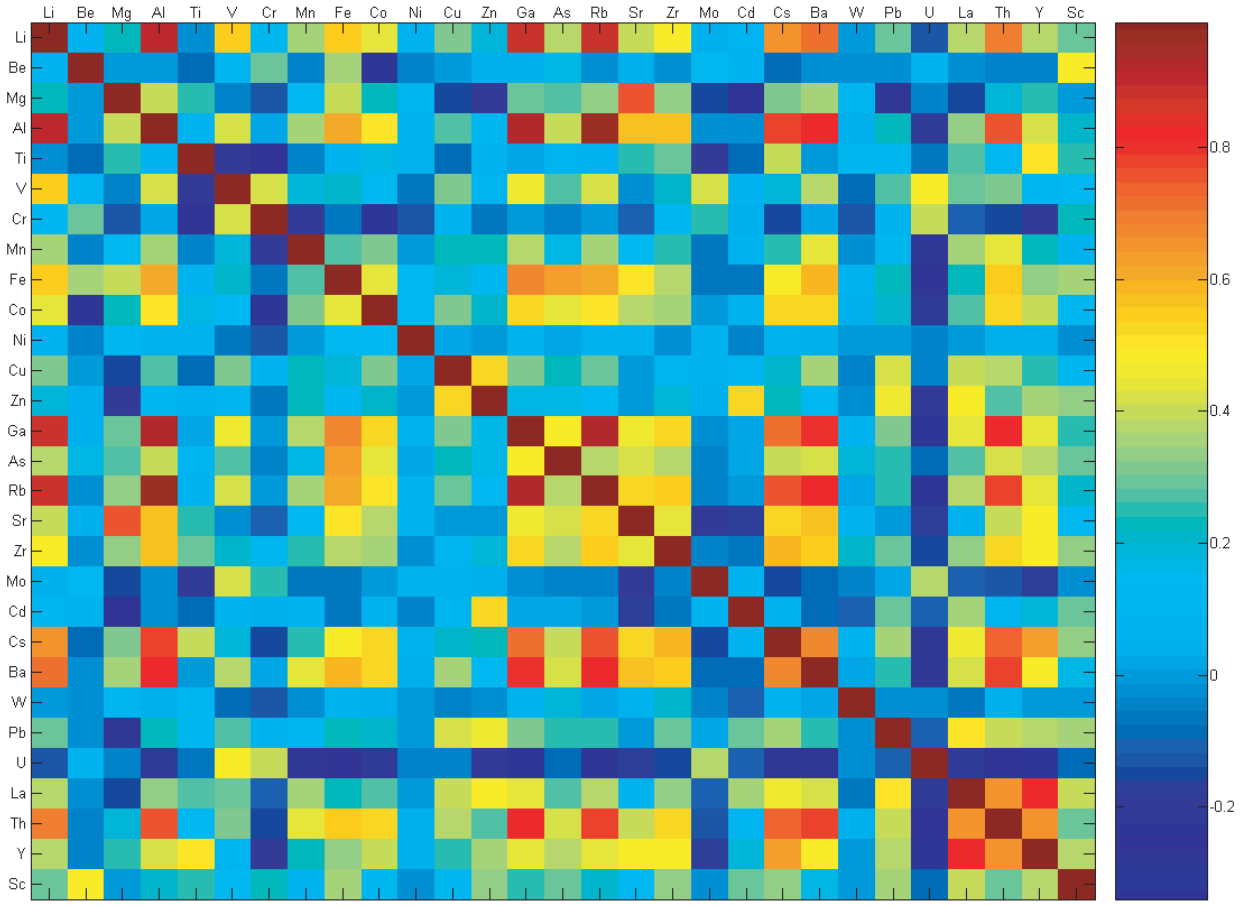

Fig. 2a. Correlation matrix, Terminilletto global system

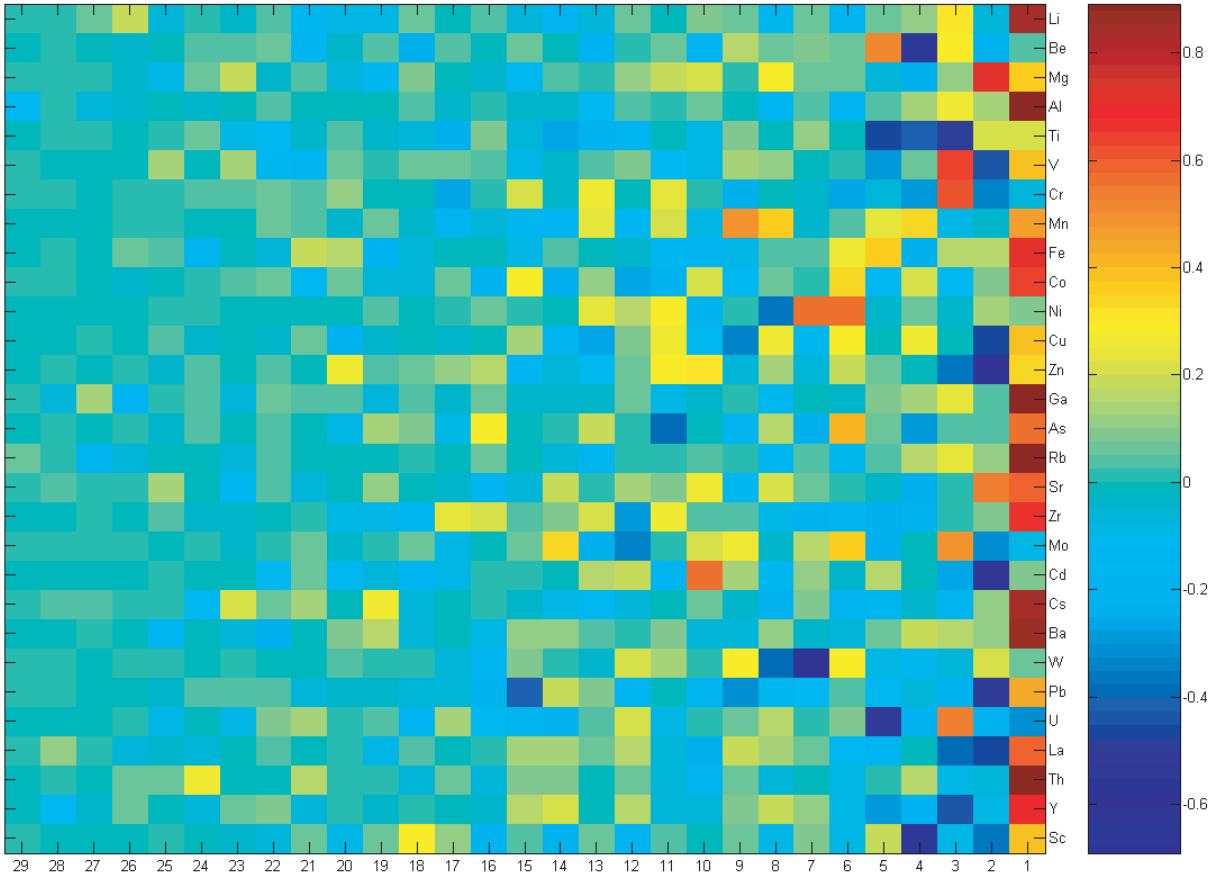

Fig. 2b. rCP matrix, Terminilletto global system

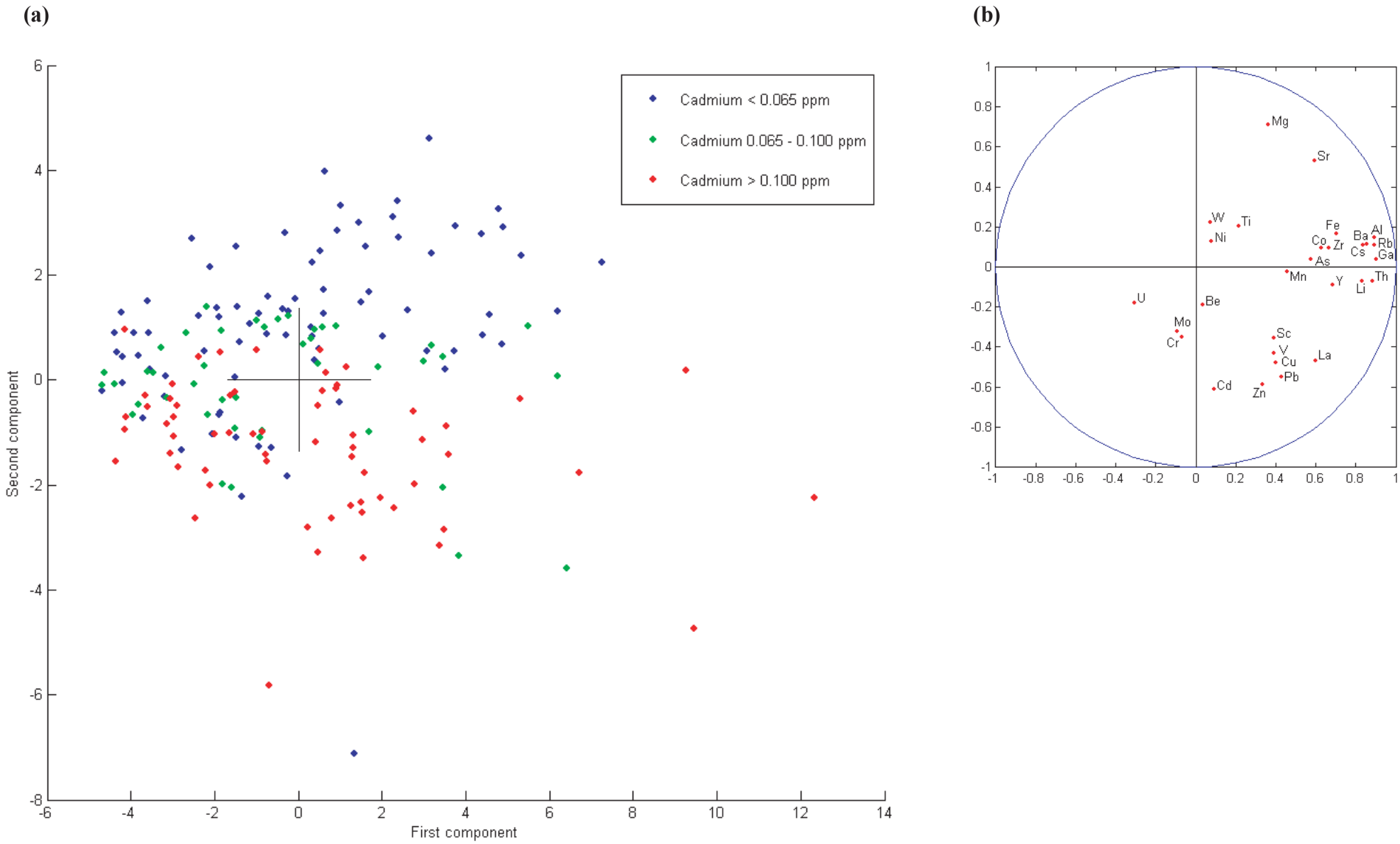

Fig. 3. Terminilletto global system.
a. First component against second component diagram.
b. Associated correlation circle (x: first PCA axis, y: second PCA axis).

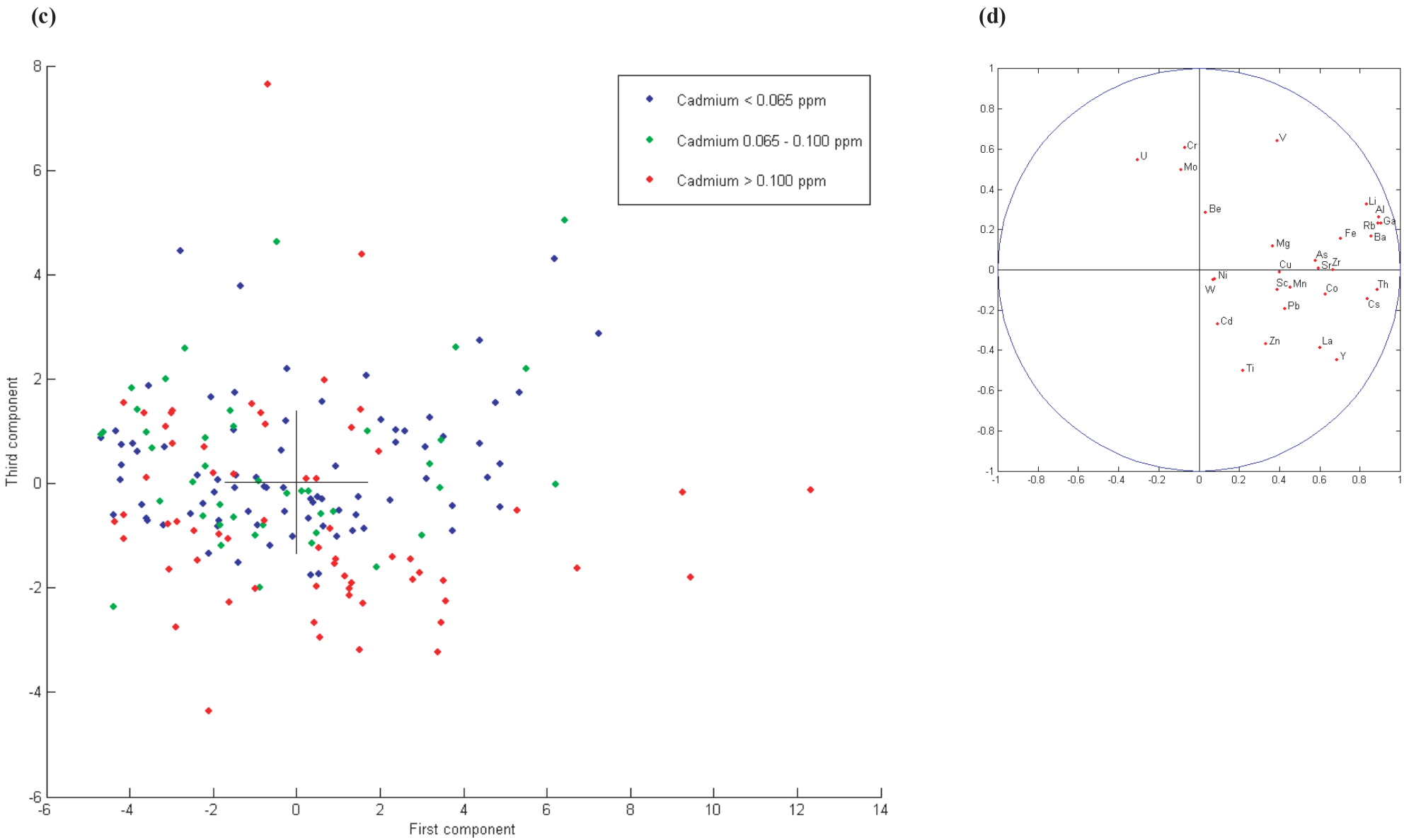

Fig. 3. Terminilletto global system.
c. First component against third component diagram.
d. Associated correlation circle (x: first PCA axis, y: third PCA axis).

(e)

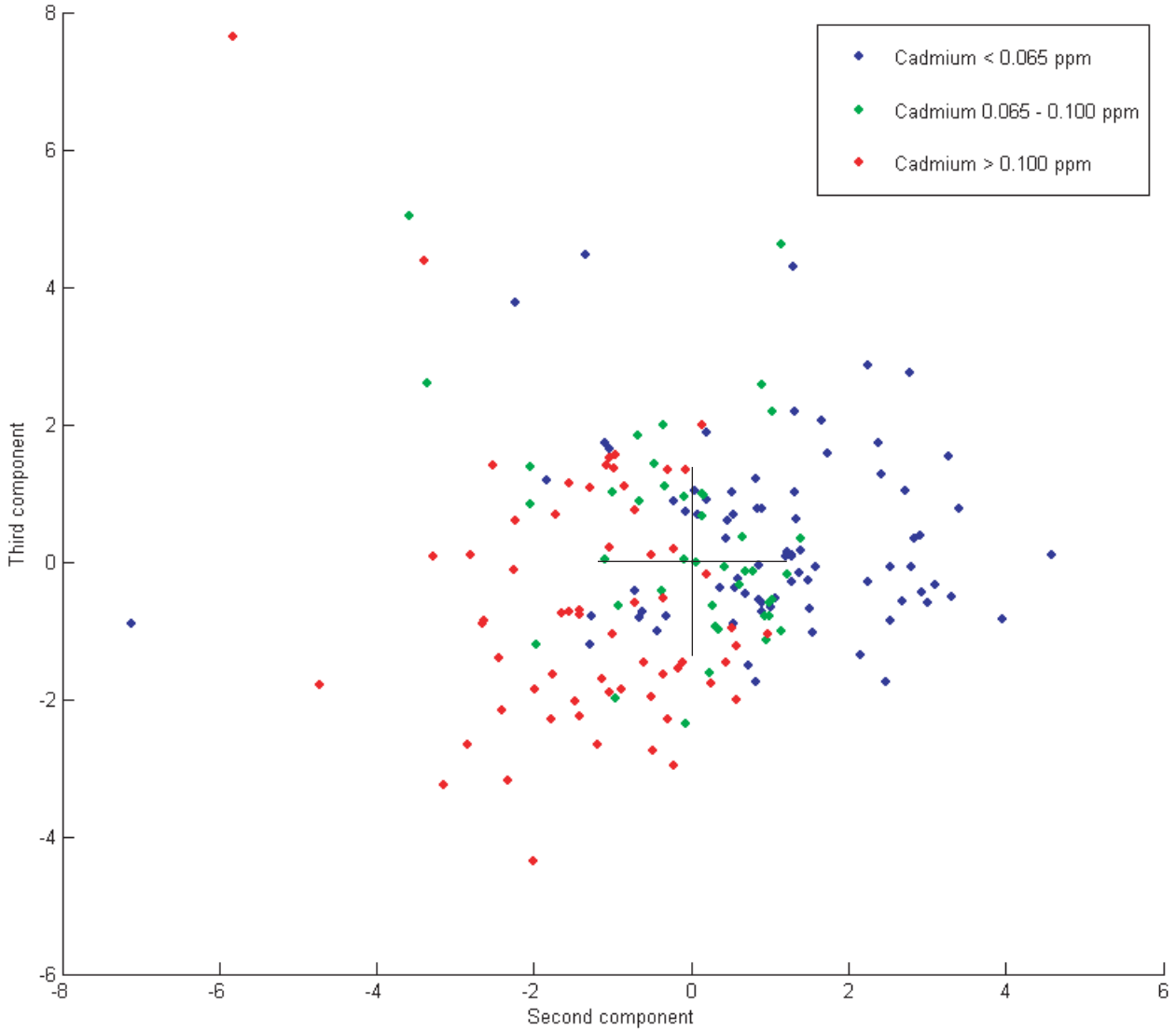

(f)

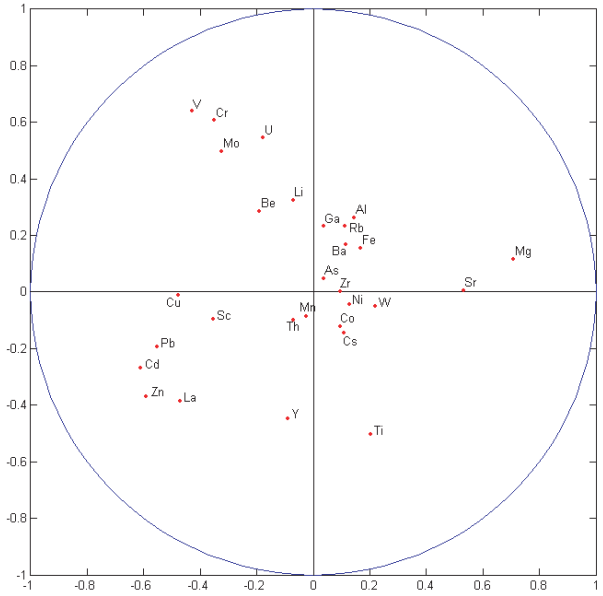

Fig. 3. Terminilletto global system.
e. Second component against third component diagram.
f. Associated correlation circle (x: second PCA axis, y: third PCA axis).

The distribution of variables between the first and third PCA axes is only poorly defined (Fig. 3d). Elements predominantly associated with the third axis (U, Cr, Mo, V, Ti) are drawn away from the circle periphery and therefore preclude a good distribution of the objects, at the possible exception of V. Variations in Li, Al, Ga, Rb, Th, and Cs are once again strongly associated with the first axis. The rest of the elements are distributed in various proportions between the first and third axes and no special group of elements can be distinguished. The corresponding distribution of objects (first principal component plotted against the third; Fig. 3c) is not well structured and no major distinction of behaviour can be made between the "normal" samples and samples which are significantly enriched in Cd.

The distribution of variables between the second and third PCA axes is clearer (Fig. 3f). Even if none of the variables is really approaching the circle periphery, three distinct associations of elements can be observed: the first one is composed of V, Cr, Mo, U, that are mostly associated with the third axis but for which a non-negligible part is anti-correlated with the second axis; at about 90° counter-clockwise, a second group constituted by Zn, Cd, La, Pb (+/-Cu) is located; and a third association including Mg and Sr is found, which is mostly positively associated to the second axis.

These three poles constitute major directions towards which clouds of objects are elongated in the second against third components diagram (Fig. 3e). "Normal" samples are mostly distributed between the first and third elemental associations, whereas the samples most enriched in Cd are located in a fan including the cluster center and elongated towards the first and second chemical groups, with some Cd-enriched samples being strongly pulled towards the first pole. "Normal" and Cd-enriched samples display a rather clearly separated behaviour in this diagram, but the transition between the two clouds of objects is ensured by the "intermediate" category of samples with regards to their Cd concentrations.

VIII-4-1-2 Terminilletto global system: interpretation

When considering the three first components of the PC matrix, Cd-enriched samples are mostly distributed between three major poles:

- Li, Al, Ga, Rb, Cs, Ba, Th, and to a lesser extend, Zr, Fe, Co, As, which constitute a mix between a group of elements that are highly enriched in the continental crust and therefore are likely to be related to external inputs (Li, Al, Ga, Rb, Cs, Ba, Th), and a group of elements that are mostly related to a "nutrient-like" behaviour (Co, As). Fe is an element that may both indicate continental inputs or increasing nutrient levels
- Cd, Zn, Pb, La, Cu, representing a mixed group between heavy metals, nutrients and rare-Earth elements. The origin of this association is less clear, but one may interpret it as reflecting ehanced volcanic inputs. Indeed, Cd, Pb, Zn and Cu have been linked to aerian volcanic exhalations by several authors (e.g., Symond et al., 1987; Hinkley et al., 1999; Allard et al., 2000).
- V, Cr, Mo, U, forming an association which indicates preferential concentration and preservation of organic matter in sediments, which may be due to the presence of dysoxic conditions during burial, and perhaps related to an increase in the nutrient pool.

On the contrary, “normal samples” are distributed due to various influences of:

- the “external” (Li, Al, Ga, Rb, Cs, Ba, Th) pole
- the “preservation(/nutrients)” pole (V, Cr, Mo, U)
- and the chemical end-member constituted by Mg and Sr, which may be considered as reflecting normal, non-perturbed marine conditions.

It is worthwhile to remark here that, in most cases both Cd-enriched and normal samples are largely distributed along lines between the centre of the point cluster and its chemical poles. This suggests that Cd enrichments are rather independent from variations in the end-members components, even if some of the Cd-enriched samples appear to be influenced by enhanced availability of elements from the “preservation(/nutrients)” group or from the group including Zn, Pb, La, Cu in the chemical system. Anti-correlation between Cd/Zn and Mg/Sr on the same PCA axes indicates that these elements share part of their behaviour within the global geochemical system; our suggestion is that Cd and Zn, whenever available, may substitute for Mg and Sr in the carbonate lattice.

VIII-4-1-3 Terminilletto “external inputs” sub-system: results

All elements belonging to the previously described “external inputs” group (e.g., Li, Al, Ga, Rb, Cs, Ba, Th), Cd and Zn, as well as Mg and Sr (as supposed indicators of normal marine conditions), has been selected to construct this sub-system.

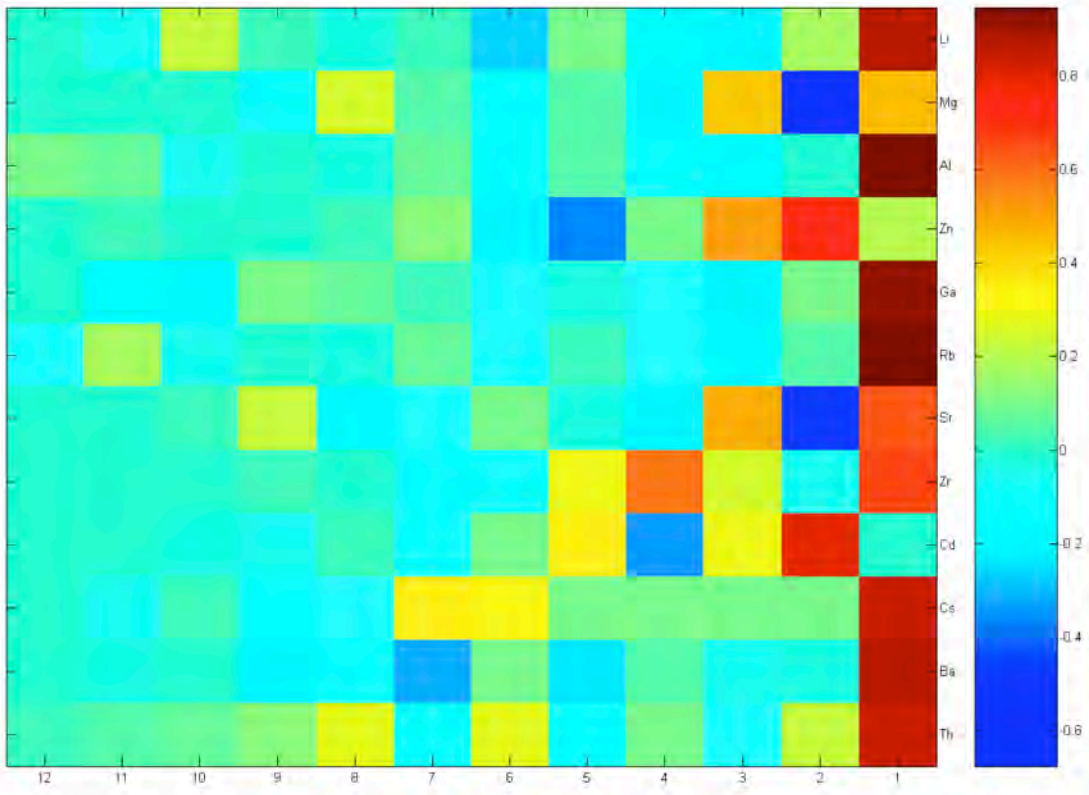

Fig. 4a. rCP matrix, Terminilletto “external input” sub-system

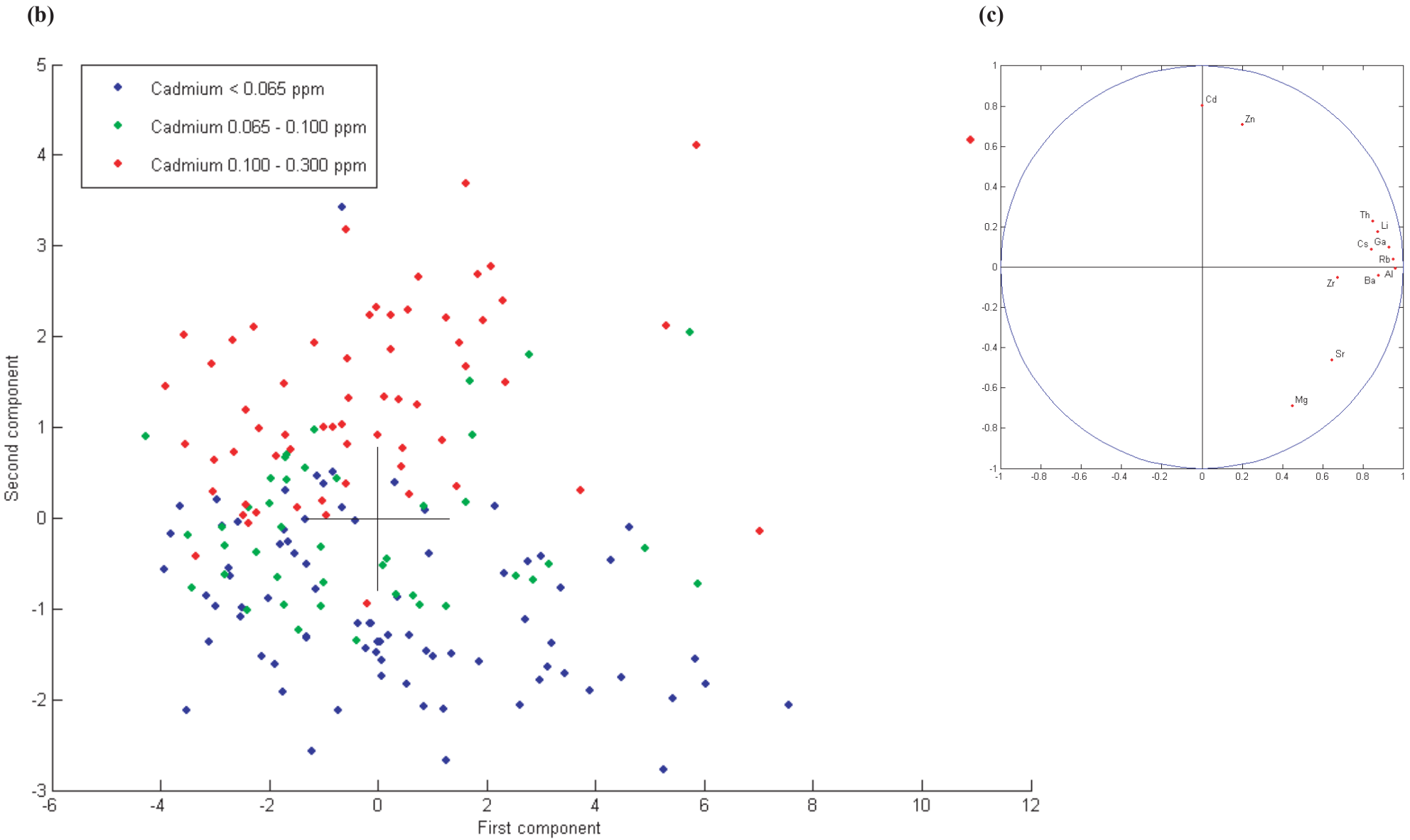

Fig. 4. Terminilletto “external” sub-system.
b. First component against second component diagram.
c. Associated correlation circle (x: first PCA axis, y: second PCA axis).

The PCA analysis permits to restrict most of the information regarding the total variance along the three first axes (80.81%, 72.59% held by the two first axes). The corresponding rCP matrix (Fig. 4a) indicates that Li, Al, Ga, Rb, and, to a lesser extend, Cs, Ba and Th, are once again strongly associated with the first axis. Most of the variability of the chemical system is therefore controlled by variations in these elemental concentrations. Cd and Zn are associated with the second axis, in anti-correlation with Mg and Sr. All these associations are more clearly visible on the correlation circle concerning PCA axes one and two (Fig. 4c).

On the diagram obtained by plotting the first principal component against the second one (Fig. 4b), we observe distributions similar to those obtained with the general system: the point cluster constituted by "normal" samples is elongated from the centre towards the Mg/Sr and "external inputs" poles, and the one constituted by samples highly enriched in Cd is pulled towards both the Cd/Zn and the "external inputs" poles. A transition between the two point clouds is ensured by the "intermediate" category of samples with regards to their Cd concentrations.

VIII-4-1-4 Terminilletto "external inputs" sub-system: interpretations

Elements that are supposed to belong to external inputs are dominating the system in terms of variance. They form a chemical pole which is clearly separated from the Cd/Zn one, and therefore share little variability with these two elements. Cd contents in samples from the Terminilletto section seem mostly independent with regard to these inputs, even if a few number of the samples highly enriched in Cd are also enriched in elements related to the "external" input group.

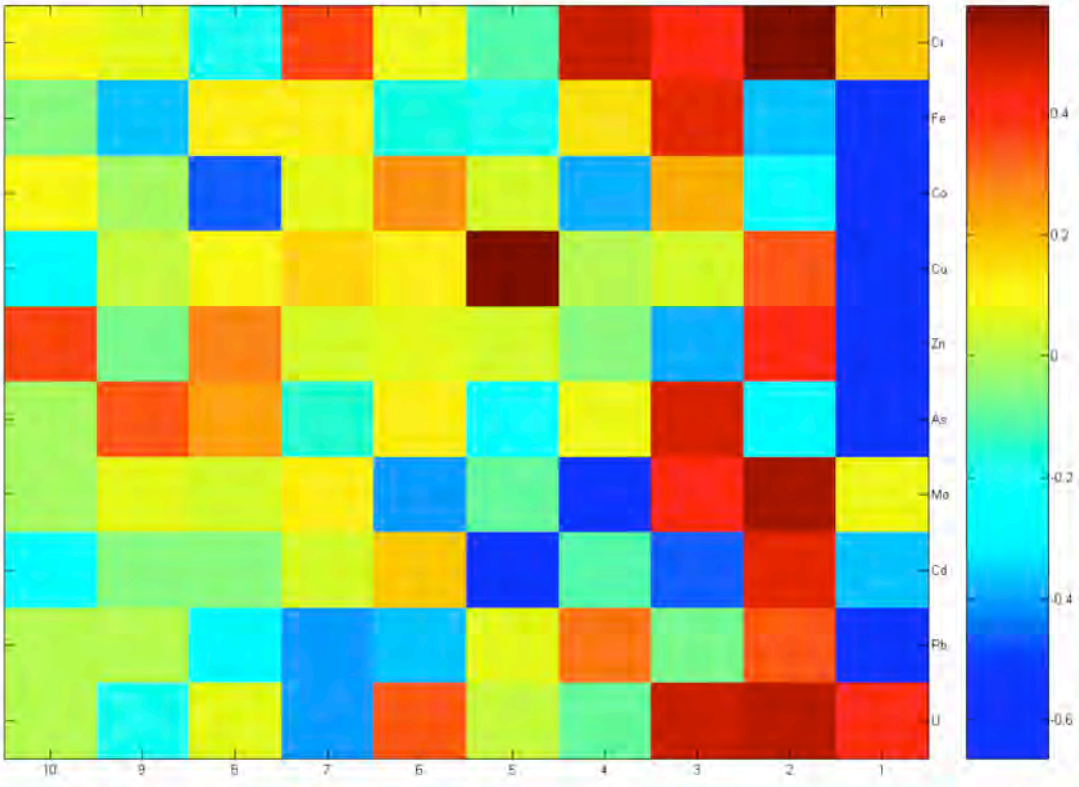

Fig. 5. rCP matrix, Terminilletto "nutrients-preservation" sub-system

VIII-4-1-5 Terminilletto "nutrients-preservation" sub-system: results

For this sub-system, we have selected variables that can be related to a "nutrient-like" behaviour (Cd, Zn, Fe, Co), preferential enrichments under sediment dysoxic conditions (U, Pb) or both (Mo, Cr, Cu, As).

The two first axes obtained by PCA only hold 46.29% of the sub-system variance, whereas the three first axes totalize 61.01% (Fig. 5). Fe, Co, Cu, Zn As and Pb are strongly anti-correlated to the first axis. Cr, Mo and U are the major elements related to the second axis, but they are only partially correlated with it. The same observation is valid for the third axis, to which are related variations in Fe, As and U, in anti-correlation with those of Cd; none of these elements are well expressed on this axis. Cd is mostly related to the fifth axis (which holds only 8.01% of the global variance), where it is in strong anti-correlation with Cu.

This sub-system therefore does not really permit to clarify the information given by the global system with regards to Cd enrichments.

VIII-4-1-6 Terminilletto "nutrients" sub-system: results

This sub-system derives from the previous one by selecting all variables that may present a "nutrient-like" behaviour (Fe, Co, Cu, As, Mo, V, Cr, Ni) in addition to Cd and Zn. The two first axes obtained by PCA analysis contain 43.44% of the global sub-system variance, reaching only 58.60% for the three first axes (Fig. 6a). However, in this sub-system Cd and Zn are both strongly associated to the third axis (Fig. 6a, 6e, 6g).

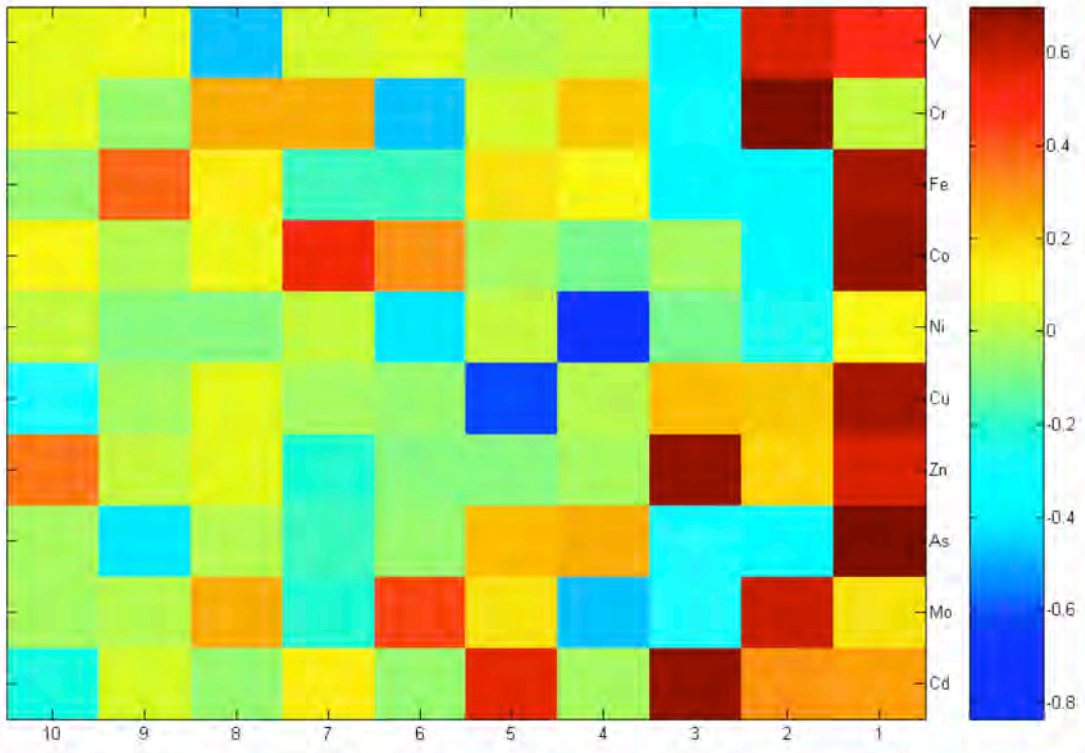

Fig. 6a. rCP matrix, Terminilletto "nutrients" sub-system

Fe, Co, Cu, As, and to a lesser extend, Zn and V, are positively correlated with the first axis (Fig. 6a, 6c, 6e), whereas Cr, and - with a decreasing correlation coefficient - V and Mo are associated with the second axis (Fig. 6a, 6c, 6g).

Tendencies are not easy to sort out from the diagram in which the first principal component is plotted against the second one (Fig. 6b), due to the numerous variables related to both the first and second PCA axes (Fig. 6c); furthermore, no major distinction can be made between the Cd-enriched and "normal" sample groups (Fig. 6b). Nevertheless, a rather well-defined group composed of Fe, Co, As can be distinguished within the variables (Fig. 6c), which may be partly responsible - together with variations in Cu - to the elongation in the point cluster along the first component. This concerns a few "normal" samples as well as a slightly more elevated number of the samples highly enriched in Cd.

Clearer relationships are shown in the diagram in which the first principal component is plotted against the third one (Fig. 6d). On this diagram, the group constituted by samples highly enriched in Cd are pulled from central values both towards a pole composed of Cd and Zn, as well as towards a chemical group composed of Cu, Co, As, Fe and V (Fig. 6e). The cluster constituted of "normal" samples is mostly elongated following the influences of the latter group.

With regards to the correlation circle related to the second and third PCA axes (Fig. 6g), it displays two well-defined poles consisting of Cd/Zn, and Mo/V/Cr, which are clearly independent, being at an angle of around 90° relative to each other. The remainder of the elements (Fe, As, Ni, Co) is too far from the circle periphery to have a significant influence on the point distribution. On the diagram in which the second principal component against the third one is plotted (Fig. 6f), we observe that most of the Cd-enriched samples are attracted towards the Cd/Zn pole. A very small number of these samples shows an increasing influence of the Mo/V/Cr pole. "Normal" samples are grouped around the centre or characterized by both a depletion relative to Cd and Zn contents, and an attraction towards the Mo/V/Cr pole.

VIII-4-1-7 Terminilletto "nutrients-preservation" and "nutrients" sub-systems: interpretation

Elements related to a "nutrient-like" behaviour, and/or to enhanced concentration and preservation in sediments seem distributed in sub-systems in a way that their variability is difficult to define. These sub-systems may be related to differences in the elemental sources, distinct behaviours in the water column - including variation in the biological uptake - and/or unequal distribution and concentration in the sediment during diagenesis. Concerning the tendencies that can be distinguished, Mo, V and Cr seem to be preferentially associated (influence of better preservation?), as well as Fe, Co and As (mostly "nutrient-like" distribution?). As for the "external inputs" sub-system, Cd-enriched samples are, in the great majority of the cases, not dominated by anything except Cd and Zn variations, even if a restricted part of them - and in this regard they present very few differences with non-enriched samples – shows influences of variations in the concentrations of one or several "nutrient-like" elements. Increasing concentrations in Cd seem therefore rather independent from enrichments or depletions in "nutrient-like" elements in the Terminilletto geochemical system.

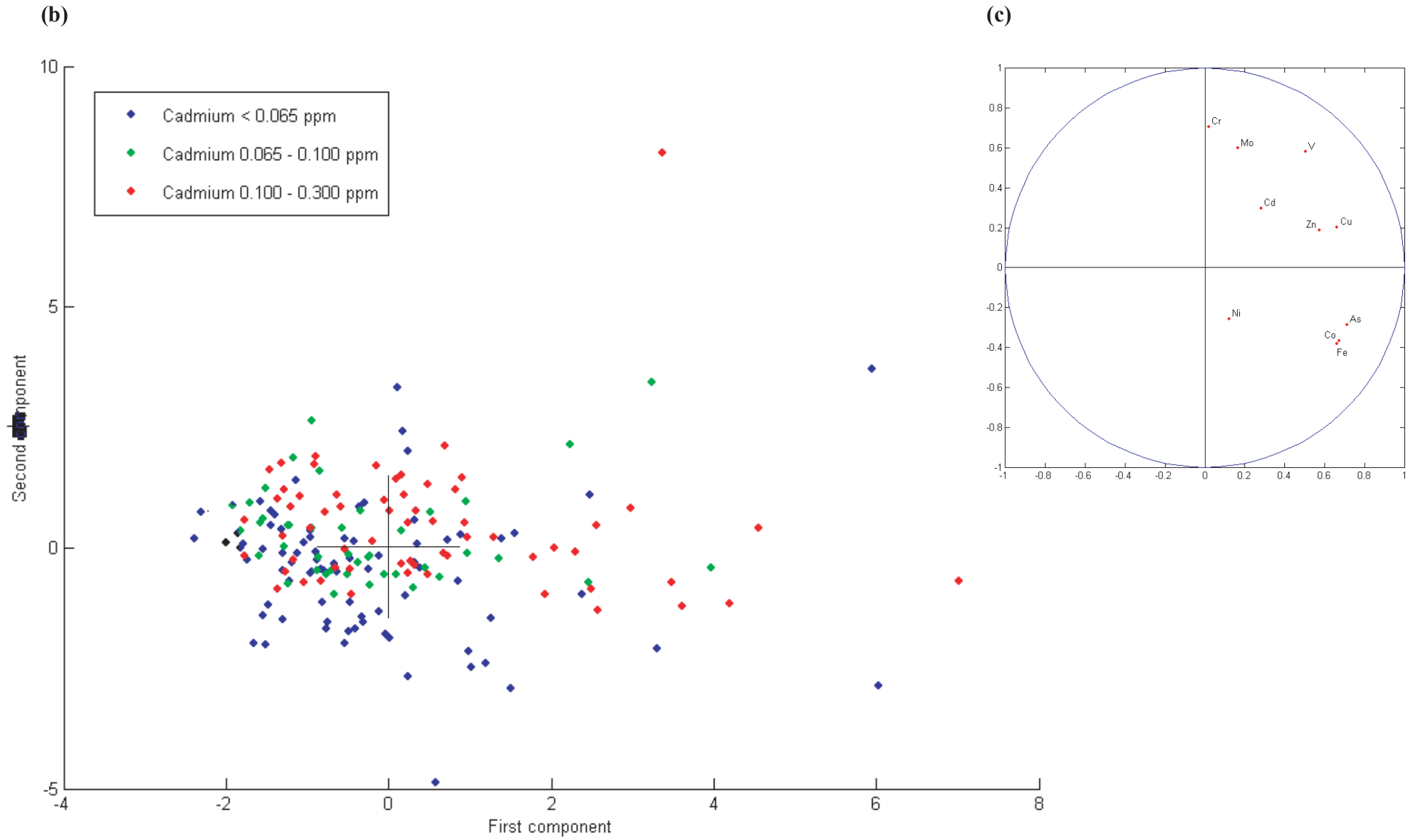

Fig. 6. Terminilletto “nutrients” sub-system.
b. First component against second component diagram.
c. Associated correlation circle (x: first PCA axis, y: second PCA axis).

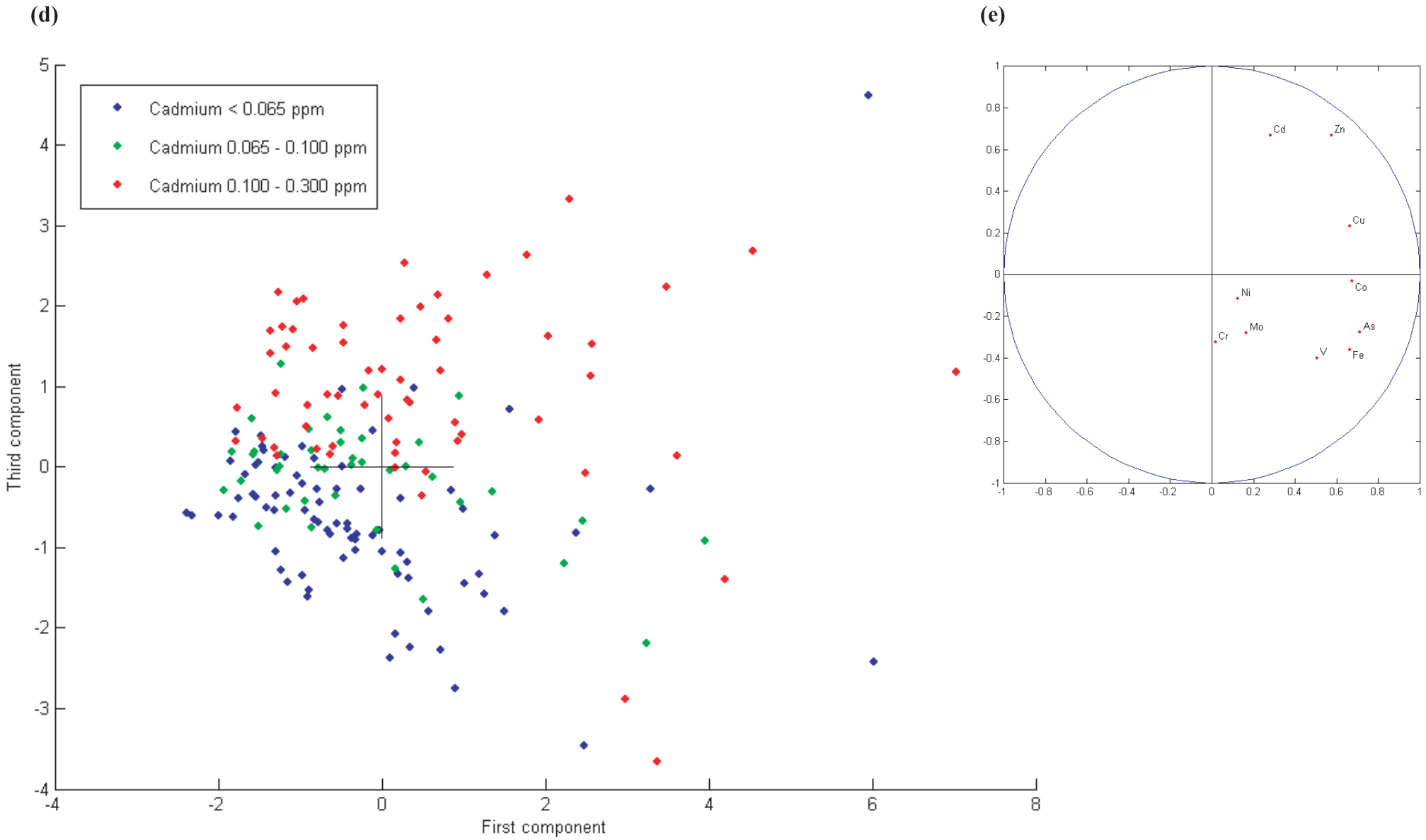

Fig. 6. Terminilletto “nutrients” sub-system.
d. First component against third component diagram.
e. Associated correlation circle (x: first PCA axis, y: third PCA axis).

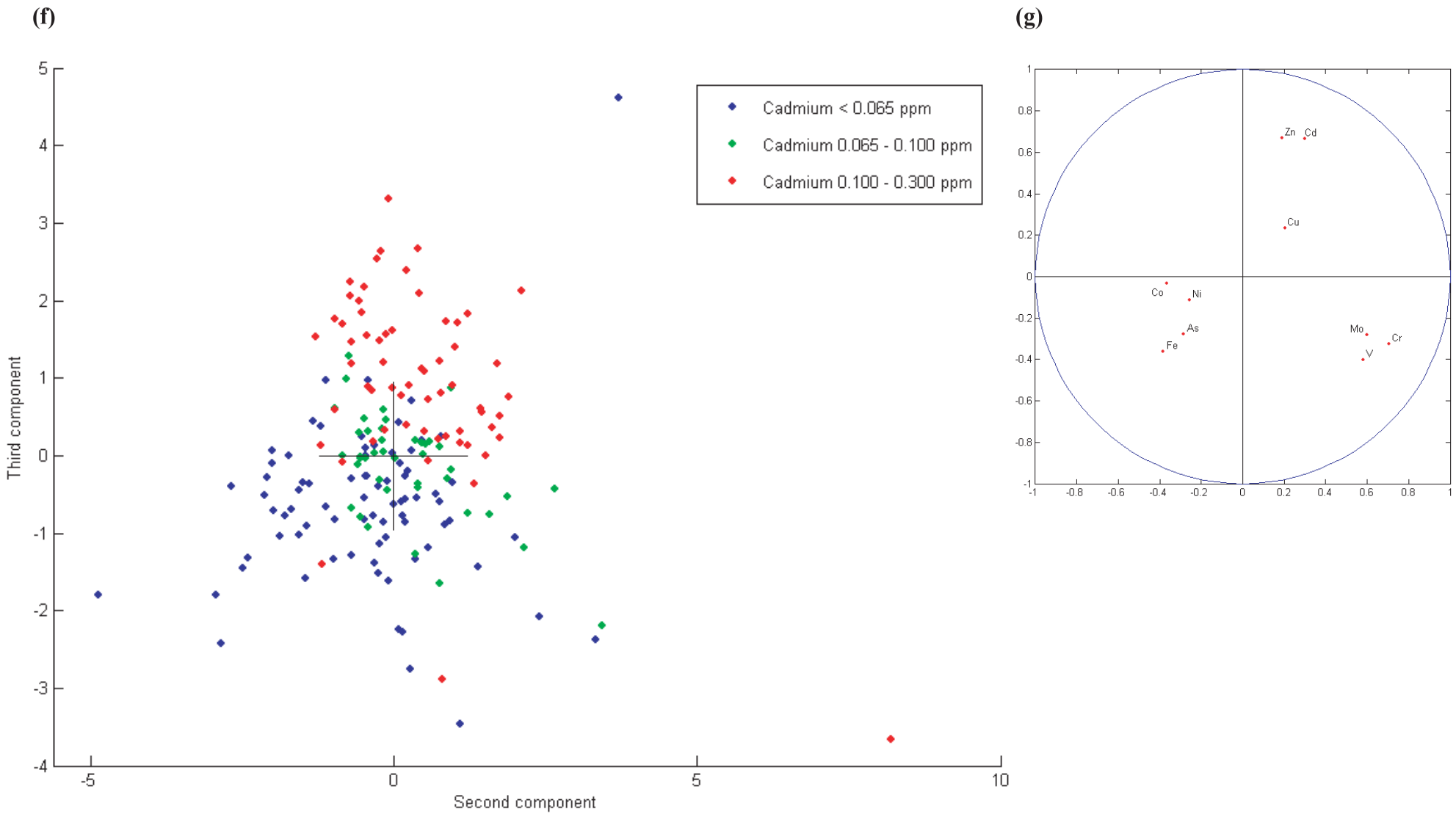

Fig. 6. Terminilletto “nutrients” sub-system.
f. Second component against third component diagram.
g. Associated correlation circle (x: second PCA axis, y: third PCA axis).

VIII-4-2 Lausen-Schleifenberg section

VIII-4-2-1 Lausen-Schleifenberg global system: results

The correlation matrix (Fig. 7a) shows a strong association between Cd and Zn. Apart from this correlation, behaviour of Cd is independent of other chemical elements. Other strong associations concern Ba and Ni, as well as As and Mo, and less well-defined ones include Ga, Rb, Cs on one hand, and La, Y, Sc (+/- Cr) on the other hand.

The PCA provides indications on the degree of complexity of the Lausen-Schleifenberg geochemical system: the first PCA axis only displays 25.19% of total variance, and six axes are necessary to surpass the 75% of variance explained.

With respect to the rPC matrix (Fig. 7b), we observe that most of the variations for Ga, Rb, Sr, Cs, La, Th is associated with the first PCA axis, whereas Sc is equally distributed between the first and second axes. V, As and Mo are anti-correlated to the second axis (17.01% of the global variance), in contrast to Cr, Y, Sc, which are positively correlated to the same axis. Cd and Zn are anti-correlated to the third axis (10.43% of the total variance), in association with As and Mo, and positively correlated to the fourth axis (8.69% of the total variance), whereas Ba and Ni show a rather strong anti-correlation with this same axis.

The diagram obtained by plotting the two first principal components (42.20% of the total variance) against each other (Fig. 8a) is very difficult to interpret due to the absence of well-defined, area-restricted chemical poles (Fig. 8b). The only point clearly visible is that the samples, Cd-enriched or not, are well distributed along the first axis, being more or less enriched in elements like Sr, Th, Rb, Ga, and Cs.

The first component against third component diagram (Fig. 8c) shows a sample distribution from the centre towards two main directions, one of them being possibly controlled by either a La/Th/Ga or a Cs/Sr/Rb chemical pole, the second one being certainly related to a Cd/Zn chemical pole, even if a contribution of the Mo/As group can not be excluded (Fig. 8d).

The second component against third component diagram (Fig. 8e) permits to clarify the respective roles of the Cd/Zn and Mo/As associations in the sample distribution. A large majority of Cd-enriched samples seems only attracted towards the Cd/Zn pole (Fig. 8f), whereas some the “normal” samples are slightly pulled towards the Mo/As pole or the Sc/Y/Cr association.

The first component against fourth component diagram (Fig. 8g), and the associated correlation circle (Fig. 8h), indicate that at least part of the chemical behaviour of Cd and Zn is clearly independent of those of the first axis-related elements, as these two variables form a clearly distinctive pole related to axis four. The distribution of a large part of the samples that are highly enriched in Cd is undoubtedly influenced by this pole, which points out a specific and unrelated chemical behaviour of most of the samples anomalously enriched in Cd.

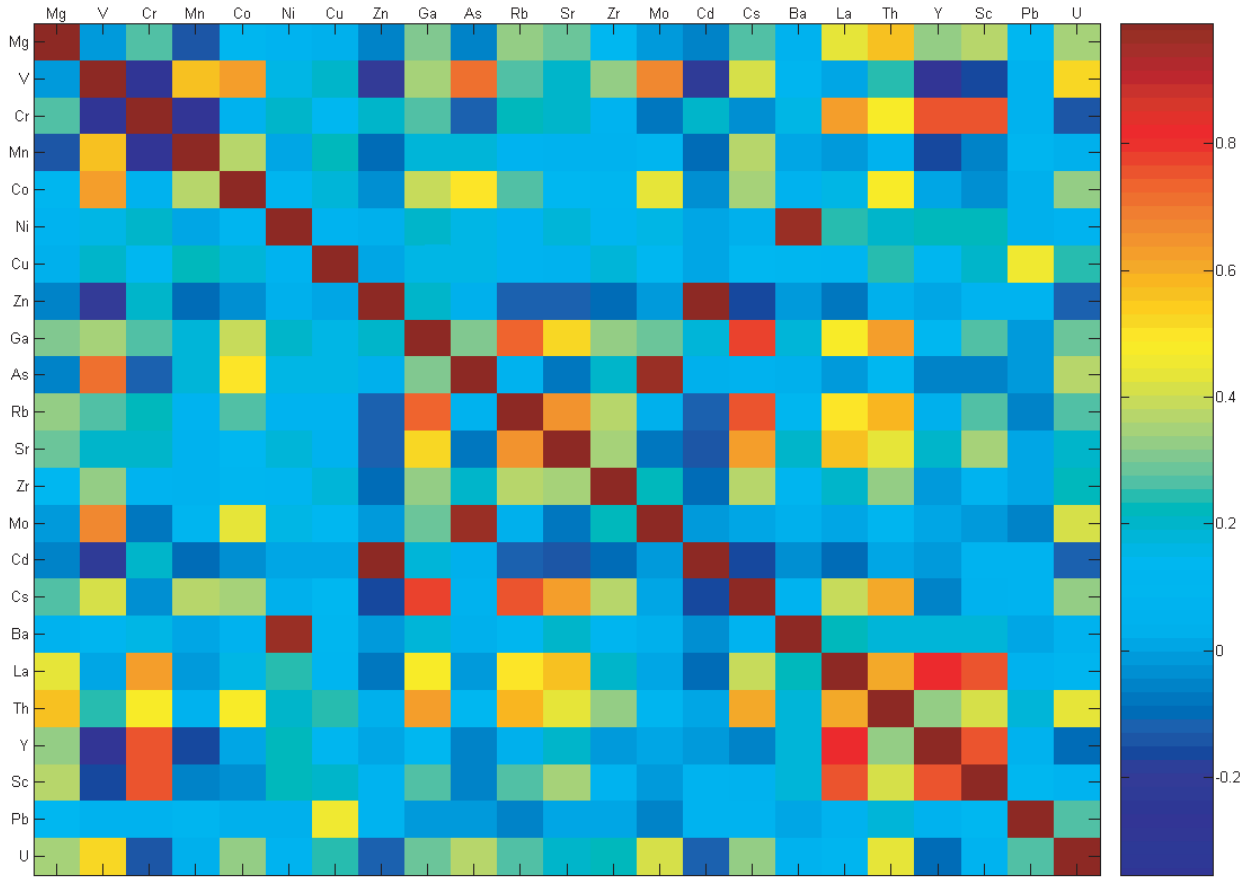

Fig. 7a. Correlation matrix, Lausen-Schleifenberg global system

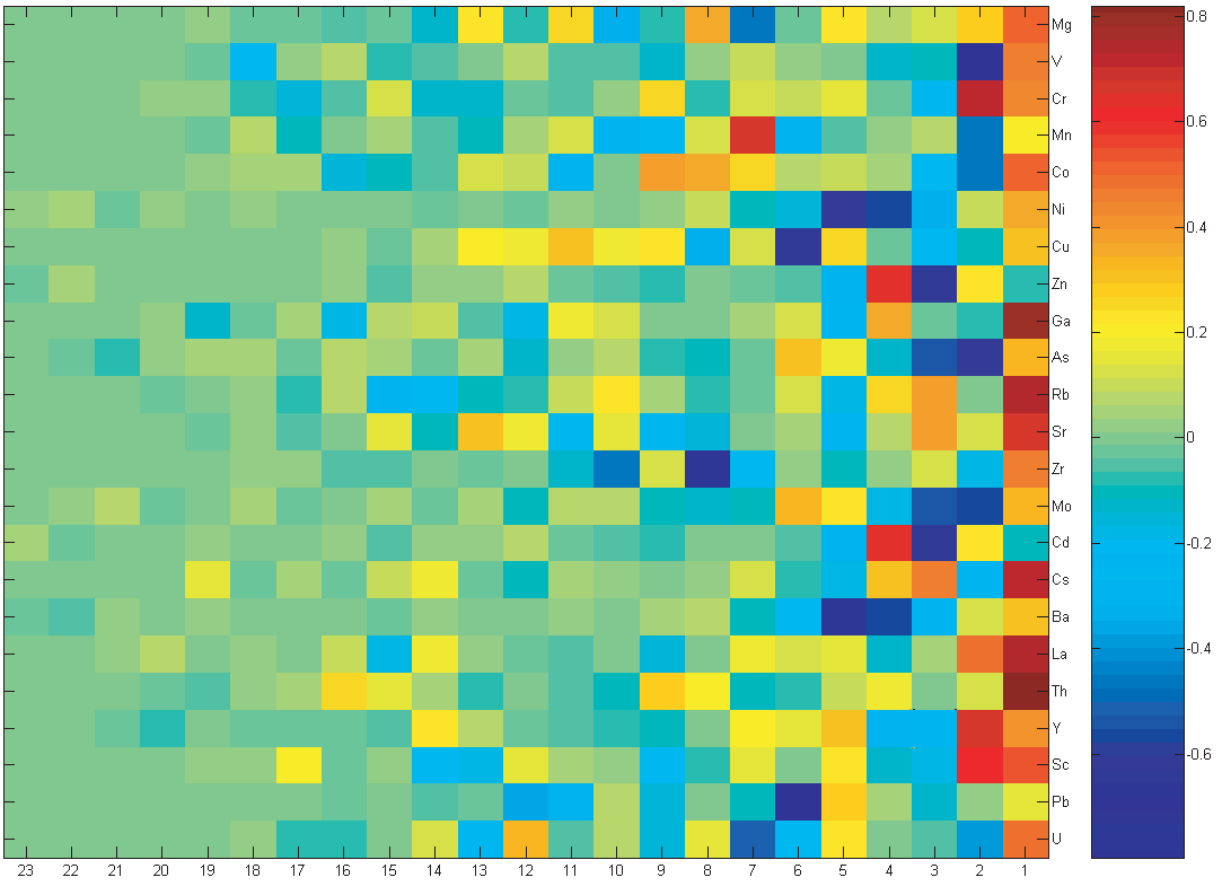

Fig. 7b. rCP matrix, Lausen-Schleifenberg global system

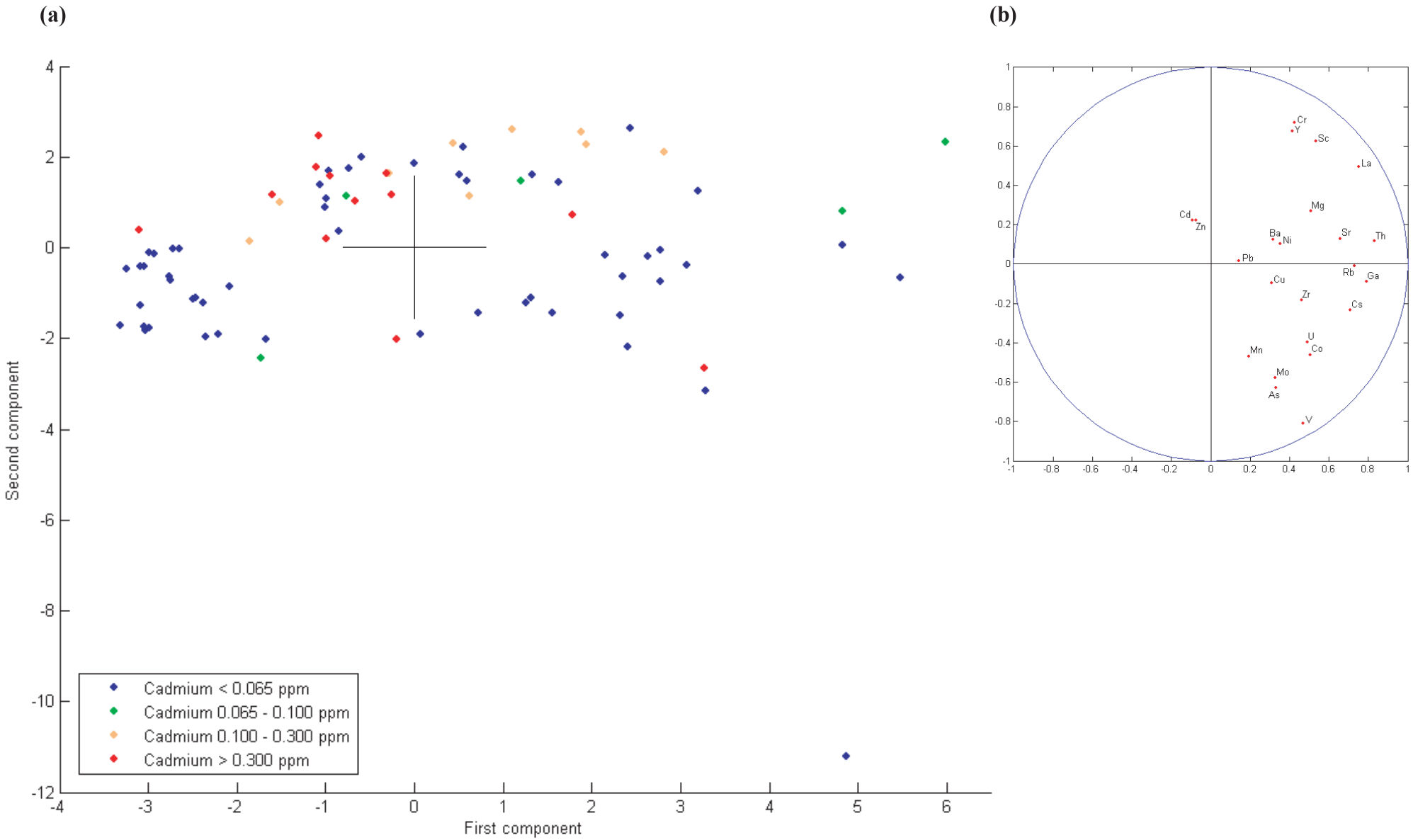

Fig. 8. Lausen-Shleifenberg global system.
a. First component against second component diagram.
b. Associated correlation circle (x: first PCA axis, y: second PCA axis).

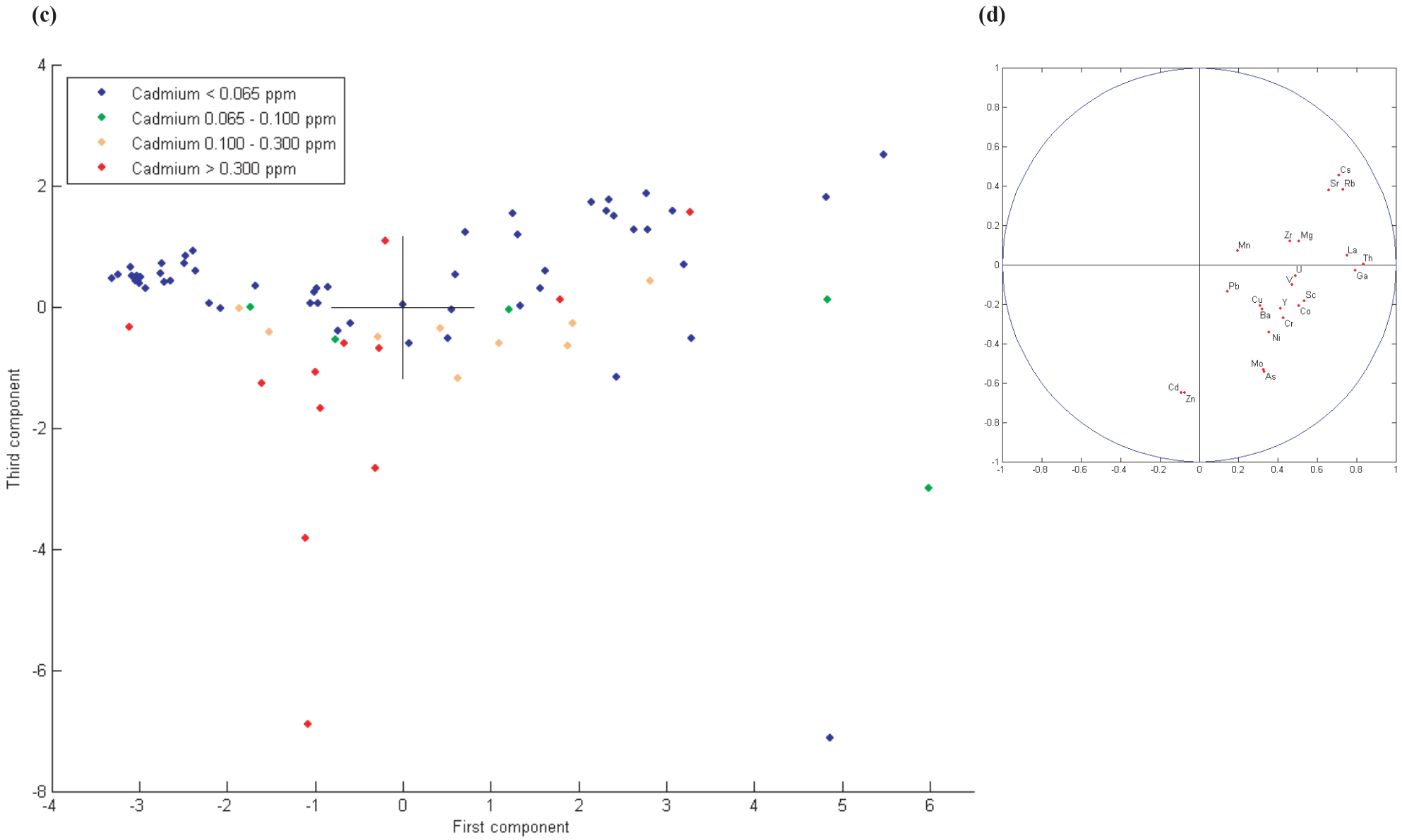

Fig. 8. Lausen-Shleifenberg global system.
c. First component against third component diagram.
d. Associated correlation circle (x: first PCA axis, y: third PCA axis).

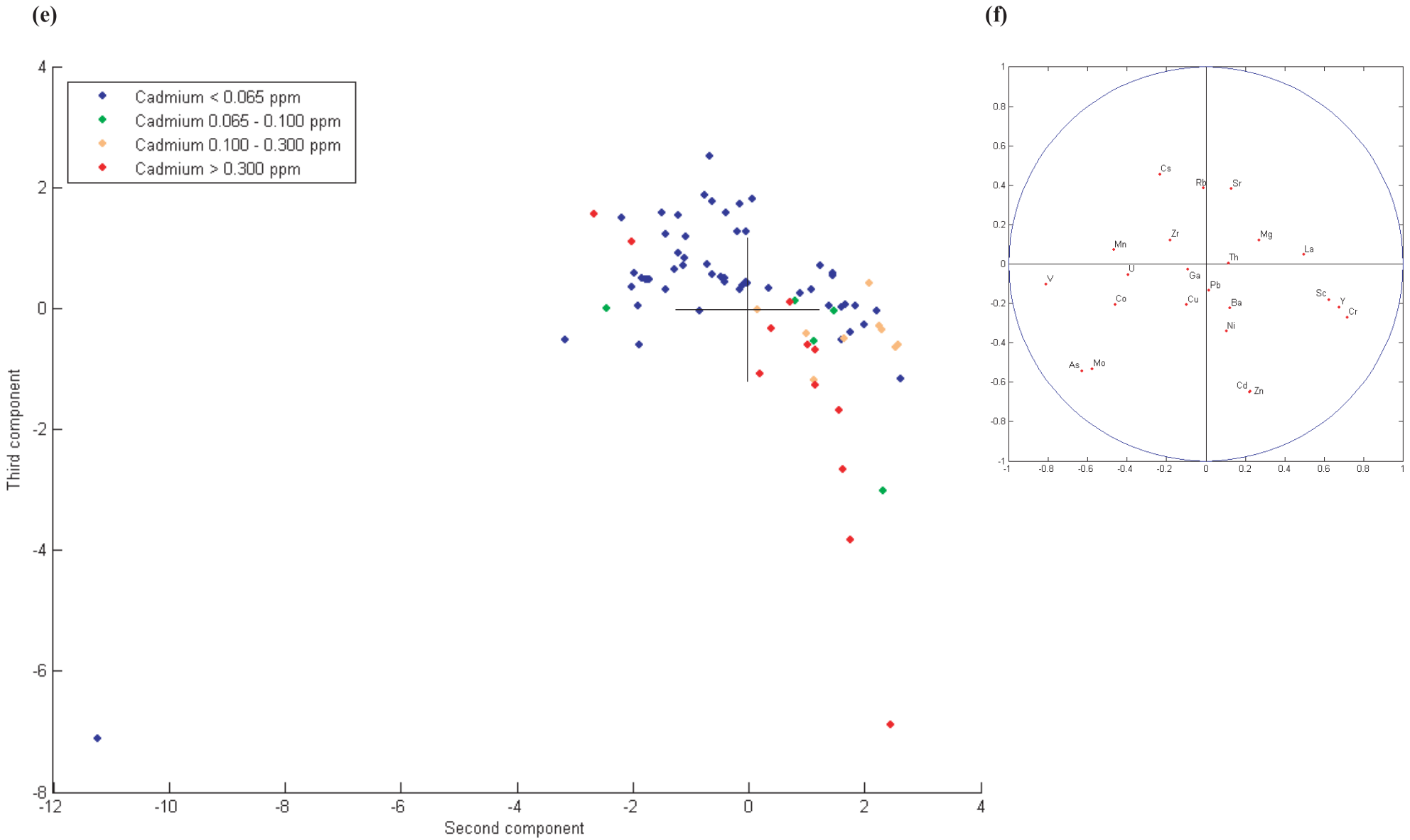

Fig. 8. Lausen-Shleifenberg global system.
e. Second component against third component diagram.
f. Associated correlation circle (x: second PCA axis, y: third PCA axis).

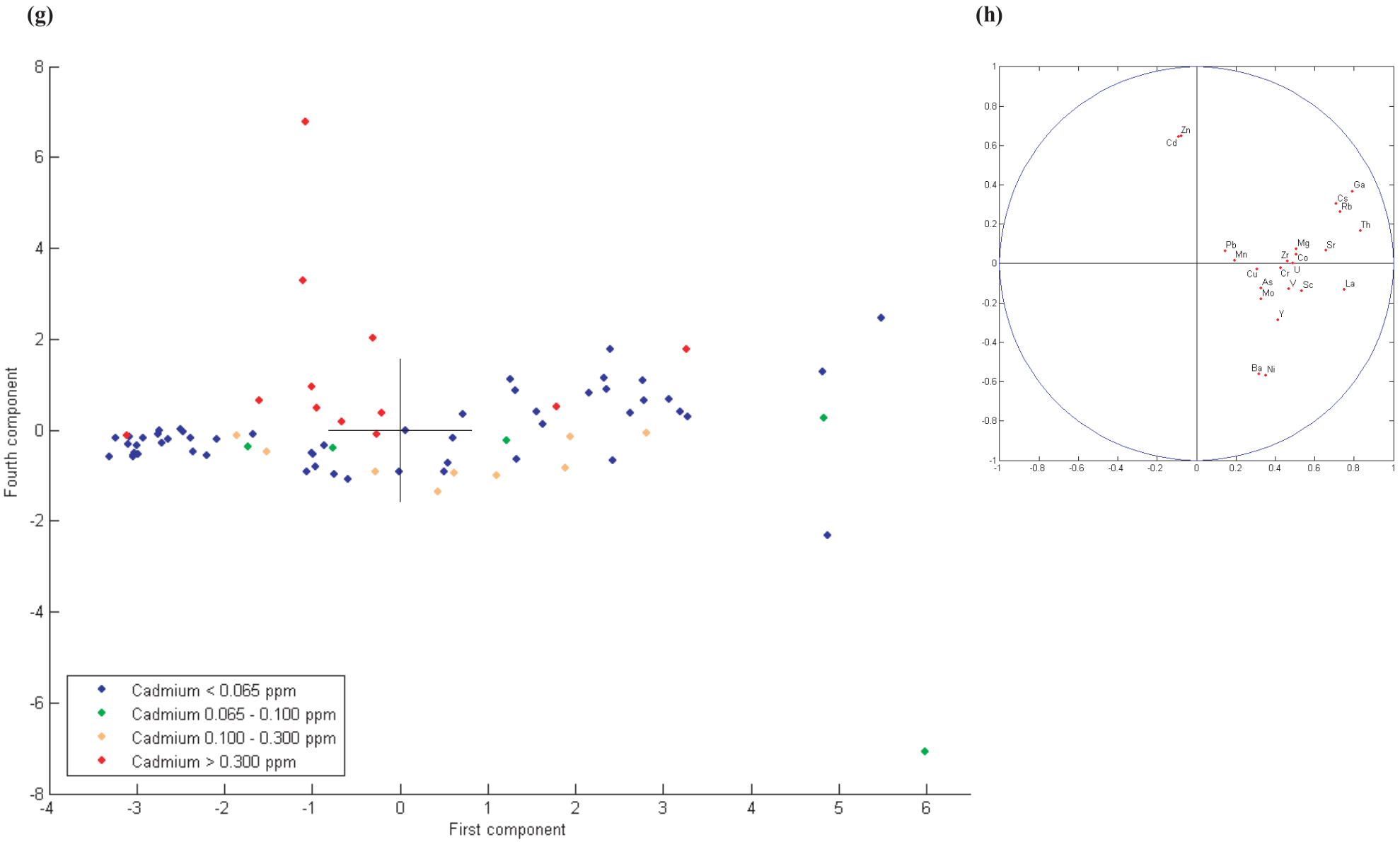

Fig. 8. Lausen-Shleifenberg global system.
g. First component against fourth component diagram.
h. Associated correlation circle (x: first PCA axis, y: fourth PCA axis).

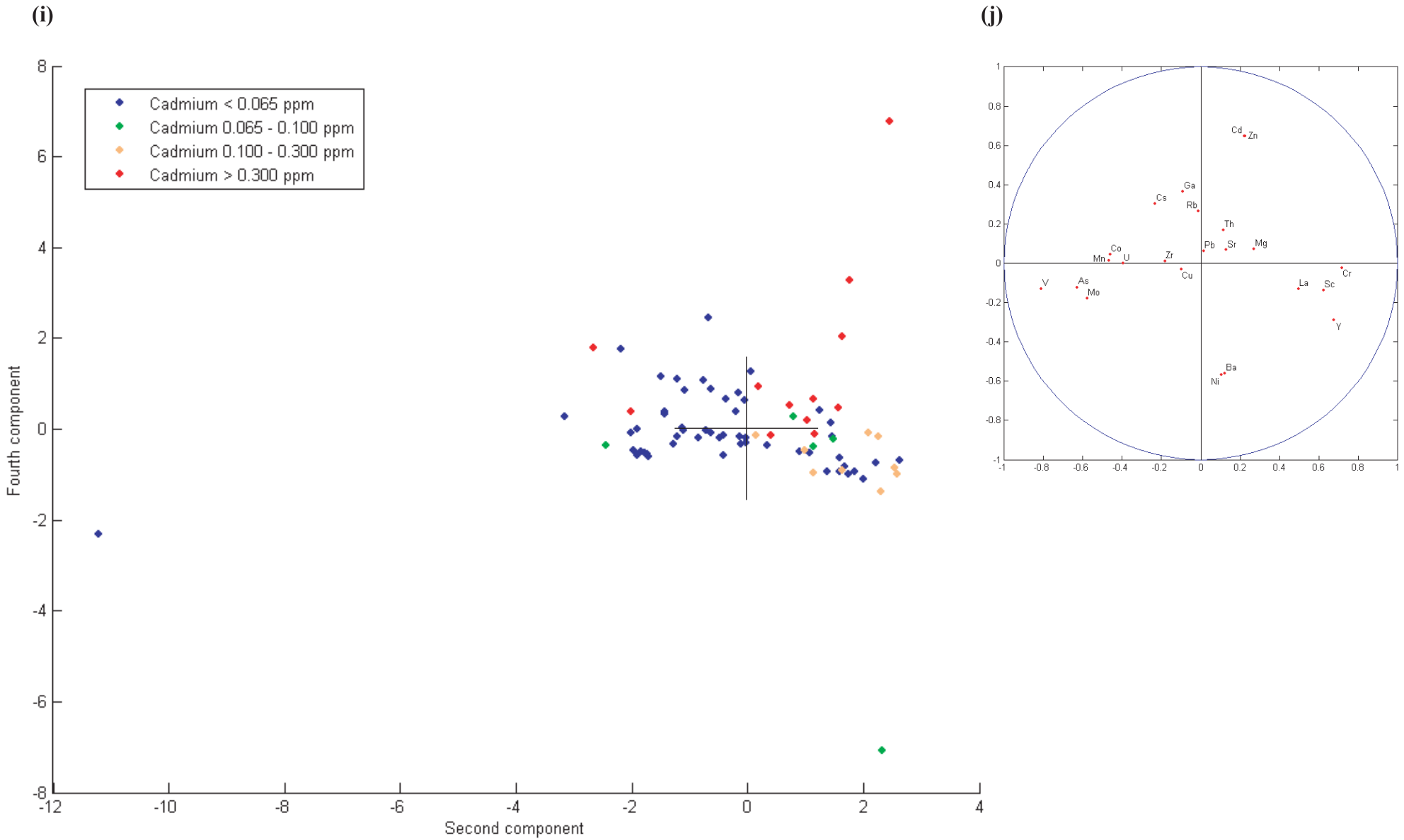

Fig. 8. Lausen-Shleifenberg global system.
i. Second component against fourth component diagram.
j. Associated correlation circle (x: second PCA axis, y: fourth PCA axis).

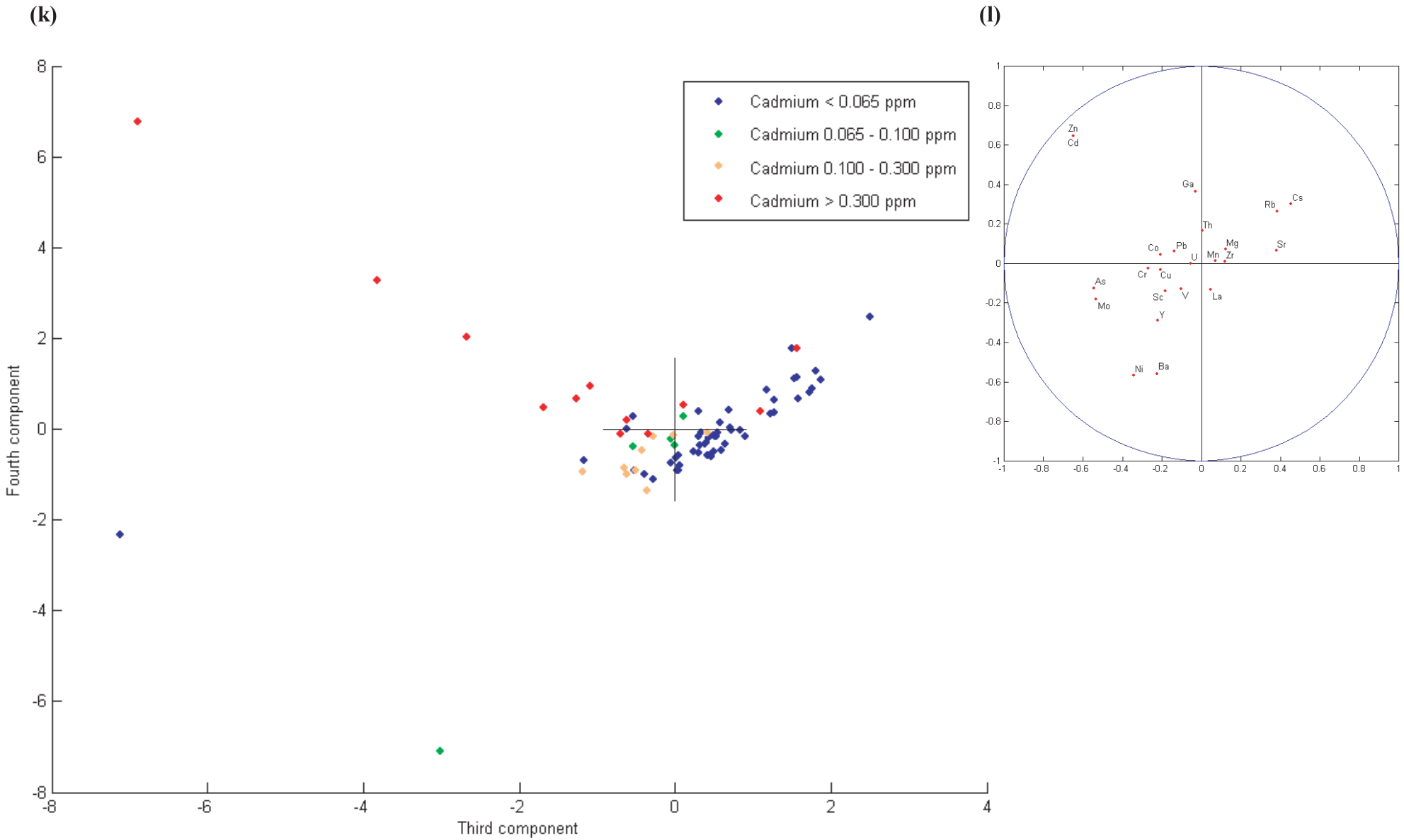

Fig. 8. Lausen-Shleifenberg global system.
k. Third component against fourth component diagram.
l. Associated correlation circle (x: third PCA axis, y: fourth PCA axis).

The diagram showing a plot of the second component against the fourth one (Fig. 8i), and the associated correlation circle (Fig. 8j), give, to a certain point, similar information: some of the samples which are highly enriched in Cd are attracted by the Cd and Zn pole, unrelated to other elements concentrations, whereas some others stay near the centre of the point cluster, and again others - like the non-enriched samples - seem more attracted by a pole anti-correlated to the second axis, which may be controlled mostly by variations in V, As, Mo (plus or minus Mn, Co, U) contents.

Complementary indications are given by both the third component against fourth component diagram (Fig. 8k), and the associated correlation circle (Fig. 8l), which also point out a specific chemical behaviour of part of the samples which are highly enriched in Cd. These latter are clearly drawn away from the point cluster centre following the attraction of the Cd and Zn pole. However, the behaviour of the rest of the samples, including part of the Cd-enriched ones, is less clearly defined, as no major chemical association is shown to control the point cloud elongation.

VIII-4-2-2 Lausen-Schleifenberg global system: interpretation

From the above follows that the Lausen-Schleifenberg system is very complex. Nevertheless, some trends can be sorted out:

- Cd and Zn are shown to be strongly associated in this chemical system, considering the correlation matrix and the results from the PCA analyses.
- Most of the variance in this chemical system is related to the concentrations of Ga, Rb, Sr, Cs, La, and Th in the samples. These elements may be related to external inputs into the global chemical system of this section.
- Sc, Y, Cr appear to form a distinct chemical pole (also related to external inputs?) as well as Mo and As, +/- V (influence of “nutrient-like” behaviour or related to better preservation and subsequent enrichment in the sediment?)
- None of these poles seem to be associated to the Cd and Zn one, indicating different mechanisms of enrichment and/or different sources for these two latter elements in comparison with the other ones. Nevertheless, a small part of the Cd-enriched samples, as well as most of the normal samples show a partial influence of the Sc/Y/Cr and Mo/As(/V) poles in their distribution.

VIII-4-2-3 Lausen-Schleifenberg “external inputs” sub-system: results

All elements which are strongly associated to the first PCA axis of the global system and suspected to be of external origin (i.e., Ga, Rb, Sr, Cs, La, Th) have been selected for the “external inputs” sub-system. Zr has been added due to its affinity for the continental crust (conservative tracer of terrestrial weathering; e.g., Morton and Hallsworth, 1999; Velbel, 1999). Zn and Cd have been selected to precise their relationships with “external” elements.

The PCA permitted to concentrate the global chemical variability of this sub-system on the three first axes (explanation of 79.00% of the total variance, 69.66% held by the two first axes).

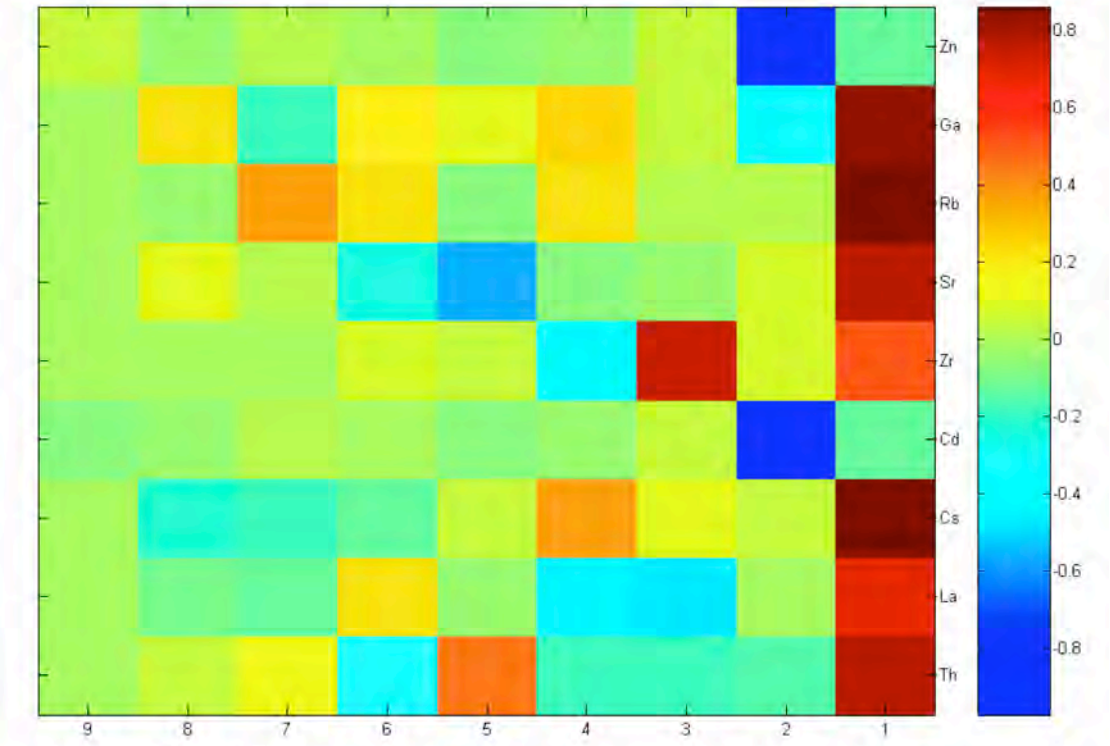

Fig. 9a. rCP matrix, Lausen-Schleifenberg "external input" sub-system

The rCP matrix (Fig. 9a) shows a strong association of all elements considered to be of external origin with the first axis, at the exception of Zr which is only partially correlated to this axis, being the principal element related to the third axis. Cd and Zn are both strongly anti-correlated to the second axis.

When plotting the first PC component against the second one (Fig. 9b), and drawing the corresponding correlation circle (Fig. 9c), we observe that - as was already suggested by the study of the global system - two very distinct chemical poles control the distribution of samples in this sub-system. One is constituted by all the elements except Cd and Zn, and the second one is composed of this two latter elements. "Normal" samples with regards to their Cd contents, as well as the "intermediate" ones, show various influences of the "external elements" group. Some of the highly Cd-enriched samples follow the same behaviour. The majority of them, however, is attracted towards the Cd and Zn pole, and does not appear to be influenced by the other chemical group. Indeed, the point cluster derive in the Cd/Zn direction, begins from the centre of the point cloud - even in the depleted part relative to "external" elements, and shows no drift towards intermediary influences.

If the here used limit separating "intermediate" and Cd-enriched samples is moved upward to 0.800 µg/g (Fig. 9d), all Cd-enriched samples would specifically follow the movement in the direction of the Cd and Zn pole, whereas "normal" and "intermediate" samples would show a greater influence from the "external elements" group.

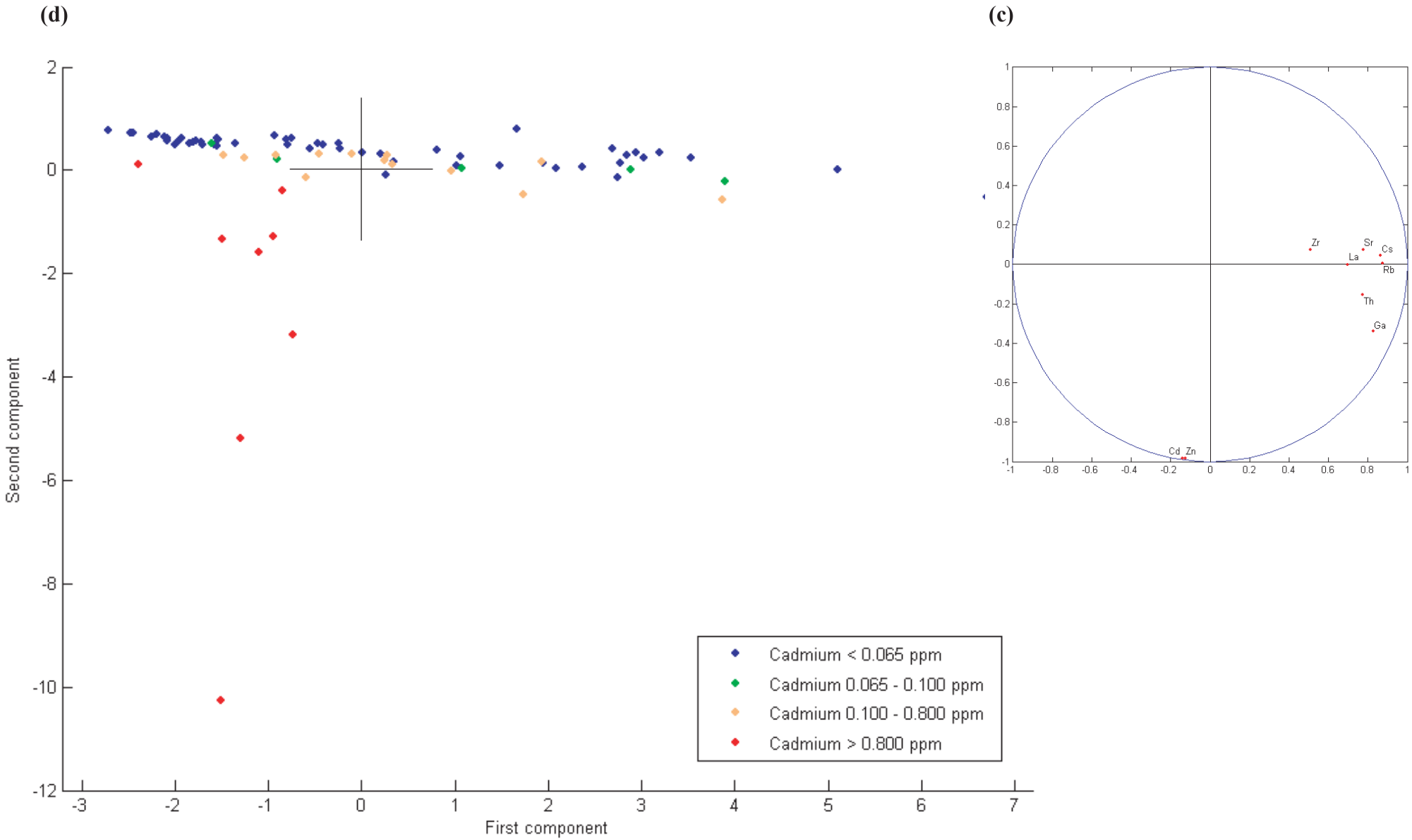

Fig. 9. Lausen-Shleifenberg “external input” sub-system.
d. First component against second component diagram.
c. Associated correlation circle (x: first PCA axis, y: second PCA axis).

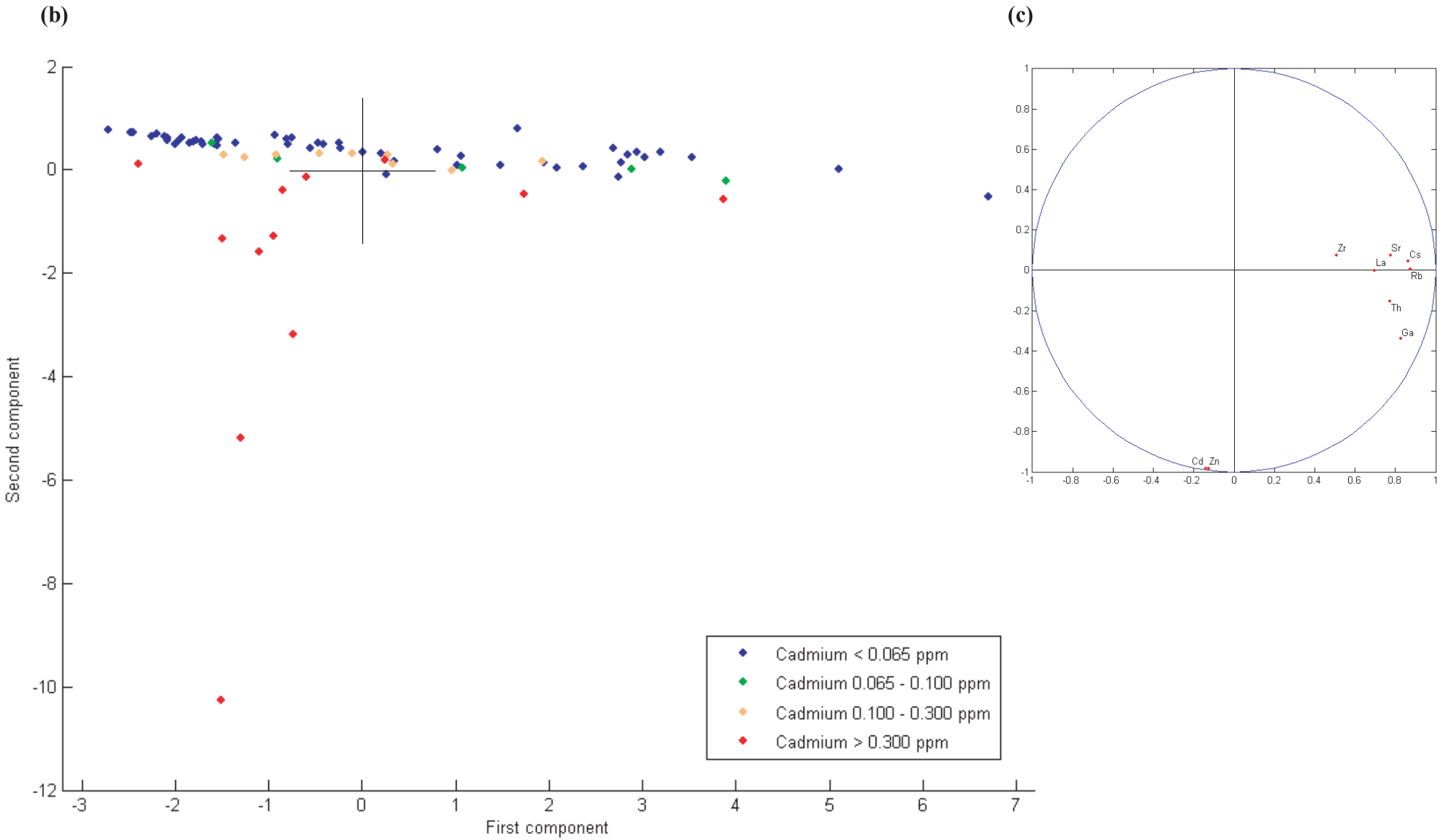

Fig. 9. Lausen-Shleifenberg “external input” sub-system.
b. First component against second component diagram.
c. Associated correlation circle (x: first PCA axis, y: second PCA axis).

VIII-4-2-4 Lausen-Schleifenberg "external inputs" sub-system: interpretations

The most important enrichments in Cd appear to be related to a mechanism which is totally independent from external inputs, as is witnessed by variations in Ga, Rb, Sr, Cs, La, and Th. Indeed, samples that are enriched in Cd to the highest levels (e.g., above 0.800 µg/g) present the lowest influence with regards to the concentrations of the external group. On the other hand, some of the "intermediate" samples show rather strong influences of the "external" elements group. This may indicates that:

- inputs of elements related to both chemical groups are synchronous, and Cd and Zn underwent a concentration process relatively to the "external" elements. The concentration process may be related to preferential biological uptake, a fixation by adsorption on different types of solid particles including organic matter, or a better preservation in sediments under reducing conditions (see Rambeau et al. in prep.b).
- the association Cd/Zn and the "external" elements are incorporated into the calcareous grains following their concentrations in the parent water at the time of carbonate precipitation, and inputs of these two elemental groups are mostly disconnected in time; this latter point is demonstrated by the behaviour of the "intermediate" samples.

A combination of both processes is equally possible, each element being taken from the parent water and incorporated in carbonates as a function of its availability, Cd and Zn being preferentially concentrated by specific mechanisms.

VIII-4-2-5 Lausen-Schleifenberg "nutrients-preservation" sub-system: results

For this sub-system we selected the elements Mo, As, and V, which are shown to form a specific chemical pole in the global chemical system - in addition to Cd and Zn. We also took Co into consideration, in order to complete the "nutrient-like" sub-system, as well as Pb and U, in order to test the influence of preservation under dysoxic conditions.

The PCA led to the construction of a new system of axes combining the different variables. The two first axes comprise 66.92% of the total variance, and the three first axes 81.48%. Considering the rCP matrix (Fig. 10a), V, As and Mo are associated to the first axis, together with part of Co (which is equally related to the fourth axis), whereas Zn and Cd are strongly correlated to the second one. Pb is mostly related to the third axis. U is partitioned between the first, third and fifth axes, but not strongly associated to one of those.

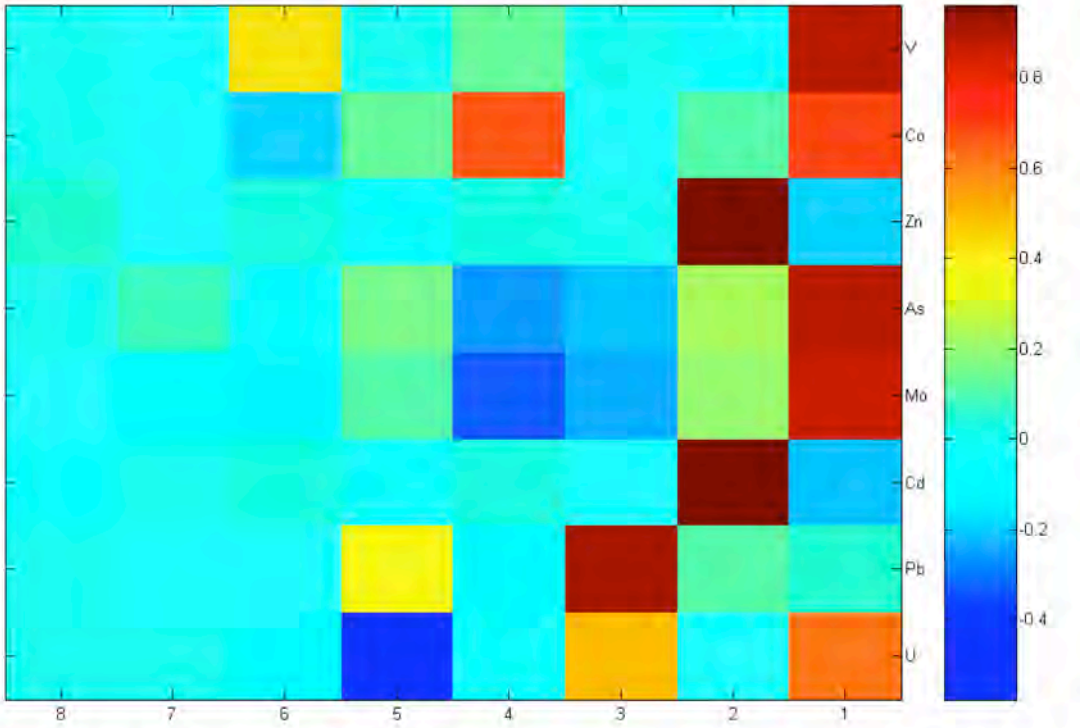

Fig. 10a. rCP matrix, Lausen-Schleifenberg "nutrients-preservation" sub-system

When considering the diagram obtained by plotting the two first PC components against each other (Fig. 10b), as well as the corresponding correlation circle (Fig. 10c), we distinguish two major elemental poles. One is constituted by Cd and Zn, and the other one is composed of As, Mo, V, and - to a slightly lesser extend - also Co and U. These two groups of elements are clearly disconnected, being positioned at an angle of 90 to 100° relative to each other on the correlation circle. Samples are unequally distributed in the diagram, under the influence of the two poles. Those which are Cd-enriched to the highest levels (above 0.800 µg/g) are elongated from the centre of the point cluster - or more exactly from a zone of the point cloud that is slightly depleted in elements belonging to the As/Mo/V(/Co/U) group - towards the Cd and Zn pole. "Normal" samples are distributed following various degrees of influence by the As/Mo/V(/Co/Cu) group, most of them being grouped around the centre, along with the "intermediate" samples.

The diagram plotting the first component against the third (Fig. 10d) shows the relative influences of the Pb, U and Mo/As/V/Co poles (Fig. 10e) on the point distribution. All these groups of elements are responsible for segregation inside the point cloud, but the samples concerned are the "normal" ones and, to a lesser extend, the "intermediate" ones with regards to their Cd contents, the highly Cd-enriched samples being untouched. The same result is obtained with the diagram plotting the second component against the third (Fig. 10g), which present distinct influences of the Pb (+/-U) pole (for part of the "normal" and "intermediate" samples) and the Cd/Zn pole (for the highly Cd-enriched samples).

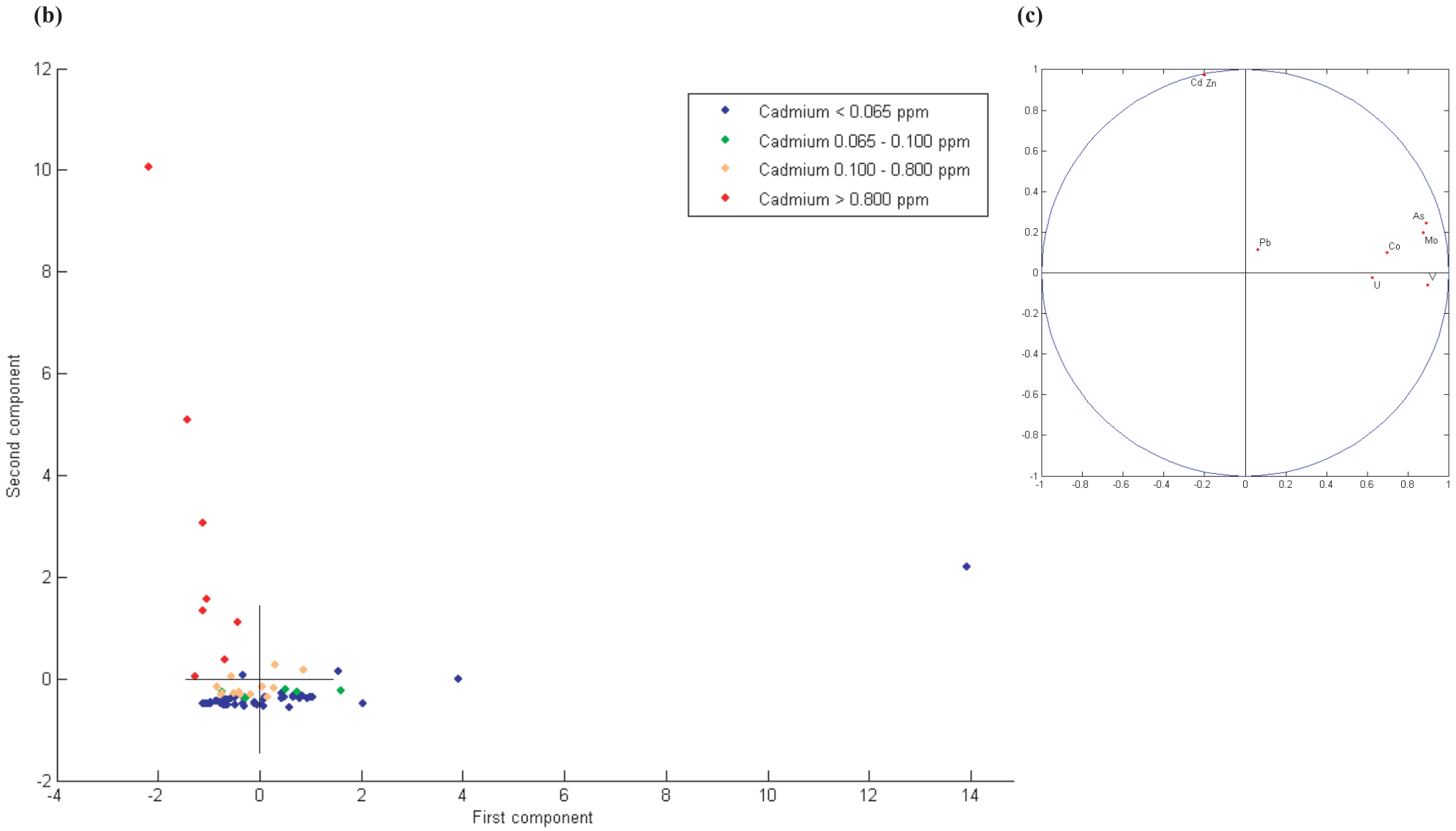

Fig. 10. Lausen-Shleifenberg “nutrients-preservation” sub-system.
b. First component against second component diagram.
c. Associated correlation circle (x: first PCA axis, y: second PCA axis).

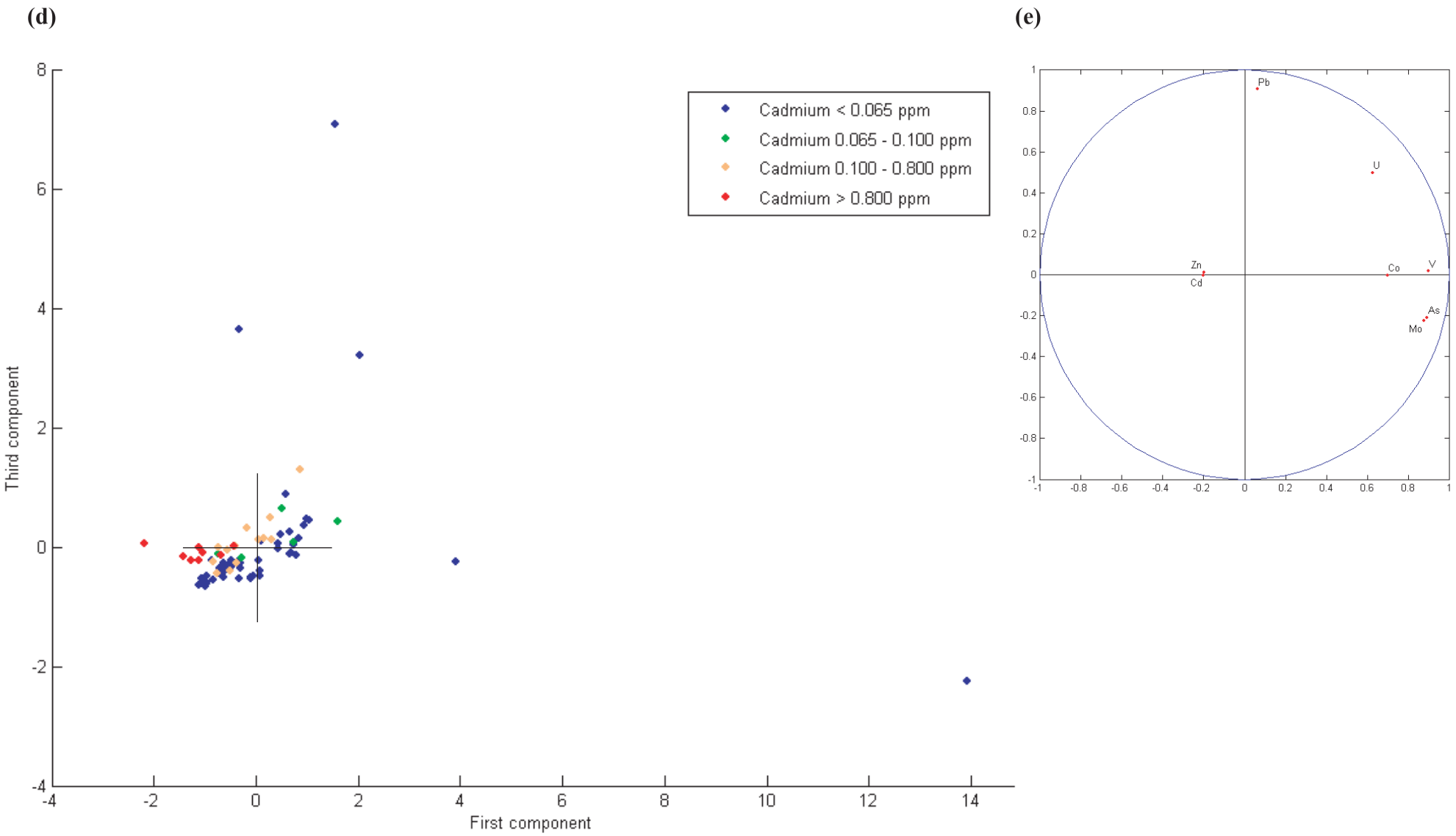

Fig. 10. Lausen-Shleifenberg “nutrients-preservation” sub-system.
d. First component against third component diagram.
e. Associated correlation circle (x: first PCA axis, y: third PCA axis).

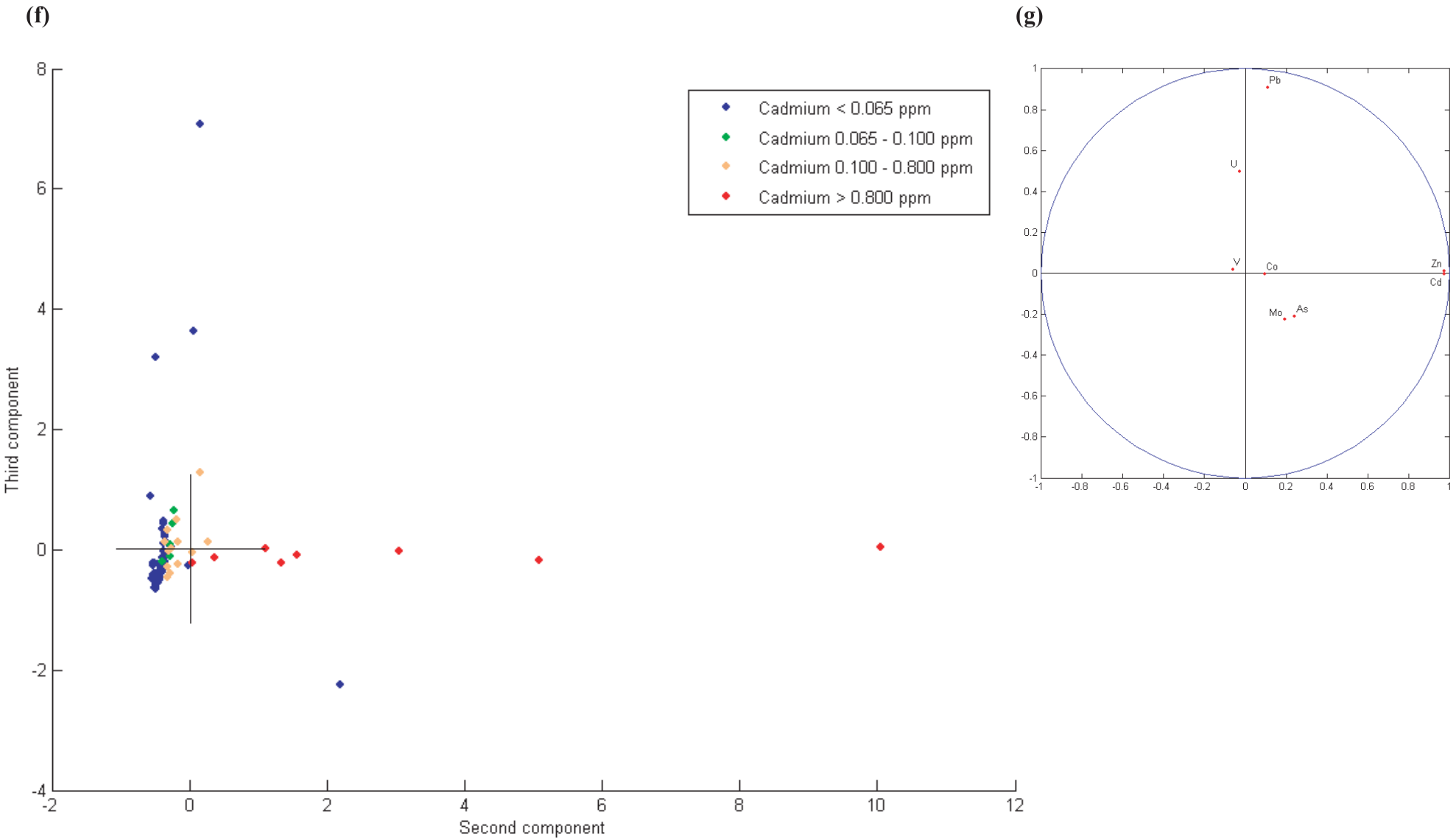

Fig. 10. Lausen-Shleifenberg “nutrients-preservation” sub-system.
f. Second component against third component diagram.
g. Associated correlation circle (x: second PCA axis, y: third PCA axis).

VIII-4-2-6 Lausen-Schleifenberg "nutrients-preservation" sub-system: interpretations

Once again, Cd enrichments appear to be related to sources and/or mechanisms that are clearly distinct from those controlling the distribution of the other elements in this sub-system. Mo, As, V and Co are preferentially associated in a chemical pole and are interpreted as witnesses of variations in the nutrient system. U and Pb are thought to represent preferential preservation inside the sediment under dysoxic conditions. However, these two elements are only associated to a certain level. The reduced number of samples which is concerned by a strong influence of the Mo/As/V/Co, Pb or U poles may indicate that large variations in the nutrients or preservation conditions are scarce. At any rate, these variations only concern some of the samples that display "normal" to "intermediate" Cd concentrations.

It is therefore unlikely that Cd enrichment in this particular section is linked with either preferential biological uptake such as by phytoplankton activity (as it would be very improbable that this uptake only concerns Cd and Zn and none of the other elements that normally present a "nutrient-like" behaviour) or enhanced preservation in the sediment linked with dysoxic conditions. It is also quite difficult to consider a process of adsorption onto organic matter as the only factor responsible for such enrichments, as organic matter contents are supposed to be related, in one way or another, to nutrient supply.

One possible explanation remains a preferential uptake via bacterial activity, as certain types of bacteria have been shown to concentrate Cd and other trace elements with great efficiency (e.g., Loaëc et al., 1997; Boyanov et al., 2003 and references therein; Kemner et al., 2005 and references therein).

VIII-4-3 Gorges du Pichoux section

VIII-4-3-1 Gorges du Pichoux global system: results

The correlation matrix (Fig. 11a) of the Gorges du Pichoux chemical system indicates strong correlations among the Li, Al, Ga, Rb, Cs, Ba, La, and Th group, which includes also associations of some of its members with Y. Zr and Cu are equally associated, and - to a lesser extend, V and Co. Cd is totally independent with regards to any other element considered in this system.

A comparative correlation matrix (Fig. 11b) constructed using the samples for which Zn, As, and W were measured, and shown here for comparison, shows that Cd and Zn are only partially associated in this system. Cd is furthermore anti-correlated with As to a certain extend.

The PCA realized on the system that does not consider As, W and Zn permit to concentrate the essential part of the information on a few axes: the three first axes explain 70.74% of the total variance, and four axes suffice to surpass the 75% mark. The comparative system, which also includes these elements but concerns a reduced number of samples, displays less well-defined results: 53.14% of the total variance is held by the three first axes, and six axes are necessary to surpass 75%. This latter result is comparable with those obtained with the sections of Terminilletto and Lausen-Schleifenberg.

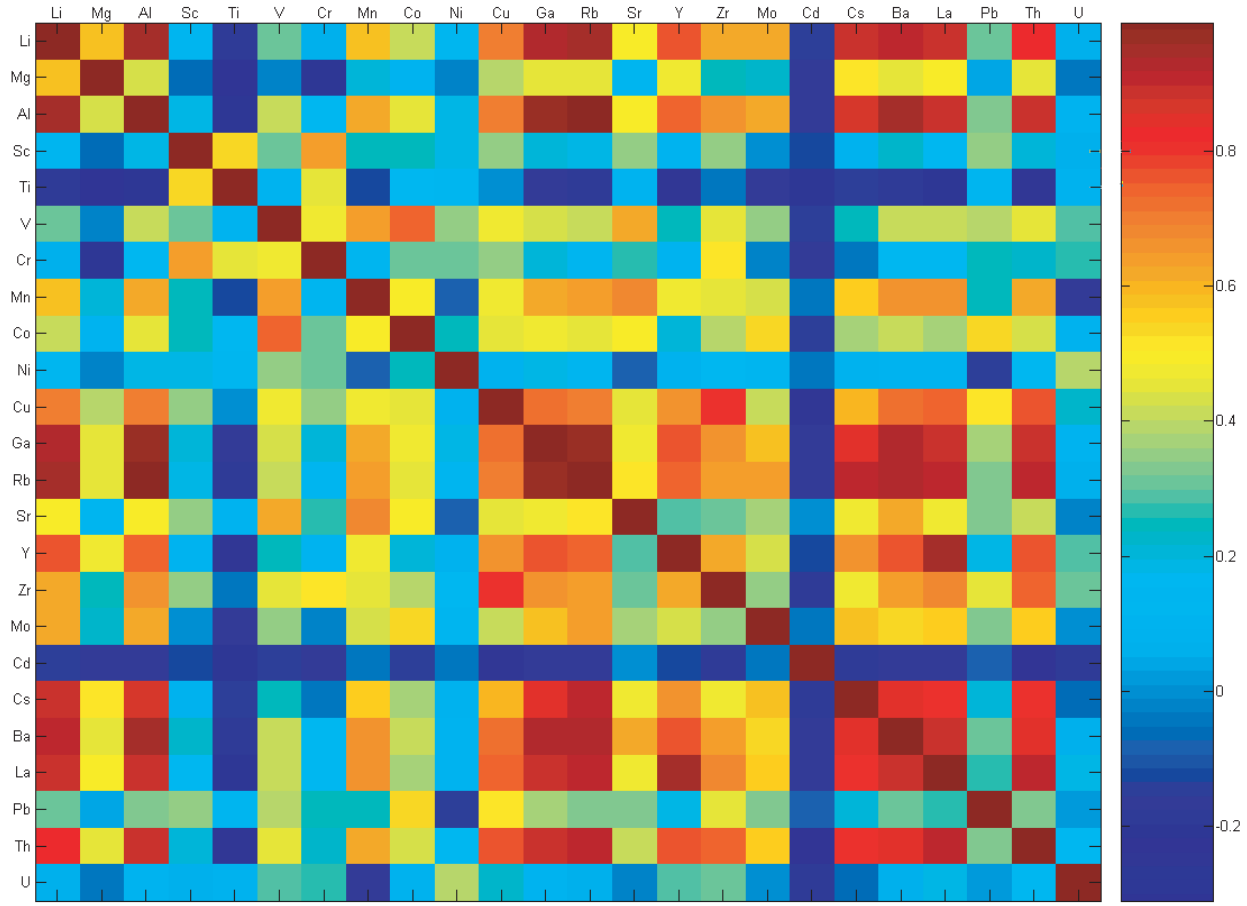

Fig. 11a. Correlation matrix, Gorges du Pichoux global system (without As, W, Zn)

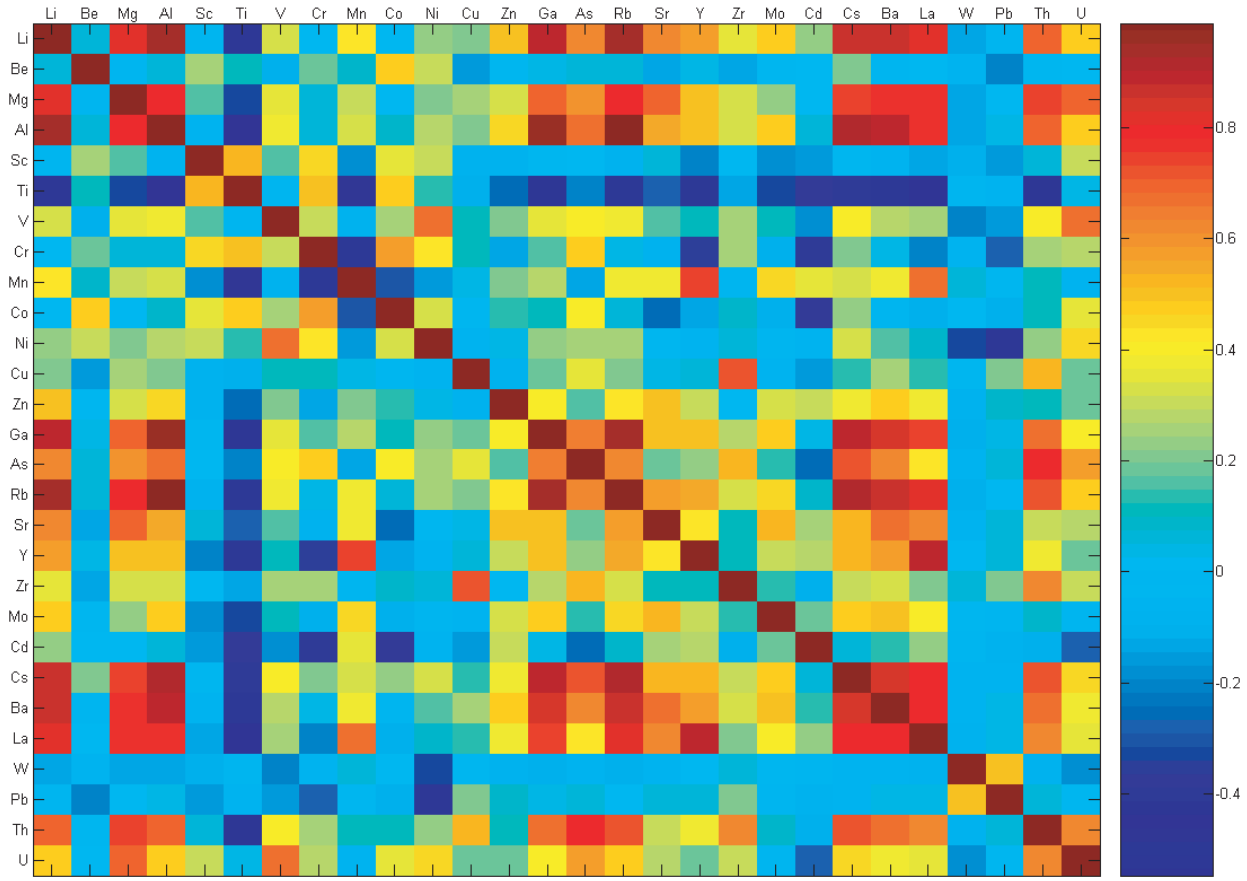

Fig. 11b. Correlation matrix, Gorges du Pichoux comparative global system (+ As, W, Zn)

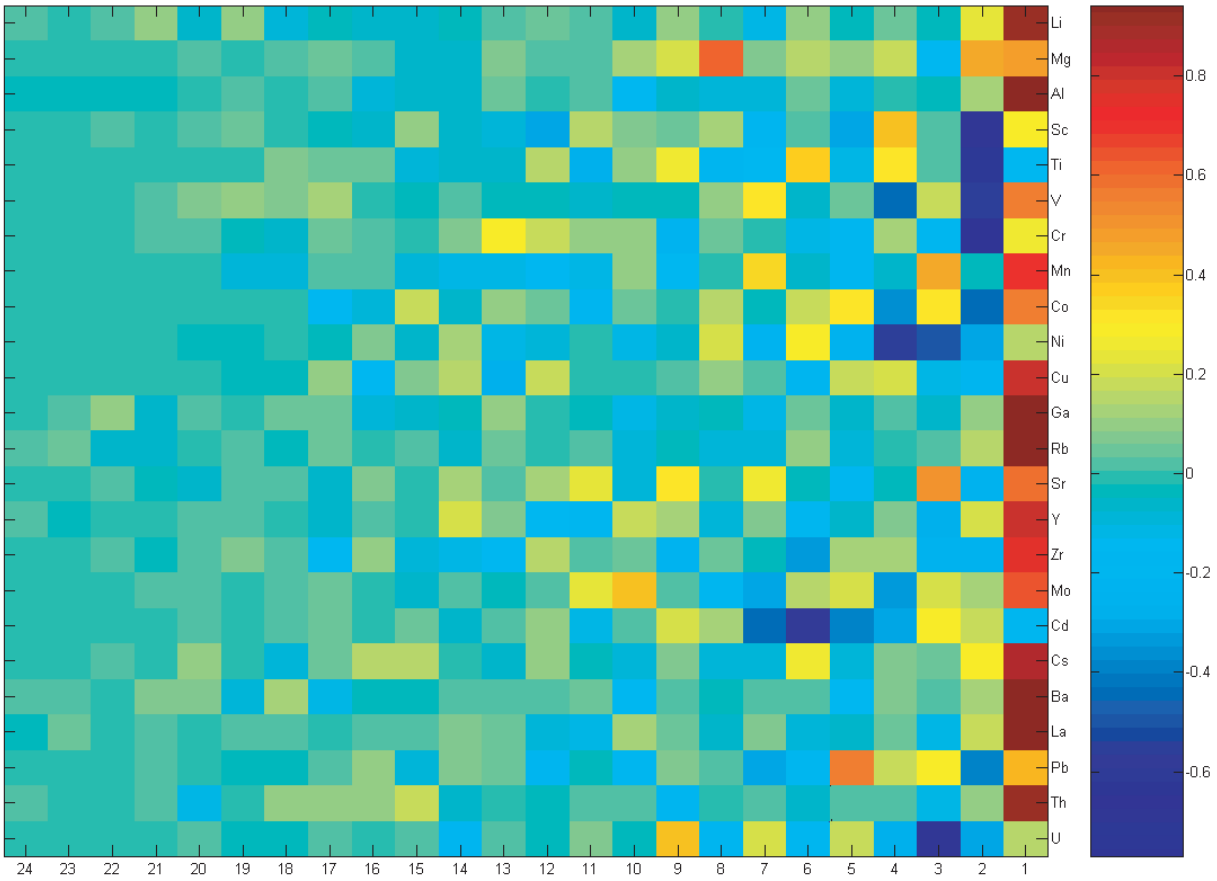

Fig. 12a. rCP matrix, Gorges du Pichoux global system (without As, W, Zn)

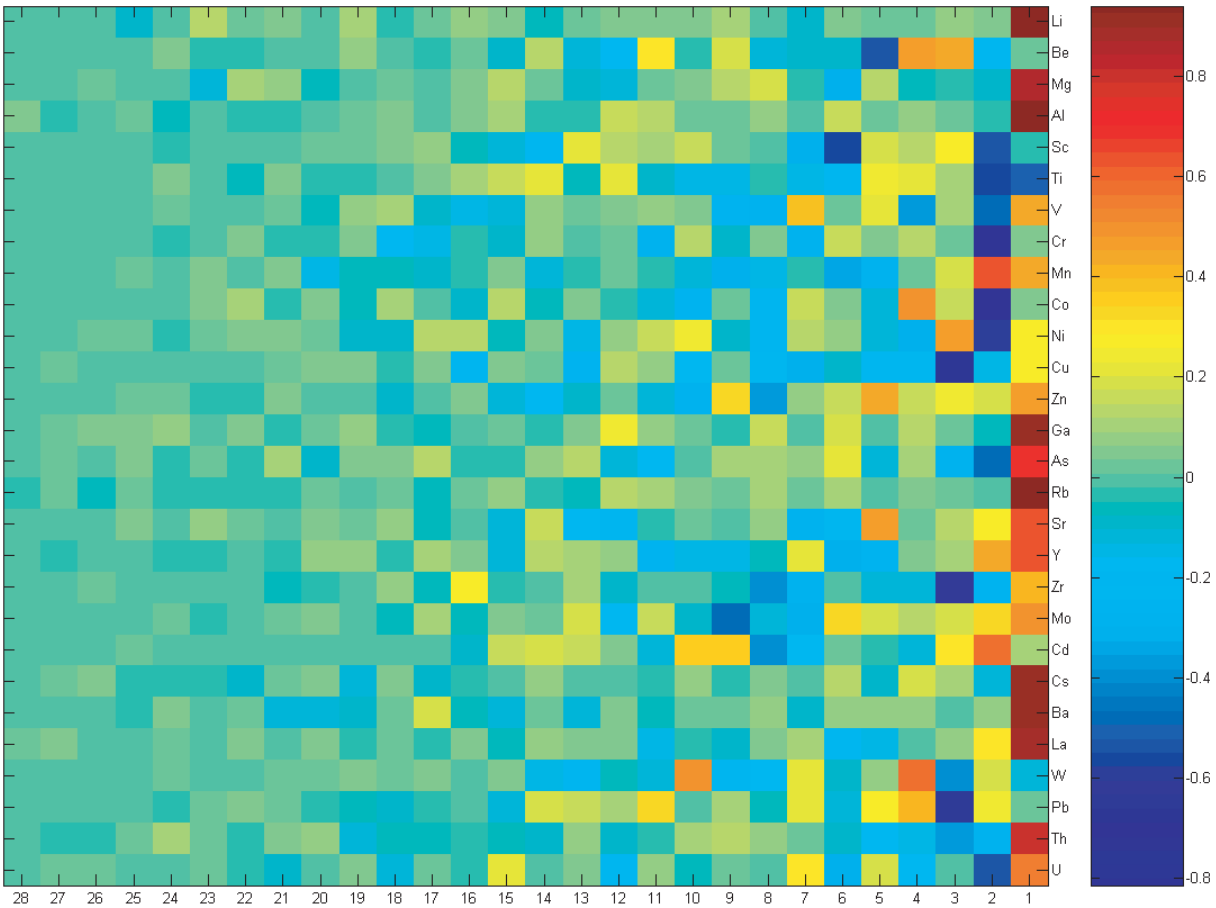

Fig. 12b. rCP matrix, Gorges du Pichoux comparative global system (+ As, W, Zn)

The rCP matrix related to the system without As, W and Zn (Fig. 12a) indicates that the variance of this system is dominated by variations in Li, Al, Ga, Rb, Ba, La, Th, and - to a lesser extend - Cu and Cs, which are strongly associated with the first axis (holding 45.64% of the total variance). Others elements like V, Mn, Co, Y, Zr, and Mo are equally partially associated to the first PCA axis. Sc, Ti and Cr are the main elements related to the second axis, with which they are in anti-correlation. U is the element that is most strongly associated to axis three. Cd is particularly related to the sixth axis. The rCP matrix associated to the comparative system (Fig. 12b) gives Li, Mg, Al, Ga, Rb, Cs, Ba, and La as the main association controlling the total variance. As is partly correlated to the first axis, as well as anti-correlated to the second axis. W is mainly partitioned between axes three and four. Cd is partly correlated to axis two and anti-correlated to axis eight. Zn is not clearly associated to any of the axes, being partly correlated to the first and fifth axis, and anti-correlated to axis eight, in association with Cd.

Relationships concerning the different variables and the three first axes of both systems are equally displayed on the six correlation circles presented in Fig. 13.

VIII-4-3-2 Gorges du Pichoux global system: interpretation

Li, Al, Ga, Rb, Ba, La, +/- Mg, Cs, and Th are the elements that control the maximum variance in this global system. These elements are mostly related to external inputs, at the possible exception of Mg. Additionally, these two global systems do not display any clear information with regards to Cd variations. Nevertheless, one striking point is that in the Gorges du Pichoux chemical system, Cd is only partially associated with Zn. However, we must consider that the relationship between these two elements was established using a reduced number of samples (but including all the samples belonging to the Cd-enriched part), so this observation is perhaps a little skewed.

VIII-4-3-3 Gorges du Pichoux "external inputs" sub-system: results

Li, Al, Ga, Rb, Y, Zr, Cs, Ba, La, and Th are intepreted here to be of an external origin. Together with Cd, these elements have been selected to construct the "external inputs" sub-system. Except for Cd and Zr, these elements are all associated to the first axis of the PCA (Fig. 14a) in anti-correlation. In contrast, Cd is strongly correlated to the second axis. Zr is equally partitioned between the first and third axes.

The diagram realized by plotting the first principal component against the second one (86.09% of the total variance; Fig. 14b) and the associated correlation circle (Fig. 14c) show that the point cluster is elongated following two major influences, which are clearly disconnected:

- "normal" samples as well as those belonging to the first intermediate category are mainly distributed following variations in the group of "external" elements
- the second intermediate category with regards to Cd concentrations shows a mixed influence of the "external" elements and Cd poles
- the highly Cd-enriched samples are distributed following only the attraction of the Cd pole, independently of the other elemental group.

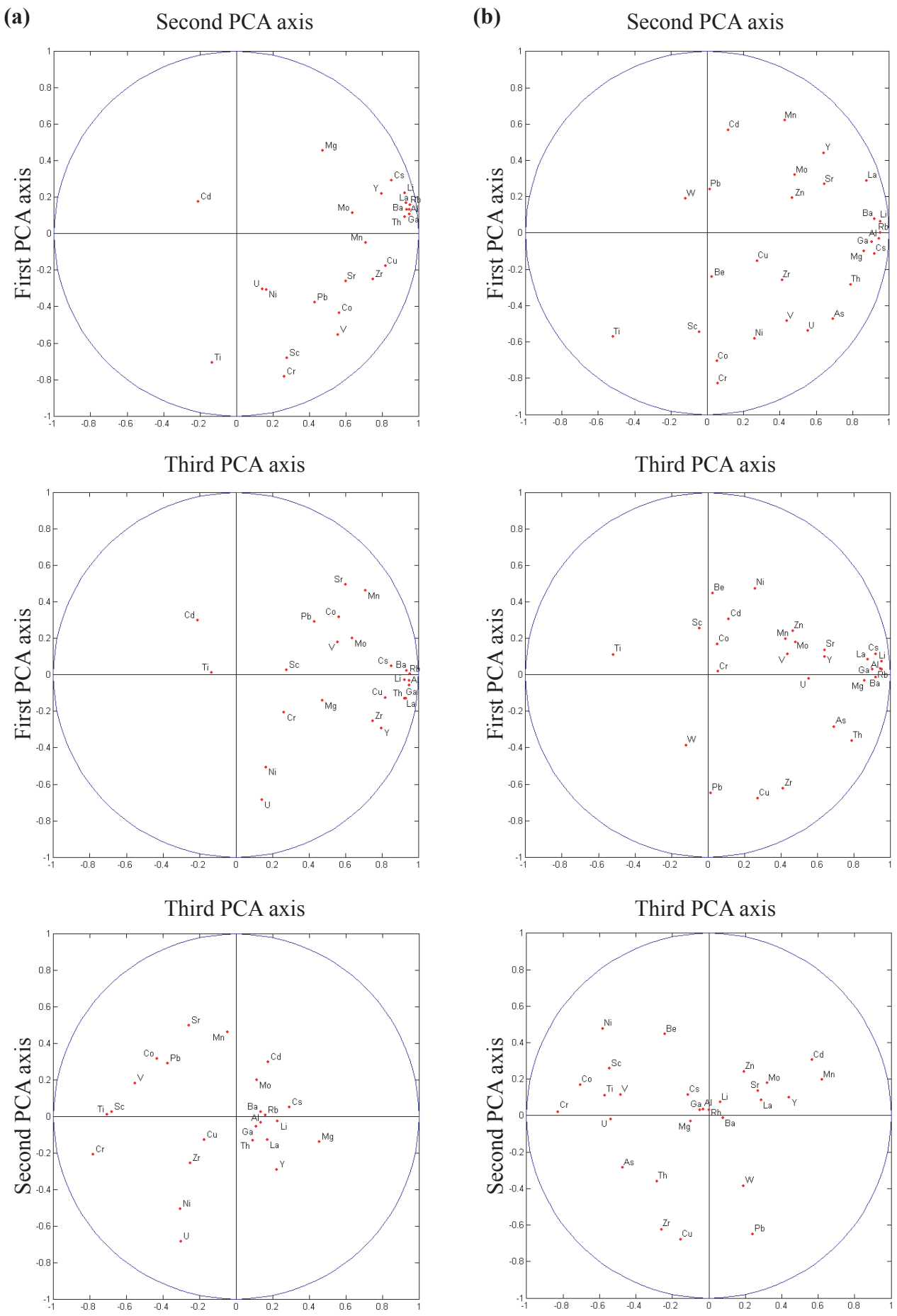

Fig. 13. Gorges du Pichoux, correlation circles relative to the three first PCA axes of:
a. the global system (without As, W, Zn)
b. the comparative global system (+ As, W, Zn)

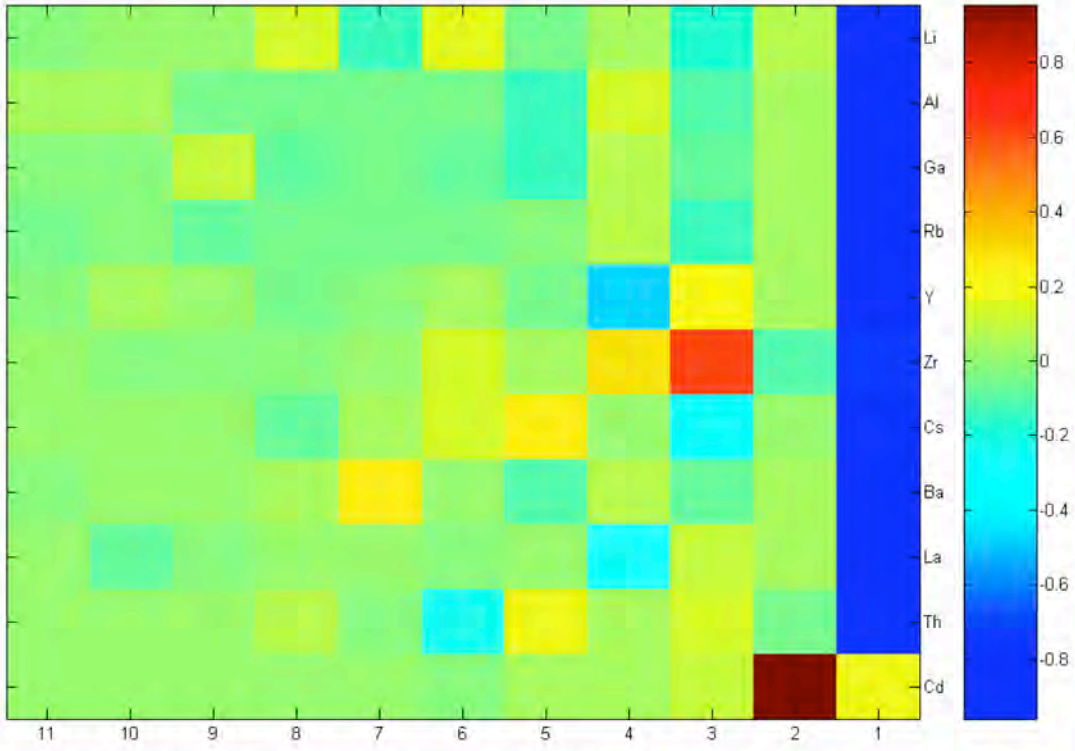

Fig. 14a. rCP matrix, Gorges du Pichoux "external input" sub-system

VIII-4-3-4 Gorges du Pichoux "external inputs" sub-system: interpretations

The mechanism that controls Cd enrichments seems once again to be totally independent of variations in the "external inputs" group of elements. The diagram obtained by plotting the two first principal components against each other intriguingly mirrors the one obtained for the Lausen-Schleifenberg "external input" sub-system. We therefore postulate that the preferential enrichment of Cd in these two sections are related to the same mechanism, which as a consequence is independent of specific ages (Bajocian or Oxfordian) and rather independent of specific carbonate facies types (oolitic or lagoonal).

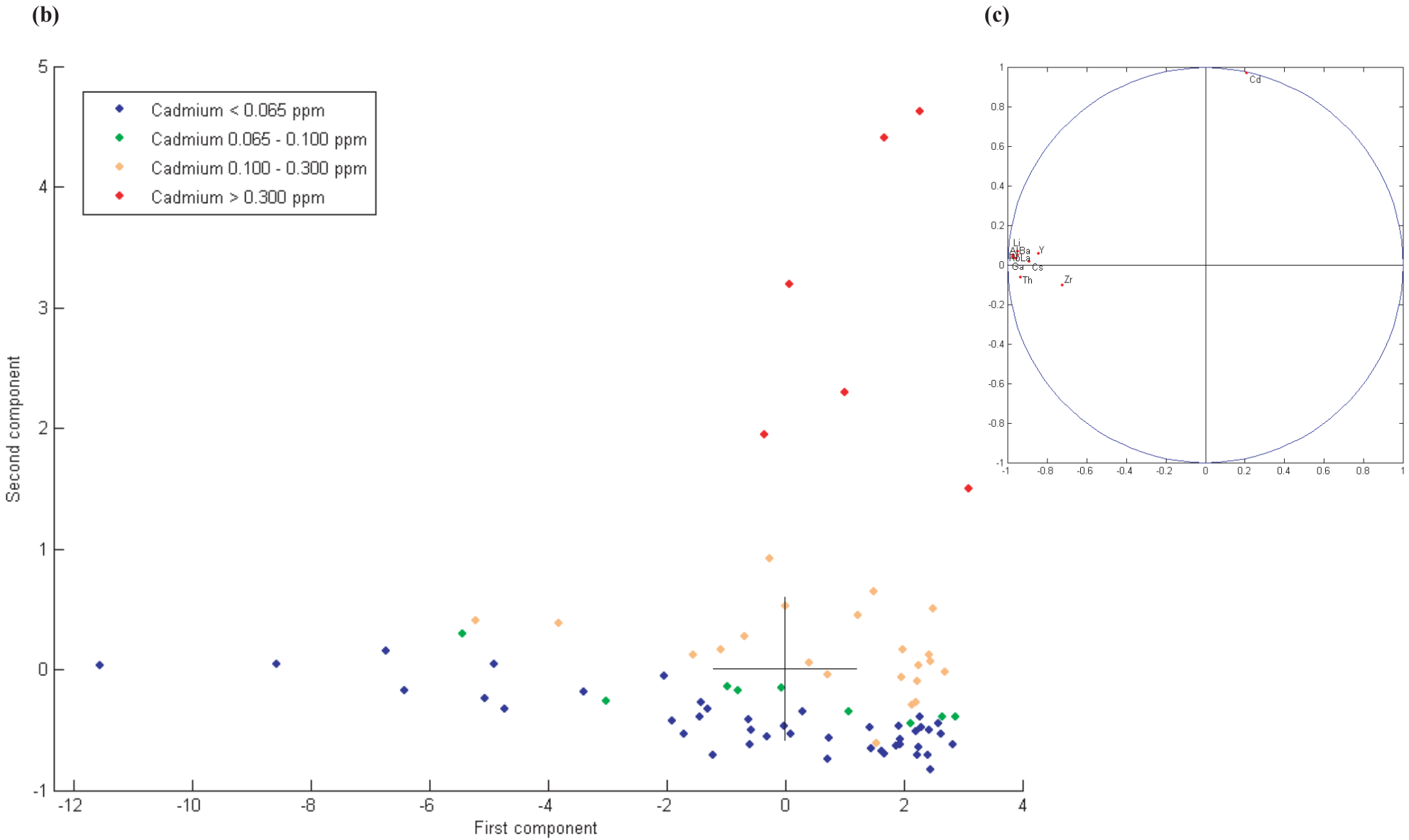

Fig. 14. Gorges du Pichoux “external input” sub-system.
b. First component against second component diagram.
c. Associated correlation circle (x: first PCA axis, y: second PCA axis).

VIII-4-3-5 Gorges du Pichoux "nutrients-preservation" sub-system: results

This sub-system has been realized using the following variables: V, Co, Cu, Mo, Cd, Pb and U. The resulting PCA system holds only 72.25% of total variance on the three first axes, the first one explaining 42.96% of it. V, Co and Cu, and Mo and Pb to a lesser extend, are strongly associated to the first axis (Fig. 15a). Cd is both anti-correlated to the second axis, and correlated to the third axis, whereas U is positively correlated to both axes, but predominantly to the second one.

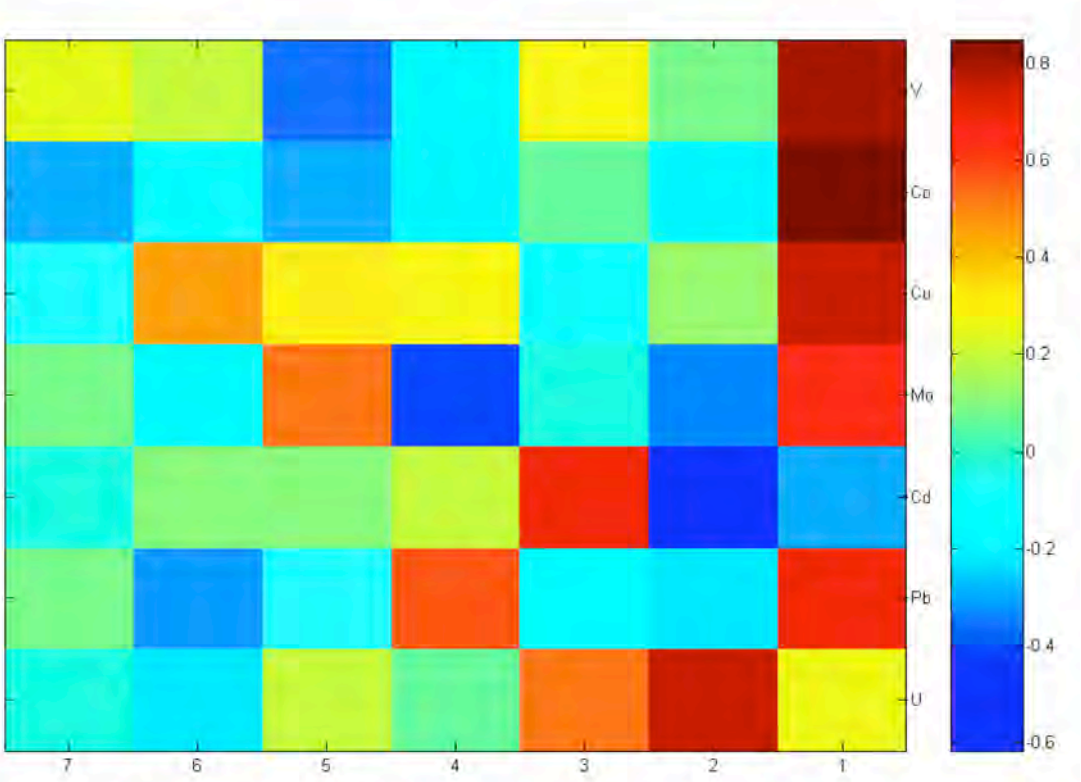

Fig. 15a. rCP matrix, Gorges du Pichoux "nutrients-preservation" sub-system

When plotting the first principal component against the second one (Fig. 15b), and considering the associated correlation circle (Fig. 15c), we observe that the point cluster constituted by the "normal" to "intermediate" samples with regards to their Cd concentrations, is distributed following various influences from both the U and Cu/V/Co/Pb/Mo poles, whereas the highly Cd-enriched samples only present an attraction towards the Cd pole.

The first against third component diagram displays a less clear distribution (Fig. 15d), and well-separated chemical poles can not be distinguished on the correlation circle (Fig. 15e).

The second against third component diagram permits to appreciate the respective influence of Cd and U on the sample distribution: all the "normal" samples as well as some of the "intermediate" ones are almost exclusively partitioned under the influence of U variations, whereas the highly Cd-enriched samples as well as part of those belonging to the intermediate group (mainly from the group above 0.100 µg/g Cd) show only influences of the Cd pole in their distribution.

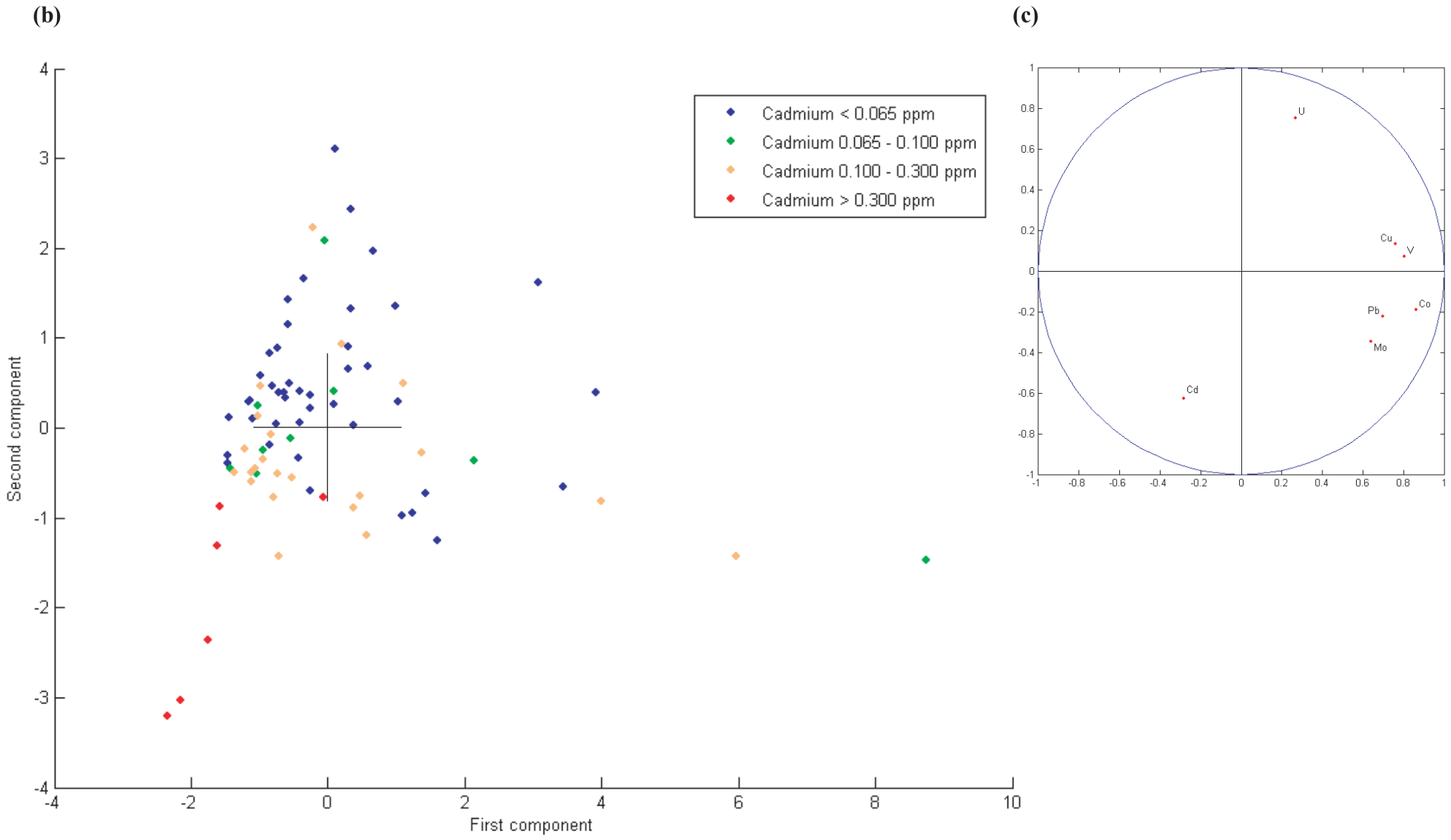

Fig. 15. Gorges du Pichoux “nutrients-preservation” sub-system.
b. First component against second component diagram.
c. Associated correlation circle (x: first PCA axis, y: second PCA axis).

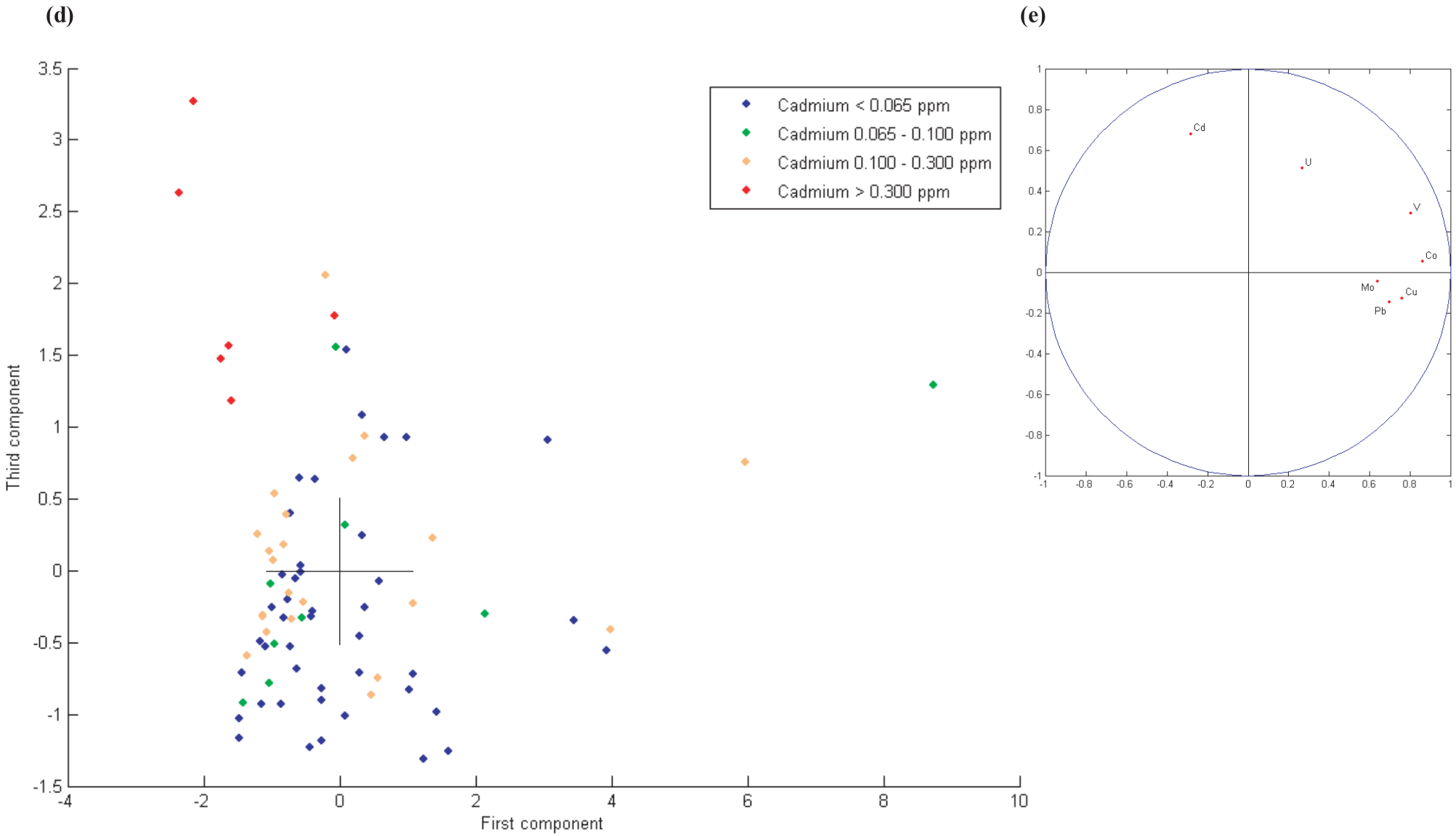

Fig. 15. Gorges du Pichoux “nutrients-preservation” sub-system.
d. First component against third component diagram.
e. Associated correlation circle (x: first PCA axis, y: third PCA axis).

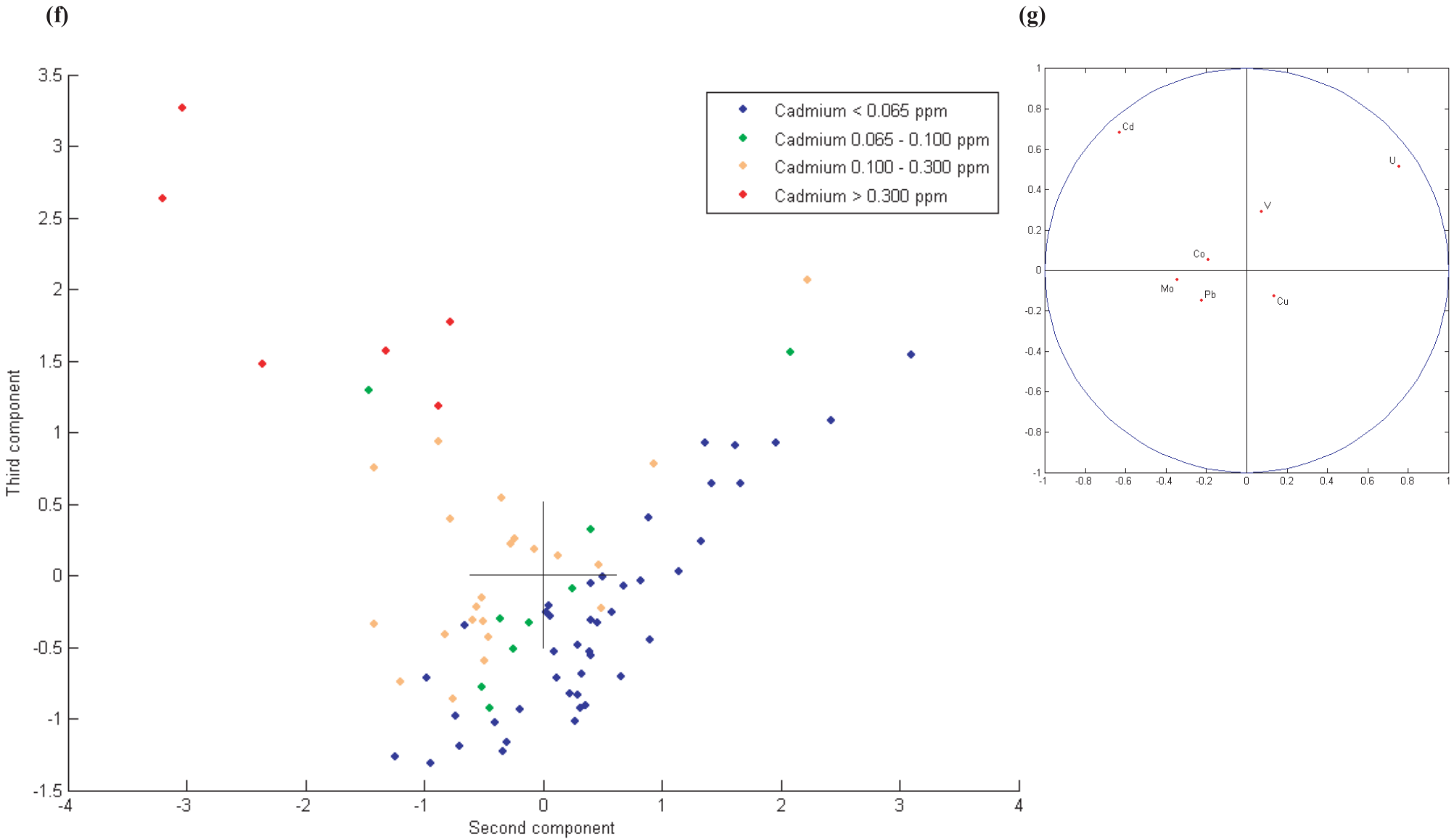

Fig. 15. Gorges du Pichoux “nutrients-preservation” sub-system.
f. Second component against third component diagram.
g. Associated correlation circle (x: second PCA axis, y: third PCA axis).

VIII-4-3-6 Gorges du Pichoux "nutrients" sub-system: results

This sub-system derives from the previous one by selecting V, Co, Cu, Mo and Cd. The first four elements are strongly anti-correlated with the PCA first axis (Fig. 16a), whereas Cd is associated to the second one. These two axes totalize 71.14% of the system variance.

The diagram plotting the first principal component against the second one (Fig. 16b) shows a distribution of the point cluster under two distinct influences: one represented by a chemical pole composed of Mo, Co, V and Cu; the other one represented by Cd (Fig. 16c).

"Normal" to "intermediate" samples with regards to their cadmium contents present a certain influence of the Mo/Co/V/Cu pole, even if the great majority of the samples remains in the vicinity of the cluster centre. On the contrary, the highly Cd-enriched samples show an exclusive attraction towards the Cd pole. This is also valid for a part of the "intermediate" samples (above 0.100 µg/g), which present a slight shift towards the Mo/Co/V/Cu pole.

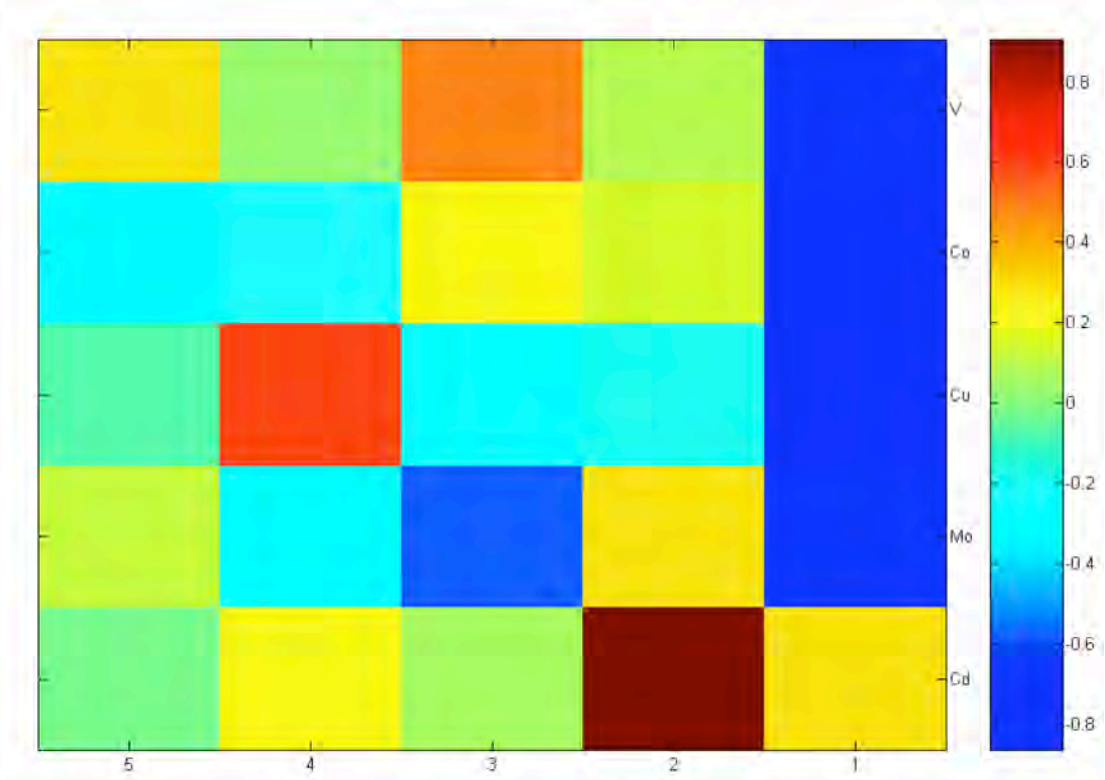

Fig. 16a. rCP matrix, Gorges du Pichoux "nutrients" sub-system

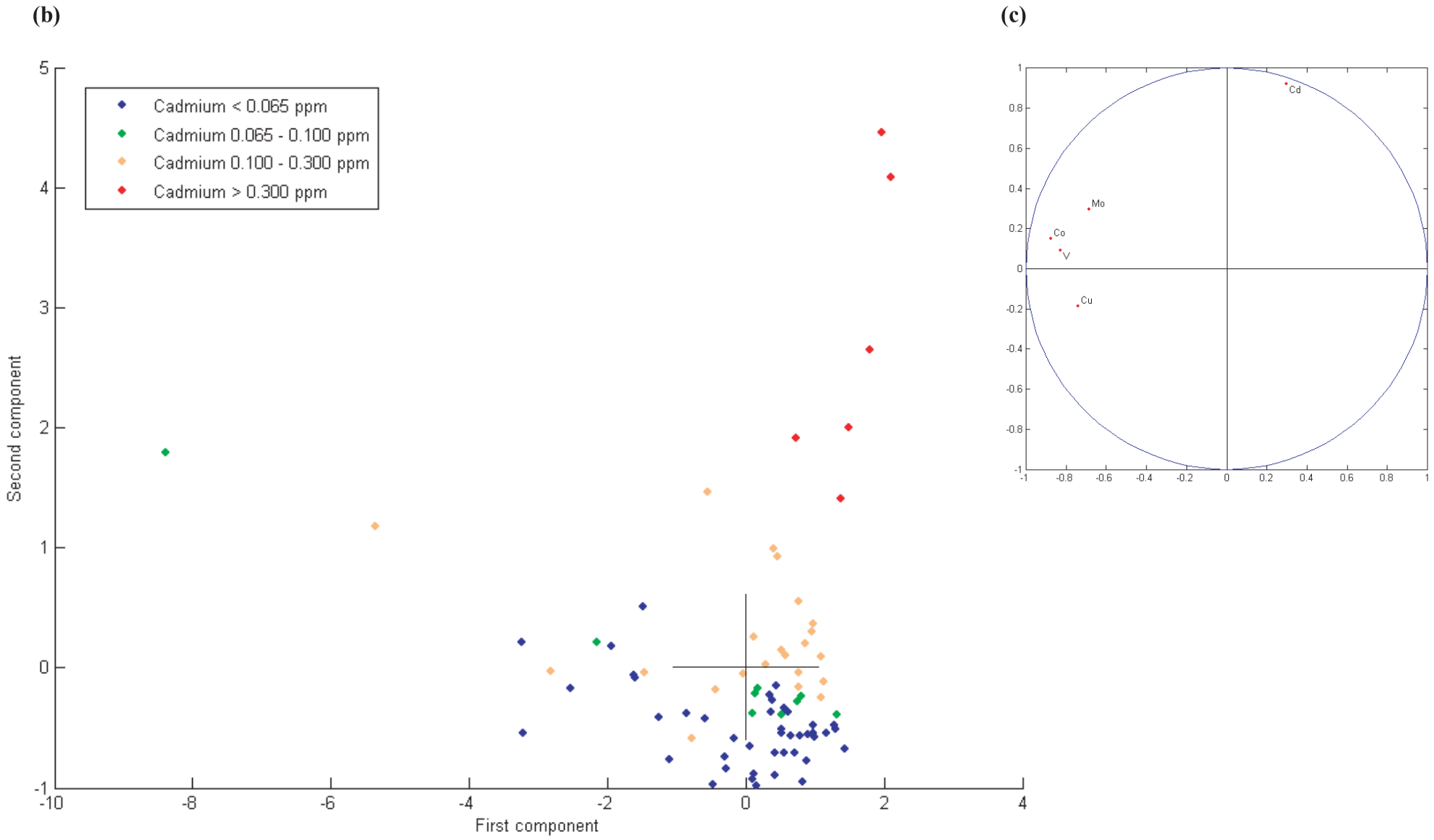

Fig. 16. Gorges du Pichoux “nutrients” sub-system.
b. First component against second component diagram.
c. Associated correlation circle (x: first PCA axis, y: second PCA axis).

VIII-4-3-7 Gorges du Pichoux "nutrients-preservation" and "nutrients" sub-systems: interpretation

As for the Lausen-Schleifenberg section, Cd enrichments in this section seem to be controlled by sources and/or mechanisms that are not directly related to those inducing the other element distributions in these sub-systems. The highest Cd concentrations may be associated to specific concentration processes, whereas in "normal" and part of the "intermediate" samples, Cd may be incorporated as a function of its presence in the parent water, similar to other elements.

VIII-5 Discussion and conclusions

VIII-5-1 General statements

In the three sections investigated, the total variance is dominated by variations in Ga, Rb, Cs, and Th, +/- Li, Al, Ba, Sr, and La. These elements are likely to be linked with external inputs by continental weathering. Related "external inputs" sub-systems were in each case easily to be defined (with most of the total variance held by the first or the two first PCA axes), showing that elements that compose this group are not affected by internal mechanisms such as biological uptake or preferential preservation following their arrival.

Elements that are related to "nutrients-like" behaviour and/or to preferential preservation in the sediment display more complex behaviour. As a consequence, "nutrients" and "nutrients-preservation" sub-systems are not so well-constrained (reduced part of the total variance expressed on the first PCA axes). Specific variations of the elements that are related to these groups may be controlled by different internal as well as external cycles (punctual inputs, influence of life, concentration under special chemical conditions related to variations in oxygenation, in pH, etc.).

In all cases, Cd enrichments have been proved to be rather independent of those of specific elements belonging to the "external", "nutrients-preservation", and "nutrients" groups, even if some of the samples showing anomalous or "intermediate" Cd concentrations can be also enriched in elements related to a "nutrient-like" behaviour or to "external" inputs.
However, the two sections corresponding to shallow-water environments (Lausen-Schleifenberg and Gorges du Pichoux) present rather different patterns with regards to the Cd-enriched samples in comparison with the deeper-water section of Terminilletto. We propose that in the deeper-water environment represented by this section, Cd, as well as other elements are included in carbonates as a function of their availability in the parent water. In the shallow-water sections, an additional mechanism appears to operate, which is responsible for the preferential concentration of Cd. Diagrams obtained for the different sub-systems in both the Lausen-Schleifenberg and Gorges du Pichoux sections are very similar, which indicates that the mechanism was the same for both the Bajocian and Oxfordian periods.

VIII-5-2 Specific mechanism of Cd enrichments in shallow-water sections

The specific enrichment mechanism discussed here concerns only Cd for the Gorges du Pichoux section and Cd and Zn for the Lausen-Schleifenberg section. These elements seem to be prefentially concentrated by certain intrinsic processes. These mechanisms do not appear to be identical with preferential biological (e.g., planktonic) uptake, as none of the other elements displaying a "nutrient-like" behaviour is equally concerned by this enrichment. An enhanced preservation in the sediment linked with dysoxic conditions is also improbable, since no links exist between the Cd/Zn pole, and elements related to preferential preservation in the sediment under oxygen-reduced conditions.

One possibility of Cd enrichment is the preferential uptake via bacterial activity. This was already proposed by several authors to have a great influence on various trace-element concentrations in aquatic environments (e.g., Loaëc et al., 1997; Boyanov et al., 2003 and references therein; Kemner et al., 2005 and references therein).

This mechanism is supposed to be of some influence for at least the Gorge du Pichoux section, since the lagoonal environment related to these carbonate successions is subjected to both intense micritization and oncoid formation.

Adsorption onto organic matter remains a possible way of carrying Cd and Zn into the sediment, especially for the Lausen-Schleifenberg section, for which Cd was already proposed to be preferentially adsorbed on organic matter particles, and transferred to the sediment, where it becomes released and incorporated to carbonates during early diagenesis (Rambeau et al., in prep.b). However, Cd (+/-Zn) enrichments may not be directly dependent on the enhanced availability of organic matter, because in such a case, they should be related to other "nutrient-like" elements, - but rather to enhanced availability of Cd and Zn in the environment.

We may attribute the difference in Cd and Zn chemical behaviour for the Lausen-Schleifenberg and Gorges du Pichoux sections, to distinct types of preferential enrichments: in the Lausen-Schleifenberg system, Cd and Zn may be associated to identical hosting phases (sulfides? Rambeau et al., in prep.b), whereas in the Pichoux system, Cd and Zn may be drawn apart by separated hosting phases due to Cd concentration by bacterial activity, and/or to preferential incorporation in carbonate lattices, related to similar ionic radii in Ca and Cd; Rambeau et al., in prep.b).

VIII-5-3 Possible sources of Cd

Even for the shallow-water sections of Lausen-Schleifenberg and Gorges du Pichoux, it is difficult to involve only a preferential enrichment mechanism as responsible for Cd anomalies in the sediment. These anomalies are indeed restricted to specific levels, which do not show particular changes in facies relative to the overlying or underlying sediments (Fig.1). The most likely explanation for such enrichments remains, therefore, some sort of mix between increased Cd availability in the environment and preferential incorporation into specific phases.

We have shown that in all investigated sections, Cd enrichments are independent of continental weathering inputs, as witnessed by variations in, e.g., Li, Al, Ga, Rb, Cs, and Th. In none of the investigated sections, a chemical pole is observed which is composed by elements preferentially concentrated in hydrothermal fluids (e.g., Mn, Al, Zn, Fe, Y, Sr, and La; Rubin, 1997; Barrat et al., 2000; Corbin et al., 2000; Pichler and Veizer, 2004). An important role for hydrothermal activity in the process of Cd enrichment is therefore ruled out.

However, in the Terminilletto section (for which the Cd behaviour does not seem to be skewed by the presence of an additional concentrative mechanism), Cd has been shown to be included in a chemical pole that also comprises Zn, Pb, La and Cu. Cd, Zn, Pb and Cu forms an association that is usually found in aerian volcanism emissions (e.g., Hinkley et al., 1999); additionally, Cd, Pb and Zn, and to a lesser extend, Cu, are particularly enriched in volcanic gases in comparison to lava extrusions (e.g., Symond et al., 1987; Allard et al., 2000).

We therefore propose that Cd enrichments in Bajocian and Oxfordian limestone are related to both specific sources and, for the shallow-water sections, additional concentration mechanisms. The source of Cd may be related to volcanic inputs, or more specially aerian volcanic gases, which may provide various other elements including Zn, Pb and Cu. Enhanced volcanism during Jurassic times may equally have led to enhanced continental weathering, by the way of climate change (e.g., towards more humid conditions) or via acidic rainfalls, thereby providing the general system with elements which are highly enriched in the continental crust, as well as with "nutrient-like" elements (as already suggested by Bartolini et al., 1996; Bartolini and Cecca, 1999; Cobianchi and Picotti, 2001). These elements may subsequently enter different sub-systems and therefore show different concentration patterns. All these different elements have been incorporated in the carbonate rocks - including some of the Cd-enriched carbonates - following their availability in the environment at the time of carbonate precipitation or diagenesis.

Possible candidates for a source of aerian volcanic gases and associated Cd are (1) the important phase of silicic volcanism related to the break-up of Gondwana which has been identified in Patagonia and in Antarctica for the Jurassic period (Pankhurst et al., 2000); and (2) the volcanic centre situated in the North Sea (Jeans et al., 2000) which was active during the Jurassic and early Cretaceous.

References

Algeo, T.J., 2004. Can marine anoxic events draw down the trace element inventory of seawater? Geology, 32 (12), 1057-1060

Allard, P., Aiuppa, A., Loyer, H., Carrot, F., Gaudry, A., Pinte, G., Michel, A. and Dongarrà, G., 2000. Acid gas and metal emission rates during long-lived basalt degassing at Stromboli volcano. Geophysical Research Letters, 27, 1207-1210

Alloway, B.J., 1995. Cadmium. In: Heavy metals in soils. 2nd edition. Blackie Academic and Professional, 122-147

Barrat, J.A., Boulègue, J., Tiercelin, J.J. and Lesourd, M., 2000. Strontium isotopes and rare-earth element geochemistry of hydrothermal carbonate deposits from Lake Tanganyika, East Africa. Geochimica et Cosmochimica Acta, 64 (2), 287–298

Bartolini, A., Baumgartner, P.O., and Hunziker, J., 1996. Middle and late Jurassic carbon stable-isotope stratigraphy and radiolarite sedimentation of the Umbira-Marche basin (central Italy). Eclogae geologicae Helvetiae, 89, 811-844

Bartolini, A. and Cecca, F., 1999. 20 My hiatus in the Jurassic of Umbria-Marche Apennines (Italy): carbonate crisis due to eutrophication. Comptes Rendus de l'Académie des Sciences de Paris, Earth and Planetary Sciences, 329, 587-595

Boyanov, M.I., Kelly, S.D., Kemner, K.M., Bunker, B.A., Fein, J.B. and Fowle, D.A., 2003. Adsorption of cadmium to Bacillus subtilis bacterial cell walls: A pH-dependent X-ray absortion fine structure spectrometry study. Geochim Cosmochim Acta, 67 (18), 3299-3311

Böning, P., Brumsack, H.-J., Böttcher M.E., Schnetger, B., Kriete, C., Kallmeyer, J. and Borchers, S.L., 2004. Geochemistry of Peruvian near-surface sediments. Geochimica et Cosmochimica Acta, 68 (21), 4429-4451

Boyle, E.A., Sclater, F. and Edmond, J.M., 1976. On the marine geochemistry of cadmium. Nature, 263, 42-44

Charrière, A., 1992. Evolution paléogéographique méso-cénozoïque du Moyen-Atlas (Maroc) en relation avec les domaines atlantique et méditerranéen. Notes et Mémoires du Service géologique du Maroc, Rabat, 366, 189-203

Cobianchi, M. and Picotti, V., 2001. Sedimentary and biological response to sea-level and palaeoceanographic changes of a Lower-Middle Jurassic Tethyan platform margin (Southern Alps, Italy). Paleogeogr., Paleoclimatol., Paleoecol. 169, 219-244

Corbin, J.C., Person, A., Iatzoura, A., Ferré, B., Renard, M., 2000, Manganese in pelagic carbonates: indication of major tectonic events during the geodynamic evolution of a passive continental margin (the Jurassic Europeann margin of the Tethys-Ligurian Sea). Palaeogeography, Palaeoclimatology, Palaeoecology, 156, 123-138

Gibbs, M.T., Bluth, G.J.S., Fawcett, P.J. and Kump, L.R., 1999. Global chemical erosion over the last 250 My: Variations due to changes in paleogeography, paleoclimate and paleogeology. American Journal of Science, 299, 611-651

Gonzalez, J.-L., Chiffoleau, J.-F., Miramand, P., Thouvenin, B. and Guyot, T., 1999. Le cadmium : comportement d'un contaminant métallique en estuaire. IFREMER publications, Programme scientifique Seine-Aval, 10, J.-L. Gonzalez (coord.), Plouzané, France, 31 pp

Gonzales, R., 1993. Die Hauptrogenstein-Formation der Nordwestschweiz (mittleres Bajocien bis unteres Bathonien). Unpublished Ph.D. thesis, University of Basel, 191p.

Gonzales, R., and Wetzel, A., 1996. Stratigraphy and paleogeography of the Hauptrogenstein and Klingnau Formation (middle Bajocian to late Bathonian), northern Switzerland. Eclogae geologicae Helvetiae, 89, 695-720.

Halliday, A.N., D.-C. Lee, Tommasini, S., Davies, G.R., Paslick, C.R., Fitton, J.G. and James D.E., 1995. Incompatible trace elements in OIB and MORB and source enrichment in the sub-oceanic mantle. Earth and Planetary Science Letters, 133, 379-395

Hinkley, T.K., Lamothe, P.J., Wilson, S.A., Finnegan, D.L. and Gerlach, T.M., 1999. Metal emissions from Kilauea, and a suggested revision of the estimated worldwide metal output by quiescent degassing of volcanoes. Earth and Planetary Science Letters, 170, 315-325

Hug, W.A., 2003. Sequenzielle Faziesentwicklung der karbonatplattform des Schweizer Jura im Späten Oxford und frühensten Kimmeridge. Geofocus, 7, 156 pp.

Jeans C.V., Wray D.S., Merriman R.J. and Fisher M.J.. 2000. Volcanogenic clays in Jurassic and Cretaceous strata of England and the North Sea Basin. Clay Minerals 35, 25-55.

Jones, C.E. and Jenkyns, H.C., 2001. Seawater strontium isotopes, oceanic anoxic events, and seafloor hydrothermal activity in the Jurassic and Cretaceous. American Journal of Science, vol. 301, 112-149

Kabata-Pendias, A. and Pendias, H., 1992. Trace elements in soils and plants. 2nd edition. CRC Press, 365 pp.

Kemner, K.M., O'Loughlin, E.J., Kelly, S.D. and Boyanov, M.I., 2005. Synchrotron X-ray Investigations of Mineral-Microbe-Metal Interactions. Elements, 1 (4), 217-221

Loaëc, M., Olier, R. and Guezennec, J., 1997. Uptake of lead, cadmium and zinc by a novel bacterial exopolysaccharide. Water Research, 31 (5), 1171-1179

Morettini, E., Santantonio, M., Bartolini, A., Cecca, F., Baumgartner, P.O., and Hunziker, J.C., 2002. Carbon isotope stratigraphy and carbonate production during the Early-Middle Jurassic: examples from the Umbria-Marche-Sabina Apennines (central Italy). Paleogeogr., Paleoclimatol., Paleoecol. 184, 251-273

Morford, J.L, and Emerson, S., 1999. The geochemistry of redox sensitive trace metals in sediments. Geochimica et Cosmochimica Acta, 63 (11-12), 1735-1750

Morton, A.C. and Hallsworth, C.R., 1999. Processes controlling the composition of heavy mineral assemblages in sandstones. Sedimentary Geology, 124, 3-29.

Niu, Y. and O'Hara, M. J., 2003. Origin of ocean island basalts: A new perspective from petrology, geochemistry, and mineral physics considerations. J. Geophys. Res., 108 (B4), 2209

Pankhurst, R. J., Riley, T. R., Fanning, C. M. and Kelley, S. P., 2000. Episodic Silicic Volcanism in Patagonia and the Antarctic Peninsula: Chronology of Magmatism Associated with the Break-up of Gondwana. Journal of Petrology, 41, 605-625.

Pichler, T. and Veizer, J., 2004. The precipitation of aragonite from shallow-water hydrothermal fluids in a coral reef, Tutum Bay, Ambitle Island, Papua New Guinea. Chemical Geology, 207, 31– 45

Rambeau, C., Föllmi, K.B., Adatte, T., Baize, D., Bartolini, A., Hug, W.A., Matera, V., Sandoval, J., Steinmann, P., and Veuve, P., in prep (a). Anomalous cadmium enrichments in Tethyan Jurassic carbonates: past and present environmental implications. In prep.

Rambeau, C., Föllmi, K.B., Matera. V., and Adatte, T., in prep (b). µ-X-Ray fluorescence determination of cadmium locations and associations with other trace-elements in Jurassic cadmium-enriched limestone - models for the enrichment of cadmium in calcareous rocks. In prep.

Reyment, R.A. and Savazzi, E.,1999. Aspects of Multivariate Statistical Analysis in Geology. Elsevier, Amsterdam, 285 pp.

Rubin, K., 1997. Degassing of metals and metalloids from erupting seamount and mid-ocean ridge volcanoes: observations and predictions. Geochimica et Cosmochimica Acta, 61, 3525-3542.

Snow, L. J.,. Duncan, R. A, and Bralower, T. J., 2005. Trace element abundances in the Rock Canyon Anticline, Pueblo, Colorado, marine sedimentary section and their relationship to Caribbean plateau construction and oxygen anoxic event 2, Paleoceanography, 20, PA3005, doi:10.1029/2004PA001093

Stimac, J., Hickmott, J., Abell, R., Larocque, A.C.L., Broxton, D.E., Gardner, J., Chipera, S., Wolff, J. and Gaueke, E., 1996. Redistribution of Pb and Other Volatile Trace Metals During Eruption, Devitrification, and Vapor-Phase Crystallization of the Bandelier Tuff, New Mexico. Journal of Volcanology and Geothermal Research, 73, 245-266

Symonds, R. B., Rose, W. I., Reed, M. H., Lichte, F. E., and Finnegan, D. L.1987. Volatilization, transport and sublimation of metallic and non-metallic elements in high temperature gases at Merapi Volcano, Indonesia. Geochim. Cosmochim. Acta, 51, 2083-2101

Taylor, S. R., and McLennan, S.M.,1985. The Continental Crust: Its Composition and Evolution, Oxford Univ. Press, New York.

Tuchschmid, M., 1995. Quantifizierung und Regionalisierung von Schwermetallen und Fluorgehalten bodenbildender Gesteine der Schweiz: Umwelt-Materialien 32 (BUWAL, Berne)

Velbel, M.A., 1999. Bond strength and the relative weathering rates of simple orthosilicates. American Journal of Science, 299, 679-696.

Weissert, H., and Mohr, H., 1996. Late Jurassic climate and its impact on carbon cycling. Palaeogeography, Palaeoclimatology, Palaeoecology, 122, 27-43.

Zempolich, W.G., 1993. The drowning succession in Jurassic carbonates of the Venetian Alps, Italy: a record of supercontinental breakup, gradual eustatic rise, and eutrophication of shallow-water environments. Carbonate sequence stratigraphy - recent developments and applications, Loucks, R.G., Sarg, J.F. (Eds.), American Association of Petroleum Geologists Memoires, 57, 63-105

IX - Other geochemical investigations

IX-1 Cadmium (Cd) contents in the section of Casa de Chimeneas and relationships with the section of Carcabuey (South Spain)

The carbonate successions from Casa de Chimeneas (South Spain) represent the lateral equivalent of part of the Carcabuey section (Chapters IV and V), for time periods ranging from the uppermost part of the Early Bajocian to the basis of the Late Bajocian (*humphriesianum* to *niortense* Zones pro part). They are mostly composed of marly limestone and marls, whereas the successions present at Carcabuey are more calcareous (Fig. 1; Chapter IV); additionally, calcareous deposits from the Casa de Chimeneas section are far less condensed than those from Carcabuey.
Carbonate rocks from the Casa de Chimeneas section exhibit higher Cd contents for the lower part of these successions, (*humphriesianum* Zone, basis of the *niortense* Zone), which tend to decrease upwards. This general trend is in accordance with the variations of the Cd curve obtain for the same time period at Carcabuey, which present high values for the *humphriesianum* Zone and a shift towards less elevated contents during the *niortense* Zone.

Cd concentrations remain rather low, but similar to those observed in basin environments, as shown for the Terminilletto section (central Italy, Chapters IV and V) or the Chaudon-Norante carbonate successions (S.E. France; Chapter IV; next paragraph).

It must be noted here that the two Cd peaks observable inside the basin carbonate successions of Carcabuey (*garantiana*/*parkinsoni* Zones; Fig.1) correspond to redeposited sediments (turbidites or tempestites; J. Sandoval, pers. comm.). The carbonates concerned by these high Cd values may therefore have been formed in shallower environments, and may have inherited their Cd contents from there.

Fig. 1. Next page. Cadmium contents in μg/g for the Bajocian hemipelagic sections of Carcabuey and Casa de Chimeneas, South Spain. The grey curves correspond to a five-point moving average.

Fig. 2. Page 163. Cadmium contents in μg/g for the Bajocian hemipelagic section of Chaudon-Norante, S.E France.

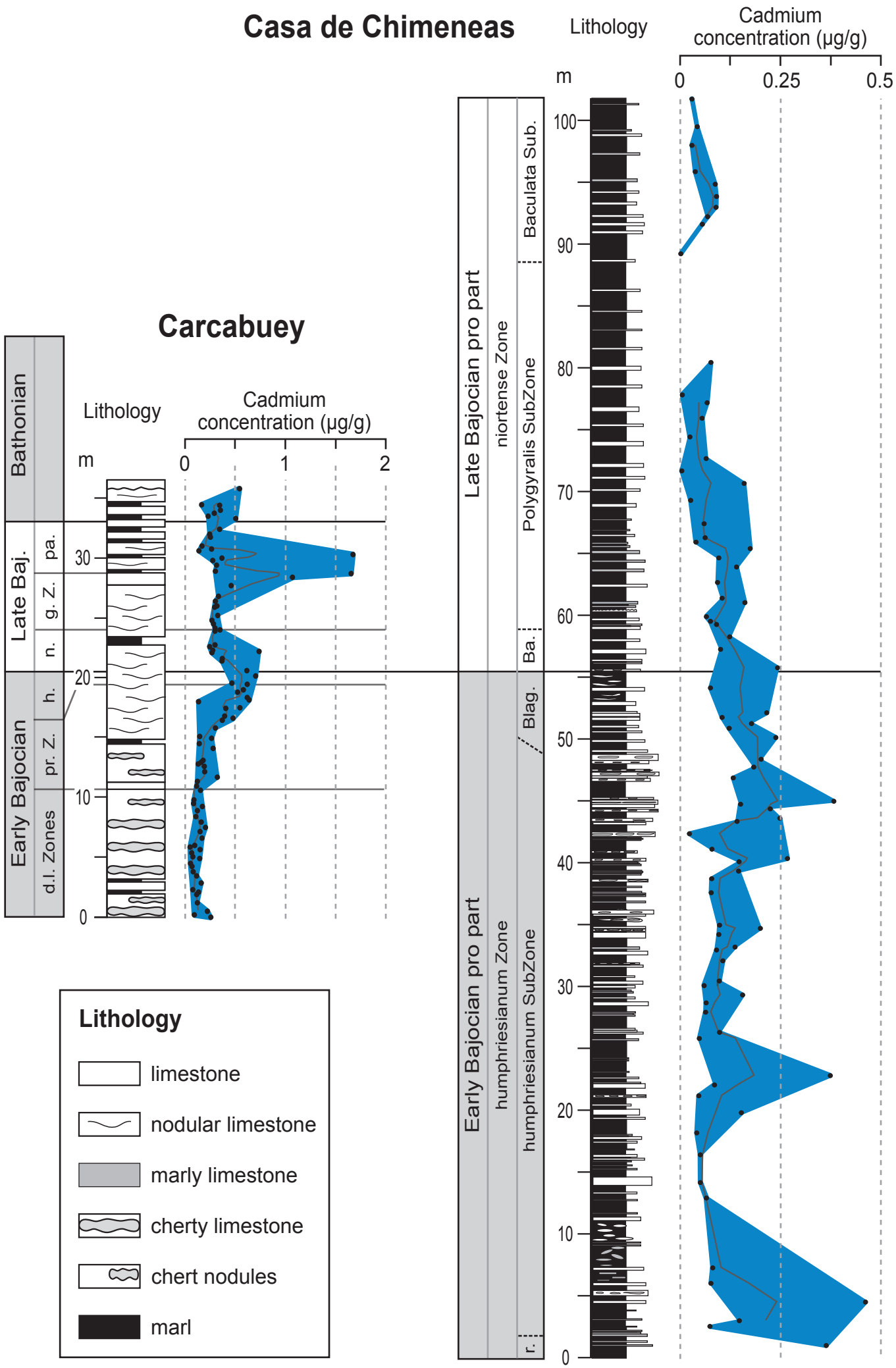
Casa de Chimeneas
Lithology
Cadmium concentration (µg/g)
m
0
0.25
0.5
100
90
80
70
60
50
40
30
20
10
0
Late Bajocian pro part
niortense Zone
Polygyralis SubZone
Baculata Sub.
Ba.
Early Bajocian pro part
humphriesianum Zone
humphriesianum SubZone
Blag.
r.
Carcabuey
Lithology
Cadmium concentration (µg/g)
m
0
1
2
30
20
10
0
Bathonian
Late Baj.
pa.
g. Z.
n.
Early Bajocian
h.
pr. Z.
d.l. Zones
Lithology
limestone
nodular limestone
marly limestone
cherty limestone
chert nodules
marl

Chaudon-Norante

Detailled section

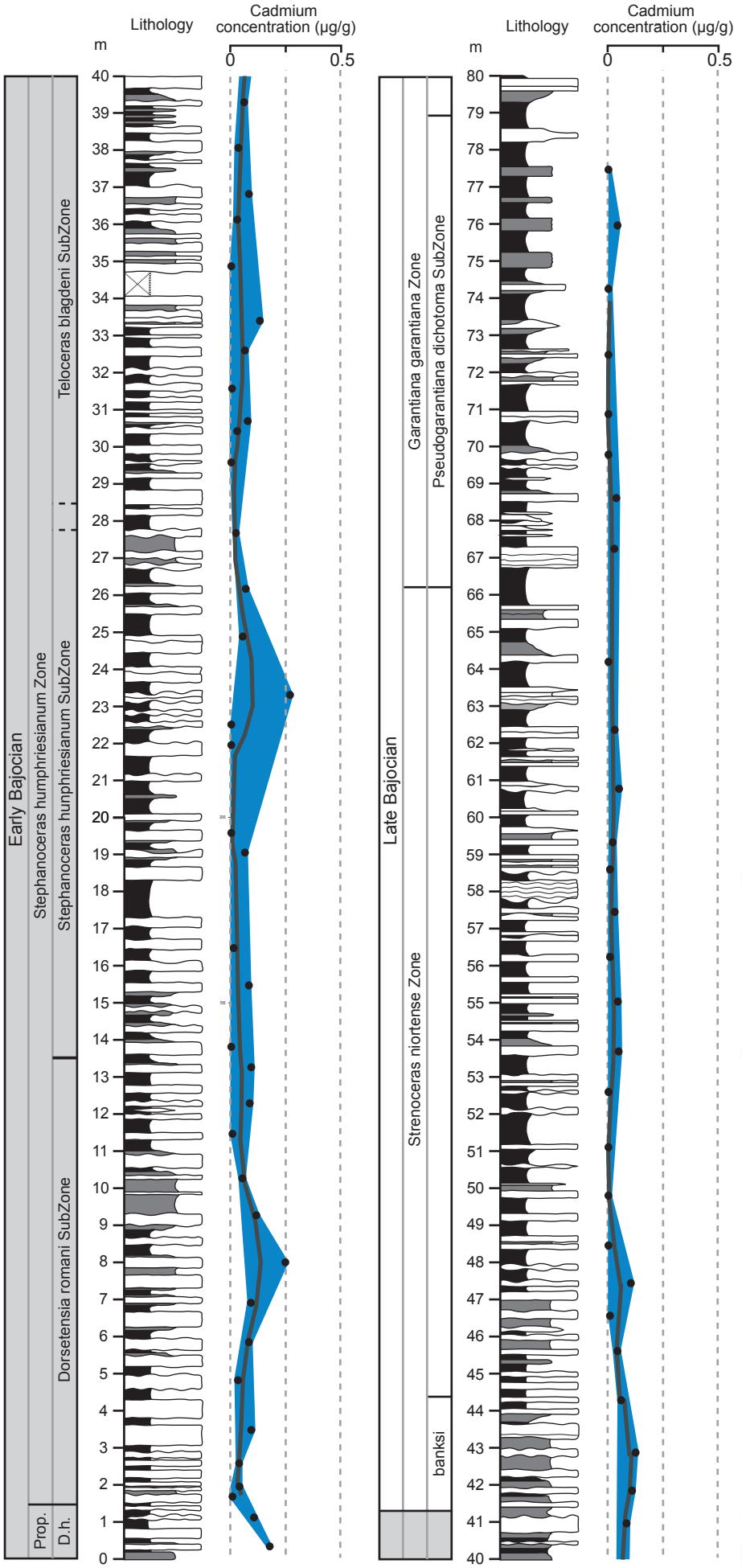

Lithology

limestone

marly limestone

marl

Prop. = Propinquans Zone;
D.h. = Dorsetensia hebridica SubZone;
Ba / banksi = Teloceras banksi SubZone
humph = humphriesianum
Z = Zone
S.Z. = SubZone

Reduced-scale section

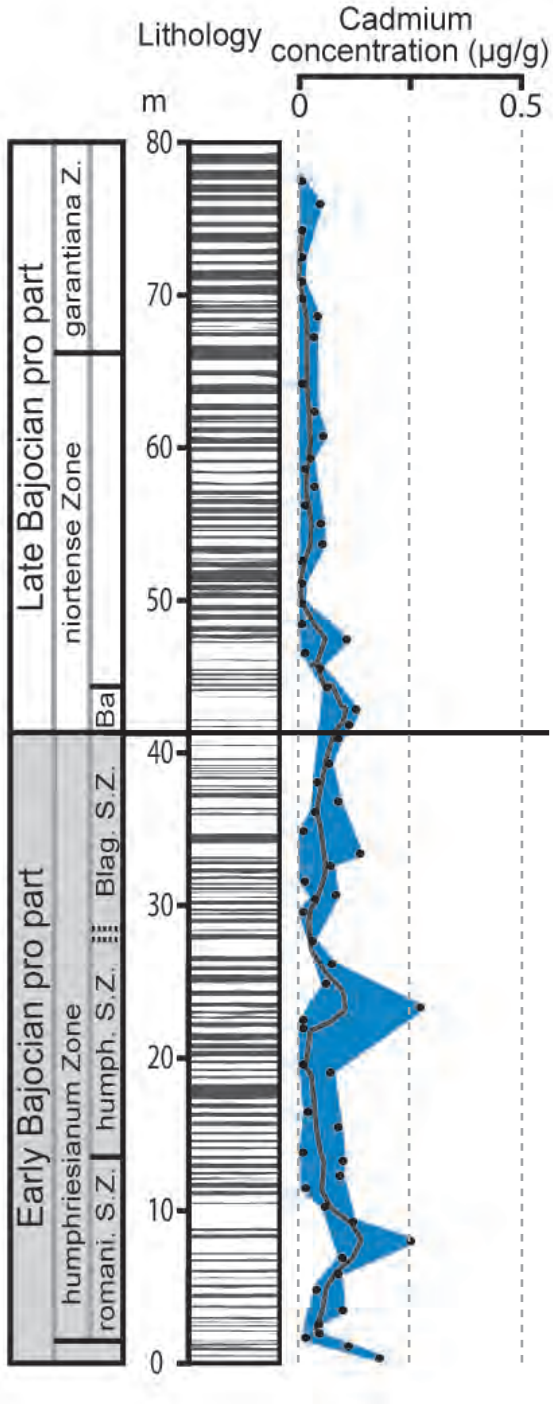

IX-2 Cadmium contents in the section of Chaudon-Norante (S.E Basin, France)

Cd contents have been measured for a selection of samples from the Chaudon-Norante section, dated by ammonites as Early Bajocian, uppermost part of the propinquans Zone, to Late Bajocian, garantiana Zone pro part (D. Bert, pers.comm.). These carbonate successions are composed of alternate layers of limestone, marly limestone and marl, deposited with a high sedimentation rate in an hemipelagic environment (Fig. 2). The black colour of the rocks, as well as the abundance of pyrite, hint at the presence of reducing conditions and/or organic matter (Raiswell and Berner, 1986; Raiswell et al., 1988) inside the sediment.

The measured Cd concentrations are generally low for these carbonate successions, even if slightly higher Cd contents are observed for the lower part of the section (Early Bajocian and basis of the Late Bajocian; Fig.2). For this part, the highest Cd values are comparable to concentrations obtained for the basin successions of Terminilletto (central Italy) dated as Early Bajocian (Chapters V and VIII).
The globally low Cd contents displayed by the Chaudon-Norante section is a further indication that Cd enrichments are rather independent of increasing organic matter contents and/or the presence of reducing conditions in the sediment (see also Chapter IV). They also confirm that carbonate successions related to basin environments generally present decreasing Cd concentrations in comparison with shallow-water environments (Chapter V and VIII).

IX-3 Cadmium anomalies outside the Tethyan realm

We have equally investigated the cadmium contents of Bajocian to Oxfordian carbonates outside the Tethyan realm, in order to better constrain the lateral extension of the cadmium events during these periods. We have analyzed carbonate rocks from Madagascar, that have been provided by Markus Geiger (Bremen university, Germany) and have been previously described by this author (Geiger et al., 2004). These carbonates correspond to ferruginous limestone, principally oolitic, and are probably Bajocian (16 samples) and Oxfordian (6 samples) in age; however, it must be noted that the age dates for these sections are rather poorly constrained. In parallel, 6 samples of Bathonian/Callovian age have been analyzed for comparison.
Results are given in Table 1.

Cadmium contents in Jurassic carbonates from Madagascar are highly heterogeneous. Most of the samples present relatively low cadmium concentrations, at the exception of two samples of probable Bajocian age (Anjeba section), which display Cd concentrations of 2.140 and 0.756 µg/g. Two other samples of Bathonian/Callovian and Oxfordian age, respectively, equally show rather high cadmium contents (above 0.400 µg/g; Table 1.)

These anomalies may be related to those observed in the Tethyan realm (Chapter V to VIII), at least for the Bajocian and Oxfordian stages, which lead to the hypothesis of a global event controlling cadmium enrichments worldwide during the Jurassic. However, considering the few data available with regards to cadmium contents in limestone from Madagascar, as well as the lack of precise time control for these carbonate successions, a generalisation is indeed difficult.

Section	Sample name	Age	Cd contents (µg/g)
Analamanga	ANA 1	Bajocian	0.059
	ANA 11	Bajocian	0
	ANA 18	Bajocian	0.058
	ANA 19	Bajocian	0.162
	ANA 23	Bajocian	0.011
	ANA 24	Bajocian	0.024
	ANA 34	Bajocian	0.006
	ANA 35	Bajocian	0.114
	ANA 36	Bajocian	0.007
	ANA 5	Bajocian	0
	ANA 8	Bajocian	0.089
Anjeba	AND 01	Bajocian	0.178
	AND 09	Bajocian	0
	AND 10	Bajocian	0.106
	AND 12	Bajocian	2.140
	AND 13	Bajocian	0.756
Amparambato	AMPARA 02	Bathonian/Callovian	0.413
Ankazomiheva	ANK 02	Bathonian/Callovian	0.063
	ANK 03	Bathonian/Callovian	0.084
	ANK 06	Bathonian/Callovian	0.097
Atainakanga	ATAIN 09	Bathonian/Callovian	0
Tongobory	TONGO 10	Bathonian/Callovian	0
Dangovato	DANGO 21	Oxfordian	0.436
	DANGO 22	Oxfordian	0.121
	DANGO 39	Oxfordian	0.008
	DANGO 40	Oxfordian	0.086
	DANGO 41	Oxfordian	0.058
	DANGO 58	Oxfordian	0

Table 1. Cd contents for a selection of Jurassic samples from Madagascar.

IX-4 Organic matter analysis in the section of Lausen/Schleifenberg

We have investigated the organic matter contents of several marly or marly-limestone levels from the Schleifenberg section (Chapters IV) by Rock-Eval analyses. Most of the investigated samples show very low organic matter contents (Table 2). Total organic contents nevertheless mark a strong increase in one sample from the basis of the section (SM 8; 1.03 %). These marls directly underlie a Cd-enriched level (S.156, up to 4.9 µg/g Cd; Annex 1). The basis of the Schleifenberg section, and the laterally corresponding Lausen section, may therefore have been characterized during the Early Bajocian by enhanced input of organic matter inside the sediment. This is in accordance with the model propose in Chapter VII, which proposed that in this special environment (oolitic platform slope), Cd was mostly transferred inside the sediment as an adsorbed phase onto organic matter particles, especially pellets.

Table 2 - Organic Matter Contents (Schleifenberg section, Swiss Jura)

Values in italics have too low TOC contents ; the HI, OI, T_{max} data are not realistic

Sample	Depth	TOC (%/weight)	HI (mg HC/g TOC)	OI (mg CO_2/g TOC)	T_{max} (°C)	C_{min} (%/weight)
SM1	8310	*0.09*	*78*	*567*	*441*	7.1
NR1	7980	*0.15*	*73*	*1040*	*390*	5.7
SM2	7015	*0.08*	*25*	*725*	*435*	6.9
SM3	1940	*0.04*	*0*	*1200*	-	6.9
133/134 NJ	1815	*0.09*	*44*	*1122*	*385*	7.4
SM4	1810	0.24	83	392	430	8
133/134 BG3	1810	0.21	105	576	423	7.7
133/134 NP	1805	*0.06*	*17*	*887*	*402*	7.8
SM5	990	*0.08*	*38*	*513*	*443*	6.4
SM6	785	0.26	62	454	443	4.4
SM7	655	0.12	67	442	428	6.4
SM8	505	1.03	106	184	423	0.8
IFP STAN.		3.29	430	24	422	3.2
VP STANDARD		1.87	460	56	421	6.4

IX-5 Phosphorus analyses in the sections of Terminilletto and Carcabuey

The interest of such investigations lies in the observation that a close correlation between cadmium and phosphorus contents in marine waters is known on a global scale, and cadmium contents in sediments have been employed as an approximation of nutrient availability at the time of their formation (Boyle et al., 1976; Bruland et al., 1978; Boyle, 1988; Elderfield and Rickaby, 2000).
A first indication of a possible link between Cd anomalies during Jurassic times is obtained by the phosphorus-accumulation curve compiled for the last 160 my, which gives a relative maximum for the Oxfordian (Föllmi, 1995). However, a detailed phosphorus record is lacking for sediments older than Oxfordian (Föllmi, 1995).
We analyzed a series of samples from the sections of Terminilletto (central Italy) and Carcabuey (southern Spain) for their phosphorus contents. No clear correlation can be established between cadmium and total phosphorus contents for the Terminilletto section, even if slightly higher phosphorus concentrations correspond to the bases of positive cadmium shifts during the late Aalenian and late Callovian/early Oxfordian (Fig. 3). The results for the Carcabuey section are even less encouraging, as correlation appears very weak between cadmium concentrations and phosphorus contents for the set of samples that have been analyzed (Fig. 3).
This may indicates :

- a preferential conservation of Cd inside the sediment in comparison with phosphorus
- or a decoupling between Cd and phosphorus cycles during times of preferential Cd enrichment.

Fig. 3. Next page.
Cadmium and total phosphorus contents in µg/g for the deeper-water sections of Terminilletto, central Italy, and Carcabuey, southern Spain. The grey curves correspond to a five-points moving average.

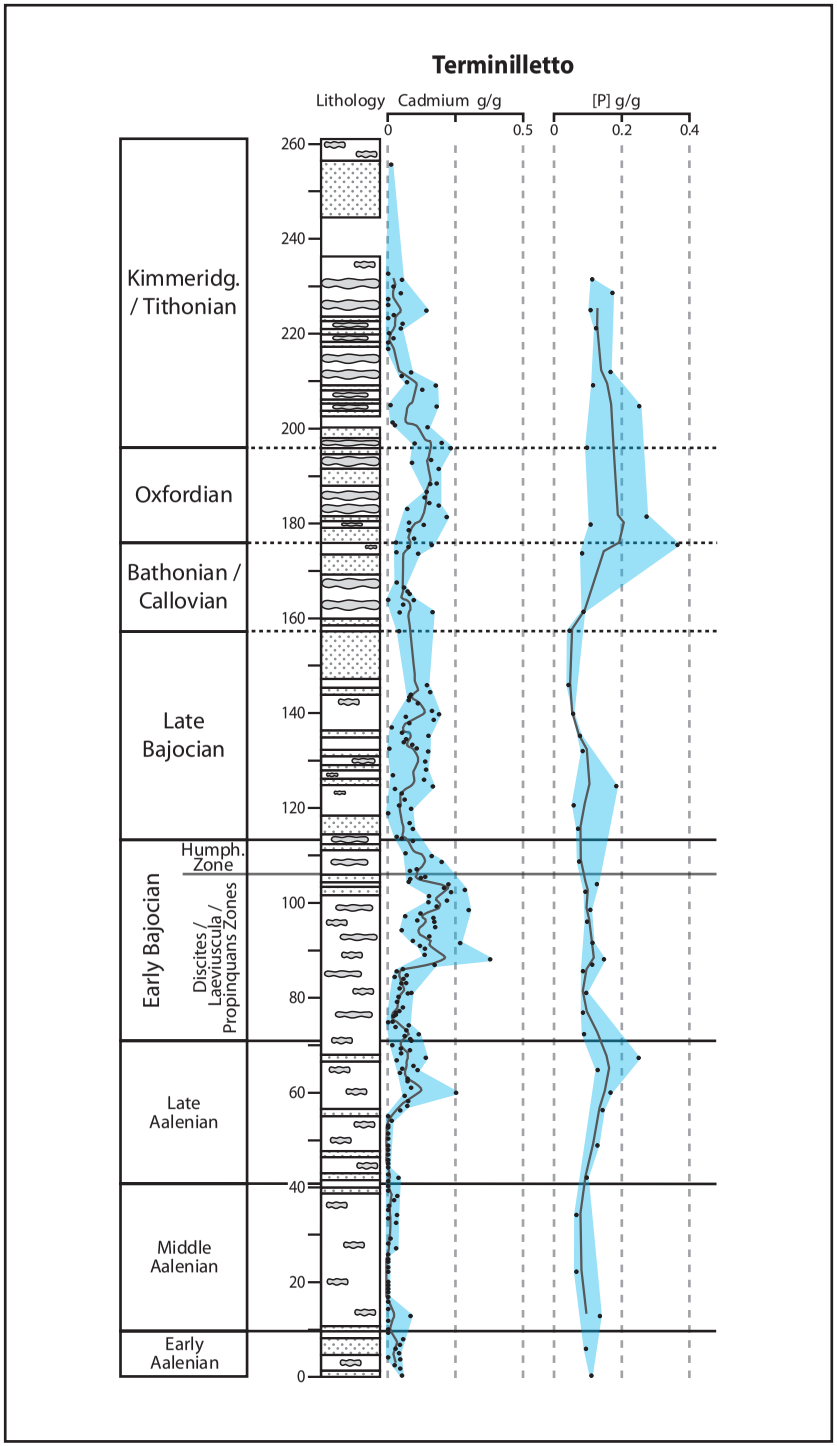
Terminilletto
Lithology
Cadmium g/g
[P] g/g
0
0.5
0.2
0.4
260
240
220
200
180
160
140
120
100
80
60
40
20
0
Kimmeridg. / Tithonian
Oxfordian
Bathonian / Callovian
Late Bajocian
Early Bajocian
Humph. Zone
Discites / Laeviuscula / Propinquans Zones
Late Aalenian
Middle Aalenian
Early Aalenian

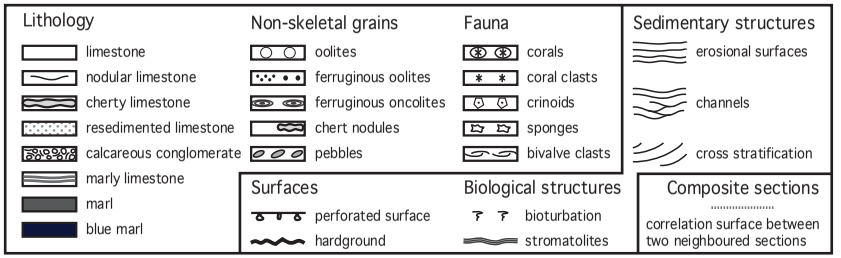
Lithology
limestone
nodular limestone
cherty limestone
resedimented limestone
calcareous conglomerate
marly limestone
marl
blue marl
Non-skeletal grains
oolites
ferruginous oolites
ferruginous oncolites
chert nodules
pebbles
Fauna
corals
coral clasts
crinoids
sponges
bivalve clasts
Sedimentary structures
erosional surfaces
channels
cross stratification
Surfaces
perforated surface
hardground
Biological structures
bioturbation
stromatolites
Composite sections
correlation surface between two neighboured sections

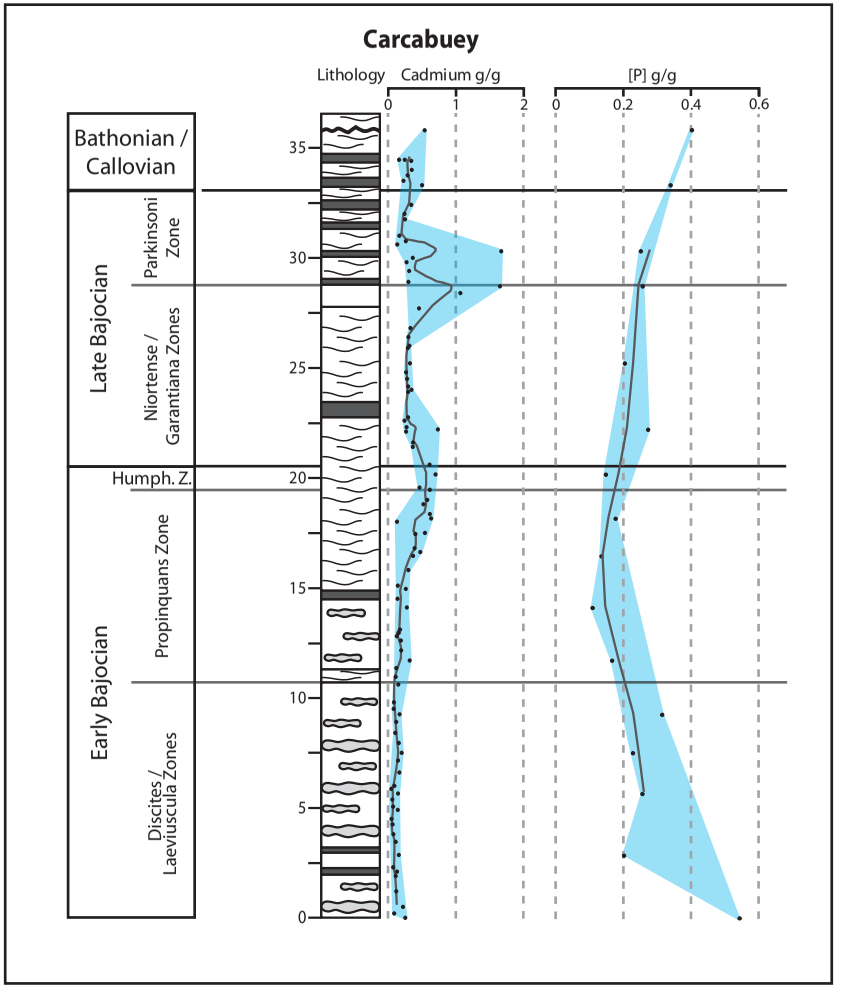
Carcabuey
Lithology
Cadmium g/g
[P] g/g
0
1
2
0.2
0.4
0.6
35
30
25
20
15
10
5
0
Bathonian / Callovian
Late Bajocian
Parkinsoni Zone
Niortense / Garantiana Zones
Humph. Z.
Early Bajocian
Propinquans Zone
Discites / Laeviuscula Zones

References

Elderfield, H., and Rickaby, R.E.M., 2000. Oceanic Cd/P ratio and nutrient utilization in the glacial Southern Ocean. Nature, 405, 305-310

Geiger M., Clark, D.N. and Mette W., 2004. Reappraisal of the timing of the breakup of Gondwana based on sedimentological and seismic evidence from the Morondava Basin, Madagascar. Journal of African Earth Sciences, 38, 363-381

Raiswell, R. and Berner, R.A., 1986. Pyrite and organic matter in Phanerozoic normal marine shales. Geochimica et Cosmochimica Acta, 50, 1967-1976

Raiswell, R., Buckley, F., Berner, R.A. and Anderson, T.F., 1988. Degree of pyritization of iron as a paleoenvironmental indicator of bottom water oxygenation. Journal of Sedimentary Petrology, 58, 812-819

Boyle, E.A., Sclater, F.R. and Edmond, J.M., 1976. On the marine geochemistry of cadmium. Nature, 263, 42-44.

Boyle, E.A., 1988. Cadmium: chemical tracer of deepwater paleoceanography. Paleoceanography, 3, 471-489.

Bruland, K.W., Knauer, G.A., and Martin, J.H., 1978. Cadmium in the northeast Pacific waters. Limnology Oceanography, 23, 618-625.

Föllmi, K.B, 1995. 160 m.y. record of marine sedimentary phosphorus burial: coupling of climate and continental weathering under greenhouse and icehouse conditions. Geology, 23, 859-862.

X - Conclusive points and discussion: Towards a model for Cd enrichments in Jurassic carbonates

We have conducted this research work with the following goals in mind:

- to trace the geographical and stratigraphical distribution of cadmium enrichments in Jurassic carbonates, in western and southern Europe,
- to develop a predictive tool to identify the presence of anomalously enriched soils related to cadmium-enriched carbonate rock substrata in the investigated areas,
- to reconstruct the sedimentary and environmental conditions that have led to these Cd enrichments in Jurassic rocks.

With these research aspects, we have explored both a sedimentological-geochemical-paleoenvironmental side of the problem of cadmium enrichment in carbonates, as well as a side related to the actual environment. The major conclusions related to each point are presented and discussed in the following paragraphs.

X-1 Geographical and stratigraphical extend of Jurassic Cd anomalies

X-1-1 Cd anomalies in the former Tethyan realm (western and southern Europe)

Our results from the analysis of carbonate sections:

- of Bajocian age, in the Swiss Jura mountains (Lausen-Schleifenberg section), in Burgundy (Lucy le Bois section) and Normandy (Ste Honorine des Pertes), France, as well as in southern Spain (Carcabuey and Casa de Chimeneas sections) and central Italy (Terminilletto section),
- as well as of Oxfordian age, in the Swiss Jura mountains (Gorges du Pichoux section), in Burgundy, France (Le Saussois section) and central Italy (Terminilletto section),

suggest that the cadmium enrichments for both periods are a general and pervasive phenomenon in the investigated basins, irrespective of the specificities of the carbonate facies. However, two major features must be distinguished:

- a general increase in cadmium "background" values (i.e., increase in mean concentrations as well as in the lowest concentrations for both periods) is recorded in both open-marine and platform settings; this shift of the Cd curves towards more elevated Cd concentrations is particularly well marked in basin environments (e.g., Terminilletto section for both the Bajocian and Oxfordian periods; Carcabuey and Casa de Chimeneas sections for the Bajocian).

- in addition, major enrichments ("Cd peaks"), with cadmium values frequently above 1 µg/g, are observed in most of the shallow-water sections (Lausen-Schleifenberg, Ste Honorine des Pertes, Lucy le Bois, Davayé-Vergisson for the Bajocian; Gorges du Pichoux section for the Oxfordian). These values largely surpass the mean value for Cd in carbonates of around 0.030 - 0.065 µg/g (Kabata-Pendias and Pendias, 1992; Alloway, 1995; Tuchschmid, 1995). The Carcabuey section, which corresponds to relatively deep-water environments, delivered two samples that are enriched in Cd to levels comparable to shallow-water sections; however, these samples differ from the rest of the sediments recorded in this section and may correspond to tempestites or turbiditic deposits (i.e., lateral transfer of sediment from shallower-water environments towards deeper-water settings). Similar Cd enrichments have been already observed by Veuve (2000), in a series of carbonate successions of Bajocian and Oxfordian age in the Jura mountains.

With regards to Bajocian times, the general increase in Cd concentrations usually begin during the Early Bajocian and continue during most of the Late Bajocian (Lausen-Schleifenberg, Ste Honorine des Pertes, Carcabuey, Casa de Chimeneas, Vergisson-Davayé), with the frequent presence of associated Cd peaks in the sections related to shallow-water environments. For the section of Terminilletto, Cd concentrations show a distinct shift towards more elevated concentrations earlier, in the uppermost part of the Late Aalenian period, and decrease at the end of the Early Bajocian. The crinoidal Lucy le Bois carbonate successions only present increasing Cd contents for the lower part of the section (probably Early Bajocian in age). The hemipelagic Chaudon-Norante section, even if displaying generally low Cd contents, locally exhibits higher Cd contents, equivalent to those obtained for the basin successions of Terminilletto, for the Early Bajocian and the basis of the Late Bajocian.

With regards to the Oxfordian, the Terminilletto section shows an increase in Cd concentrations for the whole time period, whereas the sections of Gorges du Pichoux and Le Saussois - related to lagoonal environments - present a distinct shift in Cd concentrations restricted to the *bimammatum* ammonite Zone.

In most of the sections investigated, in particular the ones related to shallow-water environments, Cd contents are highly heterogeneous, and anomalous peaks are restricted to narrow stratigraphic intervals. This renders these peaks very difficult to be identified, and a large sampling program is needed for every profile, in order to reduce chances to overlook eventual anomalies.
Cd peaks occur in a wide range of sedimentological facies, including oolitic carbonates, spongy and micritic limestone, crinoidal carbonates and lagoonal micrite with oncoids. Additionally, carbonate rocks of comparable facies may show highly variable cadmium concentrations (e.g., in the sections of Lausen-Schleifenberg, Gorges du Pichoux, Ste Honorine des Pertes…).
Nevertheless, the highest cadmium concentrations identified so far occur in oolitic packstones (upper offshore deposits, Lausen-Schleifenberg section), with Cd values of up to 21.35 µg/g.

X-1-2 Cadmium anomalies outside the Tethyan realm

Analyses of shallow-water carbonate (ferruginous, principally oolitic, limestone) samples from the Anjeba, Dangovato, Analamanga, Atainakanga, Tongobory, Ankazomiheva, and Amparambato sections, Madagascar (Geiger et al., 2004) show that increased Cd contents during the Jurassic, and more particularly the Bajocian time period, may extend to areas outside the former Tethyan realm. Indeed, one of the sample analyzed, probably Bajocian in age, shows Cd contents of more than 2 µg/g. One Oxfordian carbonate sample, as well as one sample from the Bathonian-Callovian set, equally display rather high Cd concentrations (more than 0.4 µg/g). However, due to the small number of samples analyzed, as well as to the weak time control in these sections, it is highly difficult to speculate about the Cd evolution for the Jurassic time period as preserved in the carbonate successions from Madagascar, and subsequently about the geographical extent of Jurassic Cd anomalies.

X-2 Relationships between Cd enrichments in Jurassic rocks and anomalous Cd contents in the associated soils

Soils developed from Bajocian and Oxfordian carbonates have shown a strong tendency to be enriched in cadmium to unusually high levels, especially in the French and Swiss Jura area (Atteia et al., 1994, 1995; Genolet and Dubois, 1996; Baize and De Pury, 1997; Okopnik, 1997; Benitez-Vasquez, 1999; Prudente, 1999; Baize and Sterckeman, 2001; Dubois et al., 2002; Prudente et al., 2002). Studies conducted in this geographical area have pointed out a relationship between anomalously high cadmium contents in soils and the weathering of associated bedrocks (e.g, Benitez-Vasquez, 1999; Prudente, 1999; Baize and Sterckeman, 2001; Dubois et al., 2002; Prudente et al., 2002).

The results of our investigations with regards to Bajocian and Oxfordian carbonates in the Lower Burgundy area confirm that for a large part of the soils enriched in cadmium, a chemical heritage from the weathering of the associated bedrock is the most likely source of cadmium. Bajocian and Oxfordian limestone in Lower Burgundy present a wide range of cadmium contents, which correspond to the spatial variability of cadmium contents observed in the associated soils. Furthermore, investigated carbonate sections in this geographical area exhibit intervals with increasing cadmium concentrations, which stratigraphically correspond to the parent rocks of soils displaying anomalously high cadmium contents.

Mean enrichment factors calculated for Cd in the soil relative to the associated carbonate substratum vary from 4.6 to 5.7. However, these calculations may be skewed by the wide variability of cadmium contents in the limestone as well as by the phenomena of Cd remobilization and transfer inside soil horizons that may occur after bedrock dissolution. The mean enrichment factors calculated for soils from a restricted area and fragments of bedrock sampled in the immediate vicinity of soil enrichments give values around 5.5 - 5.7. This indicates that anomalous Cd enrichments in soils may occur even if the parent rocks display rather low Cd contents (e.g., a Cd content of 0.2 µg/g may induce the development of soils which exhibit Cd concentrations up to more than 1 µg/g).

The widespread presence of Cd-enriched carbonates in investigated sections of Middle and Late Jurassic age suggests that these enrichments may occur on a larger geographical scale within western and southern Europe. This would also imply that corresponding soils have the potential to be naturally enriched in Cd, in particular for soils related to the weathering of shallow-water carbonates.

X-3 Towards the causes and mechanisms of Jurassic Cd enrichments

X-3-1 Cd location in carbonates from shallow-water sections and proposed mechanisms of enrichments

Major Cd enrichments have been shown to be related to shallow-water environments. A μXRF study has been realized for a selection of Cd enriched samples, with the following results:

- In samples related to platform margin environments, Cd concentrations not only occur in calcareous grains like ooids but also in small spots both in a micritic matrix, or within part of ooids cortices. These enrichments are either related to to Zn +/- Mo enrichments, or independent of the concentrations of other elements. Oncoids (lagoonal environments) have been shown to contain moderate but rather homogeneous Cd concentrations.
- A systematic coincidence in the locations of Cd and Zn has not been observed for the analyzed samples, even if some of the Cd enrichments equally present high Zn contents. We therefore postulate that these elements have only partially similar concentration mechanisms. Zn may be preferentially trapped inside sulphide lattices (under reducing conditions), sometimes in association with Fe. Cd may be preferentially transferred to carbonates phases as well as partially incorporated into the sulphide phases.
- In several of the investigated thin sections, the presence of Ti, Zr, Nb, Pb, and/or Rb has been observed. These elements have been proposed to be related either to detrital inputs or to aerial volcanic inputs.

A model has been established for Cd enrichment in platform settings, in association with enhanced bioproductivity and related organic matter production, high sedimentation rates on the platform slope, and the establishment of reducing conditions in the uppermost part of deposits associated with organic matter degradation and subsequent Cd transfer partly into sulphide phases and partly into surrounding carbonate grains. This is in accordance with the increasing organic matter contents measured in a marly intercalation directly underlying one Cd-enriched carbonate level at the basis of the Schleifenberg section. Calcareous ooids may also be directly enriched in Cd by the sequestration of this element within the layers of organic matter these grains may comprise.
Cd enrichments in lagoonal environments are proposed to be related to microbial activity, via micritisation and/or by direct bioconcentration in carbonate phases.

All these processes of incorporation seem to directly depend on the specific environmental conditions during the deposition of sediments, as well as on the quantity of Cd available in seawater at the time of carbonate formation. Indeed, only a reduced part of the samples of similar facies display anomalous cadmium contents, which indicates that environmental conditions, alone, are not sufficient to induce high concentrations in Cd within a sedimentary deposit.

In addition, results of multivariate statistical analyses show that, for the shallow-water sections of Lausen-Schleifenberg and Gorges du Pichoux (Bajocian and Oxfordian in age, respectively), a specific enrichment mechanism seems to operate, which is independent of preferential biological (e.g., planktonic) uptake as well as of enhanced preservation in the sediment linked with dysoxic conditions. This is a further indication that the main phenomenon involved in the formation of highly Cd-enriched levels is the enhanced presence of this element in the environment. The presence of organic matter in the environment may therefore be regarded more as a vector that permits the transfer and concentration of Cd inside the sediment, rather than a primary factor that controls Cd enrichments.

The weak relationship between Cd concentrations and total phosphorus contents, investigated for the Carcabuey and Terminilletto sections, equally hint at a disconnection of Cd enrichment mechanisms from those controlling the general nutrient cycle.

The fact that Cd high concentrations are not directly related to reducing conditions inside the sediment is also demonstrated by the results from the Chaudon-Norante section (Bajocian; SE France). This section is composed of black marls and marly limestone, which were deposited in an oxygen-depleted environment, and display generally low Cd contents.

X-3-2 The origin of cadmium and a general cadmium cycle

We suggest that in shallow-water sections Cd concentrates mostly via biological activity and the production and sedimentation of organic matter. As we have seen, the shallow-water sections deliver samples which are generally more enriched in Cd than their deeper-water counterparts. However, these latter samples display slight but remarkable increases in Cd contents during several periods of the Jurassic time (late Early Bajocian - Late Bajocian for the Carcabuey section, late Early Bajocian - early Late Bajocian for the Casa de Chimeneas and Chaudon-Norante sections, and Late Aalenian - Early/Late Bajocian boundary, as well as Oxfordian - Early Kimmeridgian, for the Terminilletto section), which mirror periods of preferential enrichment in shallow-water sections.

A purely concentrative mechanism, is, therefore, not sufficient to explain that these stratigraphically bound increases in Cd contents are observed in al investigated sections, both attributed to shallow-water as well as to deeper-water environments.

On the other hand, results from multivariate statistical analyses have shown that Cd behavior in the three investigated sections (Terminilletto, Lausen-Schleifenberg, Gorges du Pichoux) is rather independent of those of other chemical associations.

In particular, no link has been discovered between Cd and:

- chemical elements which follow a “nutrient-like” behavior in oceanic water
- elements that may be related to preferential concentration and preservation under reducing conditions inside the sediment
- elements that may mirror increasing detrital input.

In the Terminilletto section, for which the Cd behavior does not seem to be skewed by the presence of an additional concentrative mechanism, Cd has been shown to be included in a chemical pole that also comprises Zn, Pb, La and Cu. Cd, Zn, Pb and Cu are usually associated in aerian volcanism emissions (e.g., Hinkley et al., 1999); furthermore, Cd, Pb and Zn, and to a lesser extend, Cu, present enrichment patterns in volcanic gases in comparison to lava extrusions (e.g., Symond et al., 1987; Allard et al., 2000).

It is for these reasons that we propose that Cd, which is highly concentrated in shallow-water sections and more homogeneously distributed in deeper-water settings of middle and early late Jurassic age, has an external origin, and was most likely induced into the Jurassic environment by the way of volcanism.

Possible candidates are:

(1) the important episode of silicic volcanism related to the break-up of Gondwana identified in Patagonia and in Antarctica. This episode is of middle and late Jurassic age, and two major events have been dated at 172-162 Ma and 157-153 Ma (Pankhurst et al., 2000; Fig.1), which correspond to latest Aalenian to Callovian and late Oxfordian to Kimmeridgian, respectively (Gradstein et al., 2004). This volcanic activity may have reached sufficient intensity, with strong and violent explosive events, to transfer the Cd into the stratosphere and induce its redistribution worldwide

(2) the volcanic centre situated in the North Sea (Jeans et al., 2000) which was active during the Jurassic and early Cretaceous. Deposits associated with this volcanic activity have been shown to be enriched in Zn, Zr, and Nb, which are elements that are frequently present in Cd-enriched carbonates of Bajocian age (µXRF investigations).

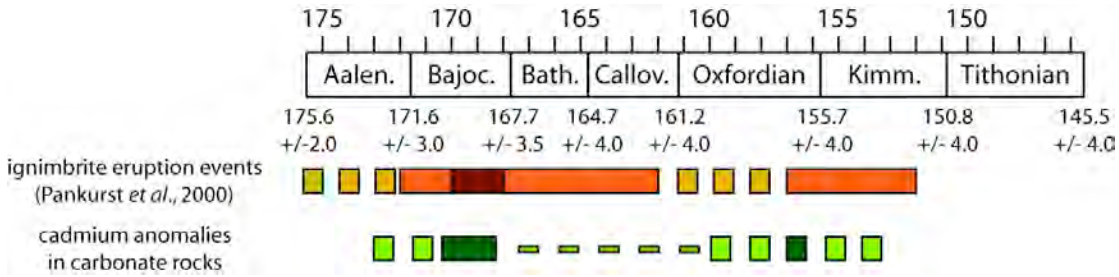

Fig. 1. Comparison of timings between Cd enrichments in Jurassic carbonates (this study) and occurrences of volcanic events in Patagonia and Antarctica (Pankurst et al., 2000). Numerical ages of the considered geological stages from Gradstein et al., 2004.

The North Sea volcanic event may have been responsible for the high cadmium enrichments observed in carbonates of southern and western Europe. But similar Cd anomalies detected in coeval carbonates from Madagascar are more difficult to explain. There the cadmium enrichment may have been related to one of the following scenarios:

- Cd is provided by the volcanic activity of the North Sea center and distributed via ash deposits in European seawaters; Cd chemical associations within seawater led to its redistribution to more remote areas, like the Madagascar coasts
- Cd input in European and Madagascar sections is due to a worldwide volcanic event (probably related to the Patagonia/Antarctica province), by the transfer of Cd gases in higher atmospheric strata and its subsequent return to the marine environment by atmospheric precipitation
- Cd anomalies in Madagascar are related to another event and/or environmental conditions leading to specific concentration in Cd.

X-4 General conclusions

Cd in calcareous rocks of the Jurassic period has been shown to concentrate in shallow-water environments depending on (1) amounts of Cd available in seawater and (2) biological activity, which may be regarded as a major vector of Cd transfer inside the carbonate rocks. Meanwhile, deeper-water sections exhibit remarkable increases in Cd contents during Bajocian and Oxfordian times, which mirror periods of preferential enrichments in shallow-water sections.

As these general increases in Cd concentrations occur on an interbasinal scale, they are likely linked to other, coeval events, such as tectonic, volcanic or climatic events. In cental Europe, the Bajocian and Oxfordian stages are usually characterized by the widespread deposition of iron- and chert-rich sediments and by the abundance of condensed horizons and omission surfaces (e.g., Burkhalter, 1995, 1996, Bartolini et al., 1996). Major sea-level rises are postulated for both stages and positive excursions in stable carbon isotopes have been identified (Bartolini et al., 1996; Weissert and Mohr, 1996), as well as faunal turnovers. Both the Bajocian and Oxfordian are periods of increasing phosphorus burial (Föllmi, 1995 and Cook and McElhinny, 1979). Carbonate platforms in the western Tethys experienced low growth rates during the period between the Late Bajocian and the Oxfordian, which was related to unfavourable conditions with regards to carbonate productivity (e.g., Bartolini et al., 1996; Weissert and Mohr, 1996; Cobianchi and Picotti, 2001 and references therein).

We propose that increases in the Cd curve during Late Aalenian to Late Bajocian and Oxfordian to Early Kimmeridgian periods are associated to general environmental changes in the Tethyan realm. These changes may be related to changes in the intensity of volcanic processes (Bartolini et al., 1996; this study), which may have led to an increase in the availability of Cd in the environment, and separately to higher biological productivity rates (e.g., Bartolini et al., 1996; Bartolini and Cecca, 1999). Enhanced volcanic activity may as well have induced increasing weathering rates, by the way of climate change (e.g., towards more humid conditions) or via acidic rainfalls.

This may in turn have led to the settling of unfavourable periods for biogenic carbonate production and to perturbations in the carbon, phosphorus and silica cycles, as expressed in the $\delta^{13}C$ record, in the estimated abundance of economic phosphate deposits and - for the Oxfordian - in the marine P burial record, as well as by the abundance of chert levels in Bajocian and Oxfordian carbonate successions.
Volcanic processes may explain both the unusual Cd contents of these carbonates and the presence of other trace-metals, like Zn, Pb, Cu or Nb, in some of the investigated samples.

In shallow-water environments, both general changes in the Cd cycle and local conditions of preferential Cd incorporation in the sediment may have coexisted during the Bajocian and Oxfordian periods, leading to high Cd contents in the calcareous rocks that now crop out in western Europe. This has important implications with regards to the present environment, as Cd-enriched shallow-water limestone have been shown to represent a non-negligible source of Cd for associated soils.

A schematic overview of possible consequences of enhanced volcanic activity during Jurassic times, including the development of Cd anomalies in carbonate rocks as well as in associated soils, is given in Fig. 2.

Fig. 2. Next page. A schematic overview of the mechanisms potentially leading to Cd enrichment in Jurassic carbonates (and soils by consequence).

Fig. 2

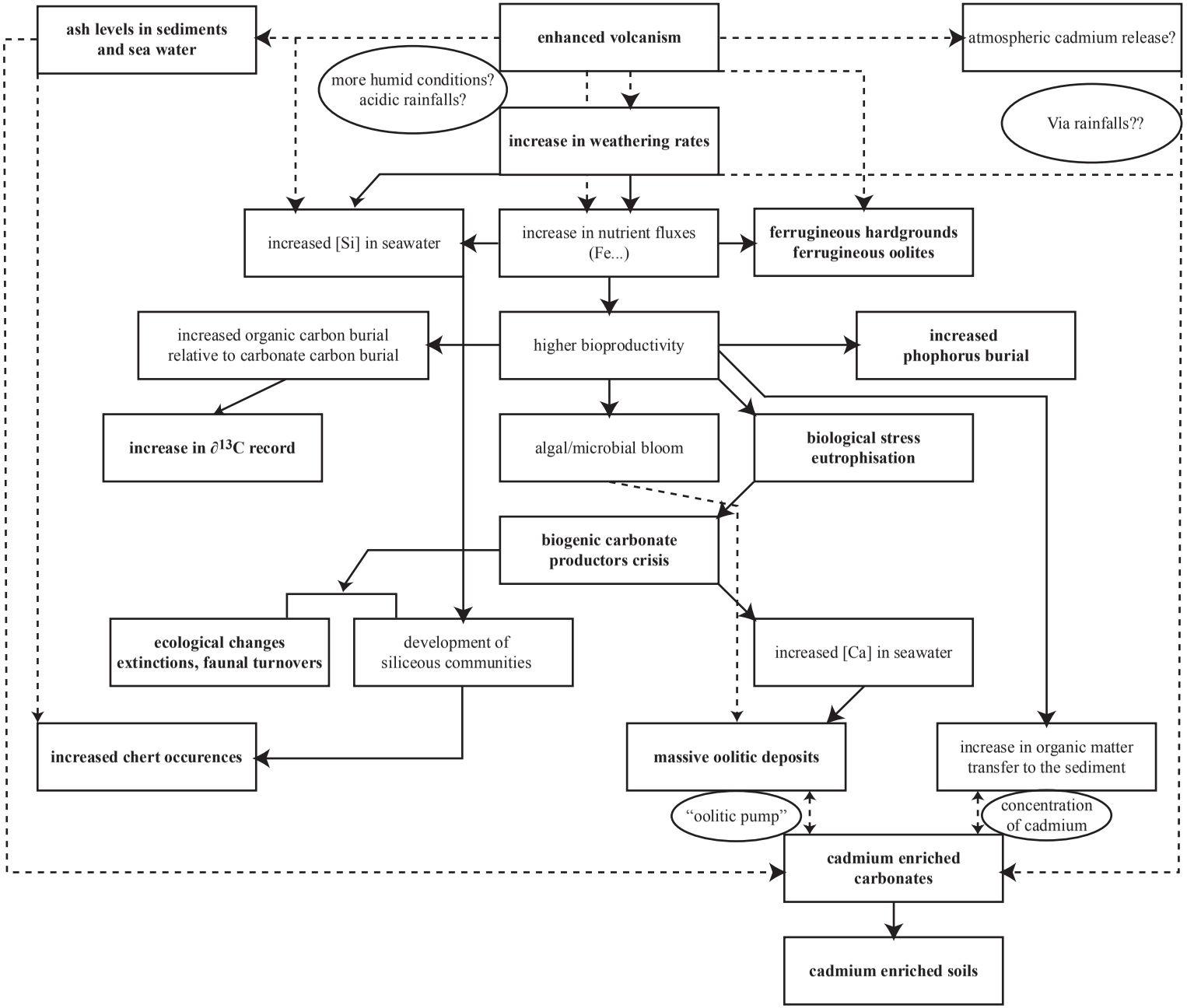
ash levels in sediments and sea water
enhanced volcanism
atmospheric cadmium release?
more humid conditions? acidic rainfalls?
Via rainfalls??
increase in weathering rates
increased [Si] in seawater
increase in nutrient fluxes (Fe...)
ferrugineous hardgrounds ferrugineous oolites
increased organic carbon burial relative to carbonate carbon burial
higher bioproductivity
increased phophorus burial
increase in ∂13C record
algal/microbial bloom
biological stress eutrophisation
biogenic carbonate productors crisis
ecological changes extinctions, faunal turnovers
development of siliceous communities
increased [Ca] in seawater
increased chert occurences
massive oolitic deposits
increase in organic matter transfer to the sediment
"oolitic pump"
concentration of cadmium
cadmium enriched carbonates
cadmium enriched soils

References

Allard, P., Aiuppa, A., Loyer, H., Carrot, F., Gaudry, A., Pinte, G., Michel, A. and Dongarrà, G., 2000. Acid gas and metal emission rates during long-lived basalt degassing at Stromboli volcano. Geophysical Research Letters, 27, 1207-1210

Alloway, B.J., 1995. Cadmium. In: Heavy metals in soils. 2nd edition. Blackie Academic and Professional, 122-147

Atteia, O., Dubois, J.P., and Webster, R., 1994. Geostatistical analysis of soil contamination in the Swiss Jura. Environmental Pollution, 86, 315-327

Atteia, O., Thélin, P., Pfeifer, H.-R., Dubois, J.-P., and Hunziker, J., 1995. A search for the origin of cadmium in the soil of the Swiss Jura. Geoderma, 68, 149-172

Baize, D. and De Pury, P, 1997. Etude de quelques fosses pédologiques sur la commune de Boncourt (Jura). Ecole Polytechnique Fédérale de Lausanne. Rapport interne. Unpublished

Baize, D. and Sterckeman, T., 2001. Of the necessity of knowledge of the natural pedo-geochemical background content in the evaluation of the contamination of soils by trace elements. The Science of the Total Environment, 264, 127-139

Bartolini, A., Baumgartner, P. and Hunziker, J., 1996. Middle and late Jurassic carbon stable-isotope stratigraphy and radiolarite sedimentation of the Umbria-Marche basin (central Italy). Eclogae geologicae Helvetiae, 89, 811-844

Bartolini, A. and Cecca, F., 1999. 20 My hiatus in the Jurassic of Umbria-Marche Apennines (Italy): carbonate crisis due to eutrophication. Comptes Rendus de l'Académie des Sciences de Paris, Earth and Planetary Sciences, 329, 587-595

Benitez-Vasquez, N., 1999. Cadmium speciation and phyto-availability in soils of the Swiss Jura: hypothesis about its dynamics. Unpublished Ph.D. Thesis, EPF, Lausanne, 132 p.

Burkhalter, R.M., 1995. Ooidal ironstones and ferruginous microbialites: origin and relation to sequence stratigraphy. Sedimentology, 42, 57-74

Burkhalter, R.M., 1996. Die Passwang-Alloformation (unteres Aalénien bis unteres Bajocien) im zentralen und nördlichen Schweizer Jura. Eclogae geologicae Helvetiae, 89, 875-934

Cobianchi, M. and Picotti, V., 2001. Sedimentary and biological response to sea-level and palaeoceanographic changes of a Lower-Middle Jurassic Tethyan platform margin (Southern Alps, Italy). Paleogeogr., Paleoclimatol., Paleoecol. 169, 219-244

Cook, P.J. and McElhinny, M.W., 1979. A re-evaluation of the spatial and temporal distribution of sedimentary phosphate deposits in the light of plate tectonics. Economic Geology, 74, 315-330.

Dubois, J.P., Benitez, N., Liebig, T., Baudraz, M. and Okopnik, F., 2002. Le cadmium dans les sols du haut Jura suisse. In: Les éléments traces métalliques dans les sols. Approches fonctionnelles et spatiales (D.Baize and M.Tercé, eds) INRA Editions, Paris, 33-52

Föllmi, K.B, 1995. 160 m.y. record of marine sedimentary phosphorus burial: coupling of climate and continental weathering under greenhouse and icehouse conditions. Geology, 23, 859-862

Geiger M., Clark, D.N. and Mette W., 2004. Reappraisal of the timing of the breakup of Gondwana based on sedimentological and seismic evidence from the Morondava Basin, Madagascar. Journal of African Earth Sciences, 38, 363-381

Genolet, F and Dubois, J.P., 1996. Etude de la teneur en cadmium dans les sols de la région de Blauen-Nenzlingen (canton de Basel-Campagne). EPF Lausanne, 1996:27

Gradstein, F.M., Ogg, J.G., Smith, A.G. et al., 2004. A Geologic Time Scale 2004. Cambridge University Press, ~ 500 pp.

Hinkley, T.K., Lamothe, P.J., Wilson, S.A., Finnegan, D.L. and Gerlach, T.M., 1999. Metal emissions from Kilauea, and a suggested revision of the estimated worldwide metal output by quiescent degassing of volcanoes. Earth and Planetary Science Letters, 170, 315-325

Jeans, C.V., Wray, D.S., Merriman, R.J. and Fisher, M.J., 2000. Volcanogenic clays in Jurassic and Cretaceous strata of England and the North Sea Basin. Clay Minerals 35, 25-55

Kabata-Pendias, A. and Pendias, H., 1992. Trace elements in soils and plants. 2nd edition. CRC Press, 365 pp.

Okopnik, F., 1997. Relation entre la variabilité spatiale du cadmium et la couverture pédologique de la région du Mont d'Amin. Travail de fin de 3e cycle. EPFL Lausanne. 45 p.

Prudente, D., 1999. Distributions des teneurs naturelles en cadmium dans les sols de la fôret communale des Fourgs (Doubs-Fr). Unpublished Ph.D. Thesis, EPF Lausanne, 68 p.

Prundente, D., Baize, D., and Dubois, J.P., 2002. Cadmium naturel dans une forêt du Haut-Jura français. In Baize, D. (ed.), Les éléments traces métalliques dans les sols. Approches fonctionelles et spatiales. INRA Editions, Paris, p. 53-70

Pankhurst, R. J., Riley, T. R., Fanning, C. M. and Kelley, S. P., 2000. Episodic Silicic Volcanism in Patagonia and the Antarctic Peninsula: Chronology of Magmatism Associated with the Break-up of Gondwana. Journal of Petrology, 41, 605-625

Symonds, R. B., Rose, W. I., Reed, M. H., Lichte, F. E., and Finnegan, D. L., 1987. Volatilization, transport and sublimation of metallic and non-metallic elements in high temperature gases at Merapi Volcano, Indonesia. Geochimica et Cosmochimica Acta, 51, 2083-2101

Tuchschmid, M., 1995. Quantifizierung und Regionalisierung von Schwermetallen und Fluorgehalten bodenbildender Gesteine der Schweiz: Umwelt-Materialien 32 (BUWAL, Berne)Veuve (2000)

Weissert, H., and Mohr, H., 1996. Late Jurassic climate and its impact on carbon cycling. Palaeogeography, Palaeoclimatology, Palaeoecology, 122, 27-43

Annex 1

Data tables

Lausen-Schleifenberg - 1/8

Sample Name	Depth (m)	Cd (µg/g)
S 1	100.060	0.109
S 1	100.060	0.331
S 1	100.060	0.164
S 1	100.060	0.127
S 2	99.660	0.321
S 5	97.910	0.061
S 5	97.910	0.156
S 7	97.110	0.078
S 9	96.260	0.080
S 9 (250 mg)	96.260	0.102
S 9 (125 mg)	96.260	0.104
S 9	96.260	0.141
S 12	94.510	0.088
S 12	94.510	0.143
S 14	93.460	0.055
S 16	91.960	0.592
S 16	91.960	0.679
S 18	90.660	0.000
S 18	90.660	0.052
S 19	90.060	0.000
S 19	90.060	0.063
S 19	90.060	0.094
S 20-1	89.410	0.090
S 20-1	89.410	0.089
S 20-1	89.410	0.112
S 20-2	89.410	0.054
S 20-2	89.410	0.053
S 21	88.660	0.040
S 21	88.660	0.054
S 21	88.660	0.043
S 22	88.010	0.000
S 22	88.010	0.066
S 22	88.010	0.049
S 23	87.810	0.000
S 23	87.810	0.096
S 23	87.810	0.059
S 24	87.110	0.000
S 24	87.110	0.094

Lausen-Schleifenberg - 2/8

Sample Name	Depth (m)	Cd (µg/g)
S 25	86.310	0.000
S 25	86.310	0.061
S 25	86.310	0.072
S 26	85.810	0.000
S 26	85.810	0.041
S 27	85.010	0.086
S 27	85.010	0.072
S 28	84.410	0.000
S 28	84.410	0.092
S 29	83.410	0.000
S 29	83.410	0.574
S 29	83.410	0.579
S 30-1	82.810	0.674
S 30-1	82.810	0.679
S 30-2	82.810	0.644
S 32-1	81.610	0.536
S 32-2	81.610	0.529
S 32-1	81.610	0.783
S 33	80.160	0.000
S 33	80.160	0.189
S 33	80.160	0.241
S 34 hardground	79.760	0.000
S 34 hardground	79.760	0.567
S 34	79.710	0.000
S 34	79.710	0.207
S 35	78.710	0.000
S 35	78.710	0.036
S 35	78.710	0.075
S 36	78.110	0.000
S 36	78.110	0.033
S 37	77.910	0.000
S 37	77.910	0.028
S 37	77.910	0.032
S 38	77.060	0.000
S 38	77.060	0.000
S 38	77.060	0.102
S 38	77.060	0.098

Lausen-Schleifenberg - 3/8

Sample Name	Depth (m)	Cd (µg/g)
S 39	75.610	0.000
S 39	75.610	0.035
S 40	74.910	0.000
S 40	74.910	0.038
S 41-1	74.360	0.000
S 41-1	74.360	0.057
S 41-2	74.360	0.051
S 42	73.560	0.000
S 42	73.560	0.028
S 45	71.460	0.000
S 45	71.460	0.036
S 46	70.360	0.000
S 46	70.360	0.026
S 46	70.360	0.018
S 47	70.060	0.000
S 47	70.060	0.043
S 48	69.160	0.057
S 49	68.310	0.071
S 50	68.110	0.091
S 50	68.110	0.086
S 51	67.360	0.043
S 51	67.360	0.032
S 52	66.710	0.037
S 52	66.710	0.023
S 52	66.710	0.028
S 53	66.010	0.099
S 54	65.160	0.089
S 55	64.510	0.081
S 55	64.510	0.119
S 56	64.010	0.170
S 57	63.810	0.122
S 58	63.410	0.232
S 58	63.410	0.233
S 59	62.660	0.134
S 60	62.010	0.194
S 61	61.510	0.172
S 61	61.510	0.317
S 62	60.810	0.162

Lausen-Schleifenberg - 4/8

Sample Name	Depth (m)	Cd (µg/g)
S 63	60.110	0.510
S 63	60.110	0.603
S 64	59.610	0.611
S 64	59.610	0.577
S 64	59.610	0.599
S 65	58.560	0.265
S 65	58.560	0.313
S 66	57.960	0.148
S 67	56.960	0.446
S 68	56.410	0.132
S 68	56.410	0.151
S 69	56.210	0.133
S 70	55.510	0.223
S 70	55.510	0.258
S 71	55.310	0.256
S 72	54.310	0.109
S 73	53.810	0.106
S 74	53.110	0.137
S 74	53.110	0.156
S 75	52.610	0.205
S 76	52.210	0.250
S 76	52.210	0.278
S 77	51.610	0.134
S 78	51.010	0.133
S 79	50.560	0.252
S 80	50.010	0.361
S 80	50.010	0.398
S 80 (250 mg)	50.010	0.408
S 80 (125 mg)	50.010	0.405
S 81	49.510	0.877
S 82	48.910	0.219
S 82	48.910	0.223
S 82	48.910	0.202
S 83	48.210	0.604
S 84	47.710	0.282
S 85	46.810	0.094
S 86	46.110	0.052
S 89	44.310	0.152
S 91	42.860	0.189
S 94	41.210	0.173
S 97	39.410	0.336
S 98	38.710	0.152

Lausen-Schleifenberg - 5/8

Sample Name	Depth (m)	Cd (µg/g)
S 99	37.960	0.325
S 100	37.310	0.400
S 101	36.860	0.087
S 102	36.360	0.144
S 103	35.760	0.219
S 104	34.810	0.109
S 105	33.910	1.489
S 106	33.310	0.251
S 107	32.560	0.255
S 108	32.160	0.235
S 109	31.560	0.191
S 110	31.360	0.514
S 111	30.910	0.406
S 112	30.310	0.303
S 113	29.710	0.044
S 114	29.110	0.185
S 115	28.210	0.000
S 116	27.360	1.392
S 116	27.360	1.270
S 116	27.360	1.369
S 116	27.360	1.498
S 117	27.010	0.100
S 118	26.460	0.173
S 119	25.760	0.196
S 120	25.210	0.058
S 121	24.810	0.040
S 122	23.910	0.061
S 123	23.410	0.418
S 124	22.760	0.243
S 124	22.760	0.280
S 124	22.760	0.200
S 124	22.760	0.264
S 125	22.360	0.153
S 126	22.210	0.117
S 127	21.310	1.259
S 128	20.660	0.296
S 129	20.160	0.225
S 130	19.710	0.093
S 131	19.110	0.317
S 132	18.560	0.749
S 133	18.410	0.088
S 134	17.810	0.437
S 135	17.360	0.259

Lausen-Schleifenberg - 6/8

Sample Name	Depth (m)	Cd (µg/g)
S 136	16.510	0.181
S 137	16.010	0.111
S 138	15.060	0.052
S 139	14.610	0.080
LA 45	14.300	0.027
S 140	14.110	0.000
LA 44	13.700	0.071
S 141	13.360	0.057
LA 43	13.250	0.060
S 142	13.160	0.156
S 143	12.510	0.108
LA 42	12.400	0.125
LA 40	12.350	0.258
S 144	12.110	0.044
LA 39	11.800	0.108
S 145	11.610	0.077
S 146	11.060	0.062
LA 38	10.850	0.024
LA 30	10.230	0.000
S 147	10.160	0.292
LA 37	10.000	0.000
LA 36	9.800	0.036
S 148	9.760	0.000
LA 29	9.380	0.012
LA 35	9.300	0.006
LA 33	9.100	0.048
LA 32	8.850	0.008
S 149	8.710	0.109
LA 28	8.530	0.159
LA 31	8.530	0.297
LA 26	8.285	0.000
S 150	8.160	0.171
LA 25	8.085	0.121
LA 24 B L1	7.936	0.923
LA 24 E-L1	7.936	0.162
LA 24 B P1	7.933	0.471
LA 24 E-P1	7.930	0.685
LA 24 C-h	7.920	3.608
LA 24 B L2	7.919	2.346
LA 24 E-L2	7.919	0.510

Lausen-Schleifenberg - 7/8

Sample Name	Depth (m)	Cd (µg/g)
LA 24 B P2	7.918	15.777
LA 24	7.910	2.550
LA 24	7.910	2.615
LA 24	7.910	2.172
LA 24	7.910	2.587
LA 24	7.910	2.574
LA 24 E-P2	7.910	21.346
LA 24 B P3	7.903	8.544
LA 24 B L3	7.901	0.262
LA 24 E-L3	7.901	0.041
LA 24 C-b	7.900	1.456
LA 24 E-P3	7.890	0.960
LA 24 B P4	7.888	5.501
LA 24 B L4	7.884	0.078
LA 24 E-L4	7.884	0.109
S 151	7.560	2.211
S 151	7.560	1.770
S 151	7.560	2.125
S 151	7.560	2.336
LA 21	7.460	0.007
LA 20	7.010	0.038
S 152	6.810	0.129
LA 19	6.710	0.036
LA 18	6.410	0.749
S 153	6.310	1.042
S 154	6.110	0.338
LA 16	5.910	0.096
S 155 p	5.460	0.024
S 155	5.460	0.103
S 155	5.460	0.063
S 155	5.460	0.070
S 155	5.460	0.038
S 156	5.110	4.911
S 156	5.110	3.461
LA 14 b	5.060	0.080
LA 13	3.710	0.000
LA 11	3.060	0.044
LA 10	2.920	0.000
LA 9	2.370	0.000
LA 8	2.170	0.043
LA 7	1.920	0.015
LA 6	1.670	0.000
LA 4	1.120	0.000
LA 3	0.650	0.010

Lausen-Schleifenberg - 8/8

Sample Name	Depth (m)	Cd (µg/g)
LA 2	0.475	0.000
LA 2	0.475	0.022
LA 2	0.475	0.046
LA 2	0.475	0.056

Gorges du Pichoux - 1/2

Sample Name	Depth (m)	Cd (µg/g)
Pi 185	79.730	0.000
Pi 184	79.099	0.016
Pi 180	77.569	0.027
Pi 179	77.283	0.026
Pi 178	75.212	0.029
Pi 177	74.932	0.074
Pi 176	74.184	0.057
Pi 174	68.552	0.077
Pi 173	67.556	0.120
Pi 171	64.249	0.475
Pi 168	60.740	0.043
Pi 167	60.375	0.071
Pi 164	57.693	0.162
Pi 163	56.638	0.061
Pi 161	55.883	0.059
Pi 159	54.665	0.028
Pi 158	53.493	0.027
Pi 157	52.680	0.145
Pi 153	51.475	0.031
Pi 151	50.792	0.000
Pi 149	50.193	0.021
Pi 146	49.750	0.068
Pi 145	47.960	0.019
Pi 144	47.263	0.038
Pi 143	46.853	0.133
Pi 141	46.117	0.215
Pi 140	45.635	0.259
Pi 139	44.672	0.123
Pi 138	43.858	0.165
Pi 137	41.911	0.080
Pi 136	41.326	0.056
Pi 135	39.112	0.029
Pi 134	38.708	0.065
Pi 133	38.292	0.064
Pi 128	35.915	0.050
Pi 120	30.951	0.018
Pi 118	28.529	0.171
Pi 116	28.268	0.105
Pi 114	27.995	0.163
Pi 113	25.814	0.249
Pi 110	23.945	0.000
Pi 108b	23.112	0.016
Pi 107	22.852	0.048
Pi 104	22.161	0.010

Gorges du Pichoux - 2/2

Sample Name	Depth (m)	Cd (µg/g)
Pi 103	21.628	0.000
Pi 101	20.977	0.000
Pi 100	19.674	0.000
Pi 99	19.271	0.051
Pi 97	18.848	0.000
Pi 95	18.203	0.000
Pi 94	16.895	0.000
Pi 92	16.439	0.084
Pi 91	15.599	0.000
Pi 90	15.365	0.104
Pi 89a	14.551	0.031
Pi 88	14.160	0.000
Pi 86	13.529	0.032
Pi 85a	12.878	0.033
Pi 82	12.474	0.024
Pi 79	11.589	0.088
Pi 78	11.263	0.143
Pi 76	10.807	0.188
Pi 74	10.026	0.095
Pi 72	9.635	0.072
Pi 71	8.555	0.147
Pi 68	7.617	0.000
Pi 65	7.292	0.144
Pi 61	6.934	0.159
Pi 40	6.283	0.065
Pi 37	5.208	0.287
Pi 34	4.779	0.222
Pi 28	4.310	1.126
Pi 26	3.828	0.301
Pi 23	3.288	0.504
Pi 20	2.773	0.766
Pi 17	2.513	1.060
Pi 15	1.758	0.165
Pi 11	1.237	0.601
Pi 7	0.749	0.000
Pi 2.1	0.195	0.042

Davayé-Vergisson - 1/2

Sample Name	Depth (m)	Cd (µg/g)
DA 1	38.100	0.154
DA 1b	37.450	0.269
DA 2	37.300	0.034
DA 3	37.150	0.516
DA 4a	37.000	1.242
DA 4b	36.950	1.315
DA 4b	36.950	0.995
DA 4b	36.950	1.307
DA 4b	36.950	1.761
DA 5	36.700	0.169
DA 6	36.600	0.101
DA 7	36.450	0.064
DA 8	36.400	0.260
DA 8.b	35.700	0.000
DA 9	35.200	0.163
DA 10	34.900	0.333
DA 1'	34.400	0.753
DA 2'h	33.700	0.099
DA 3'	32.450	0.221
DA 4'	31.800	0.174
VE 0	31.250	0.128
DA 5'	30.950	0.089
VE 1	30.950	0.190
VE 2	30.250	0.187
VE 3-2h	27.900	0.132
VE 4	27.400	0.085
VE 5	26.400	0.013
VE 6	25.150	0.182
VE 7	24.950	0.110
VE 8	24.150	0.168
VE 10	22.050	0.439
VE 11	21.500	0.914
VE 13b	20.350	0.128
VE 14	19.850	0.173
VE 15	19.500	0.350
VE 16	18.950	0.248
VE 17	18.570	0.000
VE 19	14.150	0.000
VE 20	12.650	0.013
VE 22	10.500	0.721
VE 23b	9.850	0.189
VE 25	8.600	0.054
VE 26	8.000	0.149
VE 27b	6.950	0.423

Davayé-Vergisson - 2/2

Sample Name	Depth (m)	Cd (µg/g)
VE 28	6.500	0.081
VE 29	6.350	0.048
VE 30	5.300	0.000
VE 31	4.800	0.000
VE 32	4.400	0.000
VE 33	4.200	0.098
VE 34	3.600	0.100
VE 35h	2.250	0.061
VE 36	1.000	0.069

Ste Honorine des Pertes

Sample Name	Depth (m)	Cd (µg/g)
B 1	12.700	0.038
B 2	12.300	0.045
B 3	11.600	0.000
B 3	11.600	0.007
B 3	11.600	0.000
B 3	11.600	0.018
B 4	10.800	0.036
B 5	10.300	0.005
B 6	9.500	0.000
B 7	8.700	0.000
B 8	8.050	0.000
B 9	7.950	0.024
B 9	7.950	0.038
B 9	7.950	0.038
B 9	7.950	1.011
B 9'	7.500	0.000
B 10	7.000	0.000
B 11	6.600	0.000
B 12	6.000	0.757
B 13	5.900	0.147
B 14	5.200	0.248
B 15	4.850	0.340
B 16	4.400	0.498
B 17	3.850	0.416
OOF 4	3.500	0.632
OOF 3	2.950	0.285
OOF 2	2.600	1.089
OOF 1	2.400	0.000
CON 2	2.250	0.259
MA 3 phosph	2.170	0.410
MA 3 congl	2.130	0.000
B + 7h	2.120	0.048
B + 7b	2.080	0.173
MA 1	1.900	0.221
B + 1	1.750	0.032
MA 2	1.650	0.244
B + 6	1.600	0.349
MA 4	1.400	0.121
B + 2	1.320	0.012
B + 3 b	1.100	0.169
B + 3 h	1.100	0.000
B + 4 b	0.500	0.560
B + 4 h	0.500	0.484
B + 5	0.000	0.096
B + 5	0.000	0.144

Carcabuey - 1/3

Sample Name	Depth (m)	Cd (µg/g)
JC 4 - 35.8	35.800	0.536
JC 4 - 34.45 M	34.450	0.243
JC 4 - 34.45 N	34.450	0.155
JC 4 - 34.4	34.400	0.336
JC 4 - 34.0	34.000	0.343
JC 4 - 33.75	33.750	0.282
JC 4 - 33.5	33.500	0.221
JC 4 - 33.3	33.300	0.498
JC 4 - 32.4	32.400	0.336
JC 4 - 32.0	32.000	0.237
JC 4 - 31.75	31.750	0.243
JC 4 - 31.0	31.000	0.161
JC 4 - 30.75	30.750	0.256
JC 4 - 30.6	30.600	0.131
JC 4 - 30.3	30.300	1.186
JC 4 - 30.3	30.300	0.945
JC 4 - 30.3	30.300	1.163
JC 4 - 30.3	30.300	1.668
JC 4 - 30.0	30.000	0.360
JC 4 - 29.8	29.800	0.269
JC 4 - 28.4	28.400	1.065
JC 4 - 27.7	27.700	0.453
JC 4 - 26.8	26.800	0.326
JC 4 - 26.4	26.400	0.294
JC 4 - 26.0	26.000	0.310
JC 4 - 25.9	25.900	0.285
JC 4 - 25.2	25.200	0.318
JC 4 - 24.8	24.800	0.260
JC 4 - 24.5	24.500	0.274
JC 4 - 24.15	24.150	0.291
JC 4 - 24.0	24.000	0.340
JC 4 - 23.9	23.900	0.289
JC 4 - 22.75	22.750	0.292
JC 4 - 22.6	22.600	0.239
JC 4 - 22.3	22.300	0.269
JC 4 - 22.2	22.200	0.730
JC 4 - 22.1	22.100	0.259
JC 4 - 21.6	21.600	0.363
JC 4 - 21.4	21.400	0.361
JC 4 - 20.6	20.600	0.608

Carcabuey - 2/3

Sample Name	Depth (m)	Cd (µg/g)
JC 4 - 20.15	20.150	0.696
JC 4 - 19.55	19.550	0.458
JC 4 - 19.45	19.450	0.610
JC 4 - 19.0	19.000	0.575
JC 4 - 19.0	19.000	0.623
JC 4 - 18.8	18.800	0.516
JC 4 - 18.35	18.350	0.612
JC 4 - 18.15	18.150	0.630
JC 4 - 18.0	18.000	0.127
JC 4 - 17.5	17.500	0.538
JC 4 - 17.45	17.450	0.399
JC 4 - 16.8	16.800	0.387
JC 4 - 16.62	16.620	0.471
JC 4 - 16.45	16.450	0.365
JC 4 - 15.8	15.800	0.186
JC 4 - 15.8	15.800	0.146
JC 4 - 15.8	15.800	0.191
JC 4 - 15.8	15.800	0.295
JC 4 - 15.1	15.100	0.138
JC 4 - 14.95	14.950	0.255
JC 4 - 14.5	14.500	0.134
JC 4 - 14.1	14.100	0.271
JC 4 - 13.10	13.100	0.172
JC 4 - 12.95	12.950	0.154
JC 4 - 12.8	12.800	0.090
JC 4 - 12.6	12.600	0.184
JC 4 12.15	12.150	0.156
JC 4 - 11.7	11.700	0.312
JC 4 11.35	11.350	0.083
JC 4 - 10.95	10.950	0.106
JC 4 - 10.6	10.600	0.146
JC 4 - 9.8	9.800	0.082
JC 4 - 9.50	9.500	0.078
JC 4 - 9.25	9.250	0.165
JC 4 - 8.9	8.900	0.113
JC 4 - 8.4	8.400	0.099
JC 4 7.95	7.950	0.119
JC 4 - 7.5	7.500	0.194
JC 4 - 7.15	7.150	0.142
JC 4 - 6.6	6.600	0.160
JC 4 - 6	6.000	0.087
JC 4 - 5.86	5.860	0.008
JC 4 - 5.65	5.650	0.141
JC 4 5.38	5.380	0.023

Carcabuey - 3/3

Sample Name	Depth (m)	Cd (µg/g)
JC 4 - 5.05	5.050	0.069
JC 4 - 4.9	4.900	0.138
JC 4 4.5	4.500	0.016
JC 4 - 4.25	4.250	0.061
JC 4 - 3.8	3.800	0.071
JC 4 - 3.45	3.450	0.106
JC 4 - 2.85	2.850	0.153
JC 4 2.3	2.300	0.036
JC 4 - 2.1	2.100	0.126
JC 4 - 1.9	1.900	0.106
JC 4 - 1.2	1.200	0.114
JC 4 - 0.5	0.500	0.214
JC 4 0.2	0.200	0.052
JC 4 - 0	0.000	0.248

Terminilletto - 1/6

Sample Name	Depth (m)	Cd (µg/g)
TM 255.8	255.800	0.011
TM 232.8	232.800	0.000
TM 231.5	231.500	0.051
TM 230.05	230.050	0.019
TM 228.65	228.650	0.047
TM 227.4	227.400	0.000
TM 226.15	226.150	0.000
TM 225	225.000	0.141
TM 224.05	224.050	0.021
TM 223.4	223.400	0.000
TM 222.25	222.250	0.053
TM 221.2	221.200	0.046
TM 220.2	220.200	0.004
TM 219.16	219.160	0.020
TM 218.3	218.300	0.000
TM 216.9	216.900	0.000
TM 211.93	211.930	0.085
TM 211.22	211.220	0.050
TM 209.92	209.920	0.070
TM 209.18	209.180	0.176
TM 208.3	208.300	0.126
TM 205.05	205.050	0.009
TM 204.75	204.750	0.179
TM 201.4	201.400	0.017
TM 200.8	200.800	0.025
TM 200.4	200.400	0.145
TM 197.1	197.100	0.198
TM 196.98	196.980	0.097
TM 196	196.000	0.231
TM 193.49	193.490	0.158
TM 192.9	192.900	0.088
TM 191.58	191.580	0.187
TM 188.54	188.540	0.179
TM 188.4	188.400	0.155
TM 186.75	186.750	0.142
TM 185.58	185.580	0.134
TM 184.4	184.400	0.152
TM 183.9	183.900	0.187
TM 183.2	183.200	0.070
TM 181.48	181.480	0.215

Terminilletto - 2/6

Sample Name	Depth (m)	Cd (µg/g)
TM 180.3	180.300	0.077
TM 179.8	179.800	0.132
TM 178.7	178.700	0.076
TM 176.9	176.900	0.096
TM 176.1	176.100	0.029
TM 175.54	175.540	0.160
TM 175.12	175.120	0.075
TM 174.04	174.040	0.030
TM 173.74	173.740	0.111
TM 167.68	167.680	0.031
TM 166.57	166.570	0.059
TM 165.76	165.760	0.072
TM 165.22	165.220	0.079
TM 164.02	164.020	0.000
TM 163.92	163.920	0.094
TM 163	163.000	0.055
TM 161.4	161.400	0.164
TM 161.36	161.360	0.043
TM 157.4	157.400	0.040
TM 146	146.000	0.143
TM 144.55	144.550	0.155
TM 144	144.000	0.084
TM 143.45	143.450	0.078
TM 142.8	142.800	0.076
TM 142.2	142.200	0.109
TM 140.6	140.600	0.162
TM 139.9	139.900	0.188
TM 139.35	139.350	0.065
TM 138.7	138.700	0.168
TM 138	138.000	0.079
TM 137.1	137.100	0.013
TM 136	136.000	0.075
TM 136a	136.000	0.051
TM 135.3	135.300	0.149
TM 134.6	134.600	0.066
TM 133.95	133.950	0.058
TM 133.45	133.450	0.088
TM 132.7	132.700	0.105
TM 132.6	132.600	0.005
TM 132.05	132.050	0.147
TM 129.9	129.900	0.137
TM 128.2	128.200	0.140
TM 127	127.000	0.017
TM 126.06	126.060	0.132

Terminilletto - 3/6

Sample Name	Depth (m)	Cd (µg/g)
TM 124.68	124.680	0.165
TM 124.1	124.100	0.025
TM 123.15	123.150	0.050
TM 121.9	121.900	0.061
TM 120.65	120.650	0.040
TM 119.96	119.960	0.085
TM 119	119.000	0.000
TM 116.92	116.920	0.080
TM 115.7	115.700	0.092
TM 114.05	114.050	0.031
TM 113.7	113.700	0.050
TM 113.15	113.150	0.091
TM 110.57	110.570	0.064
TM 109.97	109.970	0.161
TM 108.75	108.750	0.197
TM 107.2	107.200	0.106
TM 106.85	106.850	0.080
TM 105.58	105.580	0.137
TM 105.35	105.350	0.121
TM 105.15	105.150	0.081
TM 104.53	104.530	0.076
TM 104	104.000	0.222
TM 103.25	103.250	0.207
TM 103.25	103.250	0.130
TM 103.25	103.250	0.127
TM 103.25	103.250	0.220
TM 102.85	102.850	0.283
TM 102.38	102.380	0.232
TM 101.53	101.530	0.151
TM 100.6	100.600	0.217
TM 100.2	100.200	0.149
TM 99.35	99.350	0.179
TM 98.6	98.600	0.298
TM 97.85	97.850	0.119
TM 97.3	97.300	0.063
TM 96.9	96.900	0.167
TM 96.38	96.380	0.107
TM 96.1	96.100	0.170
TM 95	95.000	0.173
TM 94.35	94.350	0.292
TM 94.3	94.300	0.050
TM 93.05	93.050	0.151
TM 92.08	92.080	0.091
TM 91.6	91.600	0.266

Terminilletto - 4/6

Sample Name	Depth (m)	Cd (µg/g)
TM 91.05	91.050	0.117
TM 90.42	90.420	0.136
TM 89.11	89.110	0.134
TM 88.2	88.200	0.377
TM 87.02	87.020	0.171
TM 86.20	86.200	0.077
TM 86.1	86.100	0.054
TM 85.65	85.650	0.032
TM 84.90	84.900	0.086
TM 84.82	84.820	0.068
TM 84.45	84.450	0.024
TM 84.05	84.050	0.056
TM 83.2	83.200	0.066
TM 83.11	83.110	0.049
TM 82.07	82.070	0.042
TM 82.07	82.070	0.000
TM 82.07	82.070	0.000
TM 82.07	82.070	0.008
TM 81.1	81.100	0.085
TM 81	81.000	0.073
TM 80.3	80.300	0.038
TM 79.2	79.200	0.032
TM 78.05	78.050	0.054
TM 77.29	77.290	0.041
TM 76.9	76.900	0.029
TM 76.5	76.500	0.026
TM 76.2	76.200	0.021
TM 75.03	75.030	0.016
TM 74.9	74.900	0.000
TM 74.25	74.250	0.076
TM 73.9	73.900	0.027
TM 73.2	73.200	0.067
TM 72.4	72.400	0.113
TM 72.05	72.050	0.061
TM 71.4	71.400	0.082
TM 71	71.000	0.086
TM 70.1	70.100	0.016
TM 69.4	69.400	0.047
TM 69	69.000	0.080
TM 68.4	68.400	0.048
TM 67.41	67.410	0.139
TM 66.9	66.900	0.032
TM 65.73	65.730	0.094
TM 65.13	65.130	0.052

Terminilletto - 5/6

Sample Name	Depth (m)	Cd (µg/g)
TM 64.81	64.810	0.108
TM 64.23	64.230	0.043
TM 63.01	63.010	0.072
TM 62.5	62.500	0.071
TM 61.1	61.100	0.085
TM 60.05	60.050	0.251
TM 59.4	59.400	0.060
TM 58.3	58.300	0.074
TM 57.3	57.300	0.070
TM 56.36	56.360	0.044
TM 55.1	55.100	0.000
TM 54.15	54.150	0.013
TM 53.15	53.150	0.000
TM 52.75	52.750	0.000
TM 51.44	51.440	0.000
TM 50.4	50.400	0.000
TM 48.93	48.930	0.000
TM 48	48.000	0.000
TM 47.04	47.040	0.000
TM 45.9	45.900	0.000
TM 45.1	45.100	0.000
TM 44.3	44.300	0.000
TM 42.8	42.800	0.000
TM 42.15	42.150	0.038
TM 41.4	41.400	0.000
TM 40.35	40.350	0.000
TM 39.4	39.400	0.000
TM 38.3	38.300	0.034
TM 37.4	37.400	0.022
TM 36.2	36.200	0.003
TM 35.35	35.350	0.000
TM 34.3	34.300	0.033
TM 33.55	33.550	0.000
TM 32.65	32.650	0.029
TM 29.3	29.300	0.009
TM 28.25	28.250	0.000
TM 27.25	27.250	0.029
TM 25.95	25.950	0.000
TM 24.95	24.950	0.000
TM 24.45	24.450	0.000
TM 23.22	23.220	0.000
TM 22.31	22.310	0.000
TM 20.20	20.200	0.000
TM 19.45	19.450	0.000

Terminilletto - 6/6

Sample Name	Depth (m)	Cd (µg/g)
TM 18.7	18.700	0.000
TM 18.00	18.000	0.000
TM 17.00	17.000	0.000
TM 16.00	16.000	0.000
TM 14.45	14.450	0.000
TM 13.00	13.000	0.083
TM 12.00	12.000	0.000
TM 10.13	10.130	0.000
TM 9.42	9.420	0.000
TM 8.1	8.100	0.055
TM 6.9	6.900	0.043
TM 6.05	6.050	0.027
TM 5.15	5.150	0.040
TM 4.25	4.250	0.000
TM 3.84	3.840	0.044
TM 2.62	2.620	0.024
TM 1.9	1.900	0.045
TM 0.42	0.420	0.051

Madagascar

Sample Name	Depth (m)	Cd (µg/g)
AMPARA 02		0.413
ANA 1		0.059
ANA 11		0.000
ANA 18		0.058
ANA 19		0.162
ANA 23		0.011
ANA 24		0.024
ANA 34		0.006
ANA 35		0.114
ANA 36		0.007
ANA 5		0.000
ANA 8		0.089
AND 01		0.178
AND 09		0.000
AND 10		0.106
AND 12		2.140
AND 13		0.756
ANK 02		0.063
ANK 03		0.084
ANK 06		0.097
ATAIN 09		0.000
DANGO 21		0.436
DANGO 22		0.121
DANGO 39		0.008
DANGO 40		0.086
DANGO 41		0.058
DANGO 58		0.000
TONGO 10		0.000

Chaudon-Norante - 1/2

Sample Name	Depth (m)	Cd (µg/g)
CN 142	77.130	0.000
CN 140	75.610	0.040
CN 138	73.880	0.000
CN 136	72.140	0.000
CN 134	70.620	0.000
CN 133b	69.500	0.000
CN 132	68.300	0.036
CN 130	66.900	0.027
CN 127	63.650	0.000
CN 125	61.850	0.028
CN 123	60.240	0.048
CN 120	58.820	0.020
CN 117	58.110	0.007
CN 115	56.980	0.028
CN 113	55.850	0.007
CN 111	54.720	0.044
CN 109	53.400	0.047
CN 107	52.330	0.000
CN 105	50.920	0.000
CN 102b	49.650	0.000
CN 100b	48.330	0.000
CN 98	47.330	0.103
CN 96	45.560	0.007
CN 93	45.540	0.041
CN 90	44.240	0.057
CN 87	42.800	0.122
CN 85	41.850	0.108
CN 83	41.150	0.083
CN 80	39.450	0.059
CN 78	38.000	0.032
CN 76	36.750	0.080
CN 74	35.950	0.027
CN 70	34.920	0.000
CN 67	32.620	0.130
CN 64	31.770	0.063
CN 62	30.740	0.003
CN 59	29.920	0.076
CN 58	29.650	0.026
CN 56	28.750	0.000
CN 52	26.900	0.021

Chaudon-Norante - 2/2

Sample Name	Depth (m)	Cd (µg/g)
CN 49	25.450	0.065
CN 47	24.220	0.051
CN 45	22.970	0.268
CN 43	22.170	0.000
CN 42	21.620	0.000
CN 39	19.250	0.000
CN 38	18.720	0.063
CN 35	16.200	0.010
CN 33	15.200	0.080
CN 30	13.650	0.000
CN 29	13.100	0.092
CN 27	12.070	0.085
CN 25	11.250	0.005
CN 23	10.050	0.050
CN 21	9.050	0.114
CN 19	7.950	0.246
CN 17	6.800	0.090
CN 15	5.800	0.081
CN 13	4.770	0.029
CN 11	3.540	0.091
CN 9	2.590	0.035
CN 7	2.010	0.037
CN 5	1.740	0.006
CN 3	1.130	0.103
CN 1	0.400	0.174

Lucy le Bois

Sample Name	Depth (m)	Cd (µg/g)
Lu 17	8.400	0.122
Lu 16	8.000	0.011
Lu 15	7.800	0.035
Lu 14	7.550	0.000
Lu 13	7.000	0.000
Lu 12	6.450	0.000
Lu 11	6.250	0.000
Lu 10	5.250	0.139
Lu 10-b	5.250	0.099
Lu 9	4.350	0.000
Lu 8	3.900	0.000
Lu 7	3.300	0.000
Lu 6	2.850	0.027
Lu 6 surf	2.850	0.109
Lu 5	2.200	0.000
Lu 4	1.250	0.401
Lu 3	0.800	0.000
Lu 2	0.300	2.679
Lu 1	0.000	0.000

Le Saussois - Roche aux Poulets

Le Saussois

Sample Name	Depth (m)	Cd (µg/g)
SA 1	0.000	0.202
SA 2b	1.600	0.458
SA 2p	1.600	0.346
SA 4br	4.800	0.215
SA 4p	4.800	0.177
SA 2 p.	1.600	0.464
SA 3	3.500	0.495
SA 4 p.	4.800	0.100
SA 5	6.300	0.176
SA 6	8.300	0.083
SA 7	14.300	0.000
SA 8	17.200	0.000
SA 8-600	17.200	0.090
SA 8-1200	17.200	0.083
SA 9	19.500	0.023
SA 10	23.800	0.000

Roche aux Poulets

Sample Name	Depth (m)	Cd (µg/g)
ME 2	0.500	0.323
ME 3	1.600	0.250

Roche aux Poulets (Emersion facies)

Sample Name	Depth (m)	Cd (µg/g)
Fe-t	0.050	0.358
Fe-b	0.000	0.078

Casa de Chimeneas - 1/2

Sample Name	Depth (m)	Cd (µg/g)
CC 115	102.000	0.029
CC 114	99.494	0.042
CC 113	97.990	0.029
CC 112	95.860	0.037
CC 111	94.857	0.087
CC 110	93.855	0.090
CC 109	92.978	0.089
CC 108	92.226	0.068
CC 107	91.600	0.055
CC 106	89.219	0.001
CC 101	80.447	0.076
CC 100	77.816	0.005
CC 99	77.189	0.067
CC 98	75.936	0.054
CC 97	74.432	0.024
CC 96	72.678	0.064
CC 95	71.676	0.004
CC 94	70.673	0.159
CC 93	69.295	0.026
CC 91	67.415	0.059
CC 89	66.287	0.062
CC 88	65.912	0.039
CC 87	65.410	0.174
CC 86	64.658	0.096
CC 85	63.907	0.140
CC 84	62.654	0.093
CC 83	61.400	0.104
CC 82	61.025	0.161
CC 81	59.897	0.065
CC 80	59.521	0.075
CC 79	59.270	0.090
CC 78	58.268	0.123
CC 77	57.265	0.100
CC 76	55.762	0.242
CC 75	54.133	0.075
CC 74	52.128	0.215
CC 73	51.752	0.104
CC 72	51.251	0.177
CC 71	50.875	0.122
CC 70	50.123	0.238

Casa de Chimeneas - 2/2

Sample Name	Depth (m)	Cd (µg/g)
CC 69	48.369	0.201
CC 68 A	47.742	0.183
CC 67	46.865	0.132
CC 66	44.985	0.382
CC 65	44.735	0.150
CC 64	44.359	0.224
CC 63	43.607	0.248
CC 62	43.356	0.141
CC 61 A	42.354	0.023
CC 60	41.101	0.079
CC 59 ?	40.349	0.267
CC 58	40.098	0.146
CC 57	39.346	0.145
CC 56	38.720	0.078
CC 55 C	37.592	0.077
CC 54	34.961	0.098
CC 53	34.710	0.199
CC 52	34.209	0.096
CC 51	33.206	0.136
CC 50	32.956	0.090
CC 49 A	32.079	0.106
CC 48	30.450	0.097
CC 47	30.074	0.059
CC 46	29.322	0.155
CC 45	28.695	0.064
CC 44	27.943	0.063
CC 43	26.314	0.098
CC 42	25.813	0.047
CC 41	22.806	0.373
CC 40	22.054	0.085
CC 39	21.177	0.046
CC 38	19.799	0.152
CC 37 B	18.170	0.041
CC 36 A	16.415	0.050
CC 35	14.160	0.050
CC 34 A	12.907	0.065
CC 33	7.268	0.081
CC 32	6.015	0.076
CC 31	4.511	0.461
CC 30	3.007	0.147
CC 29 A	2.537	0.074
CC 28	1.000	0.363

Bedrocks Lower Burgundy - Bajocian / Oxfordian - 1/2

Bajocian- Blacy

Sample Name	Depth (m)	Cd (µg/g)
BL 1	-	0.234
BL 2	-	0.036
BL 3	-	0.045
BLC 1	-	0.632
BLC 2	-	0.321
BLC 3	-	0.336
BLF-S	-	0.259

Oxfordian

Sample Name	Depth (m)	Cd (µg/g)
1 - Frétoy Forest		
Frétoy-Maison		
FM 1	0.050	0.192
FM 2	0.050	0.195
FM 3	0.350	0.196
FM 4	0.350	0.210
FM 5	0.650	0.117
FM 6	0.800	0.152
Raboulins		
RA 1	0.050	0.267
RA 2	0.350	0.286
RA 3 (BIS)	0.750	0.340
Anus		
AN 1	0.300	0.339
AN 2	0.600	0.308
AN 3	0.900	0.356
Chapoteaux		
CH 1	0.050	0.370
CH 2	0.350	0.550
CH 3	0.650	0.291
Frétoy	0.000	
FR 1	0.050	0.197
FR 2	0.300	0.233
Frétoy Forest		
FF 1	0.050	0.388
FF 2	0.350	0.284
FF 3	0.650	0.363
FF 4	1.050	0.216

Bedrocks Lower Bungundy - Bajocian / Oxfordian - 2/2

Sample Name	Depth (m)	Cd (µg/g)
2 - Clamecy		
CL 5 - 2	-	0.521
CL 5 - 3	-	0.200
CL 5 - 4	-	0.444
CL 5 - 1	-	0.254
3 - Précy le Sec		
CRA 1	-	0.336
CRA 2	-	0.223
CRA 3	-	0.226

Sections previously described by Veuve (2000)

1 - Pont de la Baleine

Sample Name	Depth (m)	Cd (µg/g)
6-3 a	0.487	0.143
6-3 b	0.460	0.089
6-3 c	0.433	0.111
6-3 d	0.348	0.119
6-3 e	0.325	0.126
6-3 f	0.302	0.162
6-2 a	0.270	0.139
6-2 b	0.230	0.096
6-2 c	0.190	0.109
6-1 a	0.148	0.101
6-1 b	0.126	0.102
6-1 c	0.104	0.129
6-1 d	0.082	0.108
6-1 e	0.071	0.102
6-0 a	0.044	0.224
6-0 b	0.027	0.128
6-0 c	0.009	0.128

2 - Auenstein

Sample Name	Depth (m)	Cd (µg/g)
A 18	-	0.074
A 18	-	0.050

Terminilletto - Concentrations in ng/g (1/12)

Sample	Depth (m)	Li	Be	Mg	Al	Ti	V	Cr	Mn	Fe	Co
TM 27.25	27.25	1153	150	3882501	301365	200933	1098	0	229205	1204820	1166
TM 28.25	28.25	1481	79	3806358	567282	204402	1022	0	207784	1619659	1343
TM 29.3	29.30	766	0	3490379	143496	200670	0	0	229254	1038976	1069
TM 32.65	32.65	1647	0	3937897	532223	207088	767	0	200839	1454674	1128
TM 33.55	33.55	1677	0	3695116	404829	185323	311	0	200968	1751065	1407
TM 34.3	34.30	534	135	3567178	176546	203226	0	0	188780	1131315	1010
TM 35.35	35.35	1972	0	3639920	779659	193243	908	0	178743	1591947	1402
TM 36.2	36.20	651	0	3808686	328686	210584	261	0	251606	1793010	1644
TM 37.4	37.40	2591	0	3892651	1086310	185777	1698	0	230051	1571870	1156
TM 38.3	38.3	2956	331	4384574	983456	230481	3307	3400	247757	2001470	1474
TM 39.4	39.4	1816	141	4116658	560990	225282	1562	2005	306130	1544368	1261
TM 40.35	40.35	2283	0	3854782	805757	210223	2221	2292	210662	1147656	1214
TM 41.4	41.4	1903	0	2548060	675381	125541	1794	1657	175286	1239938	822
TM 42.15	42.15	946	0	4024289	367172	218094	1355	0	266259	1793763	1538
TM 42.8	42.8	1198	554	3154848	438756	157878	1256	1946	214736	1195501	1018
TM 44.3	44.3	679	0	4175580	110583	201407	979	1534	274660	726025	1083
TM 45.1	45.1	2361	0	4009651	1039162	203939	2628	2819	242651	1968816	1552
TM 45.9	45.9	2061	0	4496790	917368	245390	2428	2388	223909	1594112	1496
TM 47.04	47.04	2075	347	3766426	683923	209829	2234	0	246212	1564246	1352
TM 48	48	1645	0	3760678	685415	197680	1284	0	212111	1616084	1076
TM 48.93	48.93	2311	0	3663644	739457	194693	1555	0	360700	2066554	1772
TM 50.4	50.4	1513	402	3725866	305393	236000	1200	0	207677	1065236	1131
TM 51.44	51.44	1190	28	2051042	446857	124027	824	0	139679	767458	976
TM 52.75	52.75	958	156	3133336	485455	204157	1123	0	215289	971632	1085
TM 53.15	53.15	1450	340	3781536	451836	210773	1298	0	203083	1039852	1024
TM 54.15	54.15	1328	69	4210670	419498	213213	1235	0	196149	1028497	1018
TM 55.1	55.1	2050	93	3387314	800253	190114	1835	0	197743	1381630	1171
TM 56.36	56.36	2274	254	3607069	678026	193663	2844	552	347323	1271705	2166
TM 57.3	57.3	2323	248	3545136	606255	192560	1735	618	218997	1144498	1093
TM 58.3	58.3	1391	103	3377055	460354	199820	1657	698	236851	839706	1141
TM 59.4	59.4	1350	35	3353579	482836	200182	1810	302	245415	2356002	2144
TM 60.05	60.05	1482	383	3483446	479346	192518	1639	480	198084	790991	935
TM 61.1	61.1	1195	212	3407031	321333	186515	1533	482	145820	973511	1230
TM 62.5	62.5	1236	174	3717450	366550	177037	1118	103	198943	545343	1011
TM 63.01	63.01	3178	0	3709975	1100411	196096	2712	1911	201344	969574	1071
TM 64.23	64.23	1357	0	3446434	364117	212895	1475	965	222897	1046887	1323
TM 64.81	64.81	2188	170	3344260	762532	196740	1761	1017	318117	1632475	1667
TM 65.13	65.13	2152	88	3491406	661335	177473	1559	777	276933	1159885	1271
TM 65.73	65.73	1307	1	3395670	278783	208339	1487	925	195511	589728	918
TM 66.9	66.9	1491	389	3394836	365268	168696	1233	594	176133	701129	1076
TM 67.41	67.41	2454	0	3234998	839357	196842	2464	1252	265712	2003584	1937
TM 68.4	68.4	1282	0	3419009	308884	218689	1291	1276	205034	562019	927
TM 69	69	2200	367	3296245	735807	196668	2232	1206	209540	1761408	1669
TM 69.4	69.4	803	0	3406078	152341	219535	1270	1314	162957	670495	842
TM 70.1	70.1	1204	0	3614586	190484	196948	1467	1424	132730	364919	821
TM 71	71	1702	102	3325577	581208	192653	2051	1336	206722	928793	1368
TM 71.4	71.4	1026	0	3524455	240585	203494	1331	1352	157885	884787	1042
TM 72.05	72.05	756	32	3245511	89157	191382	1166	1616	128453	312670	898
TM 72.4	72.4	1042	64	3621776	227791	215827	1411	1047	231708	712206	1185
TM 73.2	73.2	609	28	3197948	148807	199942	1193	921	133029	564819	891
TM 73.9	73.9	1111	170	3236227	274376	206284	1574	1661	151033	606600	1141
TM 74.25	74.25	1090	97	3302198	348255	193662	1393	931	177290	627779	971
TM 74,9	74.9	1748	173	3339533	467262	101918	1825	1717	148683	772960	773

Terminilletto - Concentrations in ng/g (2/12)

Sample	Ni	Cu	Zn	Ga	As	Rb	Sr	Zr	Mo	Cd	Cs	Ba	W
TM 27.25	10400	1382	7917	196	695	624	290704	405	0	29	39	2517	36
TM 28.25	12390	3415	1241	359	920	1259	291313	657	0	0	77	4530	5836
TM 29.3	10944	1105	3087	125	0	295	217745	0	0	9	13	1770	43
TM 32.65	10989	2951	5309	313	49	1258	360056	712	0	29	74	4406	21
TM 33.55	170465	1781	2419	214	147	911	265141	0	0	0	57	3968	66
TM 34.3	9250	1111	0	112	0	375	236039	0	0	33	27	2398	20
TM 35.35	10368	3744	1030	325	0	2069	304451	0	0	0	124	5829	96
TM 36.2	11357	2142	5520	174	215	706	233679	0	0	3	64	3299	50
TM 37.4	10730	3318	0	507	97	2386	336078	0	0	22	145	6899	45
TM 38.3	10999	5725	1544	453	654	2196	310505	804	691	34	143	5257	97
TM 39.4	10826	406	27259	287	190	1440	331025	1337	223	0	66	7859	845
TM 40.35	10431	4721	0	383	371	2028	343801	489	0	0	118	8732	31
TM 41.4	6629	2614	0	395	84	1879	176681	534	0	0	105	5540	83
TM 42.15	10748	2479	0	201	559	717	255963	584	0	38	47	3540	6
TM 42.8	8061	2918	0	202	98	1444	210939	456	0	0	69	6333	37
TM 44.3	9373	238	0	143	190	160	222395	207	0	0	11	3013	0
TM 45.1	12020	4644	0	468	193	2839	338723	875	0	0	155	10388	129
TM 45.9	11981	7280	0	419	187	2077	340059	649	0	0	107	7471	34
TM 47.04	10964	3457	4274	299	507	1678	274921	315	581	0	80	7361	8
TM 48	11664	3835	3721	318	194	1965	375296	328	0	0	85	6688	91
TM 48.93	11772	2713	3883	366	350	1767	353172	702	60	0	90	7033	58
TM 50.4	12120	1452	2200	206	138	630	243502	87	0	0	27	3268	1287
TM 51.44	6753	3045	1352	162	87	1375	121997	120	0	0	57	3855	44
TM 52.75	10388	2899	3161	307	125	1228	362582	59	0	0	63	6281	0
TM 53.15	13208	4016	1513	293	452	1245	296357	0	0	0	59	4740	0
TM 54.15	12797	2693	2239	201	285	1035	339324	322	0	13	48	5074	26
TM 55.1	11324	2850	2513	345	82	2016	277283	218	0	0	99	5468	126
TM 56.36	12525	4975	9276	344	452	1613	312774	397	188	44	95	6202	58
TM 57.3	11851	6844	6574	286	263	1690	269616	523	123	70	98	5117	100
TM 58.3	11485	5162	9326	200	239	1167	323634	1020	83	74	64	5693	367
TM 59.4	15173	6139	13890	303	532	1313	271395	325	47	60	73	5687	45
TM 60.05	12627	5951	15607	218	289	1161	335273	334	56	251	59	6135	59
TM 61.1	12730	3179	6308	149	263	827	232549	200	167	85	57	4143	30
TM 62.5	11548	2143	7084	166	137	970	236629	251	8	71	48	3797	41
TM 63.01	9574	4612	904	441	345	2611	244007	745	443	72	136	5449	29
TM 64.23	9836	3087	0	226	416	946	236504	649	261	43	58	4444	67
TM 64.81	13039	8945	10138	320	522	1828	285249	516	121	108	98	5599	0
TM 65.13	10735	6270	7489	329	328	1918	318833	410	247	52	112	6555	15
TM 65.73	10113	2736	7655	156	227	756	249126	517	0	94	36	3370	886
TM 66.9	8697	4319	16466	215	198	959	240917	351	202	32	51	3983	38
TM 67.41	11842	9399	5761	428	1053	2203	467747	877	205	139	127	9303	62
TM 68.4	10113	2394	1273	227	343	879	248686	330	0	48	57	4010	109
TM 69	12863	9151	8318	386	478	1930	373702	689	0	80	110	7012	0
TM 69.4	10992	2627	2095	140	292	384	208666	278	124	47	22	2618	170
TM 70.1	10905	1968	312	90	187	557	259809	245	41	16	28	3914	0
TM 71	11434	6814	5587	275	340	1519	340213	512	48	86	80	5559	0
TM 71.4	11483	3614	1117	197	381	642	251771	184	0	82	40	3990	1
TM 72.05	10799	958	5540	72	161	227	217673	207	0	61	13	2470	0
TM 72.4	10769	5127	4937	175	264	629	294748	217	0	113	35	3604	74
TM 73.2	8974	2281	4813	90	221	367	235250	122	3	67	20	3302	30
TM 73.9	11959	3385	4703	141	317	734	263522	209	0	27	39	4299	48
TM 74.25	8975	3588	5317	181	214	854	298689	309	52	76	66	4224	28
TM 74,9	7958	1163	2986	283	133	1111	227789	590	343	0	22	3390	23

Terminilletto - Concentrations in ng/g (3/12)

Sample	Pb	U	La	Th	Y	Sc
TM 27.25	0	483	4367	104	6364	283
TM 28.25	77	446	4870	203	6814	142
TM 29.3	0	489	5331	126	7895	13
TM 32.65	0	341	5281	241	7154	93
TM 33.55	0	233	4798	140	6766	0
TM 34.3	0	536	3700	109	5172	0
TM 35.35	28	377	4091	221	6053	0
TM 36.2	566	205	5648	253	7969	0
TM 37.4	8	461	5798	337	7505	0
TM 38.3	32	648	5139	264	6808	784
TM 39.4	0	249	5277	225	7169	652
TM 40.35	0	454	4302	353	6197	86
TM 41.4	0	142	3531	219	4618	0
TM 42.15	188	210	4914	241	7089	0
TM 42.8	0	232	3974	161	5589	169
TM 44.3	0	297	4416	178	6784	23
TM 45.1	813	418	6649	343	8844	308
TM 45.9	698	242	6739	227	8923	379
TM 47.04	0	342	5489	157	7592	0
TM 48	734	81	6515	313	8736	0
TM 48.93	445	367	6638	233	8617	0
TM 50.4	0	393	4336	219	6386	0
TM 51.44	0	146	2985	132	3946	0
TM 52.75	0	90	6208	260	8735	0
TM 53.15	0	291	4683	145	6858	0
TM 54.15	0	153	5526	128	7961	0
TM 55.1	0	323	4731	162	6619	0
TM 56.36	872	427	6504	133	8601	307
TM 57.3	1423	314	5329	198	7245	407
TM 58.3	2322	222	6124	216	8576	323
TM 59.4	1879	156	5478	225	7660	230
TM 60.05	690	181	6714	291	9346	365
TM 61.1	680	430	4620	149	6659	405
TM 62.5	673	244	6059	146	8150	432
TM 63.01	699	360	7526	232	9831	62
TM 64.23	435	297	6918	145	9065	138
TM 64.81	1431	337	8449	230	11650	370
TM 65.13	1078	255	8401	341	11239	223
TM 65.73	1507	406	5840	144	8805	316
TM 66.9	389	322	4892	158	6937	57
TM 67.41	1439	376	10275	451	15182	374
TM 68.4	433	368	6056	179	8960	236
TM 69	1839	206	7947	286	11388	390
TM 69.4	152	445	6239	126	9511	52
TM 70.1	357	550	6212	107	9338	249
TM 71	746	282	7433	232	9972	414
TM 71.4	644	339	5742	97	8147	49
TM 72.05	0	576	5750	83	8924	131
TM 72.4	808	305	6987	140	10125	200
TM 73.2	396	383	5567	77	7883	4
TM 73.9	482	485	7756	165	10892	235
TM 74.25	279	390	6432	175	9456	121
TM 74,9	476	379	4230	91	5018	14

Terminilletto - Concentrations in ng/g (4/12)

Sample	Depth (m)	Li	Be	Mg	Al	Ti	V	Cr	Mn	Fe	Co
TM 75.03	75.03	976	184	3406520	238003	0	893	866	205222	452409	930
TM 76.2	76.2	1155	193	3185858	321935	202541	1264	972	140867	505197	818
TM 76.5	76.5	2006	241	3337498	677339	192227	2037	1144	157590	911682	1035
TM 76.9	76.9	1923	87	3220649	649010	202811	2125	2299	149380	1084008	967
TM 77.29	77.29	1245	0	3394268	329474	190023	1176	1091	213555	449709	1073
TM 78.05	78.05	1618	395	3243565	586981	204036	2010	2027	209077	1051001	1255
TM 79.2	79.2	765	236	3173949	178792	207509	953	2178	142980	471935	877
TM 80.3	80.3	1424	99	3468976	365342	202779	1931	1190	157154	353868	856
TM 81	81	838	355	3424222	196012	101326	958	795	132941	388449	795
TM 81.1	81.1	1075	0	3388310	227965	211033	1267	881	156571	708826	938
TM 82.07	82.07	1157	0	3464989	289304	212933	1162	806	191941	390784	947
TM 83,11	83.11	1317	0	3314166	323683	106974	2514	493	205025	3427025	1633
TM 83.2	83.2	964	99	3381350	229498	218461	911	897	211581	449316	1142
TM 84.05	84.05	1218	0	3186161	306149	206734	1346	1119	150445	832781	956
TM 84,45	84.45	519	329	3089102	115657	106482	1144	573	167653	777454	1190
TM 84.82	84.82	1315	100	3519840	423381	193552	1299	1265	211215	758782	1132
TM 84.90	84.90	2385	0	3051521	672963	1153	2067	2059	144716	1020452	1045
TM 85.65	85.65	991	236	3234083	303554	191045	1417	1150	162685	402672	843
TM 86.1	86.1	1040	0	3233968	215665	179475	986	963	140498	349803	721
TM 86.20	86.20	1301	0	2762475	313997	1153	1215	2293	132425	528106	1004
TM 87.02	87.02	2043	292	3746545	540420	192777	2849	1462	215869	522845	1135
TM 88.2	88.2	5053	115	3511513	1450620	191684	3183	478	337405	1976464	2069
TM 89.11	89.11	1258	66	2839523	368116	190572	865	987	206707	652705	1019
TM 90.42	90.42	1203	97	3251711	357088	209566	2114	583	208903	2826997	1398
TM 91.05	91.05	1037	186	3353930	250736	213632	738	0	189344	385457	882
TM 91.6	91.6	1202	0	2807754	385748	180225	1755	1043	225942	1203328	1442
TM 92.08	92.08	1753	278	3093506	488294	187456	1094	124	185343	791407	938
TM 93.05	93.05	980	67	3449045	179131	196108	1022	314	173805	319317	1218
TM 94.3	94.3	1235	59	2486074	352001	285599	1191	0	170102	508904	1439
TM 94.35	94.35	1090	0	2974136	216424	1159	1196	1858	238912	433207	1542
TM 95	95	2842	41	3113637	816768	312038	2225	1399	223071	965484	1391
TM 96.1	96.1	1101	137	3264927	317212	221663	1464	841	189182	691293	1173
TM 96.38	96.38	651	88	3109006	92702	251369	1088	504	149644	235843	767
TM 96.9	96.9	1302	104	2913964	313330	199168	1319	832	174615	528910	1233
TM 97.3	97.3	973	16	2839754	176372	288498	933	0	162573	294535	1086
TM 97.85	97.85	474	3	2613463	26921	267864	390	0	149032	141474	829
TM 98.6	98.6	1280	99	3106266	318959	176850	1541	503	219196	698353	1903
TM 99.35	99.35	1544	38	2272208	437589	4807	1193	0	165132	596420	911
TM 100.2	100.2	1159	178	3009169	309397	176279	829	550	253816	468276	1468
TM 100.6	100.6	1674	205	2825111	389609	196045	1577	561	271078	583188	3028
TM 101.53	101.53	949	0	2293753	283877	250910	472	0	268812	389642	860
TM 102,38	102.38	1557	482	3174709	315502	104056	1731	1669	192596	446125	1311
TM 102.85	102.85	1429	299	2719996	423283	183912	1385	234	221083	1200835	1155
TM 103.25	103.25	1552	67	2871274	340411	197838	1024	106	196147	684604	913
TM 104	104	1481	112	2669944	569209	315001	1355	1838	186305	709968	941
TM 104,53	104.53	736	0	2902081	226945	94809	1654	1414	213494	393109	2563
TM 105.15	105.15	1591	234	2980145	405419	181159	1154	900	214473	426319	1115
TM 105.35	105.35	1156	157	2469326	364728	311057	993	2376	130894	614015	862
TM 105.58	105.58	975	69	2862003	209860	215648	442	596	121576	172413	675
TM 106,85	106.85	2129	540	2776699	552061	101213	1531	2260	281306	832464	1059
TM 107.2	107.2	1241	113	2468530	352397	280257	1161	1378	212459	462276	1103
TM 108,75	108.75	1529	0	2601703	250138	103966	636	1084	194714	389895	655
TM 109,97	109.97	938	0	2701235	154818	94122	359	0	112837	300808	640

Terminilletto - Concentrations in ng/g (5/12)

Sample	Ni	Cu	Zn	Ga	As	Rb	Sr	Zr	Mo	Cd	Cs	Ba	W
TM 75.03	9450	3213	7880	142	93	629	248474	412	0	16	36	3524	9
TM 76.2	8762	1980	3749	164	235	797	239134	230	51	21	54	3507	9
TM 76.5	10758	3376	2993	351	434	1642	282224	322	377	26	93	4437	19
TM 76.9	9635	4520	6226	275	266	1537	243087	434	8	29	100	4382	153
TM 77.29	10783	2580	4063	180	181	706	279543	244	0	41	49	3978	0
TM 78.05	11156	5880	8840	237	505	1450	309085	655	134	54	94	5189	38
TM 79.2	11165	1809	4209	105	67	459	255479	217	88	32	29	3249	21
TM 80.3	8967	2089	4409	192	333	822	283365	0	321	38	50	3985	1
TM 81	8172	2754	3627	115	318	493	249431	154	110	73	15	2790	4
TM 81.1	9608	2855	6437	133	408	539	252652	0	157	85	38	3288	68
TM 82.07	8553	2256	6348	143	176	705	333133	0	58	42	50	4419	0
TM 83,11	12586	6839	12598	369	1563	753	305087	222	192	49	17	5150	21
TM 83.2	10569	3008	6640	116	201	563	272958	0	116	66	30	3481	2
TM 84.05	11701	3463	5612	152	235	800	267185	596	0	56	45	3804	214
TM 84,45	8186	2274	1063	117	168	321	230777	66	28	24	5	2597	0
TM 84.82	10113	3875	6820	172	141	1081	311392	0	87	68	68	4702	2
TM 84.90	11697	5303	119	325	288	1456	278789	0	0	86	12	5780	6
TM 85.65	12202	3580	3574	142	83	687	289786	313	0	32	45	3580	34
TM 86.1	10624	1360	5713	132	169	599	223055	0	72	54	39	3412	0
TM 86.20	20840	2307	5651	222	164	826	233695	0	37	77	6	3701	2
TM 87.02	9630	1815	6959	249	107	1334	226253	0	66	171	71	3522	0
TM 88.2	13480	7335	21258	643	383	3654	415206	648	255	377	197	7293	83
TM 89.11	10984	6677	7748	193	327	980	327255	0	67	134	56	4418	0
TM 90.42	11602	8499	15322	257	568	781	279353	0	41	136	97	6010	17
TM 91.05	11852	2880	9041	123	63	609	203006	174	184	117	39	2848	40
TM 91.6	12364	4984	12772	241	406	915	266829	556	0	266	120	5109	139
TM 92.08	9955	3629	9834	215	135	1152	288337	289	120	91	83	4123	5
TM 93.05	11603	3117	8577	88	52	423	191580	204	60	151	35	2603	98
TM 94.3	13072	3909	7034	226	188	757	181713	351	0	50	112	3139	32
TM 94.35	13824	3778	1577	146	209	389	181681	0	36	292	7	2323	0
TM 95	12112	6304	18103	372	535	1722	283930	724	221	173	184	5501	66
TM 96.1	11616	3315	11390	194	313	722	237582	296	47	170	89	4103	97
TM 96.38	9654	1169	8592	100	270	229	183134	130	42	107	24	1931	28
TM 96.9	11160	3054	13768	140	281	807	271807	166	45	167	120	4514	97
TM 97.3	10480	1234	10324	128	239	467	164421	305	0	63	80	2496	45
TM 97.85	10192	1145	8666	88	53	69	149066	165	0	119	8	1472	23
TM 98.6	13124	4072	14472	175	241	755	239376	243	36	298	106	3880	21
TM 99.35	10845	4317	13280	269	280	1050	232300	409	0	179	142	5136	255
TM 100.2	11794	4550	12370	141	101	736	234531	306	0	149	46	3687	15
TM 100.6	12764	10907	16728	182	386	862	352758	429	266	217	64	5692	67
TM 101.53	10453	2587	9854	191	241	715	261814	208	0	151	78	3573	184
TM 102,38	7231	2962	7520	146	355	819	204206	61	1468	232	11	3279	5
TM 102.85	11839	7757	21798	280	302	975	207730	210	20	283	107	4220	69
TM 103.25	11472	3046	15677	149	119	922	154918	154	90	207	76	2961	11
TM 104	11680	4223	15974	309	195	1240	181486	534	411	222	104	3433	539
TM 104,53	9278	4207	7175	132	307	591	177341	105	777	76	8	2598	0
TM 105.15	6529	2497	7645	205	150	969	187685	785	313	81	53	3407	541
TM 105.35	14951	4387	13656	226	279	940	130312	423	57	121	93	2366	86
TM 105.58	7472	3077	7685	109	121	619	127122	292	106	137	46	1710	0
TM 106,85	7035	6448	17745	313	207	1386	320903	160	0	80	23	4750	3
TM 107.2	13612	5245	8832	169	113	742	289131	247	0	106	76	4025	45
TM 108,75	7032	2119	11024	179	0	692	136877	107	0	197	15	2583	0
TM 109,97	4971	3663	8860	108	0	440	117774	76	0	161	8	1748	0

Terminilletto - Concentrations in ng/g (6/12)

Sample	Pb	U	La	Th	Y	Sc
TM 75.03	303	355	6128	110	9184	0
TM 76.2	86	267	4709	132	7280	0
TM 76.5	455	268	5826	168	8917	207
TM 76.9	824	289	5182	151	8100	0
TM 77.29	506	300	5432	137	9221	533
TM 78.05	783	370	6219	223	9498	0
TM 79.2	164	300	4552	79	7318	0
TM 80.3	0	444	5111	88	8214	72
TM 81	95	262	3884	64	4900	24
TM 81.1	311	319	5423	84	8680	44
TM 82.07	0	301	6050	136	9991	180
TM 83,11	2609	299	4372	135	5604	234
TM 83.2	0	290	5220	87	8060	279
TM 84.05	3883	341	5510	140	8200	340
TM 84,45	459	306	3940	90	4873	217
TM 84.82	240	255	6088	151	9550	309
TM 84.90	168	747	2508	0	0	1
TM 85.65	729	268	5968	122	8944	281
TM 86.1	0	300	3562	81	5928	135
TM 86.20	0	318	1817	0	0	1
TM 87.02	0	847	4339	198	6366	162
TM 88.2	2681	198	8758	499	12454	759
TM 89.11	158	100	7727	206	11213	77
TM 90.42	2476	94	8430	171	10766	11
TM 91.05	370	130	6374	94	7751	135
TM 91.6	1147	324	7379	246	10903	73
TM 92.08	642	128	7780	211	9720	389
TM 93.05	186	503	4465	56	6103	168
TM 94.3	242	237	6091	145	7187	0
TM 94.35	13	236	2265	0	0	2
TM 95	2366	238	9000	280	12130	543
TM 96.1	486	270	6239	136	8946	299
TM 96.38	318	395	5223	64	7034	0
TM 96.9	333	256	5800	164	8547	252
TM 97.3	768	507	4116	103	5512	0
TM 97.85	1633	351	5583	54	6843	150
TM 98.6	584	364	6274	136	9318	223
TM 99.35	2451	156	7729	318	9436	379
TM 100.2	1281	169	5789	180	8109	290
TM 100.6	899	305	8297	191	11118	395
TM 101.53	524	193	7339	228	8630	319
TM 102,38	326	326	3597	71	4295	336
TM 102.85	1795	117	9080	277	11372	645
TM 103.25	811	87	7346	120	9642	226
TM 104	2080	81	8801	273	11255	971
TM 104,53	390	716	4029	80	4790	278
TM 105.15	313	211	4412	134	6130	127
TM 105.35	2381	81	7785	177	8363	668
TM 105.58	300	45	6348	69	8052	347
TM 106,85	1098	200	5378	140	6072	230
TM 107.2	3157	200	6666	195	7823	568
TM 108,75	474	79	5508	110	5576	138
TM 109,97	651	62	4952	59	4778	0

Terminilletto - Concentrations in ng/g (7/12)

Sample	Depth (m)	Li	Be	Mg	Al	Ti	V	Cr	Mn	Fe	Co
TM 110,57	110.57	262	0	2669586	145622	106281	424	767	103645	183156	602
TM 113,15	113.15	1108	0	2783608	312481	108523	1676	1156	167494	350287	602
TM 113.7	113.7	404	128	2506358	47602	278108	892	1311	100804	163080	716
TM 114,05	114.05	1515	323	2590224	292491	95693	3378	1414	115554	261813	772
TM 115,7	115.7	396	0	2597432	47163	103332	981	1195	101573	115379	597
TM 116,92	116.92	653	0	2470398	174366	87956	1763	1335	72719	244276	358
TM 119	119	840	225	2818118	137234	105076	1052	2084	78809	250262	600
TM 119,96	119.96	603	112	2708557	102359	103689	1490	2528	82811	244896	655
TM 120,65	120.65	530	0	2862577	38450	110337	1086	1365	102768	146807	625
TM 121,9	121.9	543	0	2390960	107173	90699	1082	1210	69148	146295	533
TM 123.15	123.15	857	147	2270707	161457	293148	1197	1752	60687	191226	760
TM 124,1	124.1	1279	0	2487747	180312	102214	2271	1904	85879	298725	1086
TM 124,68	124.68	2135	0	2443294	313153	100691	1920	1727	104319	438830	2033
TM 126.06	126.06	1161	188	2172613	277959	271296	2954	1981	102113	411295	992
TM 127	127	748	0	2550348	53675	104926	1029	1538	178039	287063	700
TM 128.2	128.2	1002	1	2733945	233929	208923	2042	1411	95312	312075	1006
TM 129,9	129.9	1533	0	2693547	363393	113070	2228	2160	103566	558364	607
TM 132,05	132.05	648	178	2877866	161524	104315	1592	1892	71429	222484	821
TM 132.6	132.6	791	126	2110852	164131	272685	1309	1259	69685	169956	601
TM 132.7	132.7	1218	134	2830337	226152	203750	1880	1417	83148	332101	828
TM 133,45	133.45	1116	0	2481965	192329	94097	1281	1321	59661	205736	489
TM 133.95	133.95	1186	190	2064214	190484	259075	1348	1537	84126	247408	729
TM 134.6	134.6	784	208	2003724	162561	272546	1264	1580	66893	152723	597
TM 135,3	135.3	2034	3339	2894516	267378	119426	1990	3669	88193	4952484	0
TM 136	136	874	101	2995199	137767	207755	1245	1360	63090	134542	703
TM 136a	136	549	348	2858652	22073	110096	873	2253	50014	89982	527
TM 137,1	137.1	844	0	2495897	122051	98029	835	1591	73283	156597	485
TM 138	138	1023	94	2894892	0	338302	1604	1165	57179	213926	665
TM 138,7	138.7	1067	0	2936781	67310	105288	1657	2069	53098	164639	498
TM 139.35	139.35	539	164	2900253	54727	186826	892	981	52706	72580	586
TM 139.9	139.9	497	0	2726009	0	322938	1696	2174	84393	136820	593
TM 140,6	140.6	538	0	2576305	55280	102206	2092	2251	73908	128121	564
TM 142.2	142.2	624	54	2582704	0	309927	869	864	60465	186514	677
TM 142,8	142.8	1056	0	2701354	146191	103398	1051	1280	60042	184587	592
TM 143,45	143.45	254	0	2686381	38578	98847	1337	1715	54991	62831	446
TM 144	144	440	1029	3204102	12199	117584	1245	3001	113970	332863	191
TM 144.55	144.55	312	46	2122852	8838	254289	1155	950	53607	34816	536
TM 146	146	698	835	2922021	158465	132080	1253	2249	77820	256861	0
TM 157.4	157.4	286	256	3926983	0	308599	1511	713	71478	107862	608
TM 161.36	161.36	1353	0	2772659	255746	202786	4205	1844	170290	307105	887
TM 161,4	161.4	1574	399	2328971	309441	103245	6123	2329	145811	567243	1236
TM 163	163	940	1025	2811035	237137	130071	2687	1359	208838	390481	0
TM 163,92	163.92	1449	0	2894378	166959	120333	3051	2712	192853	292308	0
TM 164,02	164.02	1006	411	2900207	194680	0	5925	1268	195150	389624	0
TM 165,22	165.22	2770	0	2207682	655512	102359	5483	1620	339625	852556	1157
TM 165,76	165.76	4134	313	2254050	1143798	100678	5884	2684	280815	1306322	1532
TM 166,57	166.57	1155	0	2282758	250187	107502	2297	1448	297301	313214	693
TM 167,68	167.68	700	0	2646380	156562	113261	1627	1062	404201	305647	675
TM 173,74	173.74	947	0	2930270	88701	123107	2556	1139	256420	137425	0
TM 174,04	174.04	459	0	2426974	3822	107813	1153	1385	439716	87249	624
TM 175,12	175.12	2165	0	2046937	481990	112772	2590	1327	275603	1326590	2759
TM 175.54	175.54	2591	66	1938498	678257	163274	2737	1041	206311	1671447	3462
TM 176,1	176.1	297	304	2690683	0	106325	1696	1561	199976	21658	714

Terminilletto - Concentrations in ng/g (8/12)

Sample	Ni	Cu	Zn	Ga	As	Rb	Sr	Zr	Mo	Cd	Cs	Ba	W
TM 110,57	67324	3305	5345	154	0	409	122847	127	0	64	9	2074	3
TM 113,15	5921	2414	8356	131	291	578	146135	161	772	91	14	2059	6
TM 113.7	12216	1711	4349	105	102	99	130274	124	76	50	21	1782	28
TM 114,05	6888	3521	2880	98	190	724	123603	175	4053	31	13	2178	10
TM 115,7	5850	1038	1943	43	62	127	133650	0	1380	92	3	1758	0
TM 116,92	5631	1471	895	43	126	337	147917	61	1154	80	12	2495	0
TM 119	7191	1442	3912	87	252	358	171122	17	1940	0	8	2331	0
TM 119,96	6845	1856	4846	48	67	87	153244	129	1060	85	8	2042	1
TM 120,65	5825	1752	4460	24	0	79	195653	0	0	40	0	2095	0
TM 121,9	6041	1425	6333	90	123	224	134873	35	456	61	11	2126	0
TM 123.15	11891	2562	6829	102	372	374	155324	337	88	50	159	2659	86
TM 124,1	8291	2934	5611	175	184	403	170434	120	282	25	10	2279	0
TM 124,68	8362	3819	2599	208	151	715	150548	180	536	165	17	2997	66
TM 126.06	12408	4365	6091	176	281	633	144836	333	68	132	83	2960	59
TM 127	5802	2418	476	102	0	139	167967	67	0	17	4	1830	2
TM 128.2	8966	4102	10259	168	84	465	178376	263	145	140	40	2954	66
TM 129,9	8287	5583	7363	178	260	768	185275	196	254	137	20	2994	5
TM 132,05	8028	1589	5051	79	206	275	190763	82	442	147	8	2199	19
TM 132.6	11506	2188	1886	142	71	344	153314	275	0	5	34	2431	64
TM 132.7	8277	3223	6751	154	95	520	199417	245	311	105	42	2810	9
TM 133,45	6253	1868	4161	77	211	465	169889	10	291	88	7	2151	3
TM 133.95	11966	3103	4622	176	199	381	174441	313	0	58	48	2752	117
TM 134.6	11102	1841	5307	101	31	304	172391	329	0	66	42	2340	112
TM 135,3	7844	4053	6700	221	569	575	253506	91	800	149	14	2940	6
TM 136	6927	2448	5168	76	128	263	225151	303	241	75	17	2468	37
TM 136a	7219	719	0	47	22	55	227711	68	85	51	3	1795	2
TM 137,1	5833	2160	0	93	0	347	193787	72	0	13	8	2378	5
TM 138	13324	666	3794	26	256	286	207105	128	639	79	27	949	52
TM 138,7	6721	1755	3072	78	0	149	224757	112	311	168	4	2402	10
TM 139.35	9791	1421	5101	57	39	99	197757	199	176	65	11	2023	3187
TM 139.9	14485	8065	19482	69	164	912	185116	127	380	188	8	593	30
TM 140,6	6606	1754	3396	78	0	97	191413	78	0	162	3	2041	0
TM 142.2	12630	1314	1168	3	51	168	187365	299	142	109	8	666	57
TM 142,8	7351	1816	3232	113	0	323	191108	48	142	76	10	2566	5
TM 143,45	8278	660	1850	29	64	57	198264	55	329	78	1	2016	79
TM 144	11901	3096	4970	65	368	22	231679	475	457	84	2	2402	4
TM 144.55	10378	1382	4746	76	166	0	173100	7	0	155	1	1814	0
TM 146	10624	1820	11714	165	197	354	206969	62	727	143	8	2950	4
TM 157.4	13839	530	1465	0	113	21	180110	78	60	40	3	641	88
TM 161.36	7392	4893	7035	146	102	515	145077	386	143	43	46	2932	38
TM 161,4	40285	7061	9455	274	93	842	136013	267	9359	164	18	3072	11
TM 163	8615	4020	5575	176	467	553	138976	84	96	55	15	3547	0
TM 163,92	7599	2290	8301	151	74	460	155920	84	122	94	10	2482	10
TM 164,02	8659	3598	6009	210	247	496	148818	60	14	0	15	3304	3
TM 165,22	9596	11810	8083	375	242	1593	115747	294	0	79	40	6610	6
TM 165,76	8376	13662	8437	503	221	2731	118677	290	1231	72	65	8903	17
TM 166,57	7101	62262	35087	142	120	763	119107	69	783	59	18	5108	1
TM 167,68	6615	3427	2954	63	0	143	123949	112	843	31	9	2874	12
TM 173,74	8345	1262	5827	39	149	259	159981	64	0	111	5	3196	2
TM 174,04	7988	2636	8530	21	0	48	124346	5	608	30	0	1697	0
TM 175,12	9822	17032	6443	312	582	1257	119167	206	584	75	34	7496	12
TM 175.54	27741	30612	17837	470	640	1967	139445	576	116	160	174	8272	96
TM 176,1	7090	1378	5193	10	0	4	138351	5	517	29	0	1004	0

Terminilletto - Concentrations in ng/g (9/12)

Sample	Pb	U	La	Th	Y	Sc
TM 110,57	418	105	3438	57	3288	0
TM 113,15	212	552	4986	58	5122	189
TM 113.7	688	639	5349	87	6099	238
TM 114,05	0	696	2745	67	2837	220
TM 115,7	27	565	3561	41	3914	21
TM 116,92	547	518	3693	38	4517	144
TM 119	0	383	3572	40	4684	78
TM 119,96	0	759	4138	62	5264	0
TM 120,65	466	541	3810	41	4734	0
TM 121,9	0	497	2952	35	3725	94
TM 123.15	2943	467	4773	91	6486	430
TM 124,1	502	888	5686	89	7168	239
TM 124,68	563	507	4739	104	5549	150
TM 126.06	2128	962	8291	152	8801	827
TM 127	295	471	4418	33	4373	0
TM 128.2	392	648	7963	112	10078	175
TM 129,9	528	561	6997	124	6643	210
TM 132,05	440	552	5323	54	5737	83
TM 132.6	1086	503	6335	133	7440	541
TM 132.7	245	519	5418	77	7958	16
TM 133,45	13	338	2610	51	3050	179
TM 133.95	1337	525	7113	139	7960	425
TM 134.6	3664	575	6458	76	7521	151
TM 135,3	859	378	5057	54	6152	1882
TM 136	510	412	5757	55	8908	0
TM 136a	481	449	3740	21	4426	80
TM 137,1	354	310	3251	39	3809	0
TM 138	0	488	3818	0	5532	266
TM 138,7	43	642	3902	31	4665	127
TM 139.35	636	311	3269	36	5068	0
TM 139.9	816	931	6707	0	7994	196
TM 140,6	476	850	4083	25	4398	0
TM 142.2	0	392	3571	0	5022	0
TM 142,8	986	454	3204	35	3945	110
TM 143,45	236	608	3392	12	4160	175
TM 144	0	602	4423	20	5128	194
TM 144.55	0	934	5604	35	6878	0
TM 146	208	500	4051	43	4649	188
TM 157.4	495	1047	4772	0	6339	0
TM 161.36	953	793	7397	152	8874	232
TM 161,4	1599	1279	5871	87	5751	0
TM 163	138	513	5809	136	5213	289
TM 163,92	700	581	7414	169	6463	286
TM 164,02	646	1066	7816	132	6647	106
TM 165,22	1463	536	8364	328	7012	391
TM 165,76	1949	500	8414	302	8155	0
TM 166,57	2578	454	7860	145	6332	9
TM 167,68	0	403	4414	39	3907	0
TM 173,74	730	830	5147	50	4631	43
TM 174,04	220	313	5736	42	4295	0
TM 175,12	1730	228	7022	296	6534	0
TM 175.54	2512	279	11718	580	13709	539
TM 176,1	0	507	4157	16	3778	0

Terminilletto - Concentrations in ng/g (10/12)

Sample	Depth (m)	Li	Be	Mg	Al	Ti	V	Cr	Mn	Fe	Co
TM 176.9	176.9	212	155	2183191	0	316009	864	0	144339	73949	724
TM 178,7	178.7	1090	427	2443116	208337	109939	1574	1060	325619	313168	0
TM 179,8	179.8	1446	0	2528302	97385	107203	946	1088	203825	194898	459
TM 180.3	180.3	1101	1	2450838	0	285403	1506	320	351897	266823	902
TM 181,48	181.48	2389	1030	2527183	480161	120525	2515	1387	441273	706007	0
TM 183,2	183.2	1223	0	2389864	152579	110830	1341	847	213233	201693	867
TM 183,9	183.9	645	0	2355844	50938	95786	1148	1431	529081	101433	638
TM 184,4	184.4	971	231	2219215	166492	100938	1598	2026	249466	350004	599
TM 185.58	185.58	1378	169	2601279	204854	184539	1124	686	329799	538712	653
TM 186,75	186.75	1266	0	2417463	223341	108689	2037	1241	127845	288023	641
TM 188,4	188.4	271	227	2230599	7185	106655	536	1639	191002	121904	605
TM 188.54	188.54	1212	242	1759807	142348	272873	1472	0	167904	1085565	2221
TM 191,58	191.58	1685	0	2098986	327140	99989	2235	1689	321213	429417	623
TM 192,9	192.9	664	0	2113277	164236	91777	1130	1215	225387	311651	1489
TM 193.49	193.49	360	138	1957847	0	257766	355	0	302431	131734	630
TM 196	196	728	0	2083421	177462	97678	1170	1092	117876	343214	386
TM 196,98	196.98	1351	452	2217388	226343	96883	911	736	145294	438836	628
TM 197,1	197.1	1232	0	2317939	383808	102438	1459	1378	198401	765506	755
TM 200,4	200.4	2115	116	1855158	602208	93001	2296	1236	119542	1197961	663
TM 200.8	200.8	622	206	2025367	0	263165	767	0	191299	217669	1003
TM 201,4	201.4	1073	170	2221323	222069	108489	1151	470	126942	376832	482
TM 204,75	204.75	1481	0	2057246	435112	106275	1526	422	189627	2158737	849
TM 205,05	205.05	780	0	2457619	256689	107462	2145	942	423397	557738	1289
TM 208,3	208.3	2551	0	2464451	610558	100923	2019	1284	154652	845100	1251

Terminilletto - Concentrations in ng/g (11/12)

Sample	Ni	Cu	Zn	Ga	As	Rb	Sr	Zr	Mo	Cd	Cs	Ba	W
TM 176.9	13004	1040	8634	42	121	36	101202	0	0	96	5	4	182
TM 178,7	7207	1527	6126	107	152	626	140187	352	101	76	17	6237	4
TM 179,8	6782	1496	4092	37	0	297	113606	74	387	132	6	1751	1
TM 180.3	16016	2288	6029	143	102	414	110499	248	48	77	40	2924	36
TM 181,48	12400	6202	6215	309	295	1261	136091	216	86	215	27	3781	2
TM 183,2	7356	3459	1839	112	81	433	107764	99	261	70	13	3745	64
TM 183,9	5839	1469	10252	75	0	199	122161	53	134	187	3	2115	4
TM 184,4	7862	2521	7220	111	0	551	112055	105	751	152	17	4267	1
TM 185.58	7920	3197	7480	217	200	530	114894	405	255	134	48	6856	6
TM 186,75	8724	2598	3609	101	157	592	106468	161	57	142	16	3467	29
TM 188,4	6834	1984	9251	66	0	14	102918	0	520	155	0	959	1
TM 188.54	15081	7620	13630	208	404	798	88275	281	234	179	62	3245	71
TM 191,58	8123	6269	9781	296	0	895	133675	180	150	187	25	4522	15
TM 192,9	6912	1718	3772	121	35	494	100791	43	90	88	14	6565	1
TM 193.49	12256	1440	10368	122	166	145	86078	78	33	158	12	300	122
TM 196	5964	2917	6246	116	0	568	115898	84	0	231	16	2169	0
TM 196,98	5839	2516	3656	178	0	747	116554	126	0	97	21	2454	11
TM 197,1	7456	6060	8050	289	108	1193	126743	68	101	198	30	4083	4
TM 200,4	8010	5532	9858	357	329	1806	123537	285	22	145	45	3621	31
TM 200.8	13187	551	0	55	200	353	87770	0	255	25	30	290	19
TM 201,4	9870	3518	5317	168	153	680	124649	37	108	17	21	2053	0
TM 204,75	11272	6315	10498	290	468	1159	133652	140	50	179	30	4374	9
TM 205,05	8721	2587	1903	193	158	827	120547	186	277	9	21	2169	37
TM 208,3	8954	5869	9558	401	293	1627	110566	186	0	126	37	2815	30

Terminilletto - Concentrations in ng/g (12/12)

Sample	Pb	U	La	Th	Y	Sc
TM 176.9	0	318	5065	0	5046	0
TM 178,7	716	337	7132	141	6416	270
TM 179,8	636	320	4032	80	3259	0
TM 180.3	365	475	7939	135	7824	568
TM 181,48	541	526	7868	288	7378	150
TM 183,2	608	167	4478	89	4258	0
TM 183,9	575	265	4506	46	4153	0
TM 184,4	710	299	5031	124	4548	85
TM 185.58	1064	109	10489	238	11071	428
TM 186,75	0	288	6356	97	5495	253
TM 188,4	704	230	4712	33	3983	75
TM 188.54	0	122	9573	244	9673	491
TM 191,58	1725	355	7302	154	7429	41
TM 192,9	371	119	5758	127	5196	0
TM 193.49	36	68	11069	63	9725	474
TM 196	678	300	5703	116	5655	0
TM 196,98	895	133	7085	208	6367	0
TM 197,1	1786	229	8775	273	7826	282
TM 200,4	1216	303	8153	315	7139	0
TM 200.8	0	486	2990	0	2848	0
TM 201,4	926	150	6601	149	6247	149
TM 204,75	2209	152	9233	339	8463	151
TM 205,05	747	506	4317	119	3960	15
TM 208,3	1098	214	5297	187	4403	212

Lausen-Schleifenberg ; Concentrations in ng/g (1/4)

Sample	Depth (cm)	Mg	V	Cr	Mn	Co	Ni	Cu	Zn	Ga	Rb	As
S 1-average	10006	1725428	8444	12147	204028	1156	10669	4067	24671	165	450	3086
S 18	9066	2561813	9368	0	143224	980	10238	0	20585	19	0	3862
S 19	9006	2747159	9722	0	131966	867	9726	0	0	44	0	3989
S 20-1	8941	2510621	9683	0	169193	1100	10465	1850	24144	153	0	4928
S 21	8866	2452724	7897	0	147243	881	10217	0	0	0	0	3821
S 22	8801	2848545	10853	0	164899	875	11249	0	0	117	0	3688
S 23-average	8781	5636449	8978	133	109969	1927	13128	3863	40138	25	205	3067
S 24	8711	2597570	9945	0	131755	1018	13393	3955	0	121	0	3393
S 25	8631	2536956	9528	0	130809	927	10259	0	13528	28	0	2998
S 26	8581	2833736	5997	0	124482	634	10052	0	0	90	0	1828
S 27	8501	3031239	7397	5831	100944	621	6468	2984	0	175	1204	2285
S 28	8441	3229414	5970	0	118711	584	9546	0	0	141	0	1766
S 29	8341	3277834	7496	5246	150741	3210	7732	2952	19457	591	3326	2940
S 30-1	8281	3597307	8910	0	190071	1635	14219	0	8454	253	0	3164
S 31	8196	3453270	7850	4757	158631	1706	10203	661	18494	406	2271	5540
S 32-1	8161	3995269	11586	0	193591	2019	14651	2098	121857	645	16	9071
S 33	8016	3310722	15058	6740	178481	10103	16651	1841	0	273	1240	12424
S 34CR	7976	2467247	29288	0	144832	6226	35023	2788	0	534	541	188191
S 34	7971	3100671	7244	1084	125366	627	7960	2081	0	147	554	3680
S 35	7871	2222769	3191	4744	83839	648	7722	0	0	127	224	973
S 36	7811	2241478	3313	801	79960	694	5095	237	0	109	201	431
S 37	7791	2286536	3770	2331	80980	627	6662	0	0	116	188	618
S 38-average	7706	7385574	9192	1975	54122	1566	12402	1895	8329	162	989	1015
S 39	7561	2875356	3606	4003	69277	693	7998	731	0	109	388	45
S 40	7491	2661457	4151	3534	72050	728	7021	253	0	76	256	980
S 41-1	7436	2847555	4266	0	83882	810	9932	0	0	19	0	2194
S 42	7356	2721780	4329	3384	75351	678	7933	0	0	129	212	389
S 43	7266	2741090	4778	2105	85947	754	6277	0	0	146	360	853
S 44	7176	2631292	4189	0	89054	793	6848	247	0	159	351	981
S 45	7146	2717682	4051	1132	94881	782	5977	7466	0	135	450	710
S 46	7036	2824384	5970	70	104494	686	6396	595	0	162	435	377
S 47	7006	2893474	5220	69	101936	717	5103	1841	0	123	281	377
S 116-average	2736	1827398	1841	6351	74806	793	12463	325	18060	130	262	475
S 124-average	2276	2318080	4147	5765	76430	942	14204	317	19516	268	728	2280

Lausen-Schleifenberg ; Concentrations in ng/g (2/4)

Sample	Sr	Zr	Mo	Cd	Cs	Ba	La	Th	Y	Sc	Pb	U
S 1-average	358716	0	0	133	82	1589	5424	972	10331	1351	4266	302
S 18	390462	0	0	0	42	504	1718	235	3860	0	0	310
S 19	388114	0	0	0	11	1246	1743	277	3662	0	0	364
S 20-1	392509	1110	1869	90	67	1214	2150	382	4956	0	5707	527
S 21	374588	0	0	40	0	948	1568	173	3746	0	0	327
S 22	431825	0	0	0	50	1159	2300	343	4965	0	0	372
S 23-average	385776	465	93	48	117	3667	2549	1141	3719	234	29778	2180
S 24	398565	0	0	0	57	2317	2080	265	4511	0	1050	417
S 25	397128	0	0	0	11	1428	1664	271	3803	0	0	347
S 26	399309	0	0	0	27	365	1719	294	3559	0	0	379
S 27	457991	7035	0	0	225	2166	2516	1235	4174	0	0	631
S 28	485559	0	0	0	115	2071	2391	370	3905	0	0	675
S 29	554954	0	0	0	677	4149	3066	1268	4280	0	0	1487
S 30-1	555663	439	0	674	399	2679	3935	918	5764	0	3329	737
S 31	566055	0	0	0	538	3227	4089	1613	5741	0	0	502
S 32-1	664490	1681	0	601	983	4980	5363	1703	6927	0	7391	739
S 33	478406	0	0	0	371	4164	5642	2231	8565	0	0	737
S 34CR	287323	1879	22964	0	122	3439	2848	1219	5313	0	0	2403
S 34	328003	0	0	0	107	1338	2033	604	3471	0	0	2013
S 35	322978	0	0	0	46	828	1930	618	4444	0	0	332
S 36	335190	0	0	0	44	1243	2044	508	4555	0	0	197
S 37	335067	0	0	0	65	1298	1985	598	3939	0	0	208
S 38-average	337108	378	87	0	259	3815	3510	2295	4034	235	5169	3501
S 39	362394	0	0	0	106	2571	2073	570	5147	0	0	270
S 40	370286	0	0	0	38	841	2130	416	5460	0	0	226
S 41-1	398770	16	0	0	0	2356	2454	551	6254	0	1692	273
S 42	377129	0	0	0	44	1595	2499	563	6090	0	0	197
S 43	342627	0	0	0	103	1456	1882	473	4812	0	0	408
S 44	350094	0	0	0	145	1862	2077	607	4863	0	0	163
S 45	380005	0	0	0	84	1511	2138	510	4899	0	0	236
S 46	340139	0	0	0	121	745	2535	629	3774	0	0	432
S 47	497165	0	0	0	101	1353	1940	393	3402	0	0	471
S 116-average	306075	108	62	1344	14	1722	1975	217	4939	118	1737	274
S 124-average	364399	318	216	241	48	1762	2602	534	6555	123	2362	396

Lausen-Schleifenberg ; Concentrations in ng/g (3/4)

Sample	Depth (cm)	Mg	V	Cr	Mn	Co	Ni	Cu	Zn	Ga	Rb	As
LA 45	1430	5057787	4784	8861	84630	966	13632	265	4529	246	680	1752
LA 44	1370	3379294	5904	7647	83470	1422	13577	903	8412	363	1542	2807
LA 43	1325	2982295	3743	5546	54484	913	11652	398	3593	159	753	2319
LA 42	1240	7213171	5675	8308	73072	1409	14891	1123	8055	390	2069	2800
LA 40	1235	6604549	4711	9742	110539	1282	15203	893	59713	232	693	2371
LA 39	1180	3695409	3789	10108	93132	1575	15968	821	5809	226	608	2807
LA 38	1085	3163670	2982	4767	80943	1071	12430	154	11732	194	459	1303
LA 30	1023	10310562	3562	4799	91160	1149	12771	613	4241	200	1185	2788
LA 37	1000	2993868	3645	8452	77314	806	11722	594	26	109	230	4360
LA 36	980	3460039	3661	6264	92989	1134	14983	547	928	169	492	2071
LA 29	938	3282021	4513	8999	76157	945	13226	278	2678	94	577	2546
LA 35	930	9341953	4745	5696	102271	1766	13525	469	2689	385	1606	2682
LA 33	910	3551565	4165	7561	113911	1235	14136	3680	6613	187	739	3348
LA 32	885	3201843	3125	6532	90499	713	12345	1892	0	59	146	2119
LA 28	853	2943915	4014	6880	88969	1020	11793	643	10935	169	378	13603
LA 31	853	3262144	4158	5595	148205	909	13802	688	23717	185	258	1751
LA 26	828.5	2957761	4145	8788	75198	761	10329	181	3583	97	462	4518
LA 25	808.5	8265033	3877	10010	101685	1342	13845	1538	10165	231	905	6849
La 24 B L1	793.625	4752344	3137	8093	93143	1724	16872	777	181844	235	631	4134
La 24 B P1	793.25	4203025	3518	8821	94777	1297	15901	1474	87757	246	750	7490
La 24 B L2	791.875	3282071	2505	7334	86387	1243	16557	599	424437	213	284	3330
La 24 B P2	791.75	3320265	2581	7280	89451	1196	14278	1258	2288785	460	314	12764
La24-average	791	3041395	2511	8118	85342	1388	31107	478	487099	224	477	4821
La 24 B P3	790.25	3188755	2714	8410	89230	1048	14965	790	1143939	335	337	12562
La 24 B L3	790.125	3346620	2563	7926	85462	1222	16911	913	55247	130	391	3709
La 24 B P4	788.75	4238190	2967	9576	88486	1220	13821	2714	689675	260	431	8271
La 24 B L4	788.375	3396154	2705	9238	90946	1435	17778	1407	23634	170	419	3696
S 151-average	756	3786392	3893	5835	88725	1439	15116	899	343578	399	1023	5614
LA 21	746	9756459	6081	8112	94125	1524	12546	1201	221	417	2470	4864
LA 20	701	3097870	4117	5661	76699	1180	10434	588	17662	118	794	2950
LA 19	671	3865483	5655	8754	95252	1001	13146	912	16017	212	1180	4261
LA 18	641	3811713	5963	6427	88399	1295	12044	1160	177904	447	1684	4735
LA 16	591	4707535	9993	8946	105404	1800	12583	2445	12499	543	3306	9611
S 155-average	546	3584330	4670	11929	115349	1039	11809	5901	19138	250	1045	10102
LA 14 b	506	4441921	9585	9330	105538	1521	190303	2068	29756	436	1977	9606
LA 13	371	4807595	9061	4551	84066	1466	10695	2037	6413	295	2509	8783
LA 11	306	4544711	8003	5525	84247	1712	12028	1127	6812	352	2763	8930
LA 10	292	5025953	7797	5129	79771	1558	11214	318	4406	417	2908	8157
LA 9	237	4639176	7945	4198	96450	1734	11658	822	7682	368	3151	8620
LA 8	217	4486881	9544	4994	112422	1794	11440	976	10568	307	3649	8840
LA 7	192	4287439	11292	4840	91433	1737	10581	432	6784	387	4048	9373
LA 6	167	4356350	9660	5079	172667	1586	12746	626	7285	439	4670	9884
LA 4	112	4145517	9809	5361	114228	2202	10383	1164	19676	861	6823	9291
LA 3	65	4642845	8086	5947	139314	2303	12070	1622	16011	435	5058	13422
La2-average	47.5	3769143	7797	3787	115544	1900	14726	1404	16469	403	3823	10371

Lausen-Schleifenberg ; Concentrations in ng/g (4/4)

Sample	Sr	Zr	Mo	Cd	Cs	Ba	La	Th	Y	Sc	Pb	U
LA 45	475713	428	285	27	96	3726	7547	1043	13783	579	745	383
LA 44	371169	585	285	71	241	3409	7120	1485	13041	623	1195	477
LA 43	517217	414	395	60	85	2034	5398	690	10417	202	378	521
LA 42	640548	897	990	125	271	2809	6643	1189	12778	1092	835	1015
LA 40	502416	602	1533	258	88	2698	7205	1205	15001	1238	907	1030
LA 39	498159	454	913	108	80	2724	7235	1253	15300	1023	920	505
LA 38	481811	284	548	24	68	1651	5386	810	10940	167	109	551
LA 30	403429	254	706	0	152	1854	5994	1204	11502	291	528	532
LA 37	405660	256	797	0	38	1895	6427	1074	13649	309	502	398
LA 36	579564	407	244	36	57	1940	6353	720	12380	860	492	546
LA 29	455989	235	606	12	46	1654	6624	697	13661	515	248	365
LA 35	450178	355	386	6	214	2560	6618	1262	11739	506	526	461
LA 33	462983	380	657	48	93	2082	6662	874	13284	793	683	484
LA 32	543045	285	203	8	22	1072	5746	709	11425	302	228	362
LA 28	401112	382	56	159	44	1825	6866	1146	14906	451	963	387
LA 31	433137	159	174	297	41	2122	11438	681	18004	758	50	426
LA 26	503385	356	80	0	72	1296	5708	683	12039	339	241	278
LA 25	426206	319	657	121	96	1416	6666	2499	12803	556	2665	451
La 24 B L1	409408	276	259	923	19	1487	3556	1069	7686	350	2081	344
La 24 B P1	398611	31	644	471	20	2455	3616	1408	7751	548	2729	365
La 24 B L2	398780	46	237	2346	9	1804	3492	713	8109	245	1674	322
La 24 B P2	391580	66	613	15777	10	2112	3539	954	7888	453	3184	367
La24-average	394552	164	343	2499	21	1229	4179	962	8997	445	2361	336
La 24 B P3	392721	0	689	8544	9	2186	3531	1057	7949	374	2420	334
La 24 B L3	390484	40	419	262	15	1432	3540	774	7720	327	1598	343
La 24 B P4	388891	239	648	5501	16	1717	3748	1645	7651	371	2987	343
La 24 B L4	374009	74	401	78	13	1565	3537	1473	7513	411	2337	319
S 151-average	341962	202	1146	2035	63	1942	2899	575	6528	246	2131	607
LA 21	518771	898	1606	7	334	2316	7527	1635	12479	384	1196	1106
LA 20	487446	552	927	38	116	1534	5023	950	9203	0	275	752
LA 19	565156	805	1131	36	172	1578	7396	1112	13521	715	734	1029
LA 18	684194	758	1742	749	228	1858	6214	1059	10776	542	807	1103
LA 16	609742	928	2822	96	391	2543	9768	1985	14615	779	1373	1466
S 155-average	565907	316	116	63	186	2981	8834	1254	17539	787	20877	339
LA 14 b	706513	1372	1054	80	231	131141	8838	1638	13819	792	1663	810
LA 13	828475	1286	935	0	309	1714	6762	1349	6816	506	746	1335
LA 11	808577	961	1378	44	366	1993	6139	1672	6777	511	768	1126
LA 10	879975	1180	702	0	312	2656	5243	1100	5581	323	963	818
LA 9	821955	1436	684	0	398	1710	5017	1218	5513	356	1428	1041
LA 8	716604	1226	493	43	482	1758	7263	1369	7576	552	1289	1299
LA 7	702992	1412	455	15	512	2007	5944	1553	5999	292	1044	632
LA 6	467373	1252	1021	0	517	1858	5059	1184	5288	299	1410	668
LA 4	593320	1529	274	0	844	3350	9225	1852	6315	406	1410	568
LA 3	693575	1167	541	10	650	2177	9347	2185	7945	722	1691	756
La2-average	615635	777	556	31	236	2136	4010	1167	3963	206	2352	591

Gorges du Pichoux - Concentrations in ng/g (1/4)

Sample	Depth (cm)	Li	Mg	Al	Sc	Ti	V	Cr	Mn	Fe	Co	Ni	Cu
Pi 185	7973	895	2402673	562471	0	100692	8137	4932	33932	1449740	754	10375	757
Pi 184	7910	579	2486128	422324	0	94214	5359	4454	35000	1124990	526	8474	440
Pi 180	7757	471	2613822	282678	74	119390	5609	5177	29771	959691	559	9877	298
Pi 179	7728	1144	2906993	560110	170	104568	7863	5542	35553	1500190	723	10705	657
Pi 178	7521	1098	2095608	787089	0	104735	7172	4946	26552	1182264	669	9911	922
Pi 177	7493	545	1993170	525914	0	122239	10499	3444	37823		624	16121	0
Pi 176	7418	33	1440871	45995	0	121299	8194	3666	34207		529	10021	0
Pi 174	6855	35	1328463	15640	35	116186	6494	4079	18435		591	11147	0
Pi 173	6756	66	1179315	31340	70	115156	7772	4898	28065		600	10819	1867
Pi 171	6425	0	845796	19138	0	114524	5055	1953	22618		578	9698	0
Pi 168	6074	0	870030	7538	1	118961	4683	3490	27718		571	10251	0
Pi 167	6038	0	730132	21047	0	120838	3905	4806	24434		719	10523	0
Pi 164	5769	37	1343956	86297	43	136419	3786	7258	25112		675	9559	0
Pi 163	5664	62	1143889	178112	0	119319	6316	3116	27317		620	9968	0
Pi 161	5588	123	1101045	79058	0	116794	7501	4199	29213		666	9288	0
Pi 159	5467	177	1648909	28393	385	144403	7525	5889	23200		743	11884	0
Pi 158	5349	202	1083194	28187	0	119924	2554	3993	20838		534	8722	0
Pi 157	5268	108	1342219	68697	207	128007	7080	6106	24391		655	10298	0
Pi 153	5148	459	1586320	233414	162	137633	4961	5678	36343		772	10324	0
Pi 151	5079	128	1168795	100576	0	121653	4123	3274	29040		691	8766	149
Pi 149	5019	211	1342621	149175	0	106299	4206	4493	30072		664	8876	0
Pi 146	4975	360	1941954	315507	91	124084	7369	4723	37253		1103	13495	0
Pi 145	4796	272	2024153	198288	279	130495	3670	4919	28218		899	13787	0
Pi 144	4726	303	1424943	185750	142	118850	6023	4433	33828		753	10356	0
Pi 143	4685	214	1481417	100374	323	123765	5935	4601	31198		736	11082	0
Pi 141	4612	179	1239883	37442	11	118963	4188	3678	25499		701	13588	0
Pi 140	4564	184	1278268	51802	6	110128	6334	4033	31769		757	10275	0
Pi 139	4467	472	1411800	320413	72	122583	5362	7400	26390		984	11833	23
Pi 138	4386	25	946515	34010	128	123248	3237	4467	32450		697	2221	0
Pi 137	4191	0	1207808	65065	0	117951	1995	4405	23853		637	1590	0
Pi 136	4133	13	972876	31433	38	116638	1786	3336	32783		687	2237	0
Pi 135	3911	173	1305734	58672	0	117952	1627	3693	28423		589	1430	0
Pi 134	3871	26	1146012	73700	0	124393	1874	3304	38568		660	912	819
Pi 133	3829	44	1249719	30102	0	112873	2684	2353	39529		632	253	0
Pi 128	3592	176	1807821	82023	7	132972	2536	3720	39252		674	2092	1463
Pi 120	3095	82	1652667	58270	24	120768	3161	2245	31843		635	739	0
Pi 118	2853	91	1285305	84145	60	113459	3107	2316	25765		534	0	0
Pi 116	2827	87	1359813	100911	139	125305	3684	4467	33000		708	8930	0
Pi 114	2799	117	1973034	90375	281	133093	8045	7860	30196	483341	549	6584	829
Pi 113	2581	369	2472532	139191	0	122589	6456	4963	23140	340430	446	5441	851
Pi 110	2395	444	2626068	167050	0	114045	8261	5069	29828	673271	557	8775	680
Pi 108b	2311	411	2541645	159875	11	132017	9144	4527	41583	953447	636	7856	963
Pi 107	2285	2934	2397382	1319711	0	103220	9898	5744	80318	2665288	910	10049	2038
Pi 104	2216	2862	46899825	947067	12	85180	5590	4127	69252	3387439	899	7298	1656
Pi 103	2163	3191	9335231	1632037	613	122075	9732	10620	73296	3391012	1068	13607	2717
Pi 101	2098	78	3104182	195076	676	130905	3903	5761	42886	914454	734	8846	1013
Pi 100	1967	1190	3664384	750873	13	116002	7089	4256	40183	1290736	600	8014	1361

Gorges du Pichoux - Concentrations in ng/g (2/4)

Sample	Zn	Ga	As	Rb	Sr	Y	Zr	Mo	Cd	Cs	Ba	La	W	Pb	Th	U
Pi 185	8594	197	1719	1792	120478	494	593	89	0	78	1970	472	9	492	230	2941
Pi 184	5810	160	1271	1358	129672	551	355	92	16	81	1806	488	0	256	282	2683
Pi 180	1424	90	1234	825	137037	445	256	142	27	41	1561	306	8	349	122	3757
Pi 179	6897	226	2045	1717	139728	563	455	109	26	95	2069	544	4	1166	378	4349
Pi 178	11962	293	1521	2256	121306	367	438	332	29	78	2165	334	0	654	164	2479
Pi 177	5376	187	899	1342	112390	620	151	97	74	75	1625	479	7	1268	91	2154
Pi 176	4100	53	230	84	113833	275	0	90	57	3	796	122	0	0	0	2430
Pi 174	1104	30	310	10	119360	134	0	77	77	1	735	33	0	0	0	1539
Pi 173	2398	16	531	50	89562	184	814	93	120	4	892	52	33	1516	156	2035
Pi 171	1920	14	210	7	65741	175	0	31	475	2	512	54	0	0	0	1454
Pi 168	4079	16	269	0	72920	328	344	70	43	1	517	96	0	409	21	1303
Pi 167	4448	38	623	22	86334	292	209	147	71	5	1581	112	28	374	18	703
Pi 164	2740	83	311	356	114658	153	0	194	162	25	854	88	71	213	1	992
Pi 163	6806	63	249	581	96597	205	0	241	61	19	850	86	0	0	11	1502
Pi 161	5070	60	97	276	84001	196	120	24	59	13	510	92	0	1244	12	1479
Pi 159	5603	27	172	73	139350	386	168	0	28	4	841	182	0	0	13	3130
Pi 158	3387	30	161	64	110180	123	0	130	27	6	449	63	0	0	0	1289
Pi 157	4281	40	339	245	121881	114	457	156	145	17	426	86	0	0	57	1524
Pi 153	4906	96	631	549	120424	165	344	273	31	29	1001	124	0	0	40	2284
Pi 151	6082	24	118	305	100540	115	170	0	0	15	513	85	21	1236	23	1650
Pi 149	6476	84	632	456	106034	232	110	74	21	25	913	133	0	0	34	1467
Pi 146	6274	92	764	977	75675	423	152	9	68	58	979	254	0	0	108	4612
Pi 145	3382	72	585	571	82849	178	119	16	19	30	849	145	8	0	45	1952
Pi 144	16489	105	274	419	104653	194	9	192	38	23	1185	109	8	0	32	1955
Pi 143	9685	57	254	288	116857	155	78	34	133	16	1071	93	11	0	34	1616
Pi 141	4577	19	477	89	81635	213	294	112	215	5	474	81	0	0	49	1581
Pi 140	12110	27	452	116	98496	344	47	56	259	7	683	165	0	216	30	1540
Pi 139	12843	114	1503	865	127700	305	200	273	123	101	1794	189	53	0	72	1100
Pi 138	5463	52	391	40	76071	176	104	86	165	3	578	52	14	665	10	1120
Pi 137	3652	31	439	0	106379	185	62	40	80	7	803	70	1	573	6	688
Pi 136	1605	31	344	87	84104	236	112	20	56	5	627	70	9	427	9	613
Pi 135	8997	60	365	129	94208	573	153	10	29	7	909	257	1	698	19	666
Pi 134	5214	27	222	178	108843	385	171	32	65	9	738	149	23	1527	20	848
Pi 133	3595	30	301	164	95363	433	238	10	64	7	755	165	351	3300	22	1006
Pi 128	6210	38	557	244	114195	261	476	42	50	9	1065	156	21	1203	72	1459
Pi 120	1714	38	379	166	125102	289	180	121	18	11	829	166	3	1108	20	1134
Pi 118	5965	52	491	212	113230	270	172	291	171	6	901	124	30	4494	22	1566
Pi 116	4642	44	183	234	119159	276	143	17	105	18	823	145	38	610	36	2238
Pi 114		15		335	157996	318	308	134	163	21	1010	171		727	37	3055
Pi 113		63		438	167092	588	346	0	249	18	1495	336		310	27	5091
Pi 110		75		563	153651	1601	258	0	0	11	1221	993		19	60	5361
Pi 108b		116		393	148498	1487	274	9	16	24	1357	1004		0	77	4297
Pi 107		514		4234	85006	2090	995	642	48	258	3444	2067		1684	625	4752
Pi 104		419		3235	110316	1852	747	267	10	162	3134	1770		835	503	1640
Pi 103		710		5771	145616	2736	1184	635	0	304	4566	2454		2871	747	2820
Pi 101		68		601	148552	664	431	36	0	37	1871	454		1680	29	2153
Pi 100		229		2033	133453	695	337	110	0	146	2512	640		320	173	1967

Gorges du Pichoux - Concentrations in ng/g (3/4)

Sample	Depth (cm)	Li	Mg	Al	Sc	Ti	V	Cr	Mn	Fe	Co	Ni	Cu
Pi 99	1927	1503	13292108	636917	0	108727	4976	568	44301	1294448	658	6813	746
Pi 97	1885	1252	10890654	334794	0	120520	3095	1688	42843	945263	681	7235	778
Pi 95	1820	1754	31751134	510422	0	99960	3806	445	51200	1389377	663	6965	746
Pi 94	1689	1133	2862829	459930	0	111030	4285	689	43592	1365919	485	5533	523
Pi 92	1644	2898	16449540	998472	0	117165	7319	3035	72317	2608043	1170	10579	1512
Pi 91	1560	1728	15704137	840993	0	106361	4796	1303	72371	2465161	966	6395	1187
Pi 90	1536	2309	11378375	862502	0	125770	4594	1769	71973	2168612	1178	7588	870
Pi 89a	1455	1250	8425585	450823	0	113772	6654	669	67587	2686098	688	7268	579
Pi 88	1416	2838	4505401	1119955	0	105978	5897	1027	69891	2966827	1107	6942	983
Pi 86	1353	3420	5340046	1257111	239	130372	6271	6250	100065	2600433	1061	7359	1233
Pi 85a	1288	1397	4497834	648843	156	112630	11220	4249	103261	2990413	970	5820	624
Pi 82	1247	631	2585239	395074	0	111334	15633	4203	118957	3337376	767	8700	706
Pi 79	1159	477	2519229	453841	247	122452	10292	5162	105525	1431643	557	4890	468
Pi 78	1126	908	2884781	583832	526	133146	16395	7479	109804	2818245	945	7496	1008
Pi 76	1081	419	2150946	395180	14	115790	8950	4783	103004	1172628	585	5297	517
Pi 74	1003	519	2020864	457111	0	76747	8185	4545	105071	1273748	496	4104	365
Pi 72	964	1319	3270914	606153	190	116164	26683	7246	114007	7097569	3712	11239	1738
Pi 71	855	1869	3112297	1054999	150	130797	21048	6089	116564	5309081	2937	11122	1283
Pi 68	762	2068	2597172	1053879	351	125319	12577	5036	100675	4954005	1698	7410	1164
Pi 65	729	784	2329053	334393	143	127662	7038	7541	65322	666070	503	3788	277
Pi 61	693	1489	3029745	518009	645	132338	13799	9086	60036	3731551	1321	8759	2245
Pi 40	628	492	1757607	150324	581	145697	4044	5447	66683	448730	552	5961	312
Pi 37	521	483	1474814	139227	0	105613	4792	2889	55861	463532	622	7513	186
Pi 34	478	769	1803560	501980	0	96591	3251	2484	62243	544283	418	6953	0
Pi 28	431	432	1675325	134452	0	101623	4360	2198	36082	391524	364	6686	0
Pi 26	383	652	1707374	409581	0	112644	7660	3848	57135	984459	915	7967	70
Pi 23	329	1018	2570778	586395	0	107897	6220	1977	39758	975865	618	7362	0
Pi 20	277	778	1995579	425267	78	105902	2452	3194	55539	528883	475	8596	207
Pi 17	251	438	1380575	186782	13	105487	2766	2724	54483	542744	471	6944	0
Pi 15	176	267	1077185	114199	61	107018	2803	1565	59481	392967	505	8734	378
Pi 11	124	543	1885808	215088	0	104699	4498	1913	52222	406324	572	7739	0
Pi 7	75	217	1716791	87401	9	109394	6894	2670	63434	356204	456	7293	0
Pi 2,1	20	534	2404752	366357	100	108640	4257	2269	52431	445993	497	7322	446

Gorges du Pichoux - Concentrations in ng/g (4/4)

Sample	Zn	Ga	As	Rb	Sr	Y	Zr	Mo	Cd	Cs	Ba	La	W	Pb	Th	U
Pi 99		302		1871	142522	738	172	0	51	154	2761	687		0	183	1342
Pi 97		160		781	156563	585	274	80	0	127	2544	462		1082	96	1628
Pi 95		175		1922	147450	683	116	265	0	188	2007	598		319	125	1510
Pi 94		107		1433	162041	779	76	0	0	118	2013	625		0	162	971
Pi 92		432		3623	206950	1078	407	682	84	314	2900	1200		1181	359	2035
Pi 91		315		3822	160292	1112	296	792	0	406	2660	1237		587	493	777
Pi 90		369		3368	184656	1124	341	154	104	429	3277	1215		1262	305	738
Pi 89a		166		1887	151699	880	120	1050	31	143	1738	913		423	264	1309
Pi 88		385		3834	164952	1066	151	888	0	267	3013	1162		844	284	694
Pi 86		401		4413	225795	1272	684	601	32	299	3815	1496		981	262	1018
Pi 85a		287		3184	200812	928	316	120	33	231	2530	1121		0	334	979
Pi 82		161		988	150625	613	434	127	24	59	1718	634		0	124	2838
Pi 79		232		1396	210470	596	263	0	88	76	2466	717		20	239	586
Pi 78		223		1673	226669	653	450	0	143	96	2443	771		1177	207	862
Pi 76		160		1306	180217	659	321	0	188	72	2220	765		0	238	438
Pi 74		140		1530	177074	684	362	0	95	91	1990	715		0	219	461
Pi 72		234		2185	286199	825	641	1081	72	133	2607	1063		3493	401	2679
Pi 71		455		3454	223733	609	518	470	147	130	2744	857		3684	261	1753
Pi 68		396		3893	176719	659	543	675	0	185	3026	1072		2138	411	1763
Pi 65		95		1289	224490	358	227	0	144	64	1610	384		245	126	481
Pi 61		220		1684	250223	390	476	206	159	96	1925	491		4430	152	1407
Pi 40		64		451	150381	292	297	0	65	24	1084	220		898	91	1913
Pi 37	6778	58	523	168	116233	617	276	377	287	20	1125	312	10	0	29	1442
Pi 34	7887	187	67	1504	148962	397	243	717	222	68	1830	383	31	329	59	874
Pi 28	8481	12	0	424	150435	241	180	230	1126	24	1167	154	42	0	24	1194
Pi 26	13743	188	950	1265	144104	911	261	626	301	88	1574	598	36	453	75	2117
Pi 23	37894	179	631	1654	198611	558	218	322	504	64	2191	446	1	1862	72	2928
Pi 20	3606	204	158	1423	145471	650	109	114	766	64	1765	538	14	763	100	738
Pi 17	8972	77	311	537	101845	687	172	159	1060	23	1003	353	4	0	25	591
Pi 15	1648	42	65	409	83339	646	0	64	165	13	820	276	2	248	25	724
Pi 11	18544	88	133	819	142044	693	103	73	601	38	1499	483	2	176	69	1469
Pi 7	7394	19	0	539	135259	605	112	158	0	23	1113	404	0	0	46	2205
Pi 2,1	2742	116	390	1120	174406	631	146	315	42	51	1831	490	2	463	98	2128

Total phosphorus contents

Terminilletto section

Sample	Depth (m)	[P] (μg/g)	Sample	Depth (cm)	[P] (μg/g)
TM - 103.25	103.3	93.2	TM - 231.5	231.5	111.2
TM - 102.38	102.4	90.9	TM - 228.65	228.7	171.0
TM - 100.6	100.6	112.2	TM - 225	225.0	106.7
TM - 98.6	98.6	106.2	TM - 221.2	221.2	123.1
TM - 96.1	96.1	96.3	TM - 211.93	211.9	165.8
TM - 93.05	93.1	91.5	TM - 209.18	209.2	114.3
TM - 91.6	91.6	112.4	TM - 205.05	205.1	60.7
TM - 90.42	90.4	114.8	TM - 204.75	204.8	250.5
TM - 88.2	88.2	146.3	TM - 201.4	201.4	139.4
TM - 87.02	87.0	111.6	TM - 200.4	200.4	185.2
TM - 85.65	85.7	84.2	TM - 197.1	197.1	138.8
TM - 81.1	81.1	93.7	TM - 196	196.0	96.0
TM - 79.2	79.2	85.6	TM - 192.9	192.9	89.3
TM - 76.9	76.9	83.8	TM - 191.58	191.6	174.4
TM - 74.25	74.3	102.6	TM - 188.4	188.4	53.0
TM - 72.4	72.4	87.4	TM - 185.58	185.6	118.8
TM - 71.4	71.4	79.7	TM - 185.58	185.6	114.5
TM - 70.1	70.1	60.1	TM - 184.4	184.4	124.8
TM - 69.4	69.4	55.0	TM - 183.2	183.2	99.9
TM - 68.4	68.4	81.3	TM - 179.8	179.8	107.0
TM - 68.4	68.4	78.1	TM - 181.48	181.5	272.5
TM - 67.41	67.4	249.2	TM - 178.7	178.7	191.5
TM - 66.9	66.9	67.1	TM - 176.9	176.9	82.5
TM - 65.73	65.7	75.0	TM - 176.1	176.1	43.3
TM - 64.81	64.8	127.5	TM - 176.1	176.1	42.0
TM - 64.23	64.2	86.5	TM - 175.54	175.5	363.7
TM - 62.5	62.5	106.7	TM - 175.12	175.1	209.0
TM - 61.1	61.1	78.6	TM - 174.04	174.0	83.7
TM - 61.1	61.1	75.2	TM - 175.12	175.1	204.4
TM - 60.05	60.1	165.4	TM - 173.74	173.7	81.4
TM - 59.4	59.4	111.5	TM - 167.68	167.7	70.6
TM - 58.3	58.3	118.3	TM - 164.02	164.0	97.4
TM - 57.3	57.3	111.8	TM - 161.4	161.4	85.4
TM - 56.36	56.4	142.2	TM - 157.4	157.4	44.3
TM - 55.1	55.1	82.0	TM - 146	146.0	41.2
TM - 53.15	53.2	102.7	TM - 142.8	142.8	65.9
TM - 51.44	51.4	65.9	TM - 139.9	139.9	55.0
TM - 48.93	48.9	126.6	TM - 135.3	135.3	75.2
TM - 45.9	45.9	101.2	TM - 132.05	132.1	83.5
TM - 42.15	42.2	95.5	TM - 127	127.0	76.5
TM - 38.3	38.3	88.2	TM - 124.68	124.7	182.9
TM - 34.3	34.3	64.6	TM - 123.15	123.2	65.6
TM - 29.3	29.3	86.1	TM - 120.65	120.7	56.3
TM - 24.95	25.0	69.1	TM - 116.92	116.9	92.0
TM - 22.31	22.3	64.4	TM - 115.7	115.7	69.3
TM - 16.91	16.9	89.9	TM - 113.15	113.2	136.1
TM - 13	13.0	134.5	TM - 109.97	110.0	75.8
TM - 9.42	9.4	83.1	TM - 108.75	108.8	72.8
TM - 6.05	6.1	92.8	TM - 107.2	107.2	95.4
TM - 3.84	3.8	130.0	TM - 107.2	107.2	98.7
TM - 0.42	0.4	109.0	TM - 104	104.0	125.3

Total phosphorus contents

Carcabuey section

Sample	Depth (m)	[P] (µg/g)
JC4 - 35.8	35.8	400.9
JC4 - 33.3	33.3	337.3
JC4 - 30.3	30.3	249.9
JC4 - 28.7	28.7	254.8
JC4 - 25.2	25.2	202.4
JC4 - 22.2	22.2	271.4
JC4 - 20.15	20.2	146.8
JC4 - 18.15	18.2	175.1
JC4 - 16.45	16.5	133.2
JC4 - 14.1	14.1	107.1
JC4 - 11.7	11.7	164.5
JC4 - 9.25	9.3	313.2
JC4 - 7.5	7.5	226.2
JC4 - 5.65	5.7	254.2
JC4 - 2.85	2.9	199.9
JC4 - 0.0	0.0	541.6

Organic Matter Contents

Values in italics have too low TOC contents ; the HI, OI, T_{max} data are not realistic

Sample	Depth (m)	TOC (%/weight)	HI (mg HC/g TOC)	OI (mg CO_2/g TOC)	T_{max} (°C)	C_{min} (%/weight)
SM1	83.1	*0.09*	*78*	*567*	*441*	7.1
NR1	79.8	*0.15*	*73*	*1040*	*390*	5.7
SM2	70.15	*0.08*	*25*	*725*	*435*	6.9
SM3	19.4	*0.04*	*0*	*1200*	-	6.9
133/134 NJ	18.15	*0.09*	*44*	*1122*	*385*	7.4
SM4	18.1	0.24	83	392	430	8
133/134 BG3	18.1	0.21	105	576	423	7.7
133/134 NP	18.05	*0.06*	*17*	*887*	*402*	7.8
SM5	9.9	*0.08*	*38*	*513*	*443*	6.4
SM6	7.85	0.26	62	454	443	4.4
SM7	6.55	0.12	67	442	428	6.4
SM8	5.05	1.03	106	184	423	0.8
IFP STAN.		3.29	430	24	422	3.2
VP STANDARD		1.87	460	56	421	6.4

Annex 2

Curriculum Vitae and Publication list

Claire RAMBEAU

Droit des Convers 106
2616 Renan BE,
Switzerland
Phone number (office): 032 718 25 96
Email: claire.rambeau@unine.ch

Personal information

Date of birth: January 16, 1977
Birthplace: Laxou, France
Nationality: French
Marital status: Single

Education

2001 - 2005 **PhD. Thesis in Geochemistry - Carbonate sedimentology**
University of Neuchâtel, Switzerland – group of Geochemical and Environmental Analyses
Cadmium anomalies in Jurassic calcareous rocks (Bajocian – Oxfordian) in western and southern Europe

2000 - 2001 **Master « Geosystems - Evolution – Environment »**
University of Burgundy, Dijon, France. Obtained in June 2001 with honors
Geochemical variability of calcareous rocks used for concrete production (Berriasian, French Alps). In collaboration with the Geochemistry, environment, reactors and industrial crystallization department, Graduate Engineering School ENSM Saint-Etienne, France.

1999 - 2000 ***Maîtrise* in Earth Sciences**
University of Burgundy, Dijon, France. Obtained in June 2000 with honors
Multi-field study of carbonate formations - comparison between sedimentological and geochemical data (Middle Oxfordian, Lorraine, France).

1998 - 1999 ***Licence* in Earth Sciences**, University J. Fourier, Grenoble, France. Obtained in June 1999 with honors

1995 - 1997 ***DEUG* in Earth Sciences**, University J. Monnet, Saint-Etienne, France. Obtained in June 1997 with honors

Teaching

2001 - 2005 **University of Neuchâtel, Switzerland:**
Supervisor of three Bachelor students
Sedimentological and geochemical characterization of bio-induced or inorganic carbonate precipitations in actual and ancient environments
Assistant position
practical works in general geology (1st year students)
practical works in sedimentary geology (2nd year students)
participation in Geochemistry courses
field trips and excursions

1999 - 2001 **ENSM Saint-Etienne, France:**
April 2001: supervisor of one-day excursion on sedimentary geology (2nd year students)
September 2000: supervisor of one-week field trip on general geology
University of Burgundy, Dijon, France:
1999 - 2000: Tutoring for 1st year students in Earth Sciences

Other research experiences

July – Sept. 1999 **Internship,** Geochemistry, environment, reactors and industrial crystallization department, EMSE, Saint-Etienne, France: *"Solubilization of borate fibers (possible substitute of asbestos) in pulmonary fluids"*

July – Sept. 1998 **Internship,** Geochemistry, environment, reactors and industrial crystallization department, EMSE, Saint-Etienne, France: *"Diminution of the environmental pollution of metallic hydroxides (industrial products) by mixing them with concrete"*

Additional information

Languages: French (mother tongue), fluent in English.
Driving licence.
Organization of the annual meeting of Swiss students in fields related to environment "Enviro05" - vice president.
Theme for 2005: Climatic changes, impact on environment and societies.

Publications

2006 • Vincent, B., **Rambeau, C.**, Emmanuel, L. and Loreau, J.P. Sedimentology and trace element geochemistry of shallow-marine carbonates: an approach to paleoenvironmental analysis along the Pagny-sur-Meuse Section (Upper Jurassic, France). *Facies*, vol. 52, no. 1, p. 69-84.

2004 • Föllmi, K.B., Tamburini, F., Hosein, R., van de Schootbrugge, B., Arn, K., and **Rambeau, C.** (2004). Phosphorus, a servant faithful to Gaia? Biosphere remediation rather than regulation. In Schneider, S.H.,, Miller, J.R., Crist, E., and Boston, P., eds., *Scientists debate Gaia: The Next Century*, MIT Press, Cambridge, Massachusetts, p. 79-92.

Analytical report

2004 • **Rambeau, C**., Föllmi, K.B., Adatte, T., Matera, V. and Kramar, U. 2004. Cadmium enrichment in Jurassic carbonates. HASYLAB annual report 2004, Hamburg, Germany.

Scientific meetings, proceedings and communications

2005 • **Rambeau, C.,** Föllmi, K.B., Matera, V., Adatte, T. and Steinmann, P. (2005). Cadmium enrichments in Jurassic carbonates: Causes and mechanisms? Poster presented to the Goldschmidt 2005 Conference, Moscow, Idaho USA, 20-25 May, abstract volume (CD-Rom), A133.

• **Rambeau, C.**, Föllmi, K.B., Matera, V., Adatte, T. & Steinmann, P. (2005). Anomalous cadmium enrichments in carbonates of Middle and early Late Jurassic age. Oral communication during the Thirteenth Meeting of Swiss Sedimentologists – Fribourg, Switzerland, 29 January, abstract volume (CD-Rom), p. 43.

2004 • **Rambeau, C.,** Föllmi, K.B., Adatte, T., Matera, V., and Steinmann, P. (2004). Anomalic cadmium enrichments in carbonates of Jurassic age (Bajocian, Oxfordian) and in associated soils in central and southern Europe. Oral communication during the Joint Earth Sciences Meeting of the Société Géologique de France and Geologische Vereinigung, Strasbourg, France, 20-25 September, abstract volume (CD-Rom).

• **Rambeau, C.,** Föllmi, K.B., Adatte, T., Matera, V., Steinmann, P., and Bert, D. (2004). Anomalous cadmium concentrations in Bajocian carbonates of the Tethyan realm. Poster presented to the IUGS 32th International Geological Congress, Florence, Italy, 20-28 August, abstract volume (CD-Rom), p. 822.

2003

• **Rambeau, C.,** Föllmi, K.B., Adatte, T., Matera, V., Steinmann, P., and Veuve, P. (2003). Cadmium anomalies in Jurassic carbonates. Oral communication during the Special Reunion of the French Geological Society on "Mesozoic Paleoceanography", Paris, France, 10-11 July, abstract volume, p. 35.

• **Rambeau, C.,** Föllmi, K.B., Adatte, T., Matera, V., Steinmann, P., and Veuve, P. (2003). Cadmium enrichments in carbonates: A natural source of elevated cadmium concentrations in soils. Poster presented to the NCCR “Plant survival”, Site visit of the review panel 2003, Neuchâtel, Switzerland, 9 May, abstract volume, p. 16.

• **Rambeau, C.,** Föllmi, K.B., Adatte, T., Matera, V., Steinmann, P., and Veuve, P. (2003). High cadmium concentrations in Jurassic calcareous rocks. Oral communication during the EGS-AGU-EUG Joint Assembly, Nice, France, 6-11 April, Geophysical Research Abstracts (CD-Rom).

• **Rambeau, C.,** Föllmi, K.B., Adatte, T., Matera, V., Steinmann, P., and Veuve, P. (2003). Cadmium anomalies in Jurassic carbonates. Poster presented to the Eleventh Meeting of Swiss Sedimentologists, Fribourg, Switzerland, 25 January, abstract volume, p. 60.

2002

• **Rambeau, C.,** Föllmi, K.B., Adatte, T., Matera, V., Steinmann, P., and Veuve, P. (2002). Cadmium enrichment in Jurassic carbonates. Oral communication during the 6th International Symposium on the Jurassic System, Mondello, Italy, 12-22 September, abstract volume, p. 148.

• **Rambeau, C.,** Föllmi, K.B., Adatte, T., Matera, V., Steinmann, P., and Veuve, P. (2002). Cadmium anomalies in oolitic carbonates of Bajocian and Oxfordian/Kimmeridgian age in the Swiss and French Jura Mountains. Oral communication during the 12th Annual V.M Goldshmidt Conference, Davos, Switzerland, 18-23 August, *Geochimica et Cosmochimica Acta*, Volume **66**, Number 15A, p. A623.

Annex 3

Analytical report:
Cadmium enrichment in Jurassic carbonates.

HASYLAB annual report 2004,
Hamburg, Germany

Cadmium enrichment in Jurassic carbonates

C. Rambeau, K.B. Föllmi, T. Adatte, V. Matera and U. Kramar[1]

University of Neuchâtel, Inst. of Geology, Emile-Argand 11, 2007 Neuchâtel, Switzerland

[1]Universität Karlsruhe (TH), Inst. of Mineralogy and Geochemistry, Fritz-Haber Weg, 76128 Karlsruhe, Germany

Cadmium is a highly toxic trace metal, which is transferred into the biosphere by natural and anthropogenic processes. The main cause of elevated cadmium levels in the terrestrial environment, however, is human activity, despite considerable reductions in anthropogenic cadmium emission rates during the last forty years. Important natural sources are volcanic activity and weathering of cadmium-bearing ore bodies, phosphorites and organic-rich sediments. The alteration of cadmium-enriched-rocks is generally not considered to be responsible for elevated concentrations in the environment; this is in line with the observation that the majority of known cadmium-bearing parent rocks is limited in their lateral extension and act as a point or line source rather than an area source. However, we have discovered that marine carbonate rocks – a widespread lithology hitherto thought to be depleted in cadmium relative to average terrestrial crust (mean values 30 ppb and 200 ppb respectively [1,2]) – may represent an additional and important natural source of cadmium. We have identified middle and lower upper Jurassic carbonates outcropping in Switzerland, France, Spain and Italy as being considerably enriched in cadmium, independent of their facies and correlatable in time. A particularly enriched sample from the Lausen section (Bajocian, Swiss Jura) show a cadmium concentration of up to 21 350 ppb. Moreover, a relationship between carbonates with the highest cadmium contents (> 0.5 µg/g; Bajocian and Oxfordian in age) and contaminated soils and vegetation covers has already been demonstrated in Switzerland and France and is highly suspected elsewhere [3,4].

Towards a better understanding of the origin and mechanisms of cadmium enrichment in carbonate rocks: the location of cadmium in oolitic carbonates

We have used the analytical capacity of an electron synchrotron device (µX-Ray fluorescence), present at the Hasylab (DESY) to investigate the distribution of cadmium in oolitic carbonates, during two time periods of each three days. This device allowed us to produce elemental distribution maps of cadmium in thin sections.

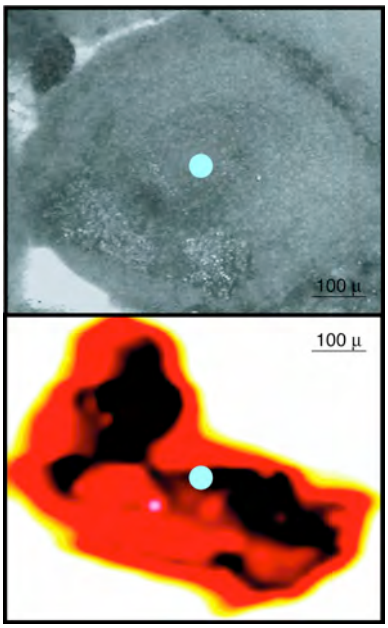

Figure 1: Above: photo of the ooid showing the area covered by analyses. The blue point indicates the location of the point measurement presented in Fig. 2. Below: cadmium concentration map of the ooid. Lowest concentrations in white, highest concentrations in black.

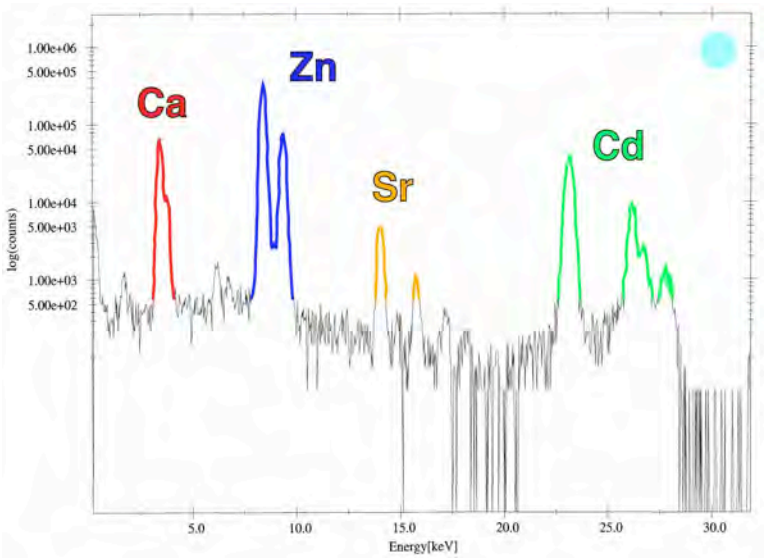

Figure 2: X-ray spectrum of the point measurement inside the ooid shown in Fig. 4 (blue point). Major peaks have been indexed on the picture. Ca=calcium, Zn=zinc, Sr= strontium, Cd=cadmium.

An interesting result of our investigations is that the cadmium distribution within oolitic carbonates may be very heterogeneous, as is shown by the analysis of an ooid within a cadmium-enriched sample of the Lausen section, which yielded a total-rock concentration of 21 350 ppb. The map of cadmium concentrations within this ooid shows a specific enrichment that is limited to certain regions within the investigated ooid (Fig. 1). This is interpreted as the result of a localized cadmium impregnation of the ooid during early diagenesis, that may have occurred very early in the sediment history. The considered ooid is surrounded by non-enriched ones; this, with the fact that whole-rock analyses performed on this very sample have shown a great heterogeneity in cadmium values, suggests that after the impregnation phase the ooids may have been reworked and resedimented, thereby also introducing heterogeneity in cadmium concentrations on a whole-rock level.

This type of analysis has been complemented by micro-X-ray spectral analyses (Fig. 2), which indicate that for this ooid the cadmium is localized in a carbonate phase, in association with zinc.

Outlook

During the next analytical run, we will focus on further cadmium-enriched ooids, in order to confirm the heterogeneity in the cadmium distribution inside these carbonate coated grains, and to better constrain the cadmium-bearing phase(s) inside this type of sediments. We also plan to realise similar investigations on different cadmium-enriched carbonate facies (for example, crinoidal or micritic limestones). Understanding the cadmium-bearing phases and the cadmium repartition inside various types of calcareous rocks will allow us to develop a general model for cadmium enrichment in carbonates. This information is crucial to predict the distribution of cadmium-enriched carbonate rocks, which controls the occurrence of potentially contaminated soils.

Acknowledgements

We highly appreciated the assistance of Dr. K. Rickers during our measurements at the Beamline L and we acknowledge financial support from the Swiss National Science Foundation (projects no. 21-65183 and 200020-101718).

References

[1] H. Gong, A.W. Rose, and N.H. Suhr, Geochim. Cosmochim. Acta 41, 1687-1692 (1977)
[2] M. Tuchschmid, Umwelt-Materialien 32 (BUWAL, Berne, 1995)
[3] O. Atteia, P. Thélin, H.R. Pfeifer, ,J.P. Dubois. and J. A Hunziker, Geoderma 68, 149-172 (1995)
[4] D. Baize, W. Deslais and M. Gaiffe, Etude et Gestion des Sols 6, 85-104 (1999)